GEOTECHNICAL SPECIAL PUBLICATION NO. 193

Material, Design, Construction, Maintenance, and Testing of Pavement



Edited by

Dar-Hao Chen, Ph.D., P.E.
Cindy Estakhri, P.E.
Xudong Zha, Ph.D.
Sheng Zeng, Ph.D.

ASCE
GEO INSTITUTE

GEOTECHNICAL SPECIAL PUBLICATION NO. 193

MATERIAL, DESIGN, CONSTRUCTION, MAINTENANCE, AND TESTING OF PAVEMENT

SELECTED PAPERS FROM THE 2009 GEOHUNAN INTERNATIONAL CONFERENCE

August 3–6, 2009
Changsha, Hunan, China

HOSTED BY
Changsha University of Science and Technology, China

CO-SPONSORED BY
ASCE Geo-Institute, USA
Asphalt Institute, USA
Central South University, China
Chinese Society of Pavement Engineering, Taiwan
Chongqing Jiaotong University, China
Deep Foundation Institute, USA
Federal Highway Administration, USA
Hunan University, China
International Society for Asphalt Pavements, USA
Jiangsu Transportation Research Institute, China
Korea Institute of Construction Technology, Korea
Korean Society of Road Engineers, Korea
Texas Department of Transportation, USA
Texas Transportation Institute, USA
Transportation Research Board (TRB), USA

EDITED BY
Dar-Hao Chen, Ph.D., P.E.
Cindy Estakhri, P.E.
Xudong Zha, Ph.D.
Sheng Zeng, Ph.D.

Published by the American Society of Civil Engineers

Library of Congress Cataloging-in-Publication Data

Material, design, construction, maintenance, and testing of pavement : selected papers from the 2009 GeoHunan International Conference, August 3-6, 2009, Changsha, Hunan, China / hosted by Changsha University of Science and Technology, China ; co-sponsored by ASCE Geo-Institute, USA ; edited by Dar-Hao Chen.
p. cm. -- (Geotechnical special publication ; no. 193)
Includes bibliographical references and indexes.
ISBN 978-0-7844-1045-5
1. Pavements--Design and construction--Congresses. 2. Pavements--Maintenance and repair--Congresses. 3. Pavements--Materials--Testing--Congresses. I. Chen, Dar-Hao, 1965- II. Changsha li gong da xue. III. American Society of Civil Engineers. Geo-Institute. IV. GeoHunan International Conference on Challenges and Recent Advances in Pavement Technologies and Transportation Geotechnics (2009 : Changsha, Hunan Sheng, China)

TE251.M3265 2009
625.8--dc22 2009022741

American Society of Civil Engineers
1801 Alexander Bell Drive
Reston, Virginia, 20191-4400

www.pubs.asce.org

Any statements expressed in these materials are those of the individual authors and do not necessarily represent the views of ASCE, which takes no responsibility for any statement made herein. No reference made in this publication to any specific method, product, process, or service constitutes or implies an endorsement, recommendation, or warranty thereof by ASCE. The materials are for general information only and do not represent a standard of ASCE, nor are they intended as a reference in purchase specifications, contracts, regulations, statutes, or any other legal document. ASCE makes no representation or warranty of any kind, whether express or implied, concerning the accuracy, completeness, suitability, or utility of any information, apparatus, product, or process discussed in this publication, and assumes no liability therefore. This information should not be used without first securing competent advice with respect to its suitability for any general or specific application. Anyone utilizing this information assumes all liability arising from such use, including but not limited to infringement of any patent or patents.

ASCE and American Society of Civil Engineers—Registered in U.S. Patent and Trademark Office.

Photocopies and reprints.
You can obtain instant permission to photocopy ASCE publications by using ASCE's online permission service (http://pubs.asce.org/permissions/requests/). Requests for 100 copies or more should be submitted to the Reprints Department, Publications Division, ASCE, (address above); email: permissions@asce.org. A reprint order form can be found at http://pubs.asce.org/support/reprints/.

Copyright © 2009 by the American Society of Civil Engineers. All Rights Reserved.
ISBN 978-0-7844-1045-5
Manufactured in the United States of America.

Geotechnical Special Publications

1 *Terzaghi Lectures*
2 *Geotechnical Aspects of Stiff and Hard Clays*
3 *Landslide Dams: Processes, Risk, and Mitigation*
7 *Timber Bulkheads*
9 *Foundations & Excavations in Decomposed Rock of the Piedmont Province*
11 *Dynamic Response of Pile Foundations - Experiment, Analysis and Observation*
14 *Geotechnical Aspects of Karst Terrains*
15 *Measured Performance Shallow Foundations*
16 *Special Topics in Foundations*
17 *Soil Properties Evaluation from Centrifugal Models*
18 *Geosynthetics for Soil Improvement*
19 *Mine Induced Subsidence: Effects on Engineered Structures*
21 *Hydraulic Fill Structures*
22 *Foundation Engineering*
23 *Predicted and Observed Axial Behavior of Piles*
24 *Resilient Moduli of Soils: Laboratory Conditions*
25 *Design and Performance of Earth Retaining Structures*
27 *Geotechnical Engineering Congress*
28 *Detection of and Construction at the Soil/Rock Interface*
29 *Recent Advances in Instrumentation, Data Acquisition and Testing in Soil Dynamics*
32 *Embankment of Dams - James L. Sherard Contributions*
33 *Excavation and Support for the Urban Infrastructure*
34 *Piles Under Dynamic Loads*
35 *Geotechnical Practice in Dam Rehabilitation*
37 *Advances in Site Characterization: Data Acquisition, Data Management and Data Interpretation*
39 *Unsaturated Soils*
40 *Vertical and Horizontal Deformations of Foundations and Embankments*
41 *Predicted and Measured Behavior of Five Spread Footings on Sand*
42 *Serviceability of Earth Retaining Structures*
43 *Fracture Mechanics Applied to Geotechnical Engineering*
44 *Ground Failures Under Seismic Conditions*
45 *In Situ Deep Soil Improvement*
46 *Geoenvironment 2000*
47 *Geo-Environmental Issues Facing the Americas*
48 *Soil Suction Applications in Geotechnical Engineering*
49 *Soil Improvement for Earthquake Hazard Mitigation*
50 *Foundation Upgrading and Repair for Infrastructure Improvement*
51 *Performance of Deep Foundations Under Seismic Loading*
52 *Landslides Under Static and Dynamic Conditions - Analysis, Monitoring, and Mitigation*
53 *Landfill Closures - Environmental Protection and Land Recovery*
54 *Earthquake Design and Performance of Solid Waste Landfills*
55 *Earthquake-Induced Movements and Seismic Remediation of Existing Foundations and Abutments*
56 *Static and Dynamic Properties of Gravelly Soils*
57 *Verification of Geotechnical Grouting*
58 *Uncertainty in the Geologic Environment*
59 *Engineered Contaminated Soils and Interaction of Soil Geomembranes*
60 *Analysis and Design of Retaining Structures Against Earthquakes*
61 *Measuring and Modeling Time Dependent Soil Behavior*
62 *Case Histories of Geophysics Applied to Civil Engineering and Public Policy*
63 *Design with Residual Materials: Geotechnical and Construction Considerations*
64 *Observation and Modeling in Numerical Analysis and Model Tests in Dynamic Soil-Structure Interaction Problems*
65 *Dredging and Management of Dredged Material*
66 *Grouting: Compaction, Remediation and Testing*
67 *Spatial Analysis in Soil Dynamics and Earthquake Engineering*
68 *Unsaturated Soil Engineering Practice*
69 *Ground Improvement, Ground Reinforcement, Ground Treatment: Developments 1987-1997*
70 *Seismic Analysis and Design for Soil-Pile-Structure Interactions*
71 *In Situ Remediation of the Geoenvironment*
72 *Degradation of Natural Building Stone*
73 *Innovative Design and Construction for Foundations and Substructures Subject to Freezing and Frost*

74 ***Guidelines of Engineering Practice for Braced and Tied-Back Excavations***
75 ***Geotechnical Earthquake Engineering and Soil Dynamics III***
76 ***Geosynthetics in Foundation Reinforcement and Erosion Control Systems***
77 ***Stability of Natural Slopes in the Coastal Plain***
78 ***Filtration and Drainage in Geotechnical/Geoenvironmental Engineering***
79 ***Recycled Materials in Geotechnical Applications***
80 ***Grouts and Grouting: A Potpourri of Projects***
81 ***Soil Improvement for Big Digs***
82 ***Risk-Based Corrective Action and Brownfields Restorations***
83 ***Design and Construction of Earth Retaining Systems***
84 ***Effects of Construction on Structures***
85 ***Application of Geotechnical Principles in Pavement Engineering***
86 ***Big Digs Around the World***
87 ***Jacked Tunnel Design and Construction***
88 ***Analysis, Design, Construction, and Testing of Deep Foundations***
89 ***Recent Advances in the Characterization of Transportation Geo-Materials***
90 ***Geo-Engineering for Underground Facilities***
91 ***Special Geotechnical Testing: Central Artery/Tunnel Project in Boston, Massachusetts***
94 ***Performance Confirmation of Constructed Geotechnical Facilities***
95 ***Soil-Cement and Other Construction Practices in Geotechnical Engineering***
96 ***Numerical Methods in Geotechnical Engineering: Recent Developments***
97 ***Innovations and Applications in Geotechnical Site Characterization***
98 ***Pavement Subgrade, Unbound Materials, and Nondestructive Testing***
99 ***Advances in Unsaturated Geotechnics***
100 ***New Technological and Design Developments in Deep Foundations***
101 ***Slope Stability 2000***
102 ***Trends in Rock Mechanics***
103 ***Advances in Transportation and Geoenvironmental Systems Using Geosynthetics***
104 ***Advances in Grouting and Ground Modification***
105 ***Environmental Geotechnics***
106 ***Geotechnical Measurements: Lab & Field***
107 ***Soil Dynamics and Liquefaction 2000***
108 ***Use of Geophysical Methods in Construction***
109 ***Educational Issues in Geotechnical Engineering***
110 ***Computer Simulation of Earthquake Effects***
111 ***Judgment and Innovation: The Heritage and Future of the Geotechnical Engineering Profession***
112 ***Soft Ground Technology***
113 ***Foundations and Ground Improvement***
114 ***Soils Magic***
115 ***Expansive Clay Soils and Vegetative Influence on Shallow Foundations***
116 ***Deep Foundations 2002: An International Perspective on Theory, Design, Construction, and Performance***
117 ***Discrete Element Methods: Numerical Modeling of Discontinua***
118 ***A History of Progress: Selected U.S. Papers in Geotechnical Engineering***
119 ***Soil Behavior and Soft Ground Construction***
120 ***Grouting and Ground Treatment***
121 ***Probabilistic Site Characterization at the National Geotechnical Experimentation Sites***
122 ***Sinkholes and the Engineering and Environmental Impacts of Karst***
123 ***Recent Advances in Materials Characterization and Modeling of Pavement Systems***
124 ***GeoSupport 2004: Drilled Shafts, Micropiling, Deep Mixing, Remedial and Specialty Foundation Systems***
125 ***Current Practices and Future Trends in Deep Foundations***
126 ***Geotechnical Engineering for Transportation Projects***
127 ***Recycled Materials in Geotechnics***
128 ***Soil Constitutive Models: Evaluation, Selection, and Calibration***
129 ***Advances in Designing and Testing Deep Foundations***
130 ***Advances in Pavement Engineering***
131 ***Contemporary Issues in Foundation Engineering***
132 ***Advances in Deep Foundations: In Memory of Michael W. O'Neill***
133 ***Earthquake Engineering and Soil Dynamics***
134 ***Soil Dynamics Symposium in Honor of Professor Richard D. Woods***
135 ***Erosion of Soils and Scour of Foundations***

136 ***Innovations in Grouting and Soil Improvement***
137 ***Legal and Liability Issues in Geotechnical Engineering***
138 ***Site Characterization and Modeling***
139 ***Calibration of Constitutive Models***
140 ***Slopes and Retaining Structures under Seismic and Static Conditions***
141 ***International Perspectives on Soil Reinforcement Applications***
142 ***Waste Containment and Remediation***
143 ***Geomechanics: Testing, Modeling, and Simulation***
144 ***Sinkholes and the Engineering and Environmental Impacts of Karst***
145 ***Seismic Performance and Simulation of Pile Foundations in Liquefied and Laterally Spreading Ground***
146 ***Asphalt Concrete: Simulation, Modeling and Experimental Characterization***
147 ***Unsaturated Soils 2006***
148 ***Advances in Unsaturated Soil, Seepage, and Environmental Geotechnics***
149 ***Site and Geomaterial Characterization***
150 ***Soil and Rock Behavior and Modeling***
151 ***Advances in Earth Structures: Research to Practice***
152 ***Ground Modification and Seismic Mitigation***
153 ***Foundation Analysis and Design: Innovative Methods***
154 ***Pavement Mechanics and Performance***
155 ***Underground Construction and Ground Movement***
156 ***Geomechanics II: Testing, Modeling, and Simulation***
157 ***Computer Applications in Geotechnical Engineering***
158 ***Contemporary Issues in Deep Foundations***
159 ***Case Studies in Earth Retaining Structures***
160 ***Dynamic Response and Soil Properties***
161 ***Embankments, Dams, and Slopes: Lessons from the New Orleans Levee Failures and Other Issues***
162 ***Problematic Soils and Rocks and In Situ Characterization***
163 ***Geoenvironmental Engineering***
164 ***Innovative Applications of Geophysics in Civil Engineering***
165 ***Geosynthetics in Reinforcement and Hydraulic Applications***
166 ***Educational Activities in Geotechnical Engineering***
167 ***Geotechnics of Soil Erosion***
168 ***Grouting for Ground Improvement: Innovative Concepts and Applications***
169 ***Soil and Material Inputs for Mechanistic-Empirical Pavement Design***
170 ***Probabilistic Applications in Geotechnical Engineering***
171 ***Advances in Shallow Foundations***
172 ***Soil Improvement***
173 ***Advances in Measurement and Modeling of Soil Behavior***
174 ***Designing Our Underground Space***
175 ***Field Measurements in Geomechanics 2007***
176 ***Analysis of Asphalt Pavement Materials and Systems: Emerging Methods***
177 ***GeoCongress 2008: Geotechnics of Waste Management and Remediation***
178 ***GeoCongress 2008: Geosustainability and Geohazard Mitigation***
179 ***GeoCongress 2008: Characterization, Monitoring, and Modeling of GeoSystems***
180 ***From Research to Practice in Geotechnical Engineering***
181 ***Geotechnical Earthquake Engineering and Soil Dynamics IV***
182 ***Pavements and Materials: Characterization, Modeling, and Simulation***
183 ***Sinkholes and the Engineering and Environmental Impacts of Karst***
184 ***Pavements and Materials: Modeling, Testing, and Performance***
185 ***Contemporary Topics in Deep Foundations***
186 ***Contemporary Topics in In-Situ Testing, Analysis, and Reliability of Foundations***
187 ***Contemporary Topics in Ground Modification, Problem Soils, and Geo-Support***
188 ***Advances in Ground Improvement: Research to Practice in USA and China***
189 ***Characterization, Modeling, and Performance of Geomaterials***
190 ***Asphalt Material Characterization, Accelerated Testing, and Highway Management***
191 ***Road Pavement Material Characterization and Rehabilitation***
192 ***Recent Advancement in Soil Behavior, In Situ Test Methods, Pile Foundations, and Tunneling***

This page intentionally left blank

Preface

This Geotechnical Special Publication (GSP) contains 28 papers addressing a variety of current issues in the Material, Design, Construction, Maintenance, and Testing of Pavement. The technical programs for the Geohunan International Conference struck a balance between the fundamental theories and field applications. These papers were presented at the Geohunan International Conference held August 3-6, 2009, in Hunan, China. This GSP includes investigations and solutions from numerous countries. It expands ranges of tools that are available to engineers and scientists.

Acknowledgments

The following individuals have assisted on preparing the GSP and reviewing the papers: Feng Hong, Jenny Li, Tom Scullion, Shongtao Dai, Xingwei Chen, Sheng Hu, and Xiaodi Hu

This page intentionally left blank

Contents

Production, Placement, and Performance Evaluation of Warm Mix Asphalt in Texas 1
Cindy K. Estakhri, Rongji Cao, Allex Alvarez-Lugo, and Joe W. Button

Adaptive Neuro-Fuzzy Inference System-Based Backcalculation Approach to Airport Pavement Structural Analysis 9
Kasthurirangan Gopalakrishnan and Halil Ceylan

Evaluations of Rehabilitation Strategies Using Grey Relational Analysis for Specific Pavement Study—5 Sites in the LTPP Program 17
Jia-Ruey Chang and Sao-Jeng Chao

Correlating APA to Field Permanent Deformation for HMA Mixes at the NCAT Test Track 25
Baoshan Huang and Xiang Shu

Improved Testing Speed and Rolling Noise Estimation in Rolling Dynamic Deflectometer Testing 31
Jeffrey L. Lee, Boo-Hyun Nam, and Kenneth H. Stokoe II

The Application of Emulsion Warm Mix Asphalt in Long Tunnel Pavement 37
Shifa Xu, Liting Xu, Jonathan Jia, and Yongqing Xie

Application of Recycled Brick-Stone Aggregate in Road Base 43
Yingbiao Wu, Yanfang Guo, and Xiuli Zhang

Workability of the 25 mm-NMAS Stone Fill HMA Mixes 49
Lubinda F. Walubita, Tom Scullion, and Joe Leidy

Predicting Pavement Condition Deterioration for the Saudi Inter-Urban Road Network 56
Muhammad Mubaraki

Use of DCP (Dynamic Cone Penetrometer) and LWD (Light Weight Deflectometer) for QC/QA on Subgrade and Aggregate Base 62
K. Kessler

A Discussion on the Optimum Bonding Condition between Semi-Rigid Base and Asphalt Surface Course 68
Hongxin Guan

Study of the Behavior of Aggregates Demolition by the Proctor and CBR tests 75
Omar Boudlal and Bachir Melbouci

Research on Dry-Shrinkage Performance of Cement-Treated Base Materials 81
Yan Wang, Fujian Ni, and Weihong Xuan

Establishment of Performance Related Specifications Using Pay Factors and Relationship between Fatigue Cracking and Pay Factors 87
Sang-Min Hwang, Suk-Keun Rhee, and Seong-Min Kim

Temperature Calibration of EICM Model in New Mexico **93**
Bin Zhang and Jie Zhang

Improvement of Coastal Silty Sand of Saudi Arabia Using Preloading Technique **100**
M. A. Dafalla

Comparative Study on GTM Method and Marshall Mixes Design Method for Large Stone Asphalt Mixes **106**
Xinjun Feng, Zhuo Gao, and Peiwen Hao

Use of Fly Ash Along with Blast Furnace Slag as Partial Replacement of Fine Aggregate and Mineral Filler in Asphalt Mix, at High Temperature **112**
Liaqat Ali and Akmal Fiaz

2D Numerical Settlement Analysis of a Slag Aggregated Test Road on Weak Soils **119**
Aykut Senol and Bilal Erol

Experimental Study of Pervious Concrete on Parking Lot **125**
Ming-Gin Lee, Chui-Te Chiu, Yu-Cheng Kan, and Tsong Yen

An Experimental Study on Pulverized Fuel Ash Concrete **132**
Wen Yi, Yonghe Wang, and Yihua Nie

Investigation of High Temperature Properties of Asphalt Mixture Containing Fibers **139**
Liang Zhou, Peilong Li, and Zhengqi Zhang

Principles of Designing Asphalt Pavement for Orthotropic Steel Bridge Decks **145**
Xianhua Chen, Wei Huang, Jun Yang, and Dawei Wang

Analysis of Semi-Rigid Asphalt Pavement with Flexible Base as a Sandwich Layer **155**
Ruibo Ren, Hiwen Li, and Zheren Wang

Properties and Early-Age Cracking Potential of Blended Cement Concrete **163**
Zhi Ge, Kejin Wang, and Zhili Gao

Evotherm Warm Mix Asphalt Technology Applied on Ultra-Thin Pavement in China **171**
Zhuohui Tao, Fujian Ni, Jinhai Yan, and Wenyuan Huang

Future Design of Perpetual Pavements: Issues and Options **177**
Rafiqul Tarefder and Damien Bateman

Field Evaluation of Damages from Super Heavy Load Moves **187**
Dar Hao Chen, John Bilyeu, and Zheng Li

Indexes

Author Index **193**

Subject Index **195**

Production, Placement, and Performance Evaluation of Warm Mix Asphalt in Texas

Cindy K. Estakhri[1], Rongji Cao[2], Allex Alvarez-Lugo[3], Joe W. Button [4]

[1] Research Engineer, Texas Transportation Institute, Texas A&M University, College Station; Email: c-estakhri@tamu.edu
[2] Vice Chief Engineer, Senior Research Engineer, Jiangsu Transportation Research Institute, 2200 Chengxin Road, Nanjing, Jiangsu, 211112, China ;
[3] Zachry Department of Civil Engineering, Texas A&M Univerisyt, College Station, USA – University of Magdalena, Santa Marta D.T.C.H., Colombia. Email: jason.yan1@gmail.com
[4] Senior Research Engineer, Texas Transportation Institute, Texas A&M University, College Station; Email: j-buttoni@tamu.edu

ABSTRACT: This paper documents the first warm mix asphalt field trial placed by the Texas Department of Transportation in 2006 using the emulsion based technology (Evotherm) developed by MeadWestvaco. The production, laydown, and compaction characteristics of warm mix were compared with a conventional hot mix asphalt control using a standard mixture design. Field-mixed, lab compacted samples were evaluated for production density, moisture susceptibility and cracking resistance. Field cores were obtained after one month and one year of service and evaluated using Hamburg Wheel-Tracking Tests and the TTI Overlay test. Cores were also evaluated using X-Ray computed tomography to determine the distribution of air voids versus depth in the compacted sample. Field performance of the warm mix is comparable to the hot mix control section after two years of service.

INTRODUCTION

This paper documents the first warm mix asphalt field trial placed by the Texas Department of Transportation (TxDOT). Evotherm, developed by MeadWestvaco Asphalt Innovations, Charleston, South Carolina, used their emulsion warm mix technology that is based on a chemical package that includes emulsification agents; additives to improve aggregate coating, mixture workability, and compaction; as well as adhesion promoters (anti-stripping agents). In this process, Evotherm utilized a high residue emulsion (about 70% binder) to improve adhesion of the asphalt to the aggregate, and the product was designed to enhance mixture workability, while lowering mixing temperatures to as low as 200°F. No plant modifications were required.

The objectives of TxDOT in conducting this field trial include the following:

- To evaluate the production, laydown, and compaction of warm mix as compared with a conventional hot mix control using a standard TxDOT mixture design.
- To evaluate the short and long-term performance of the warm mix versus a control hot mix.

PROJECT DESCRIPTION

This project was within the city limits of San Antonio, Texas. The project is located on Loop 368 (Old Austin Highway), is a four-lane roadway divided by a median, with curb and gutter and many businesses along each side. The existing pavement (prior to placement of the warm mix and control) consisted of a cold-milled asphalt surface which had been chip sealed and had been under traffic for about a month prior to the overlay. All of the paving for this project was conducted at night.

The control and warm mixtures met the gradation requirements of a TxDOT Item 341, Type C, Dense-Graded HMAC. The asphalt used for the control hot mix asphalt concrete (HMAC) was Valero PG 76-22. The base asphalt for the warm mix started as a Valero PG 64-22 prior to modification by MeadWestvaco. Once modified, the warm mix binder met the specifications of PG 76-22. The modified asphalt was then emulsified and provided to Vulcan Materials laboratory to perform the mixture design. Two aggregate sources were used for the mixtures: 88 percent of the aggregate was a limestone and the remaining 12 percent was field sand. The same aggregate sources and gradations were used for both the warm mix and the control. Both warm and control mixtures were designed using a Texas Gyratory compactor with a target density of 96.5%.

MIXTURE PRODUCTION

Both the warm mix and control were produced at Vulcan Materials plant located in San Antonio. The plant was a parallel flow Astec with external coater. The emulsion was pumped from the tanker trucks into the end of the drum through the regular plant metering system.

Production rate for the warm mix was about 190 tons per hour (conventional hot mix for this plant is around 250 tons per our). The production rate was less than expected and was due to a high moisture content in the aggregate stockpiles (primarily the field sand) from a rain that occurred the day prior to the first night of warm mix production. The combined stockpile moisture content was running between 4.8 and 5.2%. (Normal stockpile moisture content for these aggregates was between 3 and 4 percent). The limit on the production rate was due to problems with the external coater motor. It would have been desirable to have a mix discharge temperature of 200°F but at temperatures below 220°F, the plant started having trouble with the coater (asphalt too viscous), causing the motor to trip. Amperages were about 20% higher with the warm mix. The drag chain which transfers the mix up into the silos was operating normally.

On the average, the fuel consumed was the same for the warm mix as for hot mix. No reduction in fuel use was observed for the warm mix because of the high moisture content in the aggregates. There were no moisture problems in the baghouse – lots of steam was observed, but bags were not plugged up or caked over.

For the three nights that the test mixes were produced, the plant started producing mix around 7:00 pm and began shipping mix out at around 9:00 pm. About 180 tons of mix was stored during this first 2 hours of production but after the first 180 tons of

mix, there was no need to silo mix.

Temperature of the warm mix at the time of loading into the haul trucks was 220°F. Warm mix plant samples were compacted in the laboratory under three different curing conditions:

- No cure
- Curing for 2 hours at 200°F
- Curing for 2 hours at 240°F

The density of the lab-compacted warm mix specimens were comparable to the control as shown in Figure 1. The control HMAC was compacted at 300°F and all samples were compacted in the Texas Gyratory Compactor.

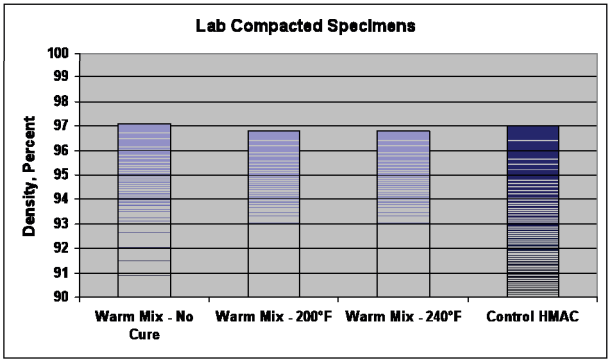


FIG 1. Compacted Laboratory Density after Different Curing Conditions for Warm Mix Compared to HMAC (Compacted in Texas Gyratory Compactor).

LAYDOWN AND COMPACTION

The mix was loaded into belly dump trucks which were all tarped and insulated. The mix was hauled a distance of 20 miles (about 25 minutes) to the jobsite. A remixing windrow elevator (Lincoln model 660 AXL) was used to transfer the mix into a Barber Greene 260B paver.

The paver had a vibratory screed which was on during the paving. One observation by the paving contractor was that "we normally heat the screed once about 20 minutes before starting, but for the warm mix, we had to relight the burners on the screed every 8 to 10 loads because the mat started to tear". Also, he observed that the angle of attack on the screed was doubled what is typically seen on hot mix.

The compacted mat thickness was about 2 inches. Both the control and warm mix were compacted using the same roller pattern: 2 passes with a vibratory roller, one pass in static mode, then between 4 and 6 passes with pneumatic. The vibratory roller was a Hamm HD120 operated at low amplitude and a frequency of about 2500 Hz (midrange). The pneumatic roller was Ingersall Rand, PT 240N, (24,000 lbs, 8 wheels). The tires were bias ply with a tire pressure of 50 psi.

Portions of the overlay were opened to traffic within 2 hours of placement. Asphalt concrete placement testing is shown in Table 1.

TABLE 1. Asphalt Concrete Placement Data.

Mixture	Mix Delivery Temperature	Placement Temperature	Average Nuclear Density, %
Warm Mix (Day 1 – Aug 30, 2006)	180 to 200°F	170 to 180°F	93.5 to 95.0
Control Mix (Day 2 – Aug 31, 2006)	315°F	305°F	94.2
Warm Mix (Day 3 – Sept 7, 2006)	220°F	205 to 210°F	92.1 to 93.8

PERFORMANCE TESTING

Hamburg Wheel-Tracking Test Results

Samples of the loose warm mix and hot mix were also sent to TxDOT's Construction Division Laboratory in Austin. These warm mix samples were reheated and compacted to 93% density using the Superpave Gyratory Compactor (SGC) at two different temperatures: 240°F and 300°F. The control samples were compacted to 93% density in the SGC at 300°F. In addition, roadway cores were obtained at one month of service and at one year.

The Hamburg test is used by TxDOT to measuring the moisture susceptibility and rutting potential of HMA layers in Texas. During the test, two 2.5 inch high by 6 inch diameter HMA specimens are loaded at 122 °F to characterize their rutting properties. The samples are submerged in a water bath and loaded with steel wheels.

The test loading parameters for the Hamburg test were as follows:

- Load: 705 N (158-lb force)
- Number of passes: 20,000
- Test condition/temperature: Under water at 50 °C (122 °F)
- Terminal rutting failure criterion: 0.5 inch (12.5 mm)
- HMAC specimen size: 6 inch diameter by 2.5 inch high

Hamburg test results for the roadway cores are compared to the lab molded plant mix samples in Figure 2. All of the warm mix samples failed the Hamburg test with the exception of the samples compacted at 300°F from the second night of warm mix production. The warm mix cores taken at one month showed no improvement in terms of rut or moisture resistance compared to the lab molded samples. However, at one year, the warm mix cores had the same results as the control mix indicating that the rutting and moisture resistance of the mix improved with time.

TTI Overlay Test Results

The TTI Overlay Tester shown in Figure 3 is used to measure the reflection cracking potential of HMA surface layers in Texas. The test loading parameters for the Overlay Tester were as follows:

- Loading waveform: cyclic triangular displacement-controlled at 0.025 in (0.63 mm)
- Loading rate: 10 seconds per cycle
- Test temperature: 25 °C (77 °F)
- Terminal cracking failure criterion: 300 load cycles (for surface mixes)
- HMAC specimen size: 6-in length by 3-in width by 1.5 in)

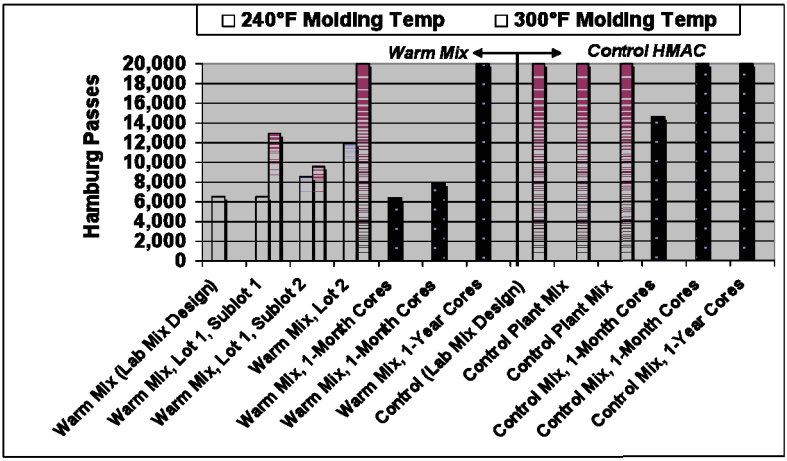


FIG 2. Hamburg Wheel Tracking Test Results for Lab Molded Warm Mix and Control Mixes Compared to One-Month and One-Year Roadway Cores.

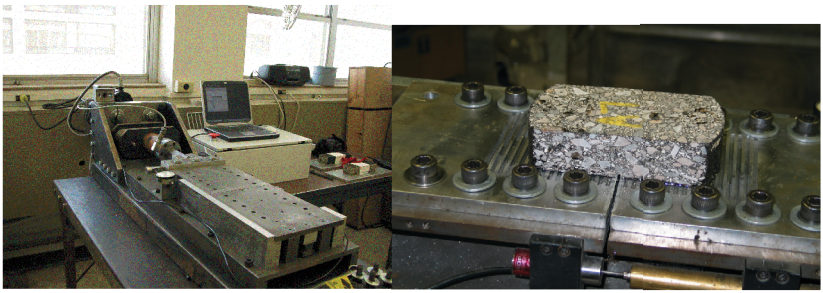


FIG 3. TTI Overlay Tester.

The overlay tester was developed to judge a mixture's resistance to thermally induced reflection cracking. However mixes that pass this test will also have good fatigue resistance. The warm mix laboratory compacted mixes did poorly in this test, as did the control mix. Newly developed criteria for TxDOT mixes recommend that standard mixes should last a minimum of 300 cycles, whereas crack resistant overlays should last more than 750 cycles.

The overlay test results seen here in Figure 4 for both the warm mix and the control mix are typical of many current TxDOT dense graded mixes. This has been a result of several factors including a) the move to stiffer binders, b) general reduction in AC content. This has been recognized by TxDOT and the overlay tester described above has been proposed to address this issue.

Overlay test results for the roadway cores are compared to the lab molded plant

mix samples in Figure 4. All of the lab molded warm mix and control HMAC specimens performed poorly in the overlay test. However, there was a significant improvement seen in the some of the cores taken at one month from the warm mix sections which was attributed to a "curing" effect which may have occurred in service.

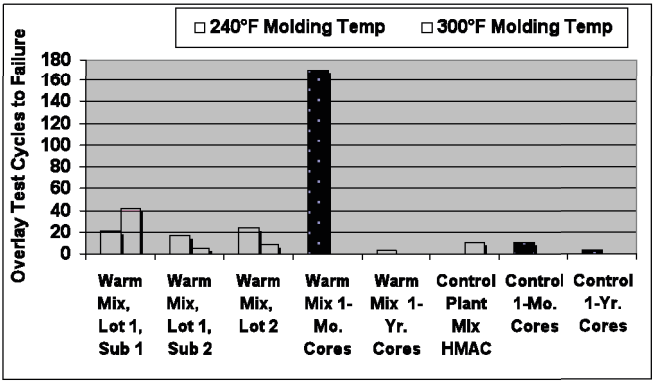


FIG 4. Overlay Test Results for Lab Molded Warm Mix and Control Mixes Compared to One-Month and One-Year Roadway Cores.

In the cores taken at one year, researchers happened to notice that the asphalt absorption into the limestone aggregate was very pronounced in the hot mix cores and yet not at all visible in the warm mix samples as shown in Figure 5.

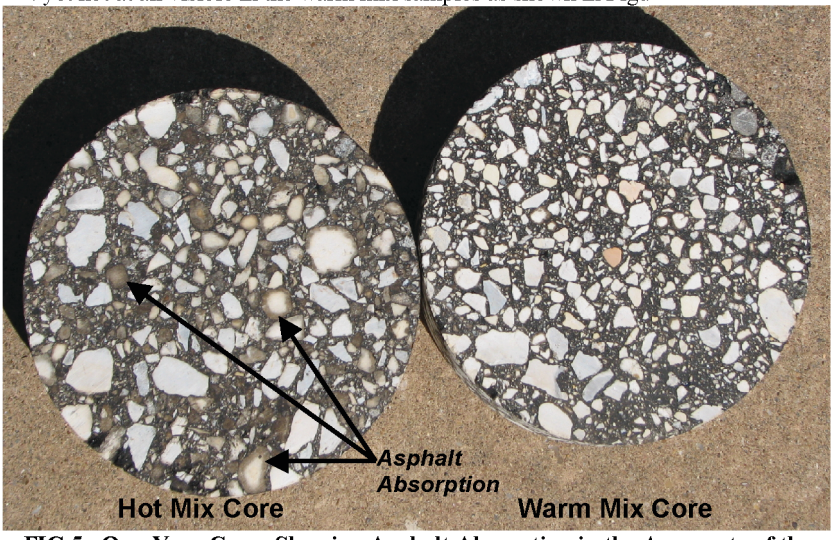


FIG 5. One-Year Cores Showing Asphalt Absorption in the Aggregate of the Hot Mix but Not in the Warm Mix Sample.

Note that the aggregate source and gradation was the same for both warm and hot mix. It is often speculated that this type of absorption means less asphalt is available to the mix to provide flexibility and cracking resistance. It is also speculated that the "lighter ends" of the asphalt are the portion which is absorbed into the aggregate leaving the "heavier" ends available in the mixture which results in a stiffer binder more prone to aging. If this were true, it might help to explain the improved overlay test results shown in the one-month warm mix cores. However, in the cores taken at one year, the overlay test results showed no benefit due to the warm mix (Figure 4).

X-Ray Computed Tomography (CT)

X-ray CT is a nondestructive test to capture the internal structure of materials. Various applications of this method are discussed by Masad (2004). The X-ray CT system at Texas A&M University was used to characterize the air void distribution of a field core taken from the warm mix and hot mix sections. The air void distribution with core depth (or position) is shown in Figure 6. For these 2 cores, the warm mix specimen has a more uniform air void distribution with depth than the hot mix core.

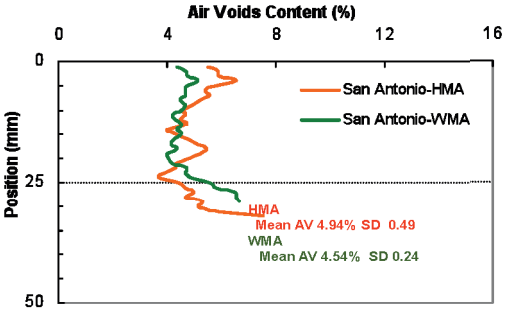


FIG 6. X-Ray CT Analysis Showing Air Void Distribution with Depth for HMA and WMA Field Cores.

SUMMARY AND CONCLUSIONS

TxDOT placed their first warm mix asphalt trial using the Evotherm process on Loop 368 in the San Antonio District in August/September of 2006. All test sections are performing well after 2 years of service. Key findings are summarized as follows.

- The warm mix was produced at a temperature of 220°F and the control was produced at 320°F.
- No reduction in fuel consumption was observed for the warm mix production and this is attributed to a heavy rain prior to production which caused the aggregate stockpiles to be excessively wet requiring more energy for plant operation.
- Warm mix was stored in silos for a maximum of 2 hours prior to load out.
- Warm mix samples were compacted in the field laboratory to densities averaging 97% which was the same as the control HMAC compacted densities. To evaluate the effect of laboratory curing on the warm mix, samples were compacted after 3 curing conditions: no cure, cure for 2 hours

at 200°F, and cure for 2 hours at 240°F. The different curing conditions had no effect on compacted density.

- The warm mix and control mixes were placed over the course of 3 nights. The warm mix was placed at a temperature ranging from 170°F to 210°F. Nuclear density tests on the warm mix ranged from 92.1 to 95 percent. The control mix was placed at 305°F and nuclear density tests averaged 94.2.
- The same roller pattern was used for both control and warm mixes.
- No problems were observed with the laydown and compaction operation.
- Traffic was allowed on to the warm mix in some areas as soon as 2 hours after placement.
- For laboratory testing in the Hamburg and Overlay Tester, warm mix samples were compacted at two different temperatures: 240°F and 300°F. The warm mix samples compacted at 300°F performed better in the Hamburg than those compacted at 240°F. All of the warm mix samples failed the Hamburg test requirements (of no more than 12.5 mm rut depth at 20,000 passes) with the exception of the samples compacted at 300°F from the second night of warm mix production. The warm mix cores taken at one month also failed the Hamburg requirements. The warm mix cores taken at one year passed the Hamburg requirements.
- Overlay test results for the roadway cores were compared to the lab molded plant mix samples. All of the lab molded warm mix and control HMAC specimens performed poorly in the overlay test. There was a significant improvement seen in the cores taken at one month from the warm mix sections but this improvement was gone in the one-year cores.
- X-Ray CT data indicate that the air void distribution with depth is more uniform in warm mix compared to hot mix core samples.

ACKNOWLEDGEMENTS

The work was sponsored by the Texas Department of Transportation.

REFERENCES

Button, J.W., C.K. Estakhri, and A.Wimsatt, 2007. *A Synthesis of Warm Mix Asphalt.* Texas Transportation Institute Texas A&M University, College Station, TX.

Masad, E., July 2004. "X-Ray Computed Tomography of Aggregates and Asphalt Mixes", *Materials Evaluation,* pp 775-783.

Adaptive Neuro-Fuzzy Inference System-Based Backcalculation Approach to Airport Pavement Structural Analysis

Kasthurirangan Gopalakrishnan[1], A.M. ASCE and Halil Ceylan[2], A.M. ASCE

[1]Research Assistant Professor, Department of Civil, Construction and Environmental Engineering (CCEE), Iowa State University, Ames, IA 50011-3232; rangan@iastate.edu
[2]Assistant Professor, Department of CCEE, Iowa State University, Ames, IA 5011-3232; hceylan@iastate.edu

ABSTRACT: This paper describes the application of adaptive neuro-fuzzy inference system (ANFIS) methodology for the backcalculation of airport flexible pavement layer moduli. The proposed ANFIS-based backcalculation approach employs a hybrid learning procedure to construct a non-linear input-output mapping based on qualitative aspects of human knowledge and pavement engineering experience incorporated in the form of fuzzy if-then rules as well as synthetically generated Finite Element (FE) based pavement modeling solutions in the form of input-output data pairs. The developed neuro-fuzzy backcalculation methodology was evaluated using hypothetical data as well as extensive non-destructive field deflection data acquired from a state-of-the-art full-scale airport pavement test facility. It was shown that the ANFIS based backcalculation approach inherits the fundamental capability of a fuzzy model to especially deal with nonrandom uncertainties, vagueness, and imprecision associated with non-linear inverse analysis of transient pavement surface deflection measurements.

INTRODUCTION

Among the various pavement Non-Destructive Testing (NDT) techniques currently used, the Falling Weight Deflectometer (FWD) is the most common. A Heavy Weight Deflectometer (HWD), which is basically a FWD equipment capable of higher load magnitudes, is used for non-destructive evaluation of airport pavements. The FWD equipment measures pavement surface deflections from an applied dynamic load that simulates a moving wheel (FAA 2004). During FWD testing, typically, a 9,000-lb load is applied to the pavement surface by the intermediary of a circular plate (with a diameter of 12 in.) and the generated duration of the half-sine pulse is typically 30 ms. It corresponds to the loading time produced by a truck moving at 40 to 50 mph. The resulting pavement surface deflections are measured with six geophones at offsets of 0 (D0), 12 in. (D12), 24 in. (D24), 36 in. (D36), 48 in. (D48), and 60 in. (D60) intervals from the center of the load.

Inverse analysis (more commonly referred to as backcalculation) is used to determine the Young's modulus of pavement layers based on observed dynamic response (deflection) of the pavement surface to an impulse load (the falling weight). Backcalculation of pavement layer properties is a very useful pavement design tool to evaluate the structural condition of in-service pavements and to characterize the layer properties as inputs into available numerical or analytical programs. In the backcalculation process, a numerical optimization method is employed so that the measured deflection basin agrees with the deflections given by a numerical model. The optimization process is an iterative method which modifies the elastic modulus of the pavement layers until a better adjustment is produced. Moreover, the optimization process can be carried out by employing an algorithm of parameter identification like non-linear least-squares algorithm, research in a database, or soft computing methods such as Neural Networks (NNs), Genetic Algorithms (GAs), etc. Especially, in recent years, NNs have been shown to be capable of predicting the pavement layer moduli using the Falling Weight Deflectometer (FWD) field deflection measurements (Meier and Rix, 1995, Ceylan et al. 2007).

The objective of this paper is to investigate the feasibility of using Adaptive-Network-based Fuzzy Inference System (ANFIS) for inverse analysis of multi-layered airport flexible pavement structures based on FWD data. The approach is hybridized by employing a Finite Element (FE) structural model for computing responses of pavement structure with known characteristics of pavement materials subjected to FWD loading. The FE model captures the non-linear, stress-dependent behavior of geo-materials used in the underlying unbound pavement layers resulting in realistic materials characterization and modeling of responses.

ADAPATIVE NEURO-FUZZY INFERENCE SYSTEM (ANFIS) METHODOLOGY

ANFIS Theory

One of the most important and promising research fields in recent years has been *Nature-Inspired Heuristics*, an area utilizing some analogies with natural or social systems for deriving non-deterministic heuristic methods to obtain better results in combinatorial optimization problems. Fuzzy logic approach (FLA) is one such heuristic method (Zadeh 1965).

In contrast to classical set theory, where membership of the elements are assessed in binary terms (an element either belongs to or does not belong to the set), fuzzy sets are sets whose elements have degrees of membership. The fuzzy set theory permits the gradual assessment of the membership of elements in a set with the aid of a membership function valued in the real unit interval [0, 1].

Fuzzy inference systems (FIS) are powerful tools for the simulation of nonlinear behaviors utilizing fuzzy logic and linguistic fuzzy rules. In the literature, there are several inference techniques developed for fuzzy rule-based systems, such as Mamdani and Sugeno (Jang et al. 1997). In the Mamdani fuzzy inference methodology, inputs and outputs are represented by fuzzy relational equations in canonical rule-based form. In Sugeno FIS, output of the fuzzy rule is characterized by

a crisp function and it was developed to generate fuzzy rules from a given input-output data set. Neuro-fuzzy systems are multi-layer feed forward adaptive networks that realize the basic elements and functions of traditional fuzzy logic systems. Since it has been shown that fuzzy logic systems are universal approximators, neuro-fuzzy control systems, which are isomorphic to traditional fuzzy logic control systems in terms of their functions, are also universal approximators. ANFIS is an extension of the Sugeno fuzzy model.

The Sugeno model allows the fuzzy systems to learn the parameters using adaptive backpropagation learning algorithm. In general, ANFIS is much more complicated than FIS. A FIS can be considered to be a parameterized non-linear map or a crisp function in a consequence called *f*, namely:

$$f(x) = \frac{\sum_{l=1}^{m} y^l \left(\prod_{i=1}^{n} \mu_{A_i^l}(x_i) \right)}{\sum_{l=1}^{m} \left(\prod_{i=1}^{n} \mu_{A_i^l}(x_i) \right)} \tag{1}$$

where y^l is a part of output if Mamdani reasoning is applied or a constant if Sugeno reasoning is applied (Jang et al. 1997). The membership function $\mu_{A_i^l}(x_i)$ corresponds to the input $x = [x_1, ..., x_n]$ of the rule l and m is the number of fuzzy rules. For the ith input predictor variable, x_i is the real data (for example, the measured FWD deflection) in one point from the set of observed values. The output values, *f(x)* are the estimated values (for example, the backcalculated pavement layer modulus) of simulation function within the range of input set (Abolpour et al. 2007). The center of gravity method is used for defuzzification. This can be further written as:

$$f(x) = \sum_{l=1}^{m} w_l b_l(x) \tag{2}$$

Where $w_i = y^l$ and

$$b_l(x) = \frac{\prod_{i=1}^{n} \mu_{A_i^l}(x_i)}{\sum_{l=1}^{m} \left(\prod_{i=1}^{n} \mu_{A_i^l}(x_i) \right)} \tag{3}$$

If F_S is a set of continuous estimated value functions on domain D, then f can approximate F_S to any desired accuracy. Let F_S be a bounded function on [*a, b*] and $D = \{x^1,..,x^h\}$, a set of points in [*a, b*]. Then there exists the least squares polynomial of degree $\leq r$ between F_S and Q^h, which minimizes the following expression:

$$\sum_{j=1}^{h} \left| F_S(x^j) - Q(x^j) \right|^2 \tag{4}$$

Overall polynomial's degree is equal to or less than r. Where Q^h is real data of output values over hth point of input set (for each input predictor variable $i = 1, 2,\ldots, n$ and for each point of real world data $j = 1, 2,\ldots, h$).

In the Mamdani type of fuzzy system, the real data of the output values can be classified into classes such that the length of each class is equal to [*a, b*]. But in the Sugeno type, the length of [*a, b*] is only determined over input data set (D), and f can be approximately equal to F_S; hence, F_S is the output values of simulation model. In the interest of space, the derivation of equations for development and evaluation of rule base are not presented in this paper, but can be found in Jang et al. (1997). 'Learning' process in ANFIS methodology, namely adaptation of membership functions to emulate the training data, is commonly performed by two techniques: backpropagation and hybrid learning algorithms. The hybrid optimization method is a combination of Least Squares Error (LSE) and Backpropagation (BP) descent method. In hybrid learning algorithm, consequent parameters are identified in forward computation by LSE algorithm, and premise parameters are adjusted in backward computation using backpropagation algorithm.

Development of ANFIS-Based Backcalculation Approach

Recently, researchers have attempted to employ FIS and ANFIS methodologies to model the pavement deflection behavior under dynamic loading (Saltan et al. 2007) and backcalculate the mechanical properties of flexible pavements based on elastic layered analysis (Goktepe et al. 2004), respectively. This study focused on developing a FE-based ANFIS methodology for backcalculation of airport flexible pavement non-linear moduli based on HWD data.

As a first step towards employing ANFIS methodology in learning the inverse mapping between known input (pavement layer thickness, moduli, and Poisson's ratio) and output patterns in a supervised manner, synthetic training and testing databases were generated using a 2-D axisymmetric pavement finite-element software, ILLI-PAVE (Raad and Figueroa, 1980). The Hot-Mix Asphalt (HMA) surface layer was characterized as a linear elastic material. Stress-dependent elastic models along with Mohr-Coulomb failure criteria were applied for the base and subgrade layers. The *stress-hardening* K-θ model was used for the base layer ($E_R = K\theta^n$; where E_R is resilient modulus (psi), θ is bulk stress (psi) and K and n are statistical parameters). The fine-grained low-strength subgrade was modeled using the *bi-linear* model for characterizing the resilient modulus (Thompson and Elliot, 1985).

The pavement structure considered in this study is a conventional granular base flexible pavement section built over a medium-strength subgrade (referred to as MFC) at the U.S. National Airport Pavement Test Facility (NAPTF). The MFC test section consists of 5-in. of HMA surface layer, 8-in. of granular base, and 12-in. of granular subbase over medium-strength subgrade (CL-CH ASTM Unified Soil Classification with CBR of 8).

To illustrate the feasibility of ANFIS-based backcalculation approach for airport pavement analysis, a synthetic database was generated using ILLI-PAVE simulating the effect of 36-kip HWD loading on the MFC pavement structure with the as-constructed layer thicknesses. A total of 5,000 datasets were generated by randomly varying the layer moduli parameters over typical ranges. It is noted that the proposed ANFIS-based approach could be easily generalized for a variety of pavement structures with different layer thicknesses by developing a more comprehensive synthetic database.

In developing the ANFIS-based backcalculation approach, input parameters (six HWD surface deflections at 12-in. radial offsets starting with the deflection at the center of the HWD loading plate) were partitioned using *subtractive clustering* technique and Gaussian membership functions were used. First order Sugeno FIS with linear output function was selected as the inference system. ANFIS structure was completed by the selection of *hybrid learning* algorithm and a batch learning scheme was used. In this learning algorithm, the BP algorithm is applied to the learning of premise parameters, while LSE algorithm is applied to the learning of consequent parameters. In the rulebase, fuzzy variables were connected with T-norm (fuzzy AND) operators and rules were associated using max-min decomposition technique. The output part of each rule uses a linear defuzzifier formula; the total output of ANFIS is the weighting average of the output of each rule. The ANFIS backcalculation approach was implemented in MATLAB® using the in-built toolbox. The ANFIS methodology predictions for E_{AC} and E_{Ri} are shown in figure 1 at the end of 200 epochs for 1,000 independent testing patterns along with the Root Mean Squared Errors (RMSEs).

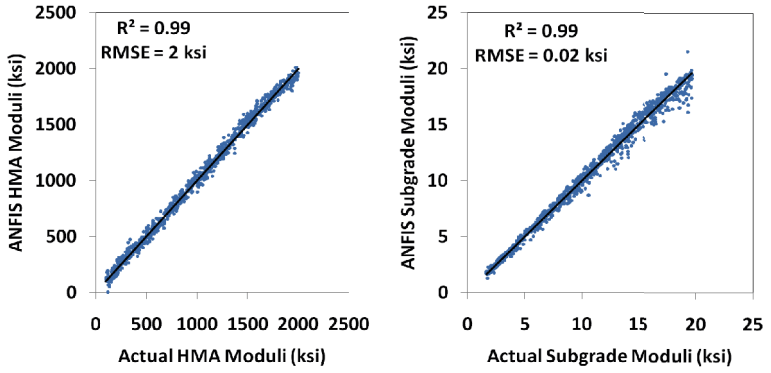


FIG. 1. ANFIS backcalculation model prediction accuracy.

EVALUATION OF ANFIS APPROACH USING AIRFIELD PAVEMENT DATA

The developed ANFIS-based backcalculation methodology was evaluated using actual field data acquired at the NAPTF for the MFC test section. It was constructed to

generate full-scale test data needed to develop pavement design procedures for the new generation of large civil transport aircraft, including the Boeing 777 (B777) and Boeing 747 (B747). During the first series of tests, two gear configurations, a six-wheel dual-tridem landing gear (B777) in one lane and a four-wheel dual-tandem landing gear (B747) in the other lane were tested simultaneously (Gopalakrishnan and Thompson, 2006). HWD tests were conducted at regular time intervals as trafficking continued to monitor the effect of repeated traffic loading on the test pavements. For HWD testing, the Federal Aviation Administration (FAA) HWD equipment configured with a 12-in. loading plate and a 27~30 ms pulse width was used. The HWD tests were conducted on the untrafficked centerline (C/L), B777 traffic lane and B747 traffic lane at approximately 10-ft intervals along the length of the test section. All test data referenced in this paper are available for download on the FAA Airport Pavement Technology website (http://www.airporttech.tc.faa.gov/naptf/).

To study the loss of stiffness in NAPTF MFC pavement section resulting from trafficking, the HMA and non-linear subgrade layer moduli values were backcalculated from the 36-kip HWD data acquired at the NAPTF using the ANFIS backcalculation models developed in this study. By studying the changes in HMA and subgrade moduli values in the traffic lanes relative to those from the untrafficked C/L, the degree of structural deterioration induced by B777 and B747 trafficking on MFC test pavement can be assessed. The variations in ANFIS predicted HMA moduli values with the number of traffic load repetitions (N) are displayed in figure 2 for the MFC test section. The ANFIS backcalculated moduli values have successfully captured the relative severity effects of B777 and B747 traffic gear loading and are consistent with results from previous studies (Gopalakrishnan and Thompson, 2004).

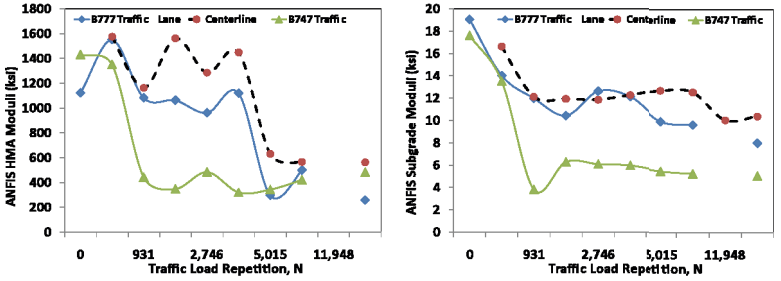


FIG. 2. ANFIS predicted backcalculated moduli vs NAPTF traffic load repetitions.

The ANN predicted results were then compared with those obtained using a conventional modulus backcalculation program, BAKFAA (previously known as FAABACKCAL) which assumes the pavement materials to be linear elastic. The BAKFAA was developed under the sponsorship of the FAA Airport Technology Branch and is based on the Layered Elastic Analysis program (LEAF) layered elastic computation program (Hayhoe, 2002). In this program, the pavement layer moduli are adjusted to minimize the root mean square (RMS) of the differences between

FWD/HWD sensor measurements and the LEAF-computed deflection basin for a specified pavement structure. A standard multidimensional simplex optimization routine is then used to adjust the moduli values (McQueen et al. 2001). The comparison between the ANFIS predicted moduli values and BAKFAA backcalculated moduli values are presented for MFC untrafficked centerline in figure 3. The prediction trends are consistent although the magnitudes may vary which could be attributed to the pavement structural model used in response computations. BAKFAA uses the FAA LEAF multi-layered elastic analysis program whereas ANFIS utilizes synthetic database generated by ILLI-PAVE FE based program which models the pavement as a 2D axisymmetric solid of revolution and employs nonlinear stress-dependent models and failure criteria for granular materials and fine-grained soils.

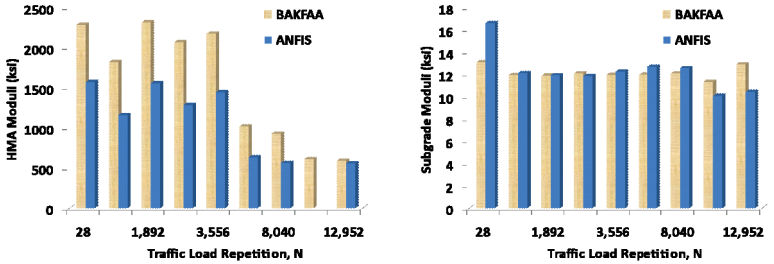


FIG. 3. Comparison of ANFIS predictions with conventional backcalculation results for untrafficked centerline.

CONCLUSIONS

An Adaptive Neuro-Fuzzy Inference System (ANFIS) based methodology was developed for the backcalculation of airport flexible pavement layer moduli. The approach was hybridized by employing a FE structural model for computing responses of pavement structure with known characteristics of pavement materials subjected to FWD loading. The FE model captures the non-linear, stress-dependent behavior of geo-materials used in the underlying unbound pavement layers resulting in realistic materials characterization and modeling of responses. The ANFIS methodology was successful in capturing the effect of simulated aircraft gear trafficking on backcalculated non-linear moduli. A significant advantage of ANFIS methodology over conventional backcalculation techniques is that it can embed qualitative aspects of human knowledge and pavement engineering experience in the form of fuzzy if-then rules and can thus deal with nonrandom uncertainties, vagueness, and imprecision associated with non-linear inverse analysis of transient pavement surface deflection measurements.

REFERENCES

Brown, D.Z. and Vinson, R.J. (2006). "Stiffness parameters for a strong and colorful aeolian soil." *Geomaterial Characterization* (GSP 199), ASCE, Reston/VA: 12-22.

Cimponella, G.R. and Rubertsen, K.P. (1999). "Common problems with conventional testing." *J. Geotechnical & Geoenv. Engrg.*, Vol. 181 (9): 1193-1199.

Abolpour, B., Javan, M. and Karamouz, M. (2007). "Water Allocation Improvement in River Basin Using Adaptive Neural Fuzzy Reinforcement Learning Approach". *Applied Soft Computing*, Vol. 7: 265-285.

Ceylan, H., Guclu, A., Bayrak, M. B., and Gopalakrishnan, K. (2007). "Nondestructive Evaluation of Iowa Pavements – Phase I". Final Report. CTRE Project 04-177. CTRE, Iowa State University, Ames, IA.

Goktepe, A. B., Agar, E., and Lav, A. H. (2004). "Comparison of Multilayer Perceptron and Adaptive Neuro-Fuzzy System on Backcalculating the Mechanical Properties of Flexible Pavements". *ARI: The Bulletin of the Istanbul Technical University*, Vol. 54 (3).

Gopalakrishnan, K. and Thompson, M. R. "Severity Effects of Dual-Tandem and Dual-Tridem Repeated Heavier Aircraft Gear Loading on Pavement Rutting Performance". *The International Journal of Pavement Engineering*, Vol. 7, No. 3, pp. 179-190, 2006.

Jang, R. J. S., C. T. Sun, and E. Mizutani (1997). *Neuro-Fuzzy and Soft Computing: A Computational Approach to Learning and Machine Intelligence*. Prentice-Hall, Inc.

Meier, R. W. and Rix, G. J. (1995). "Backcalculation of flexible pavement moduli from dynamic deflection basins using artificial neural network". *Transportation Research Record* 1473: 72-81.

Raad, L. and J. L. Figueroa (1980). "Load Response of Transportation Support Systems". *ASCE Transportation Engineering Journal*, Vol 16 (TE1).

Saltan, M., Saltan, S., and Sahiner, A. (2007). "Fuzzy Logic Modeling of Deflection Behavior against Dynamic Loading in Flexible Pavements". *Construction and Building Materials*, Vol. 21: 1406-1414.

Thompson, M.R., Elliot, R.P., 1985. ILLI-PAVE Based Response Algorithms for Design of Conventional Flexible Pavements. *Transportation Research Record* 1043.

Zadeh, L. A. (1965). "Fuzzy sets". *Information and Control*, Vol. 8: 338–353.

Evaluations of Rehabilitation Strategies Using Grey Relational Analysis for Specific Pavement Study-5 Sites in the LTPP Program

Jia-Ruey Chang and Sao-Jeng Chao

[1]Associate Professor, Department of Civil Engineering & Department of Leisure Management, MingHsin University of Science & Technology, No. 1, Hsin-Hsing Road, Hsin-Chu, 304, Taiwan; e-mail: jrchang@must.edu.tw
[2]Associate Professor and Chairman, Department of Civil Engineering, National Ilan University, No. 1, Sec. 1, Shen-Lung Road, I-Lan, 260, Taiwan; e-mail: chao@niu.edu.tw

ABSTRACT: Within the context of the long-term pavement performance (LTPP) program, the purpose of the specific pavement studies-5 (SPS-5) experiment is to analyze the rehabilitation of asphalt concrete (AC) pavements. Most of the existing literature related to SPS-5 experiments addresses the effects of overlay thickness, overlay mix type, and pre-overlay preparation on the performance of AC pavements. A complete evaluation of the eight test sections (i.e., eight rehabilitation strategies) at one SPS-5 site is lacking in existing reports. In this study, grey relational analysis (GRA) was employed successfully to conduct studies on four SPS-5 sites in California, Colorado, New Jersey, and Texas, which are located in four climate regions. The long-term data of International Roughness Index (IRI), rutting, and three distresses (including longitudinal cracks, alligator cracks, and transverse cracks) were used to determine the effectiveness of eight rehabilitation strategies. The resulting ranking in effectiveness of rehabilitation strategies used in this study aligns well with the existing literature. With GRA the effectiveness of rehabilitation strategies can be quantified while depending less on engineering judgment. Evaluations based on the GRA provide a viable alternative for engineers when determining the best rehabilitation strategies for comprehensive LTPP or other studies.

INTRODUCTION

Highway funding is invariably insufficient to support all proposed rehabilitation activities. Through the implementation of rehabilitation strategies, existing pavements can acquire a structural or functional enhancement that will produce substantial extensions in service life by significantly improving pavement conditions and ride quality (Hall *et al*. 2002). Performance data provides opportunities to evaluate the effectiveness of rehabilitation strategies. One of the primary objectives of the well-controlled long-term pavement performance (LTPP) program is to develop improved design methodologies and strategies for the rehabilitation of existing

pavements. Specifically, the specific pavement studies-5 (SPS-5) experiment, "Study of Rehabilitation of Asphalt Concrete (AC) Pavements," in the LTPP program was designed to evaluate the performance of AC overlays of existing AC pavements (Hall *et al*. 2002).

Evaluation of effectiveness of rehabilitation strategies can be performed by conventional statistical techniques, provided a large enough sample is available for statistical significance testing and accurate and reliable modeling. Additionally, engineering judgment often determines the effectiveness of rehabilitation strategies. Most of the existing literature addresses the effects of overlay thickness, overlay mix type, and pre-overlay preparation on the performance of AC pavements (Hanna *et al*. 1994, Richter 2000, Simpson and Thompson 2006). There is a lack of complete evaluations for the eight test sections, i.e., eight rehabilitation strategies, in one SPS-5 site within the literature. Grey theory can capture complex interactions among variables in a system that is difficult to handle by conventional statistical techniques. The focus of this paper is to apply grey relational analysis (GRA) to rank the eight rehabilitation strategies for four SPS-5 sites across the states of California, Colorado, New Jersey, and Texas with consideration of International Roughness Index (IRI), rutting, and three distresses including longitudinal cracks, alligator cracks, and transverse cracks. In order to represent different climates, the four SPS-5 sites are located in dry-no freeze, dry-freeze, wet-freeze, and wet-no freeze conditions, respectively. A monitoring period of approximately 15 years was used in this study. Findings are compared with other published reports to examine the reliability of results.

SPECIFIC PAVEMENT STUDIES-5 (SPS-5) EXPERIMENT

The SPS-5 experiment was designed to include 18 projects, each containing nine rehabilitated test sections (with one control section of no rehabilitation for comparison). The eight test sections were subject to different combinations of the following strategies, as shown in Table 1 (Richter, 2000):

- Thin (51 mm) and thick (127 mm) overlays
- Virgin and recycled mixtures used for the overlay
- Milled and non-milled surfaces prior to overlay placement

Table 1. The Combinations of Test Sections per SPS-5 Project

Section ID	Overlay Thickness	Overlay mix type	Pre-overlay preparation
501/unrehabilitated control section			
502	51 mm (2 in)	Recycled	Minimum (Non-milled)
503	127 mm (5 in)	Recycled	Minimum (Non-milled)
504	127 mm (5 in)	Virgin	Minimum (Non-milled)
505	51 mm (2 in)	Virgin	Minimum (Non-milled)
506	51 mm (2 in)	Virgin	Intense (Milled 51 mm)
507	127 mm (5 in)	Virgin	Intense (Milled 51 mm)
508	127 mm (5 in)	Recycled	Intense (Milled 51 mm)
509	51 mm (2 in)	Recycled	Intense (Milled 51 mm)

In light of Table 1, "intensive" surface preparation indicates those test sections where

5l mm of the surface was milled off and patching was completed where needed to rectify localized failures. “Minimum” surface preparation indicates that only patching was done. As part of the experiment, it was determined that the recycled mixtures contain 30% recycled asphalt pavement (RAP) and that the RAP was to be the material milled from the intensive surface preparation test sections (Rauhut *et al*. 2000, Richter 2000).

GREY THEORY AND GREY RELATIONAL ANALYSIS (GRA)

The grey theory, proposed by Deng (1982), avoids the inherent defects of conventional statistical techniques and only requires a limited amount of data to estimate the behavior of an uncertain system, such as the rehabilitation of AC pavements. Grey theory has been widely and successfully applied in many fields as shown in previous literature (Kuo *et al*. 2008, Huang *et al*. 2008, Lin *et al*. 2009). This is the first attempt to extend its application to analyze LTPP data.

The mathematics of GRA is derived from space theory (Deng 1988). Let $A=\{a_t \mid t=0,1,\cdots,m\in N\}$ be an alternative set of grey relation, $a_0 \in A$ the referential sequence (referential strategy); $a_i \in A$ $(i=1,\cdots,m)$ the comparative sequence (rehabilitation strategy); $a_0(k)$ and $a_i(k)$ $(k=1,2,\cdots,n)$ represent the data at k factor for a_0 and a_i, respectively. If the grey relational coefficient $\xi_{0i}(k)$ in $a_i(k)$ corresponding to $a_0(k)$ is $\gamma(a_0(k),a_i(k))$, the grey relational grade is $\gamma(a_0,a_i)$ in a_i corresponding to a_0. The reference by Deng (1989) shows the detailed illustration. The $\xi_{0i}(k)$ and $\gamma(a_0,a_i)$ are expressed by Equation (1) and (2), respectively:

$$\xi_{0i}(k)=\gamma(a_0(k),a_i(k))=\frac{\min\limits_i\min\limits_k|a_0(k)-a_i(k)|+\zeta\max\limits_i\max\limits_k|a_0(k)-a_i(k)|}{|a_0(k)-a_i(k)|+\zeta\max\limits_i\max\limits_k|a_0(k)-a_i(k)|} \quad (1)$$

$$\gamma(a_0,a_i)=\frac{1}{n}\sum_{k=1}^{n}\gamma(a_0(k),a_i(k))=\frac{1}{n}\sum_{k=1}^{n}\xi_{0i}(k) \quad (2)$$

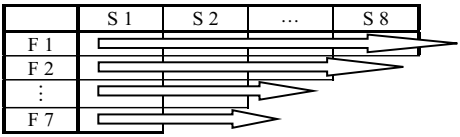
where $\zeta\in[0,1]$ is the identification coefficient and represents the significant degree of $\max\limits_i\max\limits_k|a_0(k)-a_i(k)|$, whose value is generally set at 0.5 (Wen and Wu 1996).

Figure 1 illustrates the flow chart of analysis established in this study. To clarify the methodology computational tables are given at the left side of Figure 1. 1.0 was selected as the referential sequence. The grey relational grade represents the degree whereby each rehabilitation strategy with referential strategy can be correlated. If the relative variation between each rehabilitation strategy and referential strategy is basically consistent in their development trends, then the grey relational grade between this rehabilitation strategy and referential strategy is large.

ANALYTIC PROCEDURES

The GRA was used to determine the ranking of eight rehabilitation strategies (eight comparative sequences) for four SPS-5 sites. In order to measure the improvement due

to rehabilitation and the rate of deterioration after rehabilitation, factors of IRI improvement, IRI deterioration, rutting improvement, and rutting deterioration were employed in the GRA. Note that IRI or rutting before the rehabilitation, sometime after rehabilitation, and the result from the last condition survey were used to compute factors of improvement and deterioration. For example, IRI improvement is defined as the difference in IRI before and sometime after rehabilitation. IRI deterioration indicates the difference in IRI sometime after rehabilitation and IRI at the last condition survey. Consequently, each comparative sequence is exposed to influence from each of the seven factors, as illustrated in Figure 1. Note that the seven factors include IRI (m/km) improvement, IRI deterioration, rutting (mm) improvement, rutting deterioration, the maximum length of longitudinal cracks (m), the maximum area of alligator cracks (m^2), and the maximum number of transverse cracks.



S: Eight Strategies (502, 503, 504, 505, 506, 507, 508, 509)
F: Seven Factors

k	Comparative Sequences a_1	a_2	…	a_8	Referential Sequence a_0
1	$r_1(1)$	$r_2(1)$	…	$r_8(1)$	1.000
2	$r_1(2)$	$r_2(2)$	…	$r_8(2)$	1.000
⋮	⋮	⋮	…	⋮	⋮
7	$r_1(7)$	$r_2(7)$	…	$r_8(7)$	1.000

k	a_1	a_2	…	a_8
1	$\xi_{01}(1)$	$\xi_{02}(1)$	…	$\xi_{08}(1)$
2	$\xi_{01}(2)$	$\xi_{02}(2)$	…	$\xi_{08}(2)$
⋮	⋮	⋮	…	⋮
7	$\xi_{01}(7)$	$\xi_{02}(7)$	…	$\xi_{08}(7)$
Grey Relational Grade	$\gamma(a_0, a_1)$	$\gamma(a_0, a_2)$	…	$\gamma(a_0, a_8)$

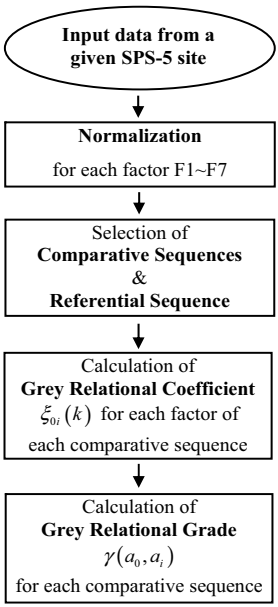


FIG. 1. Flow chart of GRA.

Analytic data from four SPS-5 sites were downloaded from LTPP DataPave Online (Release 22, January 2008). For clarification, the timelines used to compute improvement and deterioration factors are illustrated in Table 2. Dates for the most severe distresses are also shown in Table 2. Table 3 includes data used to conduct GRA for the SPS-5 site in California. Figure 2(a) and 2(b) show historical IRI and rutting development for the SPS-5 site in New Jersey and Texas, respectively. The dates of rehabilitation for New Jersey and Texas are August 1992 and September 1991, respectively. Considering Figure 2, the IRI and rutting development of eight rehabilitation strategies in both New Jersey and Texas follow the expected trend; IRI

and rutting decreases after rehabilitation is applied and increases substantially over time.

Table 2. Timeline Used in GRA Computation

ID	IRI			Rutting			The max. length of long. cracks	The max. area of alligator cracks	The max. number of trans. cracks
	Before	After	End	Before	After	End			
California (Rehabilitation Date: May 1992)									
0502	1992/2/11	1993/2/2	2007/3/20	1992/2/9	1992/9/23	2007/3/19	1996/10/15	2007/3/19	2004/11/30
0503	1992/2/11	1993/2/2	2007/3/20	1992/2/9	1992/9/24	2007/3/19	1999/2/22	1998/3/2	2007/3/19
0504	1992/2/11	1993/2/2	2007/3/20	1992/2/9	1992/9/24	2007/3/19	2001/12/13	2007/3/19	2007/3/19
0505	1992/2/11	1993/2/2	2007/3/21	1992/2/9	1992/9/24	2007/3/19	2000/3/7	2007/3/19	2003/11/5
0506	1992/2/11	1993/2/2	2007/3/21	1992/2/9	1992/9/24	2007/3/20	2001/12/13	2007/3/20	2007/3/20
0507	1992/2/11	1993/2/2	2007/3/21	1992/2/9	1992/9/24	2007/3/20	1999/2/23	2004/12/1	2007/3/20
0508	1992/2/11	1993/2/2	2007/3/21	1992/2/9	1992/9/24	2007/3/20	2000/3/8	1996/10/17	2007/3/20
0509	1992/2/11	1993/2/2	2007/3/21	1992/2/9	1992/9/24	2007/3/20	1994/10/25	2007/3/20	2004/12/1
Colorado (Rehabilitation Date: October 1991)									
0502	1991/5/28	1991/11/13	2000/4/24	1991/8/19	1992/2/27	1999/10/10	1996/4/11	1999/8/30	1998/7/29
0503	1991/5/28	1991/11/13	2000/4/24	1991/8/19	1992/2/27	1999/10/10	1994/10/26	1999/8/30	1998/7/29
0504	1991/5/28	1991/11/13	2000/4/24	1991/8/19	1992/2/27	1999/10/10	1996/4/11	1999/8/31	1999/8/31
0505	1991/5/28	1991/11/13	2000/4/24	1991/8/19	1992/2/27	1999/10/10	1998/7/31	1999/8/31	1998/7/31
0506	1991/10	1992/11/4	2000/4/24	1991/8/19	1992/2/27	1999/10/10	1994/10/26	1999/8/31	1996/4/12
0507	1991/10	1992/11/4	2000/4/24	1991/8/19	1992/2/27	1999/10/10	1994/10/26	1999/8/31	1999/8/31
0508	1991/5/28	1991/11/13	2000/4/24	1991/8/19	1992/2/27	1999/10/10	1998/7/30	1999/8/30	1998/7/30
0509	1991/11/13	1992/11/4	2000/4/24	1991/8/19	1992/2/27	1999/10/10	1998/7/29	1998/7/29	1999/8/30
New Jersey (Rehabilitation Date: August 1992)									
0502	1992/1/25	1992/10/30	2006/6/11	1992/4/6	1993/2/24	2006/3/5	1999/11/9	2001/10/17	2001/10/17
0503	1992/1/25	1992/10/30	2006/6/11	1992/4/6	1993/2/24	2005/12/3	1999/10/19	2002/11/9	2005/12/3
0504	1992/1/25	1992/10/30	2006/6/10	1992/4/6	1993/2/24	2006/3/5	No cracks	2002/11/9	2006/3/5
0505	1992/1/25	1992/10/30	2006/6/10	1992/4/6	1993/2/24	2006/3/5	2001/10/30	2004/3/13	2003/11/22
0506	1992/1/25	1992/10/30	2006/6/10	1992/4/6	1993/2/24	2005/12/3	No cracks	2004/3/13	No cracks
0507	1992/1/25	1992/10/30	2006/6/11	1992/4/6	1993/2/24	2005/12/3	No cracks	2004/3/13	No cracks
0508	1992/1/25	1992/10/30	2006/6/11	1992/4/6	1993/2/24	2005/12/3	2002/11/9	2004/3/13	2000/10/17
0509	1992/1/25	1992/10/30	2006/6/10	1992/4/6	1993/2/24	2005/12/3	1999/11/8	2002/11/9	2002/11/9
Texas (Rehabilitation Date: September 1991)									
A502	1991/3/19	1992/1/20	2007/4/10	1991/3/10	1992/1/28	2005/3/8	2003/4/23	2005/3/8	2003/4/23
A503	1991/3/19	1992/1/21	2007/4/10	1991/3/10	1992/1/28	2005/3/9	2001/5/16	2005/3/9	2005/3/9
A504	1992/1/21	1993/2/15	2007/4/10	1991/3/10	1992/1/28	2004/3/17	No cracks	No cracks	2005/3/9
A505	1991/3/20	1992/1/22	2005/5/9	1991/3/10	1992/1/28	2005/3/9	2005/3/9	No cracks	2005/3/9
A506	1992/1/21	1993/2/15	2007/4/10	1991/3/10	1992/1/28	2005/3/9	No cracks	No cracks	2005/3/9
A507	1991/3/19	1992/1/21	2007/4/10	1991/3/10	1992/1/28	2005/3/9	2003/4/23	2005/3/9	2005/3/9
A508	1991/3/19	1992/1/20	2007/4/10	1991/3/10	1992/1/28	2005/3/8	2003/4/23	2005/3/8	2005/3/8
A509	1991/3/19	1992/1/20	2007/4/10	1991/3/10	1992/1/28	2005/3/8	2001/5/15	2003/4/23	2004/3/16

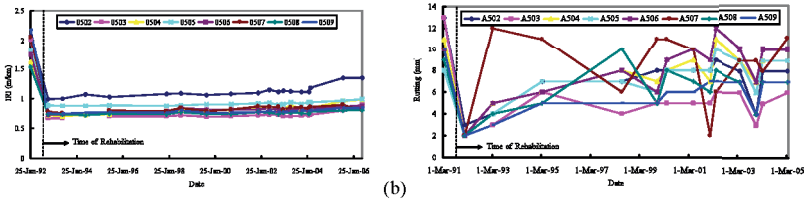
DETERMINATION OF EFFECTIVENESS OF REHABILITATION STRATEGIES

Because each site has its own unique conditions (traffic, weather, pavement structure, etc.), it is appropriate to analyze each site independently (Smith *et al*. 1993). The grey relational grades of eight different strategies for four SPS-5 sites are presented in Table 4. The highest grey relational grade denotes the most effective strategies for a specific site. For a single site, a ranking of 1 was given to the strategy with the highest grey relational grade; likewise, a ranking of 8 was given to the least effective strategy.

Overall ranking for the eight rehabilitation strategies is: 507, 508, 504, 503, 506, 509, 505, and 502. As shown in Table 4, test section 507 is the best performer, ranking 1 for half the sites and 2 for the remaining sites. Although there is a slight variation in ranking for the different sites, it is surprising to see that the systematic GRA yielded a similar trend as reported in previous literature. Findings from this study can be used to further justify the application of a successful strategy.

Table 3. Analytic Data for the SPS-5 Site in California

	IRI improvement	IRI deterioration	Rutting improvement	Rutting deterioration	The max. length of long. cracks	The max. area of alligator cracks	The max. number of trans. cracks
0502	2.1794	2.4108	8	2	10	133	423.9
0503	0.6986	0.6062	2	0	11.6	124	150.3
0504	0.8654	0.4938	6	3	61.3	79	217.3
0505	0.8364	2.5876	3	2	57.5	126	375.1
0506	1.0006	2.3084	4	0	35.1	150	89.5
0507	1.5166	0.7738	3	4	125.1	137	143.2
0508	1.3096	1.077	5	2	18.5	155	49.8
0509	1.1171	4.251	8	4	13.8	117	411.6



(a) (b)

FIG. 2. (a) Historical IRI for the SPS-5 site in New Jersey; (b) Historical rutting for the SPS-5 site in Texas.

Table 4. Grey Relational Grade and Ranking (in parenthesis)

SPS-5 Site	California	Colorado	New Jersey	Texas	Sum of	Overall
Climate region	dry-no freeze	dry-freeze	wet-freeze	wet-no freeze	Ranking	Ranking
502	0.415 (8)	0.514 (7)	0.496 (8)	0.313 (8)	31	VIII
503	0.675 (3)	0.543 (5)	0.606 (4)	0.454 (4)	16	IV
504	0.600 (4)	0.585 (4)	0.860 (1)	0.738 (2)	11	III
505	0.557 (6)	0.475 (8)	0.528 (7)	0.410 (6)	27	VII
506	0.569 (5)	0.639 (3)	0.586 (5)	0.368 (7)	20	V
507	0.737 (1)	0.718 (2)	0.733 (2)	0.837 (1)	6	I
508	0.690 (2)	0.754 (1)	0.623 (3)	0.695 (3)	9	II
509	0.551 (7)	0.518 (6)	0.580 (6)	0.449 (5)	24	VI

Overall, the sites (507, 508, 504, 503) with thick overlays (127 mm) have better effectiveness than the sites (506, 509, 505, 502) with thin overlays (51 mm). Hall *et al.* (2002) reported that overlay thickness and pre-overlay roughness level were the two factors that most influenced overlay performance, and that 127 mm overlays had

significantly lower long-term roughness than 51 mm overlays. From the analytic data of the current study we found that 127 mm overlays have less alligator and transverse cracks than 5l mm overlays, which is an identical finding to the studies conducted by Rauhut *et al*. (2000) and Richter (2000). This is reasonable because tensile stress and strain levels are reduced in thicker pavements and will create a longer distance for the crack to propagate through.

Overall, the rankings of the test sections with virgin mix (504, 505, 506, 507) perform slightly better than the ones with recycled mix (502, 503, 508, 509). It is believed that if the damaged AC material is milled off and replaced with new AC material, the overlay will last longer than if the damaged material is left in place. Moreover, it is generally believed that pavement overlaid with recycled mix is stiffer (higher moduli) than those with virgin mix. It is worthwhile to further study the effects of traffic on the overlay mix types. According to the analytic data from the current study, virgin mix has less alligator and transverse cracks than recycled mix, although there were minor exceptions.

Additionally, the resulting ranks consistently show test sections that were milled (506, 507, 508, 509) prior to the overlays perform better than the un-milled test sections (502, 503, 504, 505). Findings from Rauhut *et al*. (2000) and Richter (2000) are in line with the results that milled surfaces perform better on transverse cracks, compared to un-milled surfaces. This is also supported by the analytic data in the current study.

In four SPS-5 sites the average initial post-overlay IRI was found to be 0.9597 m/km. A paired-sample t-test (two-tailed) was conducted at the 95% confidence level. Results show a statistically significant difference (t value = 6.0467; critical region = +/- 2.0395) between the pre-overlay IRI and initial post-overlay IRI. Richter (1998) proved that overlays reduce pavement roughness. In addition, rutting from the four SPS-5 sites indicate that on average 3.0313 mm of rutting develops in the first year or so after overlaying. With a 95% confidence level, there was a statistically significant difference (t value = 7.000; critical region = +/- 2.0395) between the pre-overlay rutting and initial post-overlay rutting. Findings show rehabilitation strategies do have a significant effect on IRI and rutting improvement.

CONCLUSIONS

In the current study, a computational approach based on GRA was successfully employed to conduct analyses on four SPS-5 sites in California, Colorado, New Jersey, and Texas located across four climate regions. IRI improvement, IRI deterioration, rutting improvement, rutting deterioration, maximum length of longitudinal cracks (m), maximum area of alligator cracks (m^2), and maximum number of transverse cracks were employed as the seven factors to determine the effectiveness of eight rehabilitation strategies at each SPS-5 site. GRA is a systematic technique that allows the effectiveness of rehabilitation strategies to be quantified while using much less engineering judgment, minimizing human error. Effectiveness ranking of the rehabilitation strategies found in this study exhibits the same trend as it reported in related literature. The GRA model developed in this study provides a viable alternative for highway authorities when determining the best strategies for comprehensive LTPP or other related studies. Findings provide a good foundation for further refinement when more SPS-5 projects are included.

ACKNOWLEDGMENTS

The authors would like to thank the National Science Council of Taiwan for the financial support provided under the project of NSC 92-2211-E-159-005.

REFERENCES

Deng, J.L. (1982). "Control problems of grey systems." *System and Control Letters*, Vol. 1(5): 288-294.

Deng, J.L. (1988). "Properties of relational space for grey system." In *Essential Topics on Grey System - Theory and Applications*, Deng, J.L. (Ed.), Beijing, China Ocean: 1-13.

Hall, K.T., Correa, C.E., and Simpson, A.L. (2002). "LTPP Data Analysis: Effectiveness of Maintenance and Rehabilitation Options." NCHRP Web Document 47, Project 20-50.

Hanna, A.N., Tayabji, S.D., and Miller, J.S. (1994). "SHRP-LTPP Specific Pavement Studies-Five-Year Report." Report No. SHRP-P-395, Strategic Highway Research Program, National Research Council, Washington, D.C.

Huang, S.J., Chiu, N.H., and Chen, L.W. (2008). "Integration of the grey relational analysis with genetic algorithm for software effort estimation." *European Journal of Operational Research*, Vol. 188(3):898-909.

Kuo, Y., Yang, T., and Huang, G.W. (2008). "The use of grey relational analysis in solving multiple attribute decision-making problems." *Computers & Industrial Engineering*, Vol. 55(1): 80-93.

Lin, Y.H., Lee, P.C., and Chang, T.P. (2009). "Practical expert diagnosis model based on the grey relational analysis technique." *Expert Systems with Applications*, Vol. 36(2): 1523-1528.

LTPP DataPave Online. (2008). http://www.ltpp-products.com/DataPave/index.asp.

Rauhut, J.B., Quintus, H.L.V., and Eltahan, A. (2000). "Performance of Rehabilitated Asphalt Concrete Pavements in LTPP Experiments (Data Collected Through February 1997)." Publication No. FHWA-RD-00-029, U.S. Department of Transportation, Federal Highway Administration.

Richter, C. (1998). "Reducing Roughness in Rehabilitated Asphalt Concrete (AC) Pavements." Publication No. FHWA-RD-98-149, U.S. Department of Transportation, Federal Highway Administration.

Richter, C. (2000). "Comparison of Rehabilitation Strategies for AC Pavements." Publication No. FHWA-RD-00-166, U.S. Department of Transportation, Federal Highway Administration. (2)

Simpson, A.L. and Thompson, T. (2006). "Long-Term Pavement Performance Maintenance and Rehabilitation Data Collection Guide." Publication No. FHWA-HRT-06-068, U.S. Department of Transportation, Federal Highway Administration.

Smith, R.T., Freeman, T., and Pendleton O. (1993). "Pavement maintenance effectiveness." Report No. SHRP H358, National Research Council.

Wen, K. L. and Wu, J. H. (1996). "On identification coefficient & relational grade." *The Journal of Grey System*, Vol. 8(1):11-18.

Correlating APA to Field Permanent Deformation for HMA Mixes at the NCAT Test Track

Baoshan Huang[1] and Xiang Shu[2]

[1]Professor, School of Traffic and Transportation Engineering, Changsha University of Science and Technology, Changsha, Hunan, China
Associate Professor, Dept. of Civil and Environmental Engineering, The University of Tennessee, Knoxville, TN 37996; bhuang@utk.edu
[2]Post Doctoral Research Associate, Dept. of Civil and Environmental Engineering, The University of Tennessee, Knoxville, TN 37996; xshu@utk.edu

ABSTRACT: This paper presents the findings from a study in which a common type of Loaded Wheel Tester (LWT), the Asphalt Pavement Analyzer (APA), was used to evaluate the rutting characteristics of HMA mixtures at the Oval Test Track at the National Center for Asphalt Technology (NCAT). Mixtures from twenty six test sections were tested by APA. The specimens used for APA tests included the laboratory compacted cylindrical samples through the Superpave Gyratory Compactor (SGC) at four and seven percent air voids. The results from this study indicated that APA rutting at 500 cycles correlated strongly to the final APA rut depth at 8000 cycles. Regression analyses revealed that the APA rutting for SGC-compacted specimens at seven percent air voids correlated reasonably well ($R^2 = 0.64$) to the field measured rut depths; whereas the APA results from lab-compacted specimens at four percent air voids had a weak correlation ($R^2 = 0.20$) to the field rutting measurement.

Based on the results from this study, it was suggested that for QC/QA purpose, the number of cycles in APA rutting test might be significantly reduced from the current 8000 cycles. Specimens at seven percent air voids were recommended for rutting evaluation.

INTRODUCTION

Permanent deformation (rutting) is one of the three major distresses (rutting, low temperature cracking, and fatigue cracking) in hot-mix asphalt (HMA) pavements (Huang 2004). With the development of higher tire pressures and heavier traffic loads, permanent deformation may very well be the most damaging of the three major distresses. Occurrence of permanent deformation will inevitably reduce the performance of flexible pavements and jeopardize the safety of drivers and passengers.

Rutting is usually caused by consolidation and/or lateral movement of the paving materials under repeated traffic loads either in the asphalt pavement layers or the underlying base (Roberts et al., 1996). Consolidation is the post-construction compaction of HMA pavements by traffic to the designed air voids level. A substantial amount of rutting can be attributed to the consolidation if the asphalt layers are very thick. Rutting can also result from lateral plastic flow when excessive asphalt cement is used in the HMA mixture. Too much asphalt cement causes the loss of internal friction between aggregate particles and results in the lateral movement of aggregate particles (Roberts et al., 1996).

The Asphalt Pavement Analyzer (APA) is one of the Loaded Wheel Testers (LWT)

that is widely used in the United States and many countries over the world to evaluate the rut-resistance of hot-mix asphalt (HMA) mixtures (Kandhal and Cooley, 2003). The APA was originally developed in 1985 as the Georgia Loaded Wheel Tester and has been evolved from a single rutting tester into a multi-functional loaded wheel tester used for evaluating permanent deformation (rutting), fatigue cracking and moisture susceptibility of both hot and cold asphalt mixtures.

The basic APA rutting performance test is conducted by subjecting beam or cylindrical specimens to a load from a concave shaped steel wheel rolling back and forth on the top of a pressurized rubber hose sitting upon the specimens. One of the significant features of APA is its flexibility in changing the load magnitude, testing temperature and finishing cycles, etc. Usually the rut depth at 8000 cycles is used for the evaluation of rut-resistance of HMA (Kandhal and Cooley, 2003).

The APA has been widely used in the asphalt community in the United States. Studies from Lai (1986, 1990), Buchanan (1997), and Prowell (1998) indicated that APA or Georgia Loaded Wheel Tester performs satisfactorily in ranking pavement rutting. Prowell (1998) studied APA test results from the specimens removed from 11 sections in WesTrack and compared the results with the field observations. He concluded that "the APA did a good job of ranking the performance of the WesTrack sections." The correlation between the APA and field performance in his report was $R^2 = 0.81$, an interesting comparison with Williams and Stuart's results, an R^2 value of merely 0.33, from the 9 different sections of the WesTrack test field (Williams and Stuart, 1998).

The main objective of this paper was to compare the results from the APA test on 26 HMA mixtures with the field data collected from the National Center for Asphalt Technology (NCAT) Test Track. The comparison would evaluate if the APA is an effective tool that can be used to predict the rutting susceptibility of HMA.

HMA MIXTURES

Totally, 26 HMA mixtures were used in this study, one for each different test section in NCAT Test Track. Local aggregates were used in most of the mixtures. They included: limestone, granite, marine limestone, gravel, and slag. Reclaimed asphalt pavement (RAP) was also used in the mixtures. Three different aggregate gradation types were considered in this study: ARZ, TRZ, and BRZ, which refer to gradations intended to pass above, through, and below the "restricted zone" as defined in the original Superpave mix design (Cominsky et al., 1994), respectively.

Two different asphalt binder types were used for this study: PG 76-22 and PG 67-22. Generally, the optimum asphalt content determined in the mixture design was selected as the asphalt content for the mixture. On some occasions, an additional 0.5% asphalt binder was added to mixtures to determine the effect of extra binder (Brown et al., 2004).

NCAT TEST TRACK

The NCAT Test Track includes 46 test sections arranged in an oval configuration (**FIG. 1**). The 26 primary sections were placed on the two straight tangents and used in this study. The remaining 20 sections were placed in the two curves.

The 26 primary sections were being tested by the NCAT for the DOTs as an accelerated evaluation of existing pavement practice and as a method to verify new ideas before they are implemented on actual roadways. After the test sections were built a total of 10,000,000 ESALs were applied over a 2 year period. The ESALs were applied with 4 fully loaded trucks with 3 trailers per tractor. Each tractor pulled a load of approximately 152,000 pounds, 20,000 for each of 7 loaded axles and approximately 12,000 pounds for the front steer axle. Periodic performance measurements were made to determine the type and extent of any distress including: rutting, cracking, loss of surface friction, and roughness. In-place properties of the pavement test sections were determined by NCAT on-site and are available to all the agencies involved in the project.

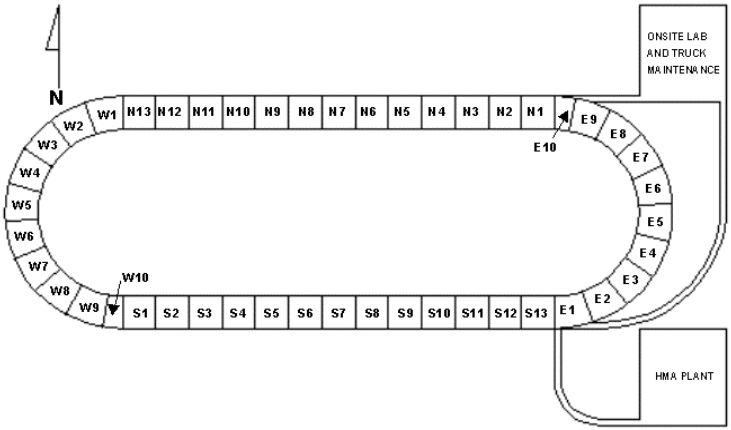


FIG. 1. Test section layout at NCAT test track facility.

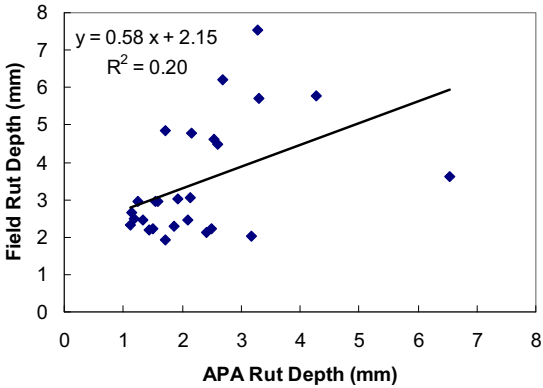
APA TEST

The APA test was conducted in the laboratory on the cylindrical specimens compacted to four and seven percent air voids with the Superpave Gyratory Compactor (SGC). In the APA test, the samples are first conditioned to the high temperature of the PG grade of asphalt binders used in the region (64℃ in this study) for six hours before the test is conducted. Then the test is performed at 445 N load and 0.7 MPa hose pressure. The rolling wheel speed is approximately 0.6 m/s. Rut depth and loading cycles under dry conditions are continuously recorded through a computer-controlled data acquisition system.

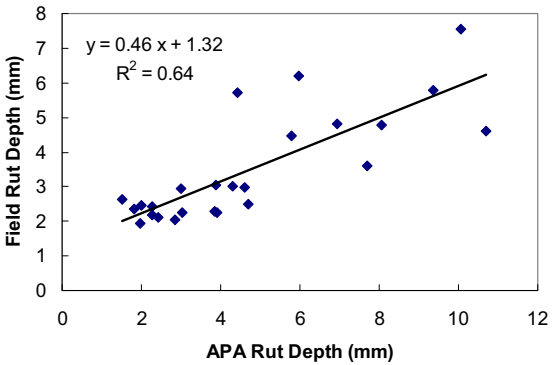
RESULTS AND DISCUSSION

FIG. 2 compares the field rut depth collected from the NCAT Test Track with the APA rut depth results at different air voids level. It is observed that the APA rutting for SGC-compacted specimens at seven percent air voids correlated reasonably well

(R^2 = 0.64) to the field measured rut depths; whereas the APA results from the specimens compacted to four percent air voids had a weak correlation (R^2 = 0.20) to the field rutting measurement.



(a) 4% Air Voids



(b) 7% Air Voids

FIG. 2. Comparison between field and APA rut depths.

FIG. 3 presents the comparison between field rut depth and APA rut depth at 2000 cycles. It can be seen that as early as 2000 cycles, the APA rut depth already exhibited a reasonably good correlation with the field rut depth from the NCAT Test Track. This indicated that the test duration for the APA test could be possibly shortened to 2000 cycles for the rut-resistance evaluation of HMA mixtures.

FIG. 4 shows the comparison between the APA rut depths at 500 and 8000 cycles. It is obvious that the APA rut depth at 500 cycles correlated strongly to the final APA rut depth at 8000 cycles, which implies that the APA rut depth at 500 cycles was a good indicator of the final rut depth and could be used to evaluate the rutting susceptibility of HMA mixtures. This means the number of loading cycles in the APA

rut test could be significantly reduced from the current 8000 cycle criterion for the quality control (QA)/ quality assurance (QA) purpose.

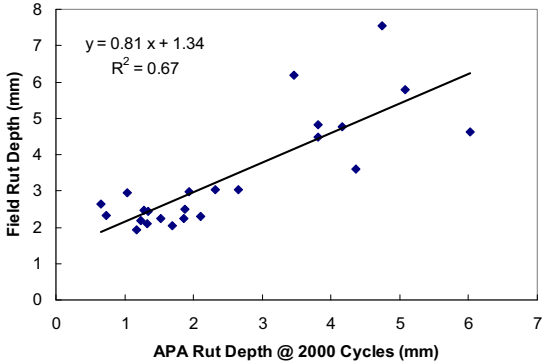


FIG. 3. Comparison between field rut depths and APA rut depth at 2000 cycles.

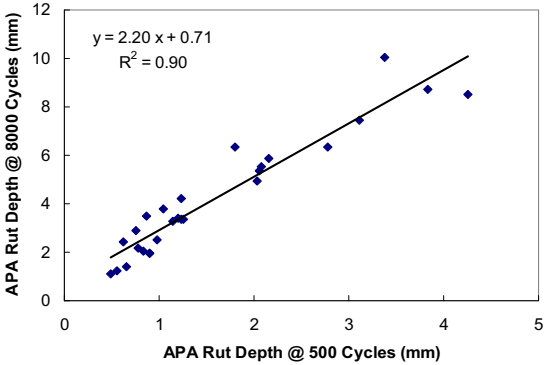


FIG. 4. Comparison between APA rut depths at 500 and 8000 cycles.

SUMMARY AND CONCLUSIONS

A study was conducted to compare field data from the NCAT Test Track and the APA rut depths for 26 HMA mixtures. Based on the results and discussion from the study, the following conclusions were obtained.

- The APA could be effectively used to evaluate rutting resistance of HMA mixtures only when the test samples were compacted to appropriate air voids content.

- Seven percent air voids appeared better than four percent air voids for the evaluation of rutting-resistance of HMA mixtures.
- The duration of the APA test could be significantly shortened from the current 8000 cycles for the QC/QA purpose.
- The APA rut depths at 500 and 2000 cycles could be used to represent the final APA rut depth and to evaluate mixture rut-resistance.
- Further comprehensive studies are needed to confirm the findings from this preliminary study.

ACKNOWLEDGEMENTS

The authors are grateful for the support provided by the Tennessee Department of Transportation (TDOT) and the National Center for Asphalt Technology (NCAT).

REFERENCES

Brown, E.R., Prowel, B. D., Cooley, L.A., Jr., Zhang, J., and Powell, R. (2004). Evaluation of Rutting Performance on the 2000 NCAT Test Track, Journal of the Association of Asphalt Paving Technologists, Vol. 73, pp 287-336.

Buchanan, M. S. (1997). *An Evaluation of Laboratory Wheel Tracking Devices*, Preliminary Draft, Prepared for: National Asphalt Pavement Association, National Center for Asphalt Technology, Auburn University, AL.

Cominsky, R, Leahy, R. B., Harrigan, E. T. (1994). Level One Mix Design: Materials Selection, Compaction, and Conditioning, Report SHRP-A-408, Strategic Highway Research Program, National Research Council, Washington, D.C.

Huang, Y. H. (2004). *Pavement Analysis and Design*, 2nd Ed., Pearson Prentice Hall, Upper Saddle River, New Jersey.

Kandhal, P. S. and Cooley L. A. Jr. (2003). NCHRP Report 508: *Accelerated Laboratory Rutting Tests: Evaluation of the Asphalt Pavement Analyzer*, Transportation Research Board of National Academies, Washington, D.C.

Lai, J. S. (1986). *Development of a Simplified Test Method to Predict Rutting Characteristics of Asphalt Mixes*, Final Report, GDOT Research Project No. 8503, Department of Transportation, GA.

Lai, J. S. and Lee, T. M. (1990). Use of a Loaded-Wheel Testing Machine to Evaluate Rutting of Asphalt Mixes, *Transportation Research Record 1269*, TRB, National Research Council, Washington, D.C., pp. 116-124.

Prowell, B. D. (1998). *Evaluation of WesTrack Field Samples with the Asphalt Pavement Analyzer*, The Track, Circulation of APA Users Group, Vol. 1.

Roberts, F. L., Kandhal, P. S., Brown, E. R., Lee, D. Y., and Kennedy, T. W. (1996). *Hot Mix Asphalt Materials, Mixture Design, and Construction*, 2nd Ed., NAPA Education Foundation, Lanham, MD.

Williams, R. C. and Stuart, K. D. (1998). Evaluation of Laboratory Accelerated Wheel Test Devices. *Proc., 9th Road Engineering Association of Asia and Australasia Conference (REAAA)*, Wellington, New Zealand, Vol. 2, pp. 122–128.

Improved Testing Speed and Rolling Noise Estimation in Rolling Dynamic Deflectometer Testing

Jeffrey L. Lee [1], Boo-Hyun Nam [2] and Kenneth H. Stokoe, II [3], M.ASCE

[1] Pavement Engineer, Hyder Consulting Pty Ltd, 199 Grey Street, South Brisbane, QLD 4101, Australia; jlee1000@gmail.com

[2] Graduate Research Assistant, Dept. of Civil Engineering, The University of Texas at Austin, 1 University Station C1792, Austin, TX 78712, USA; booda7@mail.utexas.edu

[3] Jennie C. and Milton T. Graves Chair in Engineering, Dept. of Civil Engineering, The University of Texas at Austin, 1 University Station C1792, Austin, TX 78712, USA; k.stokoe@mail.utexas.edu

ABSTRACT: The Rolling Dynamic Deflectometer (RDD) is a state-of-the-art device that has been used in project-level pavement studies to measure continuous deflection profiles along both highway and airport pavements. Because the RDD deflection measurements are made using contact rolling sensors, the physical and rolling-noise characteristics of the sensors limit the maximum RDD testing speed. In this paper, a two-part study is presented to improve the RDD testing speed and characterization of rolling noise. The first part involves development of second-generation rolling sensors. Field trials using the second-generation rolling sensors on a flexible pavement show significant improvements in testing speed and rolling-noise minimization. The second part involves improving the understanding of the noise that is simultaneously collected with the input RDD signal. This noise is referred to as rolling noise. This effort was achieved by analyzing RDD data collected from numerous project-level studies that involved different deflection levels, pavement surface roughnesses, and testing speeds. These data allowed development of a generalized rolling-noise envelope.

INTRODUCTION

The use of different nondestructive deflection testing devices to evaluate the condition of a pavement is very common in many parts of the world. In particular, some state transportation agencies in the United States incorporate this type of testing in their daily pavement management activities. The primary purpose of nondestructive deflection testing (NDT) devices is to evaluate the in-situ material properties and other characteristics (such as load transfer across cracks and joints) of pavements.

The Rolling Dynamic Deflectometer (RDD) is one type of NDT device. The RDD is shown in Fig.1. It was developed by researchers at the University of Texas at Austin (Bay et al., 1998), and is a state-of-the-art device that has been used in many project-level studies to measure continuous deflection profiles along both highway and airport pavements (for instance, Lee et al., 2005).

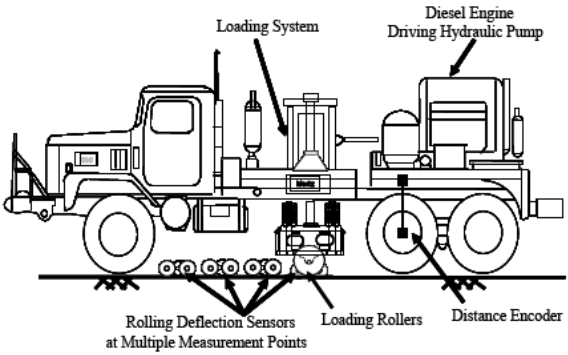
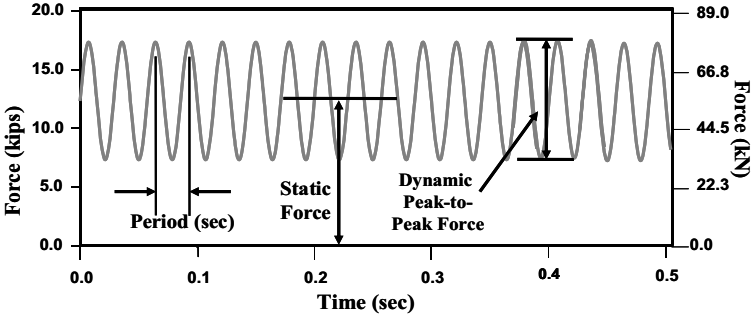


FIG. 1. Schematic Diagram of the Rolling Dynamic Deflectometer.

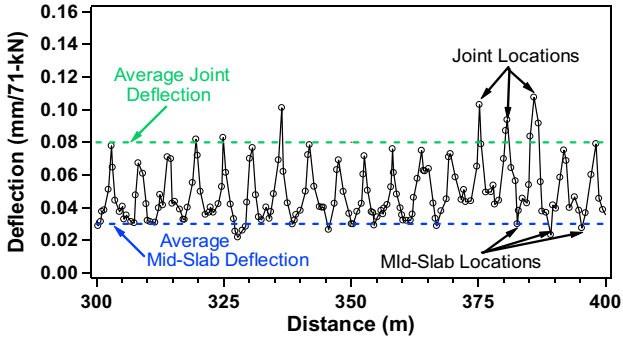
A typical RDD loading function is shown in Fig. 2(a). The loading function is composed of a constant component that is the static hold-down force and a steady-state sinusoidal component that is the dynamic force. The sinusoidal frequency is single valued, with a value between 25 to 35 Hz commonly used. The static and dynamic forces are transferred to the pavement through two polyurethane loading rollers. The applied forces are measured by four individual load cells located between the loading rollers and the upper loading platform. Rolling sensors, that are in contact with the pavement, are located at multiple points under the RDD. The rolling sensors continuously measure the dynamic deflections due to the sinusoidal loading as the RDD moves along the pavement. As a result, a continuous deflection profile is obtained as shown in Fig. 2(b).

One benefit of continuous deflection profiles is that all transverse cracks and joints are evaluated. Unlike other discrete deflection testing devices, the RDD applies sinusoidal dynamic loading and measures the resulting dynamic deflections using contact sensors called rolling sensors. The time-domain signal collected by each rolling sensor contains the sinusoidal motion created by the RDD loading and noise created by the sensors rolling along the pavement and passing traffic. Some of the time, the overall noise level in the time-domain signal can be of the same magnitude as the deflection signal. By knowing the RDD operating frequency (for instance, 30 Hz), notch-pass digital filters and signal processing are used to attenuate noise signals at frequencies outside the RDD operating frequency. As a result, only deflections at the RDD operating frequency are identified and used to calculate the continuous deflection profile.

Even though the current analysis procedure can attenuate noise effectively, it is a good practice to reduce the noise level as much as possible in the measurements. Depending on the filter characteristics of the notch-pass filter, measured noise in the range of 20 to 40 Hz can affect the accuracy of the deflection measurement. Therefore, one of the objectives is to develop second-generation rolling sensors that reduce noise over this frequency range.



(a) Static and Dynamic Components of the RDD Loading Function



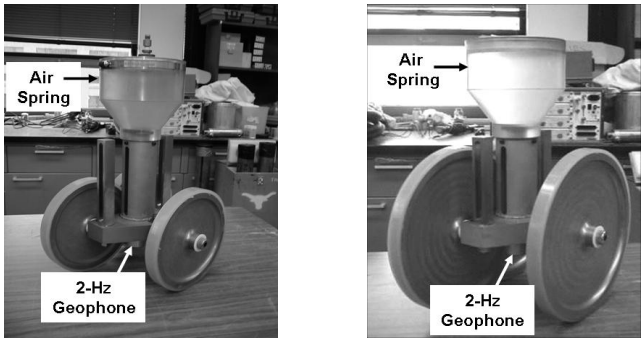
(b) RDD Continuous Deflection Profile Collected Along a Jointed Concrete Pavement

FIG. 2. RDD Loading Function and Typical RDD Deflection Profiles.

SECOND-GENERATION ROLLING SENSORS

The RDD has been a valuable tool in many project-level studies over the past decade. RDD testing has previously been limited to a testing speed of 1.6 km/hr using the first-generation rolling sensors. Second-generation rolling sensors have been developed to increase the RDD testing speed from 1.6 to 4.8 km/hr. Furthermore, the rolling noise associated with the new sensor is less around the RDD operating frequency than the first-generation rolling sensors when both sensors are moving at the same speed.

Two key factors that limit the testing speed of contact rolling sensors are: (1) negative accelerations of the rolling sensor as it moves along a rough surface, and (2) level of rolling noise measured during testing. Second-generation rolling sensors successfully address these two issues. Compared with first-generation rolling sensors, second-generation sensors have pressurized air-springs that provide an additional hold-down force which increases the allowable negative accelerations generated at higher testing speeds. Also, in second-generation sensors, the diameters of the rolling wheels have been increased from 15.3 cm to 22.8 and 30.5 cm to reduce the rolling noise. Photographs of the second-generation rolling sensors with different sized wheels are shown in Fig. 3.



(a) 22.9-cm wheel diameter rolling sensor (b) 30.5-cm wheel diameter rolling sensor

FIG. 3. Photographs of Second-Generation Rolling Sensors.

Design and Calibration of the Second-Generation Rolling Sensor

Each second-generation rolling sensor was custom-made and calibrated for its dynamic performance at the University of Texas at Austin (UT).

(Design Considerations) ─ Multiple design considerations were considered in building these sensors. Some of these are: (1) sensor frequency response, (2) hold-down force level, (3) air spring to apply hold-down force, (4) stability when moving, (5) wheel treads material, and (6) noise minimization from wheels size.

(Laboratory Calibration) ─ The calibration procedure involved vibrating a rolling sensor on a shake table and monitoring the voltage output of the 2-Hz geophone that is the sensing element. Shaking was conducted over a range of frequencies and displacement levels. A swept sine was used from 5 to 200 Hz.

(Air Springs and Air-Pressure Supply System) ─ The air springs on the second-generation rolling sensors were designed to maintain a 155 N hold-down force. Each air spring is located between the rolling sensor and a heavy frame (not shown in Fig. 3) which moves with the RDD. The air springs are pressurized by an external pressure source on the RDD.

(Field Testing) ─ Continuous deflection profiles were collected along a test site on the research test campus at UT, using the second-generation rolling sensors at 1.6, 3.2 and 4.8 km/hr. The test site consists of 3.8 cm of asphalt concrete over 20.3 cm of granular base. The deflection profiles, presented in Fig 4, show that that the deflection profiles collected at different speeds are essentially same.

ROLLING NOISE CHARACTERISTICS AND ROLLING NOISE ENVELOPE

There are a number of reasons to study the characteristics of noise in the RDD measurements. First, this knowledge allows better specifications of digital filters to effectively attenuate noise. Second, understanding the causes of the noise allows improvement in the physical design of the sensors. By analyzing first-generation rolling sensor measurements at 46 project-level studies, it has been observed that the noise characteristics depend on three parameters during testing (Lee, 2006). Table 1 summarizes the effects of the three testing parameters.

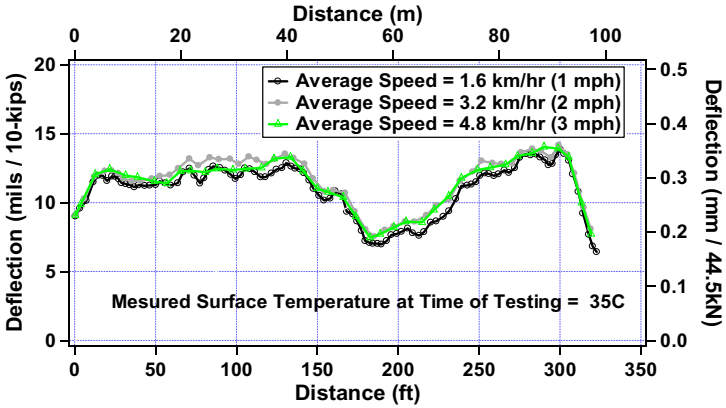


FIG. 4. RDD Deflection Profiles Collected at a Test Site Using the Second-Generation Rolling Sensor with 30.5-cm Wheels at Speeds of 1.6, 3.2 and 4.8 km/hr.

Table 1. Effects on Measured Rolling Noise

Testing Parameter	Effect on Rolling Noise
Increased Testing Speed	Increases Rolling Noise
Increased Pavement Surface Roughness	Increases Rolling Noise
Increased Level of Deflection	Increases the Signal-to-Noise Ratio

The first step in understanding rolling noise is to define a rolling noise envelope, which is basically an upper bound representation of the rolling noise. This envelope is necessary to describe the rolling noise because of the random nature of the rolling noise characteristics at any instance in time. A simplified model of the rolling noise envelope developed from analyzing the 46 project-level studies is shown in Fig. 5. Two other frequency peaks in the FFT spectrum (see Fig. 5) are due to higher order harmonics, which do not affect the RDD-generated deflections at the input frequency because their amplitudes are low enough and the digital filter attenuates them. This model is composed of two linear parts: (1) a flat envelope between 0 to 30 Hz, and (2) a sloping envelope between 30 to 100 Hz.

It is worth noting that when analyzing RDD deflection data, the relative amplitudes of the RDD deflection signal and the surrounding noise are important (i.e. in general, a higher ratio allows deflections to be resolved over shorter intervals). A quantitative parameter known as the signal-to-noise ratio (SNR) is often used to describe the relative amplitudes between a signal and the noise. There are different definitions for SNR. In this work, the following SNR definition has been adopted:

$$\text{SNR(decibels)} = 20 \log_{10} (V_{RDD_fo} / V_{20\text{-}40Hz}) \quad (1)$$

where V_{RDD_f0} = Voltage measured at RDD operating frequency, $V_{20\text{-}40\ Hz}$ = Average voltage measured in the frequency band between 20 – 40 Hz.

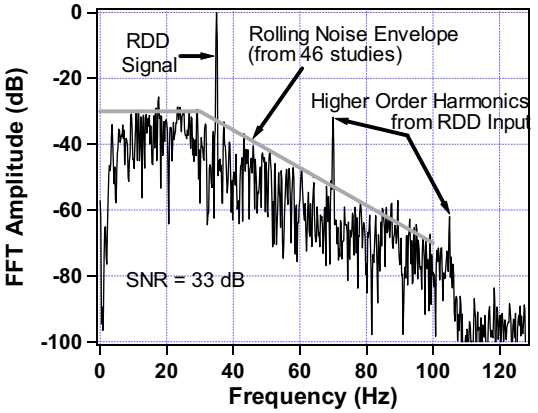


FIG. 5. Typical FFT Spectrum of a First-Generation Rolling Sensor Measurement and Rolling Noise Envelope Determined from Many Studies.

CONCLUSIONS

A two-part study is presented to improve the RDD testing speed and to improve the characterization of rolling noise in these measurements. Development of second-generation rolling sensors is presented. This type of rolling sensor can increase testing speeds up to 4.8 km/hr. Furthermore, this sensor has lower rolling noise level when compared to first-generation rolling sensors. The second part of this study involves improving the understanding of rolling noise. RDD measurements from 46 projects were investigated to evaluate the effects of deflection levels, pavement surface roughnesses, and testing speeds on rolling noise. A rolling noise envelope was developed to describe and quantify rolling noise in RDD testing.

ACKNOWLEDGMENTS

The authors appreciate the funding support from the Texas Department of Transportation (TxDOT) and the comments, support and guidance from Dr. Michael Murphy, Dr. Dar-Hao Chen, and Prof. James A. Bay.

REFERENCES

1. Lee, J., Stokoe, K., Chen, D., Garrison, M. and Nam, B. (2005), "Pavement Rehabilitation: Monitoring Pavement Changes in a Rehabilitation Project with Continuous Rolling Dynamic Deflectometer Profiles," *Transportation Research Record 1905*, TRB, Washington, D.C., pp 2-16
2. Lee, L. J. (2006), *Improved Rolling Dynamic Deflectometer Testing and Analysis Procedures*. Ph.D Dissertation. University of Texas at Austin.
3. Bay, J. A., and Stokoe, II, K. H. (1998), *Development of a Rolling Dynamic Deflectometer for Continuous Deflection Testing of Pavement*. Publication FHWA/TX-99/1422-3F. FHWA/Texas Department of Transportation.

The Application of Emulsion Warm Mix Asphalt in Long Tunnel Pavement

Xu Shifa[1], Xu Liting[1], Jia Jonathan[1] and Xie Yongqing[1]

[1] Shell (China) Limited, No.43 Liang Ma Qiao Road, Chao Yang District, Beijing, 100016 P.R.China, Senior Advisor and Application Manager, Shifa.Xu@shell.com; Engineer, Liting.Xu@shell.com; Engineer, Jonathan.Jia@shell.com; Engineer, Yongqing.Xie@shell.com

ABSTRACT: Long tunnel asphalt pavement construction, particularly due to the lack of ventilation, still handicaps the construction process in China and even in the world. Based on the actual Emulsion Warm Mix Asphalt (EWMA) long tunnel pavement project, EWMA's characteristics have been studied compared with conventional Hot Mix Asphalt (HMA). Further more, EWMA compactibility performance at various compaction temperatures has been evaluated by SGC test. The field pavement performance has been evaluated according to related specifications. The reductions in fuel consumption and gas emission of EWMA have been quantified in contrast to conventional HMA. The study shows that EWMA can reduce 30°C~40°C compaction temperature and have significant lower energy consumption and emission in tunnel construction, and increase about 10 percent rutting resistance compared with conventional HMA. Therefore, EWMA is remarkable material for long tunnel asphalt pavement construction.

INTRODUCTION

The tunnel is 1.66km long and 17m wide. The original tunnel flexible pavement structure consists of two HMA layers. The top layer is 4cm AC-13 HMA (the nominal maximum aggregate size is 12.5mm), and the bottom layer is 6cm AC-20 HMA (the nominal maximum aggregate size is 19.0mm). Because the tunnel ventilation facility has not been installed during the paving period, the heavy fume and high temperature of conventional HMA will bring big challenge and risk for paving crew. Therefore, EWMA is chosen for tunnel paving construction in this project, which is the first and longest tunnel application of EWMA in China.

1 Temperature Reduction Mechanism of EWMA

EWMA is a type of Warm Mix Asphalt (WMA) which can decrease production temperature with the additional benefit of reduced emissions from burning fuels, bitumen fumes, and odours generated at the plant and the paving site. [1] Meantime, its performances are equivalent to conventional HMA.

EWMA emulsion has higher residue content. Its application temperature is around 80°C. Most of the water in emulsion will be instantaneously vaporized when the emulsion meets hot aggregates (around 140°C in the mixing plant), and minimally retained water acts as a lubricant in EWMA. The chemical additive package, which delivered by emulsion, will provide aggregate coating, workability, adhesion, and improve compaction with no change in materials or job mix formula required. [2]

2 The Characteristics Analysis of EWMA

SBS polymer modified bitumen was used as base bitumen of EWMA emulsion for this project. The properties of SBS polymer modified bitumen and emulsion are shown in Table 1 and 2 respectively.

Table 1. Properties of SBS Polymer Modified Bitumen

Test Items		Unit	Result	Criteria [3]	Method [4]
Penetration (25°C, 100g, 5s)		0.1mm	68	60~80	T 0604-00
Ductility (5cm/min, 5°C)		cm	35	≥30	T 0605-93
Softening Point		°C	61	55	T 0606-00
RTFOT	Retained Penetration	%	75	≥60	T 0604-00
	Ductility (5°C)	cm	25	≥20	T 0605-93

Table 2. Properties of EWMA Emulsion

Test Items		Unit	Result	Method [4]
Breaking Rate		NA	Middle	T 0658-93
Particle Charge		NA	Cation	T 0653-93
Sieve Residue (1.18mm)		%	0.008	T 0652-93
Engler Viscosity E_{25}		NA	4.68	T 0622-93
Residue	Solid Content	%	68	T 0651-93
	Penetration (25°C, 100g, 5s)	0.1mm	65	T 0604-00
	Ductility (5cm/min, 5°C)	cm	33	T 0605-93
	Softening point	°C	60	T 0606-00

NA= No data available

The design method of EWMA is the same procedure as that of conventional HMA. Marshall method is used to design EWMA in this project. There are two ways to determine the optimum bitumen content of EWMA. The first way is to directly compact the EWMA samples for various bitumen content, and then to determine the Optimum Emulsion Content (OEC) based on volumetric and mechanical characteristics of EWMA specimens. The second way is to determine the Optimum Asphalt Content (OAC) for the control mix, and then substitute the EWMA emulsion by the following formula.

$$\text{OEC} = \frac{OAC}{M_{RE}} \times 100 \qquad (1)$$

where M_{RE} =Residue content of emulsion, %

The second way was recommended for this project. The OAC of AC-13 and AC-20 have been identified as 5.3 and 4.2 percent respectively. Hence, the OEC have been calculated as 7.8 and 6.2 percent respectively. The volumetric and mechanical characteristics of Marshall specimens are shown in Table 3.

Table 3. Characteristics of EWMA vs. Control Mix

Gradation	Mix Type	Va (%)	VMA (%)	VFA (%)	MS (KN)
AC-13	Control Mix	4.1	15.0	73	14.8
	EWMA	4.0	14.1	72	16.0
AC-20	Control Mix	4.5	13.6	67	11.5
	EWMA	4.3	13.3	68	11.2

Dynamic stability (DS) is a rutting resistant index of asphalt mixture from Wheel Tracking Test. The higher DS number means the higher rutting resistance of asphalt mixture. The Wheel Tracking Test specimen dimension is 300mm in length, 300mm in width and 50mm in thickness. The testing condition are: 60°C of testing temperature, 42cycle/min of wheel tracking rate, 0.7MPa of solid rubber wheel contact pressure and 60 minutes testing time. The test results are shown in Table 4.

Table 4. Rutting Test Results

Gradation	DS (Cycle/mm)		Criteria [3] (Cycle/mm)	Method [4]
	Control Mix	EWMA		
AC-13	3620	4146	≥2800	T 0719-93
AC-20	4354	5084	≥2800	

The rutting test results show that EWMA can increase about 10 percent rutting resistance compared to control mix.

Moisture sensitivity is one of the key factors of EWMA performance. In this study, the Tensile Strength Ratio (TSR) test was applied to evaluate the water susceptibility of EWMA. The test results are listed in Table 5.

Table 5. TSR Test Results

Gradation	TSR		Criteria [3]	Method [4]
	Control Mix	EWMA		
AC-13	88%	88%	≥80%	T 0729-00
AC-20	83%	81%	≥80%	

The above test results indicate that EWMA has the similar water resistance capability as control mix.

3 Compactibility Test of EWMA

In order to fully investigate the compaction characteristics of EWMA, Superpave Gyratory Compactor (SGC) is used to compact the specimens of both EWMA and control mix of AC-13 at various compaction temperature. The parameters of SGC: angle of gyration is 1.25º, contact pressure is 600Kpa, and the number of design gyration is 100. The comparison of the compaction characteristics of EWMA and control mix is shown in Figure. 1.

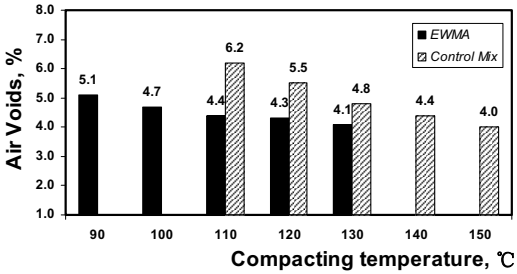


FIG. 1.Compactibility comparison of EWMA vs. Control Mix

The test results show:

At the same compaction temperature, the air voids content of EWMA is lower than that of control mix.

At the same air voids content, the compaction temperature of EWMA is over 30°C lower than control mix.

The compaction temperature susceptibility of EWMA is lower than that of control mix.

As a result, the compaction temperature window of EWMA is wider than that of control mix.

4 Fume Emission and Fuel Consumption Comparison

Fume emissions can be significantly reduced because of the lower mixing temperature during the production of EWMA. EWMA production can lead to over 60 percent reduction in CO_2 and SO_2 emissions, over 70 percent reduction in NO_X, over 50 percent reduction in flue dust according to measured data from asphalt plant by Chinese National Environment Analysis and Test Center. It shows that EWMA can effectively lower the greenhouse gas emission.

The fuel consumption for EWMA and HMA at asphalt plant is summarized in Table 6.

Table 6. Fuel Consumption at Asphalt Plant

Mix Type	Mix Temperature	Fuel Consumption	Energy Saving
HMA	165°C	7.0kg/t	20%
EWMA	130°C	5.6kg/t	

The comparison of gas emission for both EWMA and HMA monitored on paving site is listed in Table 7[5].

Table 7. Fume Emission of Paving Site Test Results

Properties	Unit	HMA	EWMA	Reduction (%)
Bitumen Fume	mg/m^3	21.1	2.06	90.2
Benzene-Soluble Organics	mg/m^3	19.5	0.58	97.0
Benzopyrene	mg/m^3	0.094	0.019	79.8

All the measured data indicate that EWMA can not only save fuel consumption, but also reduce the gas emissions significantly. Therefore, it is a good solution for poor ventilation tunnel paving job.

5 Field EWMA Pavement Performance Inspection

The paving and compacting of EWMA in the tunnel was carried out safely and smoothly although with no ventilation. Pavement quality inspection has been carried out after EWMA tunnel paving construction. The test results are shown in Table 8.

Table 8. Pavement Quality Inspection Results of EWMA (AC-13)

Test Items	LL	RL	Criteria [3]	Method [6]
Standardize division (Roughness)	0.62	0.62	<1.2mm	T 0932-95
Permeability Factor (ml/min)	49	9	<300	T 0971-95
Texture Depth (mm)	0.8	0.7	>0.5	T 0961-95
Friction Factor (BPN)	78.3	73.0	>45	T 0964-95
Compaction (%)	98.5	98.7	≥96	T 0924-95

LL: Left lane; RL: Right lane

The results show that the pavement construction quality of EWMA can fully meet the requirements of the Chinese Technical Specifications for Construction of Highway Asphalt Pavements.

CONCLUSIONS

Following conclusions can be drawn based on lab and on-site tests:

- The mixing, paving and compacting temperature of EWMA can be dropped up to 30°C compared with control mix. The operation temperature window of EWMA is wider than control mix.
- The volumetric properties and mechanical performances of EWMA are equivalent to that of control mix, while it has a 10 percent rutting resistance improvement.
- EWMA can effectively improve the construction environment especially in long tunnel paving work site by reducing operation temperature and consequently cutting more than about 50 percent of harmful gas emission.
- EWMA pavement quality can fully meet the related requirement of Chinese Specifications.

REFERENCES

1. Http://www.fhwa.dot.gov/pavement/asphalt/wma.cfm.
2. Graham C. Hurley and Brian D. Prowell. (2006). “The Evaluation of Evotherm® for Use in Warm Mix Asphalt.” NCAT Report 06-02.
3. The Ministry of Communication of the People’s Republic of China. (2004). “Technical Specifications for Construction of Highway Asphalt Pavements” JTG F40, MOC Publishing House
4. The Ministry of Communication of People’s Republic of China. (2000). “Standards Test Methods of Bitumen and Bituminous Mixtures for Highway Engineering”, MOC Publishing House.
5. Huang Songchang. (2008). “The development and application of warm mix.” CAEC.
6. The Ministry of Communication of People’s Republic of China. (1995). “Field Test Methods of Subgrade and Pavement for Highway Engineering”, MOC Publishing House.

Application of Recycled Brick-stone aggregate in Road Base

Yingbiao Wu, Yanfang Guo, Xiuli Zhang

Municipal Engineering Company of Cangzhou, #26 Huanghe East Road, Cangzhou City,Hebei province, China; 061000; szgcgs-1@heinfo.net

ABSTRACT: Construction rubbish including waste bricks and concrete blocks, can be recycled into brick-stone aggregate through pre-screening, crushing, screening and blending. Using proper mix proportions of lime-fly ash, cement, or cement-fly ash stabilizes the material which can then be used as pavement base material. The unconfined compressive strength, modulus, frost resistance and anti-brushing performance of this recycled material can meet the required specifications. Through three experimental sections, the conclusion above is validated.

INTRODUCTION

With increased construction, more and more construction rubbish is being produced from old buildings and other construction projects. So much so, that it has become a significant environment problem [1, 2]. Typically rubbish bricks and concrete blocks make up approximately 80% of construction waste. Through pre-screening, crushing, screening and blending this waste, it can become brick-stone aggregate used as a road base material. A series of laboratory experiments show that the brick-stone aggregate mixed with chemically stabilizing materials such as lime-fly ash, cement, or cement-fly ash can become a stable material for use in road base construction and can meet required performance standards. To further check the performance of these chemically stabilized brick-stone aggregate materials in the field, three experimental test sections were constructed. These experimental test sections have been trafficked more than two years, and the pavement conditions are still very good.

1. Crashing Technique of Brick-stone Aggregate Materials

Construction rubbish can not be directly used as pavement materials without pre-processing. It must be processed with a special machine. First it is pre-screen to get rid of fine soil. Second it is crushed. Then, the magnetic segregator removes the steel and scrap iron. Final it is screened to remove over-sized grains or screen into different sizes then blended to meet the gradation requirement

2. Experimental Test Study

There are many differences between the brick-stone aggregate materials and natural aggregate in performance [3]. In brick-stone aggregate the modulus of elasticity is low, the crushing value is large, the water-retaining rate is high, and the coefficient of permeability is large. These properties affect the performance of base material and therefore were confirmed through an experimental test.

For the chemically stabilized brick-stone aggregate materials, the major source of strength is in adhesion and cohesion between the binder and aggregate, not the internal friction resistance and embedding and crushing force between the grains. The strength of grain of brick-stone aggregate is lower than the strength of crushed stone. The

embedding and crushing process between the grains diminishes contact between the brick-stone grains. In order to acquire the maximum strength and stability, the suspended skeleton compact structure is chosen in this test study.

2.1 Experiment Summary

A series of lab tests were conducted to evaluate mechanical properties of the chemically stabilized brick-stone aggregate materials with lime-fly ash, cement, and cement-fly ash. The experimental mixing proportions in the lab are shown in Table 1.

In the recycled brick-stone aggregate materials, the content of fine aggregate, with size smaller than 2.36 mm, is 31.1%. In the coarse aggregate with size larger than 2.36 mm, the concrete grain content is 42.6%, and the brick grain content is 26.3% (quality ratio). The whole quality of Ⅲ grade calcareous drowned lime, effective calcium oxide and magnesium is 56.5%. The fly ash adopted is silicon-aluminum fly ash, the bulk density of dry fly ash is 0.68 g/cm^3, and the slow-setting cement is adopted. The basic properties of the raw materials are shown from Table 2 to Table 5.

Table 1. Lab Testing Mixing Proportion (Quality Ratio)

Lime-fly ash stabilized brick-stone aggregate (lime: fly ash: brick-stone aggregate＋Cement)			Cement stabilized brick-stone aggregate Cement dose (%)	Cement-fly ash stabilized brick-stone aggregate(Cement: fly ash: brick-stone aggregate)
7:13:80	7:13:80+1%	7:13:80+2%	4.5	3:6:91
5:15:80	5:15:80+1%	5:15:80+2%	5.0	3:9:88
4:16:80	4:16:80+1%	4:16:80+2%	5.5	2:7:91

Table 2. Physics Performance Index of Brick-stone Aggregate Materials

Natural accumulation density (kg/cm^3)	Tap density (kg/cm^3)	Crushing value (%)	Water absorbing capacity (%)	Cubage water absorbing capacity (g/cm^3)	Coefficient of permeability (cm/s)	Fine grained soils below 0.6mm	
						Water limit(%)	Index of plasticity
1.313	1.522	30.9	16.3	0.072	0.656	32.3	6.4

Table 3. Grain Formation of Brick-stone Aggregate Materials

Size of sieve pore (mm)	37.5	31.5	26.5	19.0	9.50	4.75	2.36	1.18	0.60	0.075
Percentage of the passing quality (%)	100	95.5	88.2	75.8	53.7	40.8	31.1	22.4	16.2	3.4

Table 4. Chemistry Component Analysis of the Fly Ash

Percentage of the passing quality in sieve pore (%)			Ignition loss (%)	SiO_2 (%)	Al_2O_3 (%)	Fe_2O_3 (%)	CaO (%)	MgO (%)	SO_2 (%)
0.3mm	0.15mm	0.075mm							
100	99.1	87.6	10.28	46.55	32.15	5.19	3.93	2.02	0.45

The cylinder test specimen of 150×150mm is adopted, and the optimum moisture content and maximum dry density of the materials are confirmed according to the heavy

duty compacting method. The major testing contents are shown in the following: ① Saturation Unconfined compressive strength of long age and multi-age in 7, 28, 90, and 180 days; ②Splitting strength; ③Modulus of resilience； ④Frost stability testing: after being saturated in water sink of 20℃ for 24h, being kept frost at -18℃ for 16h, the test piece is taken out and thawed in the water sink of 20℃ for 8h. After 5 freezing and thawing cycles like the above steps, the freezing and thawing freezing and thawing retained strength is acquired to evaluate the frost stability. ⑤ Anti-brushing performance testing: after being vibrated for 60min, the erosion percentage of test piece saturated for 24h is measured (see Figure 1). From ② to ⑤, lime-fly ash stabilized brick-stone aggregate is detected after 180 days, cement stabilized brick-stone aggregate is detected after 90 days, and cement-fly ash stabilized brick-stone aggregate is detected after 120 days.

Table 5. Physics Mechanical Strength Properties of Cement

Cement grade	Fineness (%)	Standard fineness (%)	Time of Setting （min）		Compressive Strength(MPa)		Antiflex Strength (MPa)		Soundness
			Initial setting	Final setting	3d	28d	3d	28d	
32.5	1.7	27.6	433	527	18.5	40.2	3.7	8.3	Acceptable

2.2 The Analysis of the Testing Results

2.2.1 Mechanical Strength Properties

The mechanical strength properties testing results of lime-fly ash stabilized brick-stone aggregate is shown in Table 6～Table 8.

As shown in Table 6 and Figure 2, under the condition of the same amount of cement, lime-fly ash stabilized brick-stone aggregate of 7:13:80 have the highest strength. The strength and resilience modulus of materials are in positive correlation with the cement amount. Through adding a little cement, the compressive strength of materials can be further improved. After adding 1% cement, the splitting strength of materials is twice of that without adding the cement, but the splitting strength after adding 2% cement is only slightly higher than splitting strength after adding 1% cement. Thus, in order to improve the splitting strength, the addition of 1% cement is more economical.

As shown in Table 7 and Figure 3, both the strength and resilience modulus of cement stabilized brick-stone aggregate are in positive correlation with cement content, and the cement content 5.0% is most economical. The later strength of cement stabilized brick-stone aggregate is lower than cement stabilized crushed stone and lacks a rapid strength increase within 28 days as cement stabilized crushed stone.

As shown in Table 8 and Figure 4, the 7d compressive strengths of the two groups cement-fly ash stabilized brick-stone aggregate with the cement content of 3% are very close to each other and higher than the cement-fly ash stabilized brick-stone aggregate with the cement content of 2%, therefore, the cement content is the main factor for the 7d compressive strength of the cement-fly ash stabilized mixture. Of the three kinds of chemically stabilized brick-stone aggregates, the modulus of cement-fly ash stabilized brick-stone is relatively low. The reasonable mix proportion is 3:6:91 for cement-fly ash

stabilized brick-stone aggregate, the splitting strength of which is slightly higher than other mix proportion aggregate.

Table 6. Mechanical Strength Properties Testing Results of Lime-fly Ash Stabilized Brick-stone Aggregate

lime: fly ash: rick-stone aggregate+cement (Quality ratio)	Unconfined compressive strength (MPa)					Splitting strength (MPa)	modulus of resilience (MPa)
	7d	28d	60d	90d	180d	180d	180d
7:13:80	1.00	1.74	2.2	3.2	3.6	0.35	1171
7:13:80 +1%	1.18	2.6	3.5	4.3	6.2	0.68	1640
7:13:80 +2%	1.86	3.6	4.0	4.5	6.0	0.76	2202
5:15:80	0.96	1.34	1.94	2.1	2.4	0.22	1019
5:15:80 +1%	0.98	1.42	2.6	2.9	3.5	0.49	1711
5:15:80 +2%	1.61	3.0	3.5	4.1	5.6	0.52	2149
4:16:80	0.58	1.14	1.64	1.94	2.7	0.26	1504
4:16:80 +1%	0.86	2.1	3.4	3.4	4.4	0.57	1794
4:16:80 +2%	1.54	2.7	3.9	4.0	5.5	0.71	1874

Table 7. Mechanical Strength Properties Testing Results of Cement Stabilized Brick-stone Aggregate

Cement: brick-stone aggregate (Quality radio)	Unconfined compressive strength (MPa)					Splitting strength (MPa)	modulus of resilience (MPa)
	7d	28d	60d	90d	180d	180d	180d
4.5%	3.6	3.9	4.9	5.1	6.0	0.42	934
5.0%	3.6	4.7	5.0	5.8	6.6	0.60	1285
5.5%	3.9	4.8	5.4	5.8	7.1	0.61	1520

Table 8. Mechanical Strength Properties Testing Results of Cement-fly ash Stabilized Brick-stone Aggregate

Cement: fly ash: brick-stone aggregate (Quality radio)	Unconfined compressive strength (MPa)					Splitting strength (MPa)	modulus of resilience (MPa)
	7d	28d	60d	90d	180d	180d	180d
3:6:91	2.4	2.8	3.6	3.8	4.7	0.39	871
3:9:88	2.6	2.8	3.5	3.2	3.6	0.30	841
2:7:91	1.88	2.3	2.3	2.6	3.2	0.23	373

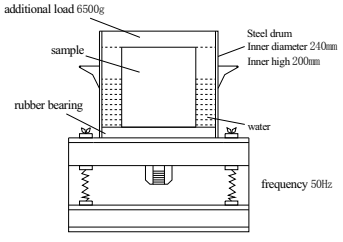


FIG.1. Anti-brushing Test Equipment

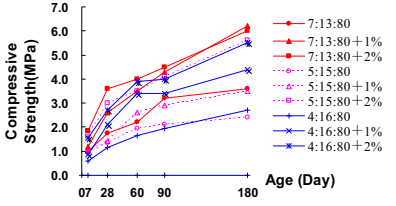


FIG.2. Unconfined Compressive Strength Increasing Curve of Lime-fly Ash Stabilized Brick-stone Aggregate with Age.

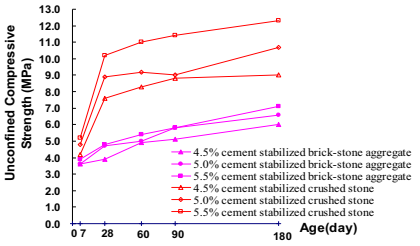


FIG.3. Strength Increasing Curve of Cement Stabilized Brick-stone Aggregate (Crushed Stone) with Age.

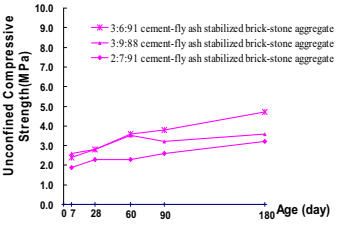


FIG.4. Strength Development Rate Curve of Cement-fly Ash Stabilized Brick-stone Aggregate.

2.2.2 Stability

The results of the 5 time freezing-thawing test and the results of the brush test for the chemically stabilized brick-stone aggregate are listed in Table 9 and Table 10 respectively. The frost resistance and anti-brushing performance of other cement-fly ash stabilized brick-stone aggregates have a relatively good performance except for the aggregate of 2:7:91. If the lime-fly ash stabilized brick-stone aggregate of 7:13:80 is mixed with cement content of 1%~2%, the frost resistance and anti-brushing performance are improved. Therefore, the lime-fly ash stabilized brick-stone aggregate should be mixed with a little cement so as to improve the stability of aggregate. The aggregate with mix proportion of 7:13:80 admixed with 1% cement is more economical. The cement content of 5.0% for cement stabilized brick-stone aggregate is more economical and the mix proportion of 3:6:91 for cement-fly ash stabilized brick-stone aggregate is better.

Table 9. Ratio of remnant compressive strength after 5 times freezing-thawing

Lime-fly ash stabilized brick-stone aggregate 180d			Cement stabilized brick-stone aggregate 90d			Cement-fly ash stabilized brick-stone aggregate 120d		
7:13:80	7:13:80+1%	7:13:80+2%	4.5%	5.0%	5.5%	3:6:91	3:9:88	2:7:91
66.7	74.2	80.3	76.5	82.8	81.0	83.3	70.6	39.3

Table 10. Total amount of brushing within 60min (%)

Lime-fly ash stabilized brick-stone aggregate 180d			Cement stabilized brick-stone aggregate 90d			Cement-fly ash stabilized brick-stone aggregate 120d		
7:13:80	7:13:80+1%	7:13:80+2%	4.5%	5.0%	5.5%	3:6:91	3:9:88	2:7:91
3.2	0.8	0.5	3.9	2.7	2.8	1.4	3.5	9.7

3. Actual engineering application of chemically stabilized brick-stone aggregate

To further check the performance of these chemically stabilized brick-aggregate materials in the field, the cement lime-fly ash stabilized brick-stone aggregate of 7:13:80 and the cement content of 1%, the cement stabilized brick-stone aggregate with the cement content of 5.0% and the cement-fly ash stabilized brick-stone aggregate of 3:6:91 had been paved in the Qiantong Road of Cangzhou City which were used as road base test sections directly. During paving, the stabilized brick-stone aggregate materials were sampled and the mechanical strength properties were characterized in the lab during the paving, the test results are listed in Table 11. Field cores (Figure 5) were taken in the test section. Currently these experimental test sections have been trafficked

more than two years, and the pavement conditions are still very good. Monitoring of these long-term test sections is planned. More information will be reported later.

Table 11. Chemical Strength Test Results in Test Sections

Type and Mix Proportion of Aggregate	Unconfined Compressive Strength of Aggregate in lab(MPa)				
	7d	28d	60d	90d	180d
Lime-fly Ash Stabilized Brick-stone Aggregate of 7:13:80 and Cement Content of 1%	0.94	2.6	3.4	5.2	6.4
Cement Stabilized Brick-stone Aggregate with Cement Content of 5%	2.6	2.6	2.8	3.3	4.7
Cement-fly ash Stabilized Brick-stone Aggregate of 3:6:91	2.1	3.0	3.8	3.9	4.7



(a) (b) (c)

FIG. 5. 180 days field cores of chemically stabilized brick-stone aggregate: (a) lime-fly ash stabilized;(b) cement stabilized;(c) cement-fly ash stabilized.

CONCLUSIONS

The suitable structure for the chemically stabilized brick-stone aggregate should be suspended framework sense structure. Using proper mix proportions mechanical properties, stability and durability of all three kinds of chemically stabilized brick-stone aggregates meet the road-use performance requirements.

The optimal water content of chemically stabilized brick-stone aggregate is much higher than that of stabilized crushed stone. Because of the strong water-absorbing property of the brick-stone aggregate, the structural surface needs only to be kept wet when curing.

REFERENCES

1. Sha Qinglin, Asphalt Pavement for semi-rigid base of High Level Highway [M], Beijing People's Publishing House, Vol. 11,1997.
2. Yin Jian, Xu Yunfeng, Li Yijin. Anti-brushing Performance Study of Recycled Cement Stabilized Aggregate Base Mixture [J]. Journal of Railway Science and Engineering, 2007, 4 (6):44-49
3. Zhang Chao, Ding Jizhong etc. Application of Recycled Waste Cement and Concrete in Semi-rigid Road base [J]. Journal of Chang'An University (Natural Science Edition), 2002, 25(5):1-4

Workability of the 25 mm-NMAS Stone Fill HMA Mixes

Lubinda F. Walubita[1], M. ASCE, Tom Scullion[1], and Joe Leidy[2]

[1]Texas Transportation Institute (TTI), Texas A&M University System College Station, TX 77843, USA. Phone (979) 845-9919, Fax (979) 845-1701, Email: lfwalubita@gmail.com
[2]Flexible Pavements, Texas Department of Transportation (TxDOT), Austin, TX 78717, USA. Email: jleidy@dot.state.tx.us

ABSTRACT: As of 2001, the Texas Department of Transportation (TxDOT) has been using a 25 mm nominal maximum aggregate size (NMAS) Stone Fill HMA (SFHMA) mix as the main structural rut-resistant layer in perpetual pavement structures. The SFHMA mix-design basically consists of moderately low asphalt-binder content with a relatively stiff performance-graded (PG) asphalt-binder on the order of about 4.2% content and a 25 mm NMAS coarse aggregate gradation. To date, over eight different SFHMA mix-designs have been utilized on different in-service perpetual pavement projects in Texas. The objective of the work presented in this paper was to review and document the workability characteristics of these coarse SFHMA mixes as observed both in the laboratory (during mix-design and material property characterization) and in the field (during construction). In general, these SFHMA mixes were found to have poor workability characteristics. Remedial measures as employed both in the lab and field to improve the SFHMA mix workability and other material property characteristics are also presented in the paper.

INTRODUCTION

As of 2001, the Texas Department of Transportation (TxDOT) recommended using Stone Filled Hot-Mix Asphalt (SFHMA) mixes in perpetual pavement (PP) structures (TxDOT, 2001; Scullion, 2007; Walubita et al., 2007; APA, 2002; Newcomb et al., 2001). For the main structural rut-resistant layer, which is at least 200 mm (8 inch) thick, a 25 mm nominal maximum aggregate size (NMAS) SFHMA mix is typically used. This 25 mm NMAS mix is often denoted as 1" SFHMA, where 1" stands for 1-inch NMAS. The 1" SFHMA mix-design characteristics basically consists of moderately low asphalt-binder content with a relatively stiff performance-graded (PG) asphalt-binder on the order of about 4.2% content and a 25 mm NMAS coarse aggregate gradation. The aggregate blend characteristics consists of a relatively higher proportion of the coarser rock compared to traditional Texas dense-graded mixes. Fig. 1 shows the 1" SFHMA gradation specification and an example of the resultant coarse surface texture.

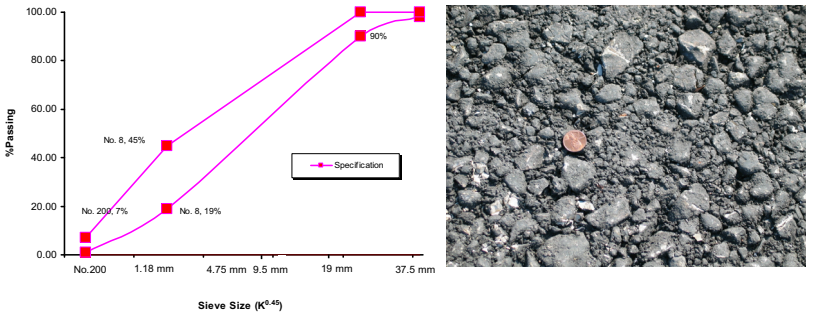


FIG. 1" SFHMA Coarse Aggregate Gradation Specification and Coarse Surface Texture.

On majority of the existing Texas PP projects, the most commonly used asphalt-binder type and aggregates are PG 70-22 and limestone, respectively (Walubita et al., 2007). Anti stripping agents in the range of 0.5% to 1.5%, mostly hydrated lime, are also often added to improve moisture damage-resistance characteristics.

However, perpetual pavements are a relatively new concept to Texas, and so is the 1" SFHMA mixes. With this in mind, the objective of this paper was to evaluate the workability and constructability characteristics of these coarse-graded 1" SFHMA mixes as experienced and observed both in the laboratory (during mix-design and material property characterization) and in the field (during construction). Remedial measures as employed both in the laboratory and field to improve the mix workability and other material property characteristics are also presented in the paper.

SFHMA WORKABILITY – LABORATORY EXPERIENCE

For HMA mixes, workability often refers to the compactability of a mix and how easy it is to handle and/or handwork the mix. This is the context within which workability is defined in this paper. The text below discusses the compactability of the SFHMA mixes as experienced/evaluated in the laboratory together with some remedial measures for improvements.

SFHMA Compactability

Because of the coarser aggregate gradation and relatively low asphalt-binder content, the 1" SFHMA mixes were found to be less workable than conventional Superpave and Texas dense-graded mixes in the laboratory. At an equivalent temperature and for the same target height and air void (AV) content, the SFHMA mix required more compactive effort. Fig. 2 illustrates this comparison.

The results shown in Fig. 2 represents a 1" SFHMA mix with 4.0% PG 70-22 asphalt-binder and limestone aggregates. The TxDOT Type C is a typical Texas dense-graded mix (⅝" [≅16 mm] NMAS) consisting of 4.4% PG 70-22 plus limestone while the ¾" Superpave mix (¾" [≅19 mm] NMAS) consists of 4.2% PG 70-22 plus limestone aggregates.

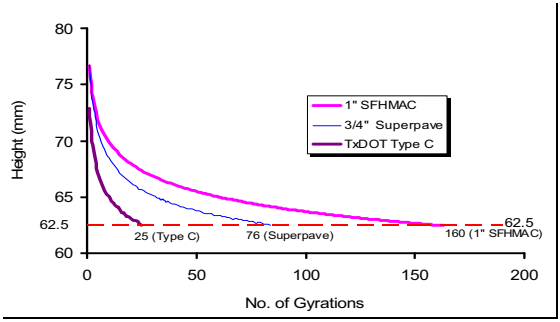


FIG. 2. Laboratory Comparison of 1" SFHMA Mix Compactability.

Clearly, Figure 2 shows that the 1" SFHMA mix required more compactive effort; about 6 times (160 versus 25) more gyrations than the Texas dense-graded TxDOT Type C mix and about 2 times (160 versus 76) more than the ¾″ Superpave mix, respectively, for the same 62.5 mm target height. Consistent with the PG asphalt-binder grade, all the mixes were compacted at 135 ℃ (275 ℉) to 7±0.5% air void (AV) content (TxDOT, 2004; Walubita et al., 2007).

Effects of Asphalt-Binder Content

From laboratory experimentation, it was observed that increasing the asphalt-binder content improved the workability and compactability of the 1" SFHMA mixes considerably. Measured in terms of the number of gyrations and for a target height of 62.5 mm, a 1% increase in the asphalt-binder content reduced the compactive effort by over 9%; thus making the mix more workable with greater potential for attaining the target density. Fig. 3 shows this relationship for a 1" SFHMA mix with 4.1% PG 70-22 asphalt-binder and limestone aggregates. The compaction temperature was 135 ℃ (275 ℉) at a 7±0.5% target AV.

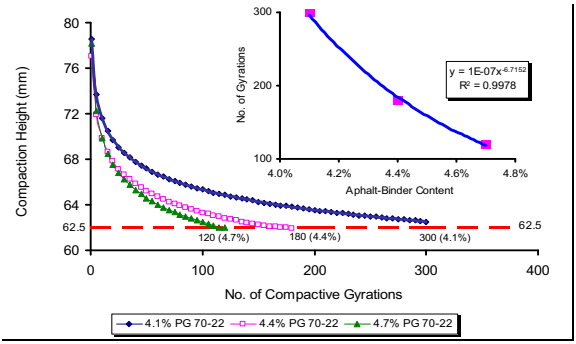


FIG. 3. Asphalt-Binder Content versus the 1" SFHMA Compactability

Clearly, Fig. 3 shows that increasing the asphalt-binder content reduces the required compactive effort for the same target thickness and AV content. About 2.5 times more gyrations were required for the 4.1% versus the 4.7% mix and 1.5 times more for the 4.4% versus 4.7% mix for the same asphalt-binder type, target height (62.5 mm), compaction temperature (135 ℃ [275 ℉]), target AV (7±0.5%), and aggregate type (limestone). These data imply that the mix with 4.1% asphalt-binder content may exhibit greater compactability problems in the field and may require more rolling compaction passes to attain the target density. In fact, the measured AVs for the samples were 6.80%, 7.01%, and 7.53% for the 4.7%, 4.4%, and 4.1% asphalt-binder content, respectively. Note that asphalt-binder also helps in lubricating the aggregate during compaction and therefore, mixes with low asphalt-binder content are generally difficult to compact because of inadequate lubrication; whereas mixes with high asphalt-binder content will compact easily (but may shove under heavy roller loads). This is one of the reasons less absorptive aggregates (less than 2% water absorption capacity) such as gravels and granites are often desired. Based on the data in Fig. 3, a design asphalt-binder content level that is greater than 4.1% would be desired for ease of workability in terms of compaction. However, 4.1% was used for this mix.

On top of improving workability (compactability), increasing the asphalt-binder content also improves the cracking resistance and durability characteristics of the SFHMA mix. However, since these 1" SFHMA mixes are designed predominantly for rutting resistance, care should be exercised when modifying the mix-design not to jeopardize this property. If; (1) the cracking resistance is expressed in terms of the number of cycles to cracking under the Overlay test at 25 ℃; (2) rutting resistance is expressed in terms of the rut depth after 20,000 load passes under the Hamburg test at 50 ℃; and (3) durability is indirectly expressed in terms of the asphalt-binder film thickness (TxDOT, 2004), then the effect of increasing the asphalt-binder content on these properties is as shown in Table 1.

Table 1. Effects of Asphalt-Binder Content on the SFHMA Mix Properties.

Asphalt-Binder Content	Hamburg Rut Depth (mm)	No. of Overlay Cycles to Cracking	Asphalt-Binder Film Thickness (microns)
4.1%	4.7	60	11.8
4.4%	5.6	75	12.7
4.7%	6.7	130	13.6
Threshold	≤12.5	≥300	≥10

Clearly, Table 1 shows that there is a significant increase in the number of Overlay cycles to cracking, in particular when comparing 4.1% versus 4.7% asphalt-binder content. The asphalt-binder film thickness also increased when the asphalt-binder content was increased; suggesting improved cracking resistance and durability. Also, all the rut magnitudes in Table 1 are less than 8 mm. So, if 12.5 mm is used as the threshold (TxDOT, 2004), all the asphalt-binder contents would be judged as producing mixes with sufficient laboratory rutting resistance. These laboratory results also corroborate Scullion (2007)'s observations that as long as these SFHMA mixes pass the Hamburg rutting test (i.e., laboratory rut depth less than 12.5 mm), the asphalt-binder content could still be increased to enhance workability and cracking

resistance, without compromising the rutting resistance characteristics of the mix.

Additionally, other ways to improve workability would be to increase the fines content in the aggregate gradation proportions, reducing the NMAS, or use of less absorptive aggregates such as crushed gravel or granite. However, majority of the SFHMA mix-designs utilized limestone aggregates, which are considered to be absorptive with an average water absorption capacity greater than 2%. Thus, it is possible that asphalt-binder absorption by the aggregates may have reduced the effective asphalt-binder content which ultimately contributed to the poor workability of these SFHMA mixes, particularly those fabricated with limestone aggregates. In one instance, the extracted asphalt-binder content from a field core where limestone aggregates were used was 3.3% versus 4.0% design; suggesting about 17% absorption (or loss).

SFHMA WORKABILITY – FIELD EXPERIENCE

Because of the relatively low asphalt-binder content and their coarseness nature, these mixes generally exhibited dryness and were generally associated with constructability (workability and compactability) problems in the field. Even with the increased number of compactive rolling passes, the 96% in-place target density was hardly achieved on most of the PP projects; about 8% core AV versus the 4±% target. Field non-destructive testing indicated considerable surface density variations while laboratory testing of field cores indicated very poor AV distribution structure (Walubita et al., 2007). There were, in general, wide spread localized locations of high voided areas (with potential for moisture entrapment), debonding, and vertical segregation. Fig. 4 shows some examples of vertical segregation and debonding from extracted cores.

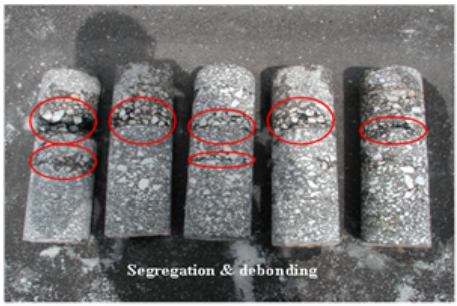


FIG. 4. Example of Aggregate Vertical Segregation and Debonding

Temperature inconsistency in the mat was also observed as one of the contributing factor to the compactability problems and non-uniformity in the final in-place density. However, use of the Roadtec as the material transfer device (MTD) for the hot mix lay-down operations tended to improve the mat temperature distribution profile and compactability of the mix, resulting in a relatively more uniform and consistent in-place density. The Roadtec yielded a more consistent mix due to remixing and more temperature uniformity in this MTD set-up. By contrast, the Windrow pick-up MTD system did not produce uniform surface temperature profiles; see Fig. 5.



FIG. 5. Comparison of Material Transfer Devices and Mat Temperature Profiles (Target Compaction Mat Temperature = 300 ℉ [149 ℃], Red Color; Blue Color = Cold Spot) (Walubita et al., 2007)

In general, improving the compacting rolling pattern, reducing the compaction lift thickness (from 5 inches [≅125 mm] to about 3 inches [≅75 mm]), adding more fines, increasing the asphalt-binder content, changing the MTD, and maintaining a consistently uniform high mix and mat temperatures improved compactability and in-place density attainment of the SFHMA mixes.

SUMMARY

In comparison to the traditional Texas dense-graded HMA mixes, the 1" SFHMA were found to be of relatively poor workability (constructability and compactability) characteristics. This was primarily attributed to the mix-design characteristics which comprised of moderately low asphalt-binder content (an average of about 4.2%) and coarser aggregate gradation. In the field, the 1" SFHMA mixes were associated with surface density variations, localized high voided areas, aggregate vertical segregation, and debonding problems. Field in-place density attainment was as difficult as it was in the laboratory during the mix-design process and material property characterization tests. Summarized, the major findings and observations from this study are as follows:

- Use of low asphalt-binder content and coarse aggregate gradation with low fines content (such as in the 1" SFHMA mixes) may often result in a less workable HMA mix, particularly in terms of compaction and in-place density attainment.
- Coarser graded aggregate mixes (such as in the 1" SFHMA) are more susceptible to surface density variations and non-uniform AV distribution structure, often with high localized voided areas that could even trap moisture.
- Coarser graded mixes such as the 1" SFHMA, because of the high proportions of larger rocks in the aggregate gradation matrix, are more prone to vertical segregation and honey combing.

- The choice and type of the MTD device used for the mix lay-down operations appears to have an influence on the mix-mat temperature uniformity and consistency; which is essential for both mix compactability and uniform in-place density attainment. A MTD set-up with a remixing capability, such as the Roadtec observed in this study, tends to yield better results.

Overall, improving the mix-design characteristics such as increasing the asphalt-binder content, increasing the fines content, reducing the NMAS, decreasing the larger aggregates proportions, and use of high quality less absorptive aggregates (such as crushed gravel and granite) tended to improve the workability of the 1" SFHMA mixes. In the field, increasing the number of compactive rolling passes, reducing the compaction lift thickness, use of the Roadtec MTD, and ensuring temperature consistency in the hot-mix yielded a more uniformly compacted mat with acceptable in-place density. However, because of workability and constructability problems experienced with these mixes, TxDOT is currently shying away from using these 1" SFHMA mixes and are researching other alternative mixes to serve as the main structural rut-resistant layers in future perpetual pavement designs.

ACKNOWLEDGEMENTS AND DISCLAIMER

The authors are thankful to TxDOT for funding this research study. Special thanks are also due to Simate G. Simate and Sihle A. Ndlovu for their technical comments. The contents of this paper reflect the views of the authors who are solely responsible for the facts and accuracy of the data presented herein and do not necessarily reflect the official views of any agency nor does the paper constitute a standard of any kind. Trade names were used solely for information and not for product endorsement.

REFERENCES

APA. *Asphalt Pavement Alliance: Perpetual Pavements – A Synthesis, APA 101*. MD, US, 2002.

Newcomb, D.E., Buncher, M., and Huddleston, I.J. "Concepts of Perpetual Pavements," Transportation Research Board, TRC No. 503, Washington D.C., December 2001, pp 4-11.

Scullion, T. Perpetual Pavements in Texas: The State of the Practice, Technical Report FHWA/TX-05/0-4822-1, Texas Transportation Institute (TTI), College Station, Texas, USA, 2007.

TxDOT. Memorandum on Full-depth Asphalt Pavements, Flexible Pavement Design Task Force Implementation, Texas Department of Transportation (TxDOT), Austin, TX, US (April 23), 2001.

TxDOT. *Standard Specifications for Construction and Maintenance of Highways, Streets, and Bridges*, Austin, TX, USA, 2004.

Timm H.D. and A.L. Priest. "Material Properties of the 2003 NCAT Test Track Structural Study" NCAT Report 06-01, Auburn, 2006.

Walubita, L. F. and Scullion, T. Perpetual Pavements in Texas: The Fort Worth SH 114 Perpetual Pavement in Wise County, Technical Report FHWA/TX-05/0-4822-2, TTI, TX, US, 2007.

Predicting Pavement Condition Deterioration for the Saudi Inter-Urban Road Network

Muhammad Mubaraki

PhD research student, Nottingham University, School of Civil Engineering, Nottingham Transportation Engineering Centre (NTEC). NG7 2RD, evxmam@nottingham.ac.uk

ABSTRACT: The Ministry of Transport (MOT) in Saudi Arabia uses Pavement Condition Rating (PCR) to report pavement condition. The PCR was developed by the World Bank in 1986. PCR is based on International Roughness Index (IRI), Rutting (RUT), Cracking (CRA), and Raveling (RAV). The MOT collects pavement condition data using a digital inspection vehicle (DIV). On some expressways, the MOT measures the Skid Number (SN) using a Skid Test Unit as complimentary measurement for safety issues. The objective of this paper is to develop a general prediction model for The Saudi Arabia Inter-Urban road network. Two models have been developed for the Inter-Urban road network using 10 years survey data for overlaid sections on some expressways in the network. One model is for PCR and the other one is for IRI. The PCR model is a function of pavement age (T), Traffic Volume (TV), and IRI. The IRI model is a function of RUT, RAV, and CRA. Overlaid sections across the entire network have been selected to study the mechanisms of pavement deterioration, to develop the model and to draw conclusions.

PAPER BACKGROUND

Pavement deterioration is a complex process and it involves not only structural damage but also many functional pavement distress types. It results from the interaction between traffic, climate, material and time. Deterioration is used to represent the change in pavement performance over time. The ability of the road to satisfy the demands of traffic and environment over its design life is referred to as performance. Due to the great complexity of the road deterioration process, performance or deterioration models are the best approximate predictors of expected conditions. The ability to accurately predict pavement performance, in terms of International Roughness Index (IRI), Rutting (RUT), Cracking (CRA), Raveling (RAV), and Skid Number (SN), is essential for a Pavement Management System (PMS) (Hass et al, 1994; Hajek and Hass, 1987; Shahin, 1994). However, in this

paper, the objective is to develop a prediction model as a function of IRI. The PCR is influenced by IRI and the IRI is influenced by pavement distress. Pavement surface roughness is a major concern associated with driving quality. Pavement roughness accelerates pavement deterioration because pavement roughness causes an increase in vertical stress received by the pavement and the aggravation of pavement fatigue. Pavement distress will also result in a deterioration of the pavement roughness index value. Therefore, pavement distress and pavement roughness have a mutually causal relationship, affecting one another in both directions. IRI reflects pavement distress conditions and it is feasible to express IRI as a function of PCR which reflects pavement performance in general, and consequently the IRI data will provide the most valuable information for the MOT to evaluate the network. The data collection tasks of large road networks like the Saudi network consume substantial cost of money and time. It is therefore reasonable to rely on IRI for managing network maintenance (Dong Lin et all, 2003).

FACTORS AFFECTING FUNCTIONAL DISTRESS OF PAVEMENTS

Pavement Condition Rating (PCR)

The Ministry of Transport (MOT) uses PCR to report pavement condition. The PCR was developed by the World Bank in 1986 and is based on International Roughness Index (IRI), Rutting (RUT), Cracking (CRA), and Raveling (RAV). The MOT collects pavement condition data using a digital inspection vehicle (DIV). The PCR ranges from 0 to 100. A value of 100 represents the highest performance point. On some expressways, the MOT measures the Skid Number (SN) using Skid Test Unit as complementary measurement for safety issues. The SN is basically the average coefficient of friction across the test length. It is calculated by dividing the horizontal force by the vertical load and then multiplying by 100 to get a whole number. It is basically an estimate of how much available friction for braking and stopping is available at a given section of road (MOT, 2008; MOT–PMS Unit, 2008).

Maintenance Types

The various options which have been applied on the MOT Network are overlay, patching, crack sealing, and pothole treatment. Due to the lack of information about the exact date of road network construction, this research has focused only on the overlaid road network as the overlay is a major maintenance and it will bring the pavement condition approximately to the highest performance point. It has been assumed that the pavement condition is 100 after applying an overlay and before opening the overlaid road to traffic. Therefore, the pavement age can be defined as the time that has passed since the overlay.

Pavement Characteristics

Due to the general similarities in pavement type, layer thickness, and material characteristics, and due to the lack of detailed pavement data such as mix design properties and pavement strength, it has been assumed that all the roads are structurally similar for each functional classification for the MOT network.

Traffic Volume

Average Annual Daily Traffic (AADT) is available for Rural Expressways since 2000. There was a need to do back projection for the years before 2000 based on the vehicle growth factor.

Climatic Condition

The climatic conditions across Saudi Arabia are fairly similar in terms of temperature and rainfall.

SCOPE

In order to address the major independent variables (i.e., age, traffic), the design of this research study considered the entire population of the Saudi Inter-Urban road network. All selected sections of pavements were overlaid pavement sections. This provided age, uniform material, construction and uniform pavement segments for analysis.

DATA COLLECTION

Data have been being sourced from the Ministry of Transport (MOT) where these data are categorized as historical data and pavement survey data. Historical data includes the maintenance type and date, while the survey data are traffic load, pavement condition, and pavement functional distress measurements.

DATA ANALYSIS

Brief Background

Regression models for the dependent variables PCR, IRI, RUT, RAV, and CRA were sought for the Inter-Urban roads in Saudi Arabia. The data over a ten year period were used in the model development. The independent variables used in the model are the pavement age (T) and average annual daily traffic (AADT). **IRI** is the International Roughness Index, the average of the left and right wheel path readings in inches per mile.

RUT is the average rut depth of the right and left wheel path in inches. **RAV** is the progressive disintegration of a hot mix asphalt layer from the surface downward as a result of the dislodgement of aggregate particles. **CRA** is Series of interconnected cracks caused by fatigue failure of the hot mix asphalt surface (or stabilized base) under repeated traffic loading. The pavement age (T) is the difference between the last major maintenance and the year of data collection in years.

Several analyses were conducted on the data set. The initial analyses were carried out to see the response among variables and statistical tests were performed on the developed models, namely the coefficient of determination and level of significance. The main tests conducted to validate the models were:

- Coefficient of determination (R^2).
- Level of significance at 0.05
- The homogeneity of variance (D value)
- The standard error
- Mallows' Cp value.

The coefficient of determination (R^2) and level of significance at 0.05 are the main criteria to be taken into account in the selection of good model. The coefficient of determination (R^2) describes the strength of the association between variables. If the p-value (P) of a coefficient is less than the chosen a-level, such as 0.05, the relationship between the predictor and the response is statistically significant.
The standard error of estimation is a measure of the accuracy of predictions made with a regression line. A model with a low value of standard error is preferred. One of the main assumptions for the ordinary least squares regression is the homogeneity of variance of the residuals. The Durbin Watson Statistic (D value) has been used to show the homogeneity. The D value ranges from 0 to 4 where the best value is 2. A small Mallows' Cp value indicates that the model is relatively precise (has small variance) in estimating the true regression coefficients and predicting future responses.

ANALYSIS PROCESS

First Step (Finding the best subset regression for pavement condition formula)

The MOT database contains four measurements namely IRI, RUT, RAV, and CRA. The PCR values are recorded which are calculated from the four measurements. Also the pavement age and the traffic volume are known. As the research aims to understand the possible trend shapes for the pavement condition rating, from engineering point of view, the PCR can be a function of time, traffic volume, and IRI. IRI can be a function of three distress measurements namely RUT, RAV, and CRA. The trend models could be linear, power, logarithmic, and a sigmoid. Several subsets regressions, stepwise regressions, and multiple regressions have been conducted to find the best subset that would be modeled based on different combinations and trend shapes. The time and traffic volume factors are highly significant with respect to pavement condition; the PCR model should therefore contain these two factors. The

IRI indicates the pavement performance for a given road. Therefore, a model to describe pavement condition could have these three predictors. As the pavement condition contains the IRI predictor, the IRI also can be modeled separately as function of three distress types. The Data has been subjected to analyses to find the best combination and trend shape. A good model should have high R^2, small standard error (s), and small Mallows Cp value. Different forms were tested and it was found that the PCR as function of T,TV,SQRT (IRI) is the best combination as the R^2 is high (79.9 %), Mallows Cp is small (4.0), D value is 1.25551, and the standard error of estimation is 6.64. The best combination for IRI was to raise each distress to power 0.25 and to add all the values together. The R^2 is high (93.0 %), Mallows Cp is small (3.0), D value is 1.13787, and the standard error of estimation is 0.210119.

Second Step (Regression Analysis based on the best combination and appropriate form concluded from first step)

The PCR was assigned as dependent variables; a significance level of 0.05 was set. IRI was assigned as independent variable, and significance level of 0.05 was set. The following models were developed with their own characteristics.

- PCR Model

PCR = 115 - 1.37 T - 0.00598 TV - 12.9 SQRT (IRI)
R^2 = 79.9%
P-value for all predictors and for the regression=0.0
D value = 1.25551
Mallows Cp = 4.0
Standard Error = 6.64674

IRI Model

IRI = 0.722 RUT^ 0.25 + 0.161 RAV^0.25 + 0.0979 CRA^0.25
R^2 = 93. %
P-value for all predictors and for the regression=0.0
D value = 1.13787
Mallows Cp = 4.0
Standard Error = 0.210119

Third Step (Validation of the Developed Model)

Two models have been developed during the regression process. The following are prominent indicators to show that the models are usable in a Pavement Management System (PMS).

- Coefficient of Determination R^2

The PCR model has an R^2 value of 0 799. This illustrates that 79.9% of the variation in the PCR in relation to IRI. However, the R^2 of the IRI model indicates 93 % of the variation related to RUT, RAV, and CRA.

- Standard Error of Estimation.

Standard error of estimation needs to be relatively small, meaning a small error in estimating the relationship in the equation. The value of 6.64764 and 0.210119 for the two models are considered small and acceptable.

- Durbin Watson Statistic (D Value).

The D values for the two models are 1.25551 and 1.13787 which are good and compared to other subsets. However, values close to 2 are the best. This means that the variance of the residual is almost constant which indicates the homogeneity of the variance.

CONCLUSION

In this paper, 10 years of data from overlaid sections on Saudi Inter—Urban roads have been employed in modeling pavement condition rating as a function of IRI, Traffic Volume, and time. The developed models could provide a reasonable prediction of pavement condition. Since the developed PCR model is a function of IRI, the developed IRI model can be inserted into the PCR model. In summary, the regression equation for a particular road network takes the following form:

PCR = 115 - 1.37 T - 0.00598 TV - 12.9 SQRT (IRI)

REFERENCES

Ministry Of Transport web site www.mot.gov.sa

Ministry Of Transport, Maintenance Department-PMS Unit 2008

Haas, R., Hudson, R. and Zaniewski, J., "Modern Pavement Management", Krieger Publishing Company, Malabor, Florida, 1994.

Hajek, J., and Hass, C., "Factors Analysis of Pavement Distresses for Surface Condition Prediction" Transportation Research Record (TRR), No. 1117, 1987, PP. 125-133.

Shahin, M., "Pavement for Airports, Roads, and Parking Lots", Chapman & Hall, New York, 1994.

Dong L, Tyng Y, Liang-H, "Correlation Analysis Between International Roughness Index (IRI) and Pavement Distress by Neural Network", 82th Annual Meeting, Washington, January 2003

Use of DCP (Dynamic Cone Penetrometer) and LWD (Light Weight Deflectometer) for QC/QA on Subgrade and Aggregate Base.

K Kessler
President. Kessler Soil Engineering Product, Inc. e-mail: ken@kesslerdcp.com

ABSTRACT: The DCP (Dynamic Cone Penetrometer) and LWD (Light Weight Deflectometer) are becoming ever more popular as mechanistic-empirical pavement design/construct procedures evolve. These instruments provide the ability to quickly, accurately, and economically measure shear strength and stiffness of in-place base course and subgrade material, thus obviating the need for density testing. These instruments are rugged, portable, easy to operate and do not have the regulatory disadvantages of a Nuclear Density Gauge. This paper outlines the genesis of the DCP for soil testing and the respective applications for various DCP configurations. The various types of LWDs and the results they produce are described. Finally, on going efforts in the use of these instruments as well as standards for QC/QA (Quality Control /Quality Assurance) for subgrade and aggregate base for roads are discussed.

KEY WORDS: DCP, LWD, Quality Control, Stiffness, Modulus, Deflectometer, Design/Build, roads, pavement, Subgrade, Base course.

1.0 INTRODUCTION

1.1 Currently many roads are being resurfaced every 5 to 10 years. These roads were built using maximum dry density for QC/QA. This paper will discuss the tools and procedures that could be used to give better pavement performance
1.2 Minnesota Department of Transportation found:
The specified density method is simple in theory but presents a number of challenges – sand cone test are time consuming, imprecise, difficult to perform on large particles and potentially unsafe for inspectors to perform. Additionally, compaction applied during a standard Proctor test does not represent compaction methods applied on today's construction sites. A materials density can be a poor indicator of performance compared to measuring stiffness and strength which are both sensitive to moisture content and stress state. Variation in density can have large effects on properties determining pavement performance. Therefore, accumulated errors in the specified density procedures can greatly influence the load bearing capacity of the soil. (Beyer *et al.* 2008)
1.3 Both South Africa and Germany produce roads lasting 20-25 years before they need resurfacing. This longevity is attributed to quality subgrade conditions which, in recent years, has been assured with stringent QC/QA testing using the DCP in South Africa (Method ST6) and the LWD in Germany.

2.0 BACKGROUND:

3.0 2.1 DCP HISTORY AND DEVELOPMENT**:** There are numerous DCPs that use a sliding hammer to drive a probe in the ground. The DCP with an 8kg

hammer (ASTM D-6959-03) is the only DCP used extensively for roads and airfields (see Figure 1).

An Australian County engineer in 1948 made a break through in field soil testing by correlating CBR to the penetration rate of a DCP (16mm driver rod with 20mm diameter, 60 degree point advanced with an 8kg sliding hammer dropped 575mm). This DCP was designed for base-course and sub-base material with aggregate less than 2". It was adopted by the South African ministry of Transportation in 1984 for QC/QA.

The US Army Corps of Engineers modified the hammer (show in Figure 1 below) so the mass could be reduced to 4.6kg making it usable in weak soil with a CBR 2% or less. The Corps also added disposable cone tip so that the instrument could be easily extracted from stiff or cohesive soils.

ASTM-D-6959 standard includes the correlation of the penetration rate to CBR. However, it is becoming more common to use the penetration rate in mm/drop rather that a correlation to CBR or further correlation to bearing capacity (pounds/sq ft).



Figure 1. DCP with 8 kg hammer



Figure 2. LWD with accelerometer

2.2 LWD HISTORY & DEVELOPMENT

The LWD was developed with the same principles in mind as the Falling Weight Deflectometer (FWD). However the FWD was used primarily on finished asphalt. They are expensive and are too heavy to use on subgrade testing so a lighter, portable version was developed, the LWD.

LWDs induce a soil response by dropping a weight onto a plate resting on the test layer. They have been correlated by the manufacture to the static plate load test (ASTM-D-1195). For the most part they are durable, light (< 35 kg), and fast (< 1 minute) and cost much less than an FWD (Falling Weight Deflectometer). Some LWDs have a load cell (ASTM-E-2583) that determines the force of the 10kg sliding hammer that is dropped 0.5m to 1.0 m. The time of loading is between 20 and 30 msec. The force is transmitted to a loading plate usually 200 mm or 300mm in diameter and the deflection is measured with a sensor, usually a geophone. Other LWDs use a fixed drop height (1.0 m or 0.5m) and a 10kg sliding hammer to determine the force (ASTM pending). The time of loading is between 20 and 30 msec. The force is transmitted to a loading plate 200mm to 300mm in diameter and the deflection is measured with a sensor, usually an accelerometer.

In Europe the 300mm diameter plate is preferred because it is also used on the Plate Load Test device and the FWD. In the US some prefer the 200mm plate because the depth of influence of the force is a factor of 1 to 1.5 times the diameter of the loading plate. The drop height of 0.5m rather than 1.0m makes the instrument less awkward to get in and out of a vehicle and to move it around the job site.

3.0 FACTS

3.1 To build the best possible road one needs know the engineering properties of the underlying material. Measurement and analysis of these properties is complex, not only because soil is not homogeneous but also because clays, silts and granular materials react differently to loading. The major properties of interest are density, moisture, shear strength, and stiffness/modulus.

3.2 **Density** is used extensively for QC/QA. It is relatively easy to obtain in practice but is linked to the Proctor Test that may not accurately represent the max dry density due to differences in compaction effort and/or variations in on-site soil composition. It is often measured in the field with a nuclear density gauge, sand cone or balloon device.

3.3 Knowing the **moisture** content of the material is essential. The ability to compact a soil to maximum density is a function of the moisture content. The shear strength and stiffness also vary with the amount of moisture in the soil. The Nuclear Density gauge, direct heat and Speedy moisture methods are used in the field today.

3.4 The CBR (California Bearing Ratio ASTM-D-883) was an original effort to define soil **shear strength**. Like wise the unconfined compression strength test (ASTM-D-2166) in an excellent indicator of soil shear strength. In the field, the DCP (ASTM-D-6951) is becoming increasingly popular due to its accuracy and ease of use for in-situ testing.

3.5 **Stiffness and modulus** (figure 3) can be measured in the field with a Static Plate Load Test (ASTM-D-1195) or a LWD. Both devices give measurements of the subgrade reaction to loading. The plate load test is reliable, but takes too long.

3.6 Modulus Determination: The commonly used method for extracting soil modulus from LWD test results is derived from the theory of a homogeneous, isotropic, linear elastic half-space subjected to a static load applied over a circular area. The relationship between the applied force via a circular plate and the surface displacement is given as:

$$\delta = 2F(1-\nu) / AGB \qquad \text{(Mooney } et\ al \text{ 2008)}$$

Where w is the vertical displacement of the center of the plate, G and v are the shear modulus and Poisson's ratio of the soil; A is the contact stress distribution parameter. The following equation, A=4 for an inverse parabolic distribution, πfor a uniform

distribution and $3\pi/4$ for a parabolic distribution (Timoshenko and Goodier 1951). Employing the relationship between G and Young's modulus E yields:

$$\mathbf{E = 4F(1-\nu^2) / AB\,\delta}$$ (Mooney *et al* 2008)

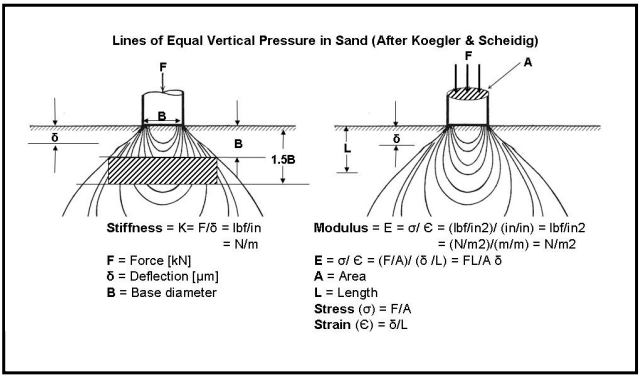


Figure 3

3.7 In South Africa they have produced virtually perpetual pavements. The Ministry of transportation gives credit to their preparation of the base course and subgrade. The DCP has been the standard QC/QA tool since 1984.

3.8 In Germany, the road builder guarantees the road. It is in the builder's best interest to build the best possible road and LWD helps them do just that. The LWD, with an accelerometer, is the instrument of choice for QC/QA. There are over 3000 of these units in a country the size of the states of Washington and Oregon.

4.0 ASSUMPTIONS

4.1 Most roads are designed using the lab tests for the subgrade material, for k (modulus of subgrade reaction), M_R (resilient modulus), or the CBR (California Bearing Ratio) sheer value. Ideally one would like to do QC/QA by measuring these same engineering properties in the field.
4.2 In-situ testing of compacted material for shear strength and stiffness/modulus better reflect future pavement performance than density.

4.3 Often highway departments seek to build roads at the lowest cost and then they assume the risk of maintenance and repair. The builder need only meet the QC/QA specifications during construction for density and moisture established by the respective highway department. This procedure results in the cheapest, but not necessarily the best possible road.

4.4 Adopting QC/QA methods which can more accurately predict pavement performance enables road builders to warrantee their work as is done in Germany.

5.0 IMPLEMENTING THE DCP AND LWD FOR QC/QA

5.1 TARGET VALUES: Highway Departments establish target values for the DCP penetration index and stiffness/modulus for the material being used in construction. Below, in Figure 4, is a sample chart from a draft report depicting the target modulus based on a soil's gravimetric moisture content for a given plastic limit. (Beyer *et al.* 2008)

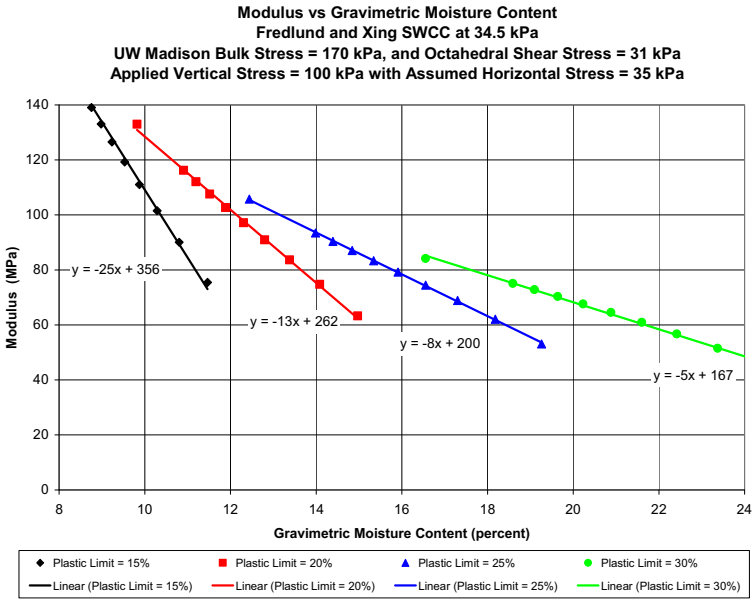


Figure 4

5.2 QC/QA TEST METHODS

5.2.1 DCP Road Testing Procedures

- Establish & record maximum allowable values
- Select test site, place DCP and record site information and initial DCP readings.
- Holding shaft perpendicular to ground, release weight and record penetration depth. Repeat five more times for a total of six drops at each location.
- The first 3 drops are seating drops. If the following is true, the test fails.

  Seat reading – initial reading > allowable seat
- The final 3 drops are used to calculate DPI (DCP Penetration Index). If the DPI is greater than the max allowable depth the test fails.

  DPI = final depth – seating depth

- Last determine if the layer is adequate it is adequate if the following is true.

Final reading – initial reading < test layer depth

- Testing for granular subgrade follows the same procedure, however comparative specifications differ.

5.2.2 LWD PROCEDURES

- Select test site & set up LWD connecting to its computational unit.
- Enter test site information according to established test procedures.
- Holding shaft perpendicular to ground, release weight, and record results manually and electronically. Repeat five more times for total of six drops.
- The first three drops are seating drops. The last three are data collecting drops used in data analysis. (Discard any erroneous data during testing).
- Analyze data using supplied software. Compare computed modulus to desired results.

5.2.3 MOISTURE Reading should be taken with each DCP and LWD test.

6.0 CONCLUSIONS

The implementation of QC/QA testing procedures that measure foundations properties of shear strength and stiffness/modulus more accurately reflect the road bed's suitability to handle traffic than older density testing procedures. The DCP and LWD would improve test precision; reduce inspection time, cost, and inspection personnel's exposure to traffic. The DCP and LWD do not require special handling, safety training, or certification. Additionally, timely direct verification of values can be accomplished. AASHTO incorporated modulus in design and build specifications in the 2002 draft guide. The instruments (DCP and LWD) and the methodology are available to implement these design specifications. They should be embraced and implemented now on a grand scale.

REFERENCES

1. METHOD ST6: (1984) Measurement of the In Situ Strength of soils by the Dynamic Cone Penetrometer (DCP), Special Methods for Testing Roads, Drag TMH6, Technical Methods for Highways (TMH), ISBN 0 7988 2289 9, Pages 19 to 24, 1984.
2. Beyer, M., Camargo, F., Davich, P., Jensen, J., Merth, S., O'neal, C., (Draft 2008) Using the Dynamic Cone Penetrometer (DCP) and Light Weight Deflectometer (LWD) For Construction Quality Assurance, LRRB Investigation 860 Draft Report V.5 MnDOT, St Paul, MN 55155
3. Mooney, M., Miller, P., (2008) Analysis of Light Falling Weight Deflectometer Test based on In-situ Stress and Strain Response, Colorado School of Mines, Golden, CO 80401 USA.
4. Tschebotarioff, G., (1951) Soil Mechanics, Foundations, and Earth Structures, An introduction to the theory and practice of design and construction, p.207, McGraw – Hill Book Company, Inc., New York.

A Discussion on the Optimum Bonding Condition between Semi-rigid Base and Asphalt Surface Course

Guan Hongxin

Communication and Transportation Engineering School, Changsha University of Science & Technology, Wangjiali Road 960#, Changsha City, P.R.C, PH (086) 0731-5258575; Fax (086) 0731-5219375; Email: guanhxin@sina.com

Abstract: The influence of bonding condition between surface course and uncracked base course on pavement structure mechanical response has been studied for many years. All research indicate that the bonding condition should be firm as far as possible to decrease the flexural stress at bottom of layers. It is inevitable for semi-rigid base course to crack due to temperature shrinkage and moisture shrinkage. Shear stress at crack tip due to offset load applying on one side of crack was calculated at different friction coefficient between surface course and cracked base course. Flexural stress at crack tip due to temperature dropping was also calculated at different friction coefficient between surface course and cracked base course. The calculated data show that shear stress and flexural stress at crack tip both increase when the friction coefficient increases, which indicates that the bonding condition should be as smooth as possible for cracked pavement structure. For actual pavement structure, there exists uncracked section between two adjacent cracks. It is discussed based on stress data to estimate which section cracks firstly. The results indicate that there exists the optimum bonding condition between surface course and base course.

Key words: *surface course, semi-rigid base, crack, optimum bonding condition*

Introduction

The bonding condition between pavement layers plays an important role on pavement structures performance. Xue Liang (2006) studied tensile stress and shear stress in pavements, and suggested avoiding the appearance of the slipping between the layers. Ziari Hassan (2007) analyzed the effects of interface condition on the life of

flexible pavements. Ai Changfa (2007) analyzed structural responses of asphalt pavements under combined factors of temperature, horizontal forces and vertical forces. Mariana R.Kruntcheva (2005) analyzed the pavement structure using a layered linear elastic program taking into account different degrees of interface bond between pavement layers and a static horizontal load in addition to the standard vertical dual load. Romanoschi (2001) discussed the effects of interface condition and horizontal wheel loads on the life of flexible and semirigid pavements.

The studies mentioned above all indicated that the bond between pavement layers should be as firm as possible. Moreover, calculating models they used were all uncracked pavement structure. It is well known that cracks developing in semi-rigid base courses are inevitable due to temperature shrinkage and moisture shrinkage. The influence of bonding condition between layers on pavement structure with cracked base course is unknown, which may be the real reason for reflective crack. In this paper, shear stress and flexural stress at the bottom of surface course will be calculated at different bonding conditions between the surface course and the cracked base course to study whether there exists the optimum bonding condition.

F.E.M. Analysis

In order to discuss the effect of bonding condition between surface course and cracked semi-rigid course on structure mechanical response, a pavement structure whose properties are shown in Table 1 was selected.

Table 1 Pavement properties

Layer	Thickness (cm)	Material	Stiffness (Mpa)	Poisson's ratio
upper surface course	4.0	AC13	2000	0.35
middle surface course	6.0	AC20	1800	0.35
bottom surface course	8.0	AC25	1200	0.35
base course	18.0	5% cement stabilized crushed stone	3800	0.35
subbase	18.0	lime and fly ash stabilized soil	2400	0.35
subgrade	-	soil	40	0.4

A three dimensional model was developed to simulate the pavement structure, which was 10m long (x axial direction) and 10m wide (y axial direction). The crack lying in the base course were 2mm wide in x axial direction, 10m long in y axial direction and 18cm high in z axial direction (depth direction). Other layers were all continuous and no crack existed in these layers.

F.E.M. was used to calculate structural response by means of ANSYS. Flexural stress at top of the crack induced by temperature changing and shear stress at top of the crack induced by offset load applying on one side of the crack were calculated separately. In order to minish the influence of stress singularity at crack tip, element solid 95 was used to mesh the area around crack tip. The axial load was treated as two circle uniform vertical pressure whose values were all 0.7Mpa.The radius of loading circle was 10.15cm and the distance between centres of the two circles was 30.45cm. In order to minish calculating time, the offset load on one side of the crack was equivalent to symmetrical pressure + antisymmetrical pressure, which is shown in Figure 1. The letter "A" in Figure 1 is the intersection point of crack area and loading circle. The radius of loading circle is also 10.15cm in Figure 1. The distance between the centres of two circles in Figure 1 is also 30.45cm. The letter "q" in Figure 1 represents 0.7Mpa. In Figure 1, symmetrical area and antisymmetrical area are all the crack area.

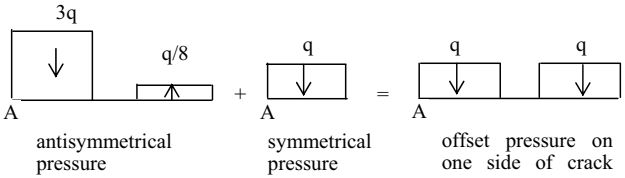


Fig. 1 An equivalent loading way for offset pressure on one side of crack

The influence of temperature changing was treated as temperature dropping amplitude varying with depth according to the study of Zheng Jian long (2001). In this paper, temperature dropping amplitude was assumed as $\Delta T(z) = \Delta T_0 e^{-z/30}$, where z is the distance from pavement surface(cm), and ΔT_0 is the temperature dropping amplitude of pavement surface(z=0). Assuming that ΔT_0 is -15℃, then the distribution of temperature dropping amplitude in pavement structure is calculated with ANSYS steady thermal analyzing module. Firstly, define the formula $\Delta T(z) = \Delta T_0 e^{-z/30}$ as temperature function in ANSYS to apply to analyze pavment structure; then set thermal analyzing parameters of pavement materials in ANSYS to be very small; Start ANSYS steady-state thermal analyzing to obtain temperature field. If the reference temperature is set at 0℃, the temperature of any point in analyzing pavement structure could be regarded as temperature dropping amplitude.

When vehicle moves through the place where semi-rigid base course is uncracked, another three-dimensional model was developed to compare structural response of this

uncracked model with that of the cracked model. Based on this uncracked model, flexural stress in different bonding conditions between the surface course and the semi-rigid base course were calculated. The geometrical size of this uncracked model was the same as the size of the cracked model except for no crack. The wheel pressure was symmetrically applied on this uncracked model.

Results and Discussion

When offset pressure applied on one side of the crack, shear stress at the top of the crack was calculated under different bonding conditions, which results are shown in Fig. 2. When temperature in cracked model drops, flexural stress at the top of the crack was calculated under different bonding condition, which results are shown in Fig. 2.

Fig. 2 Stress at crack tip varying with friction coefficient under axial load

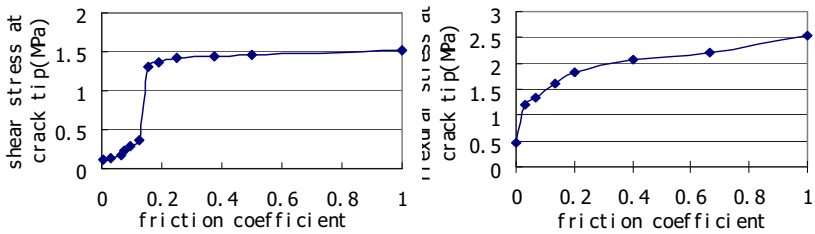


Fig. 2 shows that shear stress and flexural stress at crack tip increase rapidly firstly and then increases slowly when friction coefficient increases. It indicates that the bonding condition between surface course and base course should be set as smooth as possible when crack exists in semi-rigid base course.

If no crack exists in the base course, many scholars have studied stress varying trend. Uncracked-model-based results about flexural stress are shown in Fig. 3.

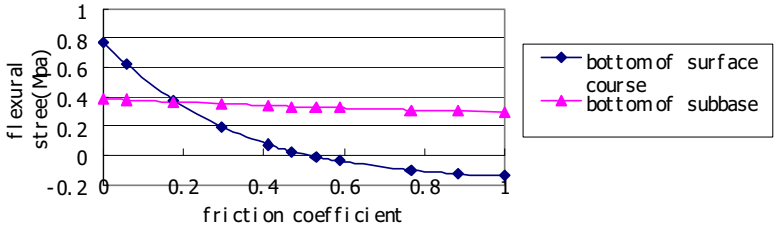


Fig. 3 Flexural stress at the bottom of layers varying with friction coefficient under axial load

Fig. 3 shows that flexural stress at the bottom of surface course and subbase both decrease when friction coefficient increases. The flexural stress at the bottom of surface course even becomes pressure stress when bonding strength between surface course and uncracked base course exceeds a certain value. It indicates that the bonding condition between surface course and base course should be set as coarse as possible when there exists no crack in the semi-rigid base course.

Obviously, two contrary results are obtained based on the calculated data mentioned above. For an actual pavement structure, the crack in semi-rigid base course is inevitable before the pavement opens to traffic and the distance between two adjacent cracks is relatively long. That is to say, the crack in the base course may reflect to the surface course firstly, or the bottom of surface course corresponding to the uncracked base course may crack firstly when the bonding condition varies.

Now a simple fatigue life analysis can be developed to discuss the optimum bonding condition. The splitting strength of bottom surface course σ_S is assumed as 1.0Mpa and the antishear strength of bottom surface course τ_S is assumed as 3.8Mpa. It must be explained that shear stress at crack tip in Fig.2 is not the real stress because of the stress concentration effect. The shear stress is only used to show the influence trend of bonding condition on structure mechanical characteristic in this paper.

According to "Chinese Specifications for Design of Highway Asphalt Pavement", the flexural fatigue life can be calculated as $N_f = \left(\frac{\sigma_s}{0.09\sigma_c} \right)^{4.55}$, and the shear fatigue life can be calculated as $N_f = \left(\frac{\tau_s}{0.33\tau_c} \right)^{6.67}$, where σ_c is flexural stress, τ_c is shear stress. Then the fatigue life corresponding to flexural stress and shear stress in Fig. 2 and Fig. 3 were calculated in terms of formulas mentioned above. The calculated results are shown in Fig. 4. The curve marked "uncracked structure flexural fatigue" was not drawn in Fig.4 when friction coefficient is larger than 0.48, because the flexural stress at the bottom of surface course turns to pressure stress at that time.

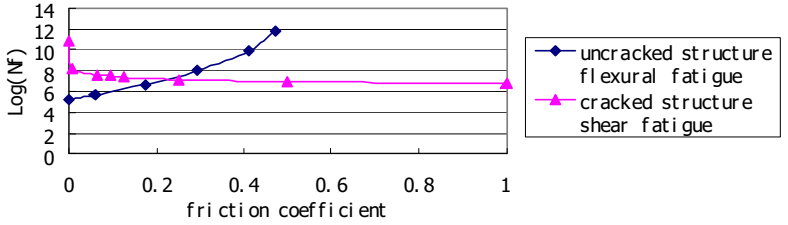


Fig. 4 Fatigue life comparing between the uncracked structure due to flexural stress and the cracked structure due to shear stress in different bonding conditions

Fig.4 shows that crack occurs earlier at the bottom of surface course corresponding to uncracked base course when friction coefficient is less than 0.22, while crack in base course reflects earlier when friction coefficient is larger than 0.22. So, it is necessary to compare fatigue life btween cracked structure and uncracked structure to obtain fatigue life of a asphalt pavement containing cracked base course section and uncracked base course section.

In addition, the flexural stress level at the crack tip due to temperature dropping is also serious, which may induce reflective crack occur only after few temperature varying cycles if bonding strength between surface course and base course is very firm.

Conclusions

From mentioned above, we can draw conclusions as follows:

Shear stress at crack tip due to offset load applying on one side of crack increases when friction coefficient between surface course and cracked base course increases;

Flexural stress at crack tip due to temperature dropping increases when friction coefficient between surface course and cracked base course increases;

Taking into account flexural stress decreasing with friction coefficient, the optimum bonding condition between surface course and base course is existent in theory, which will extend fatigue life of the whole pavement structure which contains cracked base course section and uncracked base course section as long as possible.

References

Xue Liang, Zhang Wei-Gang, Liang Hong-Jie (2006). “The mechanical response analysis of asphalt pavement in different interface condition between layers”. *Journal of Shenyang Jianzhu University (Natural Science)*, Vol. 22(4): 575 - 578

Ziari, Hassan and Khabiri, Mohammad Mahdi(2007). “Interface condition influence on prediction of flexible pavement life”. *Journal of Civil Engineering and Management,* Vol. 13 (1): 71 - 76

Ai Changfa, Qiu Yanjun, Mao Cheng , Lan Bo(2007). “Influence of Interlayer Conditions on Structural Responses of Asphalt Pavements”, *International Conference on Transportation Engineering 2007 (ICTE 2007)*:272-277

Mariana R.Kruntcheva ;Andrew C.Collop ;and Nicholas H.Thom(2005). “Effect of Bond Condition on Flexible Pavement Performance”. *JournalofTransportationEngineering*, Vol. 131(11): 880-888

Romanoschi, Stefan A.; Metcalf, John B(2001). “Effects of interface condition and horizontal wheel loads on the life of flexible pavement structures”. *Transportation Research Record*, n 1778:123-131

JIA Lu, SUN Lijun, HUANG Likui, QIN Jian(2007). “A Numerical Temperature

Prediction Model for Asphalt Concrete Pavement". *JOURNAL OF TONGJI UNIVERSITY(NATURAL SCIENCE)*, Vol 35(8):1039-1043

Zheng Jian long, Guan Hong xin(2001). "A finite element analysis based on thermal viscoelasticity theory of reflective crack resulting from low temperature shrinkage", *China Journal of Highway and Transport*, Vol. 14(3):1-5

Study of the behavior of aggregates demolition by the Proctor and CBR tests

Omar Boudlal[1] and Bachir Melbouci[2].

[1]Doctorant, Geotechnical Laboratory (L.G.E.A), Department of civil engineering; University Mouloud Mammeri of Tizi-Ouzou, Algeria; boudlal_omar@yahoo.fr
[2]Professor, Geotechnical Laboratory (L.G.E.A), Department of civil engineering; University Mouloud Mammeri of Tizi-Ouzou, Algeria.

ABSTRACT: The present study is a part of a large project on the valorisation of concrete demolition aggregates in order to contribute to their re-use in the field of the civil – engineering, particularly in roads. After the recycled aggregates are sorted and selected, their characterization is based on the comparison of their physical and mechanical behaviors with the natural aggregates (sand and gravel). Then their responses under the Proctor and the CBR tests are studied before and after treatment with sand, cement and clay additions. However, the results obtained showed that the characteristics of the recycled aggregates are lower than those of the natural aggregates. We thought then to improve them by the additions quoted herebefore. The addition of these materials, allowed to appreciably ameliorate some of their physical and mechanical characteristics approaching those obtained for the natural aggregates.

INTRODUCTION

The recycling of the concrete is more imposed in these lasts years. The various activities of civil engineering (construction, rehabilitation, demolition…) and earth-quakes generate mountains of aggregates stored or abandoned around the damaged cities and can thus have dangerous effects on the environment.

At the time when the demand for aggregates is very important and the careers are often unable to satisfy the needs for construction, the use of recycled materials offers three major advantages : economy of the discharges; economy of the careers and economy in transportation because they are local materials [Destombes and al, 2003].

The following study consists on treating these remains with cement, sand and clay to subject them to the Proctor and CBR tests for better knowing their behavior under the different requests before and after treatment.

IDENTIFICATION TESTS

The identification of the demolition aggregates or concrete aggregates (C.A) was made in many countries, but considering that their composition differs from a country to another [Canal, S. 1999], it is thus necessary to obtain these identification tests in this study to have specifics results to the studied local materials.

THE CONCRETE AGGREGATES (C.A)

The Physical characteristics obtained at the laboratory give the following results: a density of the grains (ρ_s = 2.62 g/cm^3), a dry density (ρ_d = 2.62 g/cm^3), a natural water contents (w = 2.40 %), a void ration (e = 49 %) and a degree of saturation (Sr = 1.5 %).

The "hardness" is evaluated by the Los Angeles (LA) and the Micro-Deval (MDE) tests in the presence of water. The results checks the condition (LA $\leq$ 40, MDE $\leq$ 35 and LA + MDE $\leq$ 65) of XP P 18-540 code, which classifies the aggregates studied in the E+ class distinguished in the class E. The aggregates concerned with this classification can have better applications compared to materials of class E, they can particularly be re-used in roadways under heavy traffics.

THE ADDITIONS (SAND, CEMENT AND CLAY)

- The sand equivalent at sight (ES < 60) and the sand equivalent by piston (ESV < 65). It is "clayey sand", it is rejected for the quality concretes.
- We used a composed Portland cement: CPJ - CEM II/A 42.5 NA 442.
- The Atterberg limits determined at the laboratory: liquid limit (w_L = 43.5 %); plastic limit (w_P = 20.15) and the plasticity index (I_P = 23.35) showed that it is a not "very plastic clay".

MECHANICAL TESTS

After identification, samples before and after treatment by the various additions (sand, cement and clay) with proportions of (5, 10, 15, 20 and 25%) are subjected to compaction test with modified Proctor process and California Bearing Ratio (CBR) test before and after immersion during 4 days.

MODIFIED PROCTOR TESTS

The first series of test consists on compaction the samples before and after treatment by the various additions with the modified Proctor process.

The best results obtained with well defined proportions of additions are illustrated on figure (1).

At first sight, the Proctor curves of the concrete aggregates treated by the various additions are more pointed than those of the untreated aggregate that showed the sensitivity of mixtures to water, particularly those containing the cement.

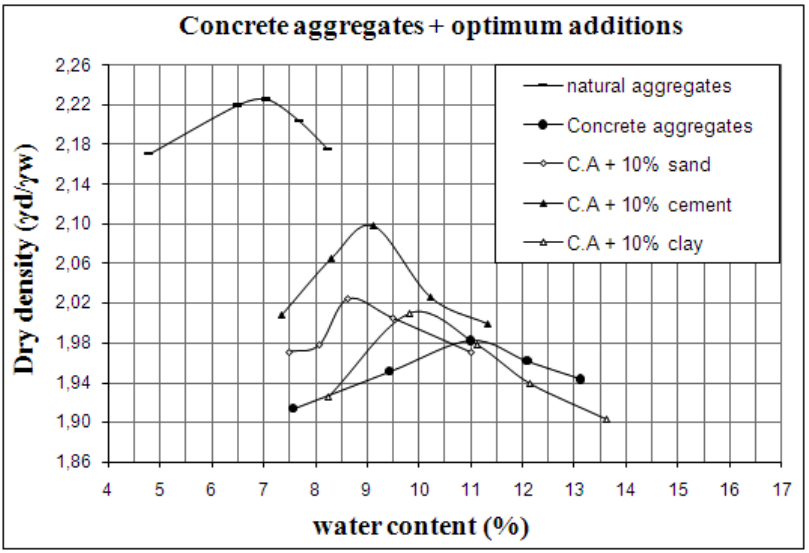


FIG. 1. Proctor curves of the concrete aggregates with the various additions.

The Proctor curves, presented on figure (1), show that an optimum addition of 10% of (sand, cement or clay) makes notable improvements to the compaction. On one hand, the dry densities are higher and on the other one, the water contents are reduced.

The concrete aggregates after treatments are better compacted and show better characteristics at the compaction.

The mixtures are compacted with a less quantity of water, in particular with 10% of cement or sand where the optimal water content does not exceed 9%. That led to an invaluable saving in water which is rare in the desert areas.

The dry density is appreciably improved with the various additions and reached its maximum value of 2.1 for the concrete aggregates mixed with 10% of cement. However, we noticed that the addition of 10% cement gives the most appreciable results and approach advantage of those obtained with the compaction of the natural aggregates under the same conditions of laboratory.

CALIFORNIA BEARING RATIO (CBR) TESTS

The second series of test consists on measuring the bearing pressure of the mixtures. With this intention, the samples having given the best maximum dry densities during the modified Proctor tests were punched with the CBR press before and after immersion during 4 days.

The results of the CBR tests (CBR index: CBR, CBR index after immersion: CBR_{imm} and the relative linear swelling: G) obtained at the laboratory are presented in the table (1).

Table 1. Results of the CBR tests.

Materials	CBR (%)	CBR_{imm} (%)	G (%)
Natural aggregates	76	58	0.00
Concrete aggregates	84	128	0.01
Concrete aggregates + 10% sand	88	124	0.02
Concrete aggregates + 10% cement	150	200	0.02
Concrete aggregates + 10% clay	34	44	0.03

The two CBR indexes (CBR and CBR_{imm}) obtained during the punching of recycled concrete aggregates before and after treatment by the various additions (except for the clay addition), are very satisfactory, they translate thus a positive behavior at the time of their implementation under traffic engines and after their startup face the aggressive climatic agents.

The treatment obtained by cement appears more interesting. Indeed, the addition of 10% cement made it possible to modify the bearing pressure of the mixture and to bring about an increase of its CBR and all the more to its CBR_{imm} index, which one considers equal approximately 200% (maximum value recorded compared to all the other additions) this confirms the results obtained by [Lamara, 2005 and Singh, 2008]. That can be due to the reactions of cement with water. Let us recall that 10% cement, corresponds to the percentage giving the highest dries densities during the modified Proctor tests.

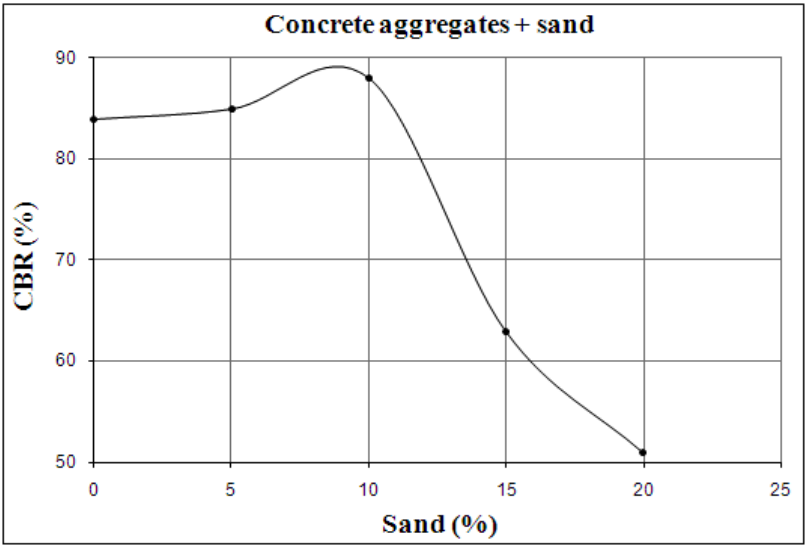


FIG. 2. Evolution of CBR Index according to the sand addition.

The CBR index improves gradually with the addition of sand to reach its maximum value of (88) with the optimum addition 10% of sand. Beyond this quantity, the CBR index decrease until to reach its minimal value of (51) with 20% addition of sand. The quantity 10% of sand is that suitable to fill the existing vacuums between the recycled concrete aggregates, thus offering to the mixture a better dry density and a better bearing pressure.

The relative linear swellings (G) presented in table (1) are very weak, they vary between 0.01 and 0.03 %. They can be thus regarded as null. That shows that these aggregates (mixtures), practically do not present variations of volume, thus giving them a good stability even in the presence of water.

CRUSHING OF THE GRAINS

The fracture of the grains occurs on a large scale during the compaction of the grounds, particularly in the road fields.

Indeed, crushing appears when the constraints imposed on the grains exceed their own resistance. This crushing improves the performances of material by decreasing its compressibility and its permeability; it is evaluated by comparing spreading out of the sieve curves test before and after test [Biarez and Hicher, 1997].

The results obtained at the Proctor tests for sand additions of 5, 10 and 25 % are presented on the figure below:

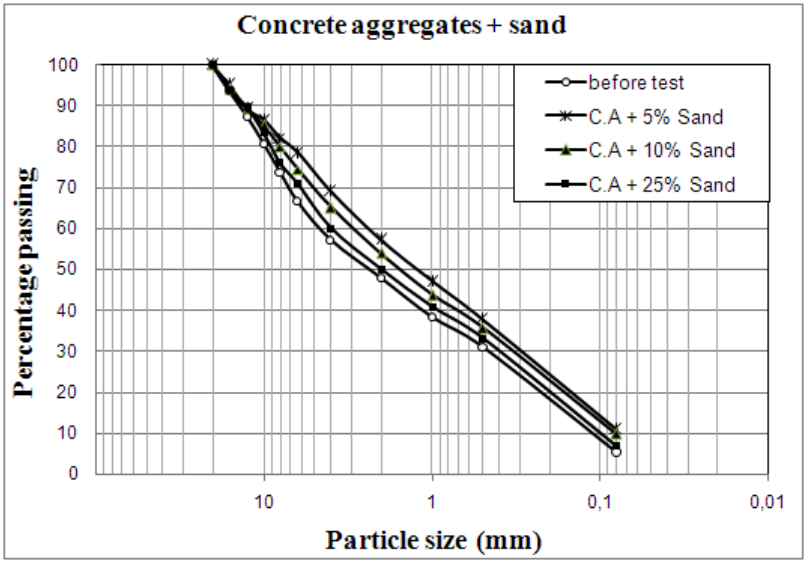


FIG. 3. Evolution of the crushing degree according to the sand percentage.

This curves shows that, the more sand addition is significant the more crushing decreases. Indeed, on one hand the number of point of contact increases and the effort concentrated between the grains decreases, on the other hand the small particles are more likely to move under the effect of the forces than to be crushed, which generate a fall decrease of crushing compared to material without sand.

VI. CONCLUSIONS

The results obtained by this study showed the improving role of the various additions, particularly cement, in the mechanical behavior of the recycled aggregates subjected to the various efforts (Proctor and CBR tests).

The treatment with cement and sand has certainly very appreciable results at CBR tests but this improvement does not reach the performances of the natural aggregates to the compaction tests.

The characterization of these aggregates made it possible to conclude that they cannot be regarded as residues in the discharges in particular after their treatment by the various additions. However, some of the studied mixtures will constitute materials being able to be re-used in roadway to weak or average traffic.

This study will be supplemented by other types of tests such as the direct shear tests and the triaxial compression tests (in particular cyclic tests) to have a better understanding of the long term behavior of these materials under the influence of the traffic.

VII. REFERENCES

Biarez, J. et Hicher, P. Y. (1997). "Influence de la granulométrie et de son évolution par ruptures de grains sur le comportement mécanique de matériaux granulaires". *Revue Française de génie civil.* Volume 1- N°4/1997, p 607-631.

Canale, S. (1999). "The utilisation of the material from demolition in the roads construction. " *Congress proceedings* R99, Vol 3, Geneve Switzerland, PP 353-357, 1999.

Destombes, M. et Al. (2003). "Les bétons et produits de démolition recyclés." *Guide technique pour l'utilisation des matériaux régionaux d'Il de France*, Décembre 2003.

Lamara, M., Lakhdar, M.F., Gouali, I. (2005). "L'ajout des particules fines pour ameliorer la capacité portante des assises de chaussées" *Seminaire sur le compactage*, 25-26 mars, Hammamet-Tunisie 2005.

Singh, S.P. (2008)., Tripthy, D.P., Ranjith, P.G. (2007). "Performance evaluation of ciment mobilized fly ash-GBFS mixes as a highway construction material." *Elsivier Waste Management* 28 (2008) 1331-1337.

Research on Dry-shrinkage Performance of Cement-treated Base Materials

Wang Yan[1], Ni Fujian[2], Xuan Weihong[3]

[1]PH.D, Faculty of Built Environment and Engineering, Jinling Institute of Technology, 99 Hongjing Road, Nanjing, Jiangsu province, PRC, 211169; wangyan.seu@gmail.com
[2]Professor, School of Transportation, Southeast University, 2 Sipailou Road, Nanjing, Jiangsu province, PRC, 210096; nifujian@gmail.com
[3]Professor, Faculty of Built Environment and Engineering, Jinling Institute of Technology, 99 Hongjing Road, Nanjing, Jiangsu province, PRC, 211169; xwh@jit.edu.cn

ABSTRACT: Shrinkage cracks are easy to occur in cement-treated macadam base when temperature and humidity change. In order to study the drying shrinkage and cracking performance of different cement-stabilized macadam base materials, dry-shrinkage performance tests were carried out by mixing the cement-stabilized macadam mixture with different gradations and cement dosages, ranging from 2% to 5%. Hence, a model for evaluating the dry-shrinkage performance of cement-stabilized macadam mixture was made on the basis of the mixture's dry-shrinkage performance's relationship with water loss rate, exposure time, cement dosage, gradation and other elements. The experiment shows that the mixture's dry-shrinkage performance is the best when mixed with fine gradations and the cement is added by 3% to 4%.

INTRODUCTION

When the shrinking stress caused by the change of the humidity in the base course is higher than the material's strength of tension, shrinking cracks come into being in transverse direction in the cement-stabilized macadam base. With the formation of the cracks, rainwater sinks into the pavement structure through the cracks and spreads all around, which can bring the great damage of sludge slopping and net-shaped cracking under the repeating load pressing of vehicles and cause the decrease in the bearing capacity of the base course. Though a lot of research has been done in the anti-erosion capability[1)] and durability[2)] of the semi-rigid base and lately researchers began to study the shrinking performance[3)] of cement-stabilized macadam material, no effective solution in controlling the dry-shrinkage cracking of cement-stabilized macadam base has been proposed.

The indoor dry-shrinkage performance is carried out to analyze how water loss rate, exposure time, gradation, cement dosage and other factors affect the dry-shrinkage performance of the cement-stabilized macadam mixture. A dry-shrinkage strain and dry-shrinkage coefficient evaluating formula in cement-stabilized macadam-based

layer is set up with the help of the experimental data. This research will provide an experimental and theoretical basis for choosing the reasonable cement-stabilized base materials and reducing the base course dry-shrinkage cracking in practical construction.

THE RAW MATERIAL'S CHARACTERISTICS AND GRADATION DESIGNING

The cement employed is the 32.5# composite silicate cement, the fineness degree of which is 3.2%, the primary solidifying time of which is 5.3h while the final solidifying time 7.4h. The aggregate consists of No. 1, No. 2, No. 3 and No. 4. The crushing value of the aggregate is examined to be 22.8%; the liquid limit and plasticity index should also be examined if the grain diameter is below 0.6mm. The rest of the capability data of the cement and aggregate all meet the criterion[4].

Three gradations employed in this experiment are: the medium value of the standard gradation range, i.e. fine gradation (marked as "z"), the rough gradation of the standard gradation range (marked as "c") and the skeleton gradation[5] determined by the compacting test (marked as "g"). The gradations are shown in Table 1.

Tab.1 Composition of Different Aggregate Gradation

Gradations	Sizes of Sieve Pores(mm)							
	31.5	26.5	19	9.5	4.75	2.36	0.6	0.075
z	100.0	94.7	82.6	54.3	42.0	27.2	13.9	2.5
c	100.0	92.5	75.2	43.1	30.6	14.8	7.5	1.4
g	100.0	-	47.6	36.0	26.4	16.2	8.3	1.5

2% to 5% of cement of three gradations is chosen in the dry-shrinkage performance experiment so as to find out the classic cement-stabilized macadam-based materials on the basis of the drying shrinkage characteristics.

The original water content of specimens and the maximum density of every kind of gradations obtained by compaction test were as follows.

Tab.2 Results of Compaction Test

Cement dosage (%)	The optimal water content (%)			The maximum density (g/cm3)		
	z	c	g	z	c	g
5.0	5.6	5.4	4.8	2.39	2.38	2.39
4.0	5.4	5.2	4.6	2.39	2.35	2.39
3.0	5.0	5.2	4.6	2.38	2.34	2.36
2.0	5.0	5.0	4.2	2.38	2.27	2.33

THE DRY-SHRINKAGE EXPERIMENT

The dry-shrinkage experiment is performed at the temperature of 25 degree centigrade and with the humidity of 50%. The beam specimen chosen for the experiment measures are about 100mm * 100mm * 400mm. Strain gauges are pasted on

both sides of the specimen to test the straining change (Figure 1(a)). The strain data are collected by computers while the water content change of the specimen is recorded manually. The test time interval is once every six hours on the first day, once every twelve hours from the second to the fifth day, once every twenty-four hours thereafter until the water content basically stops changing. All the valid results of dry-shrinkage test can be found in Figure1 (b). (Notes: Some data are eliminated due to their great variability.)

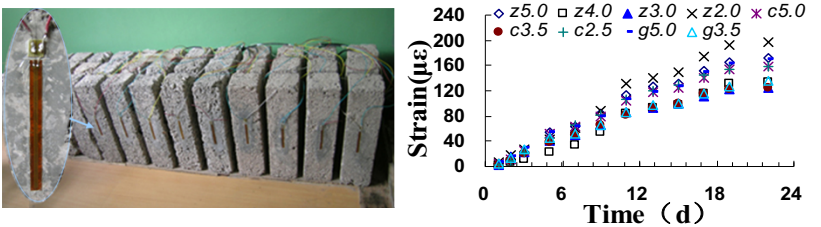


FIG.1. Test Photo and Results

THE EFFECT ON DRY-SHRINKAGE CHARACTERISTICS CAUSED BY WATER LOSS RATE

The water loss rate is obtained by dividing the water loss by the dry weight of the specimen and used to evaluate the dry-shrinkage characteristic of different mixtures under certain conditions of water loss. As the mixture's dry-shrinkage characteristic changes are similar in terms of the change of the water loss rate under conditions of different cement dosages 5% of the cement dosage is taken as an example (the same as follows) to analyze the rule of how the dry-shrinkage strain of the mixture and the average dry-shrinkage coefficient changes in accordance with the water loss rate.

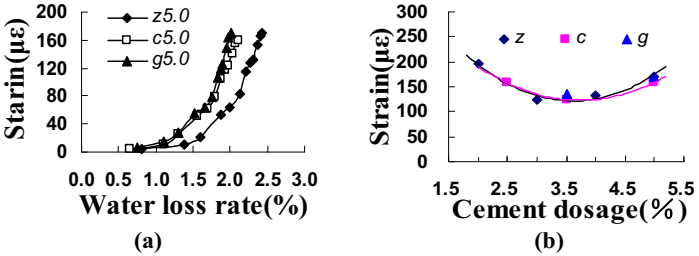


FIG.2. Rules of Dry-shrinkage Strain Changes with Different Factors

According to Figure 2(a), when the water loss rates are the same, the dry-shrinkage strain in fine gradation are low while the dry-shrinkage characteristics in rough

gradation and skeleton gradation are not so different, because the high porosity factor in rough gradation can provide sufficient room for the mixture's shrinking. A conclusion can be drawn by observing the experiment that during the prior period the water content of the specimen loses fast and the water loss rate increases fast, as a result of which the water loss rate of the first three days occupies 60% of the total. The shrinking strain capacity reaches only 20% of the total shrinking capacity during this period. Thereafter the water loss rate slows down until it becomes stable. Finally the water content of the mixture reaches around 2%, which is the same as the conclusion of the documents[6].

With the increase in the exposing time, the water loss and water loss rate increase constantly. For different gradations, the finer the aggregate is, the higher the maximum water loss rate is, because the optimum water content in fine gradation is much higher than that in rough gradation; on the other hand, when the cement dosage is higher while the gradations remain the same, the water loss rate is low even though the optimum water content increases a bit, probably because the hydrating process needs more water while the cement dosage is high.

THE EFFECT ON DRY-SHRINKAGE CHARACTERISTICS CAUSED BY THE CEMENT DOSAGE AND GRADATION

Since the cement dosage and gradation are the key factors that affect the strength of the cement-stabilized macadam base, the cement dosage and gradation's effect on the dry-shrinkage performance of the base material must be analyzed in order to determine the cement-stabilized macadam with best shrinkage characteristics.

The experimental result of the mixture's dry-shrinkage strain under the conditions of different gradations and cement dosage is shown in Figure 2(b). The gradation has no significant effect on the maximum dry-shrinkage strain. The average dry-shrinkage coefficient calculated by test results in fine gradation is a bit lower than that in the other two gradations. The lower the cement dosage is, the more obvious the difference will be. One reason might be that with much fine aggregate in fine gradation, the cement can hydrate completely and there isn't much water lost inside the mixture except the free water on the surface. Another reason is that the strength in fine gradation is high, the void ratio is low and the coarse aggregate and cement agent produced in the cement hydrating process inhibit the shrinking to a great extent.

Under the same gradation, with the increase in the cement dosage, the maximum dry-shrinkage strain and the average dry-shrinkage coefficient of the mixture both decrease first, and then increase. There is an optimum cement dosage value from 3% to 4% which can make dry-shrinkage strain and average dry-shrinkage coefficient reach their minimum degree.

SETTING UP THE EVALUATING MODEL

Since the experiment has confirmed the effect caused by the cement dosage, gradation and other factors on the dry-shrinkage performance of cement-stabilized macadam mixture, a dry-shrinkage performance evaluating model(formulae 1 and 2) for cement-stabilized macadam mixture, which can be affected by different gradations, cement dosages, water loss rate and exposing time, is set up in order to facilitate the

design and choice of the base course material and realize the non-linear regression of the experimental data by composing the program with the software-MATLAB[6]. The evaluated optimum value of the parameters is shown in Table 3.

$$y_1 = (a \cdot P_1 + b \cdot P_2) \cdot (C_e^2 + c \cdot C_e + d) \cdot (W_a^2 + f \cdot W_a + g) \cdot T_d \quad (1)$$

$$y_2 = (a \cdot P_1 + b \cdot P_2) \cdot (C_e^2 + c \cdot C_e + d) \cdot (Exp(f \cdot W_a)) \cdot T_d \quad (2)$$

Where, y_1: Dry-shrinkage strain, y_2: Dry-shrinkage coefficient, P_1, P_2: Gradation coefficient, C_e: Cement dosage, %, W_a: Water loss rate, %, T_d: Exposure time. h.

Table.3 Optimal Estimate Parameters for the Two Formulas

Variables	Regressive coefficient						Correlative coefficient
	a	b	c	d	f	g	
y_1	-0.001	-0.046	-7.540	19.115	-0.776	-31.355	0.971
y_2	0.061	2.104	-7.540	19.136	-0.572	—	0.962

Step-by-step antitheses intend to draw a conclusion by analyzing the observation data obtained in pairs through an experiment done under the same condition in order to compare the two products, two instruments, two methods, etc[7]. As t-statistic is employed to test in the hypothesis testing. The test is called t-test based on the paired data or t-test based on the paired observation value. T-test is adopted to inspect the validity of the model. After the respective bilateral t-tests on the evaluating model's paired data on the significance level of 0.05, the result can be seen in Table 4.

Table.4 Analyzed Result of T-Test

Variable type	y_1		y_2	
	Measured value	Calculated value	Measured value	Calculated value
Average value	81.478	81.190	37.796	37.659
Square deviation	2857.982	2822.512	479.4	471.5
Observed value	108	108	180	108
Poisson related coefficient	0.985		0.981	
Hypothesis average deviation	0		0	
Statistical variable-t	0.329		0.332	
P(T≤t) bicaudate	0.743		0.741	
t-bicaudate criticality	1.982		1.982	

Note: The calculated value in Table 3 means the fitted values based on the developed models.

The analyzed result shows that all the absolute value of t-statistic of the model is lower than the bilateral critical value. It brings forward such a conclusion that the measured value and evaluated value don't have any distinct difference; the model is valid and can be adopted to determine the dry-shrinkage performance of different mixtures.

As the shrinking performance evaluating model is set up on the basis of the indoor experiment, it works with great accuracy when the experimental condition conforms to or is close to that of the research. Any change in the experimental condition, e.g. the environmental humidity and the temperature, can affect the result of the experiment. Hence the model should be further amended and verified with more indoor and outdoor detecting data, so as to accurately evaluate the dry-shrinkage performance of the cement-stabilized macadam mixture.

CONCLUSION

The following conclusions have been reached from this study.

1. After dry-shrinkage experiments with different types of cement-stabilized macadam mixtures, the dry-shrinkage performance of the mixture with the fine gradation and cement dosage ranging from 3% to 4% is found to be optimum.
2. A dry-shrinkage performance evaluating formula of cement-stabilized macadam mixture is set up and verified. Though the model works with great accuracy under certain conditions, it should be further amended and verified with more practical project data.

More details about how to transform the test result to final shrinkage crack's controlling can be found in correlative literature[6].

ACKNOWLEDGMENTS

The authors appreciate the support of the Jiangsu Transportation Research Foundation, as well as thank my co-worker Li Zaixin, Li Qiang etc. for their valuable assistance.

REFERENCES

1. Hu Liqun and Sha Ai-min. (2003). "Experiment and Mechanism Analysis for Anti-erosion of Cement Stabilized Soil Material Base-course of Bituminous Pavement" *J*. China Journal of Highway and Transport, Vol. 23(01) 15-18.
2. Sha Qinglin. (1998). "Asphalt Pavement on Semi-rigid Road base for High-class Highways" *M*. China Communications Press.
3. Yang Wen-ding (2004). "Research on Shrinkage Performance of Semi-rigid base Materials" *D*. Chang'an University.
4. JTJ E42-2005. "Test Methods of Aggregate for Highway Engineering". *S*. China Communication Press.2005.
5. Li Zaixin. (2006). "Research on the Performance of Cement Stabilized Aggregate Mixture and Indexes Correlation-ship". *D*. Southeast University.
6. Wang Yan. (2008). "Research on the Mechanism and Design Method of Cracking in Cement-treated Base Asphalt Pavements". *D*. Southeast University.
7. Wang Yufang, Hao Feng(2001). "Process Control and Statistical Technique". *M*. China Metrology Publishing House.

Establishment of Performance related Specifications using Pay Factors and Relationship between Fatigue Cracking and Pay Factors

Sang-Min Hwang[1], Suk-Keun Rhee[2], and Seong-Min Kim [3]

[1]Graduate Research Assistant, Department of Civil Engineering, Kyung Hee University, 1 Seocheon, Kiheung, Yongin, Kyunggi 446-701, Korea; jsddd23@hanmail.net.
[2]Professor, Department of Civil Engineering, Kyung Hee University, 1 Seocheon, Kiheung, Yongin, Kyunggi 446-701, Korea; skrhee@khu.ac.kr
[3]Associate Professor, Department of Civil Engineering, Kyung Hee University, 1 Seocheon, Kiheung, Yongin, Kyunggi 446-701, Korea; seongmin@khu.ac.kr

ABSTRACT: This study aims to address the development of performance based payment adjustment methods. First, this study describes the cases in which the pay adjustment has been applied and influential factors used in forty states of U.S. Based on those preliminary studies, it has been determined that the applicable factors that can be used for the pay adjustment of asphalt pavements in Korea. This study develops a more systematic and reliable algorithm that can be trusted by both builder and vendee. The percent within limit (PWL) has been analyzed as a rational estimation and measurement tool for asphalt pavements. The correlation between fatigue cracking and pay adjustment factors has also been investigated in this study. The fatigue life was increased or decreased due to changing asphalt content, density and gradation.

INTRODUCTION

Recently, Korea has spent a considerable budget and effort on the road pavement. However, since the quality of product is rarely standardized, significant and inconsistent expense costs to maintain and utilize the pavement after completion. Because of insufficient data, lowering and unpredictable quality of the final product is frequently observed and considered problematic in terms of management and maintenance on the road pavement. The budget for the pavement maintenance was almost up to 20% of total budget of road construction per year.

On the other hand, many European nations and U.S states have focused on efficient and effective management of the road for performance in the field of road pavement, establishing performance related specifications for maintenance and operation. Besides,

U.S. states strictly manage the road construction applying pay adjustment for the pavement design and construction to maintain road performance. About 40 states of the U.S. adopted pay adjustment, applying their own factors which affects on the performance greatly such as density or asphalt content.

Thus this research was performed to select the applicable factors that are considered for pay adjustment of asphalt road pavement in Korea. Rational estimation and measurement tools for the payment of asphalt road management and operation are also suggested. This study also has been analyzed of the correlation between fatigue cracking and pay adjustment factors to expect the fatigue life due to changing pay adjustment basic factors.

PRESENT PAY ADJUSTMENT IN U.S.

Pay adjustment is universally applicable to many U.S. states based on individual specification. Furthermore, pay factor is estimated by PWL method, are measurement tools for payment of asphalt road management to apply probability theory. AASHTO proposes Pay Factor as a equation like P.F=55+0.5PWL(percentage within limit).

U.S. states adopt the pay adjustment based on almost 8 basic factors, including density. In the case of the density is most frequently used among the pay adjustment basic factors, it has been used as a basic factor in 32 U.S. states. Also, the asphalt content has been used in 30 U.S. states including Florida. Especially there are 8 states including Minnesota that has been adopting pay adjustment about superpave method.

On the other hand, most U.S. states rarely adopt the thickness as a pay adjustment basic factor, whereas Korea agencies adopt the thickness for the inspection provision to accept the road pavement construction. Figure 1 explains the frequency of application.

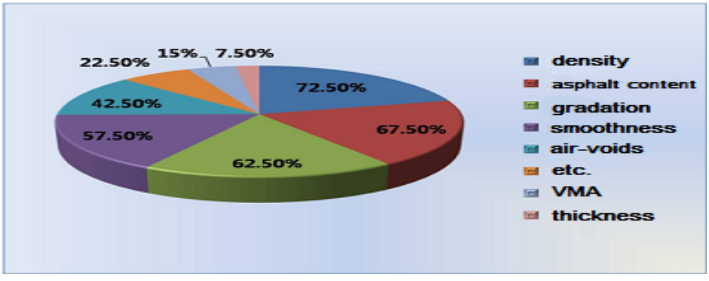


FIG 1. Frequency of application of pay adjustment factors

SELECTING PAY ADJUSTMENT FACTORS

The performance of asphalt mixture can be forecasted by some factors such as asphalt binder content, in-place density, air-voids, gradation and VMA. Therefore, the analysis of factors with regard to asphalt binder contents, air voids is very important procedure to

evaluate the pavement performance, and the most critical factor to affect the asphalt pavement These factors can be classified by three standardization as following Table 1

Table 1 Influence factors to performance of asphalt road pavement

Division	Factors
Quality Management Factors	In-place density, Air-voids, Asphalt Binder Contents, VMA, Gradation
Permit for Completion Factors	Thickness, Smoothness
Construction Management Factors	Temperature

43 U.S. states have been applied pay adjustment stand on pay factor, managing the pay adjustment basic factors which affect road pavement performance. Generally, final payment is figured out by composite pay factors according to the D.O.T. provisions depending on two or four pay adjustment basic factors. This is called "composite pay factor". On the other hand, Korea has been only applied thickness and smoothness as completion permit. This means excluding factors which affect pavement quality such as the density and the asphalt content. Thus we assumed five pay adjustment standard factors(asphalt binder content, In-place density, gradation, thickness, smoothness), considering the interior permit completion and influence on the pavement quality which is frequently used in the U.S.

SELECTING QUALITY MEASUREMENT METHOD

This study was conducted to suggest reasonable quality measurement methods of asphalt pavements to be used in the pay adjustment. The pay adjustment is a method to adjust the construction cost according to the pavement quality based on the statistic theories. Many U.S states use pay adjustment and the PWL(Percent with in Limit) is calculated using their quality index tables. The PWL for a lot can be estimated by using the quality index, Q. The Q-statistic is used with a PWL table to determine the estimated PWL for the lot. A PWL table is shown in table 1. Conceptually, the Q-statistic, or quality index, performs the same function as the Z-statistic, except that the reference point is the mean of an individual sample, X , instead of the population mean, μ, and the points of interest with regard to areas under the curve are the specification limits.

$$Q_L = \frac{\overline{X} - LSL}{S} \quad \text{and} \quad Q_U = \frac{USL - \overline{X}}{S} \tag{1}$$

Q_L = quality index for the lower specification limit

Q_U = quality index for the upper specification limit

LSL = lower specification limit
USL = upper specification limit
$\overline{X}$ = sample mean for the lot
S = sample standard deviation for the lot

QL is used when there is a one-sided lower specification limit, while QU is used when there is a one-sided upper specification limit. For two-sided specification limits, the PWL value is estimated as:

$$\mathbf{TPWL=UPWL+LPWP-100} \quad (2)$$

UPWL= percent below the upper specification limit (based on *QU*)
LPWL= percent above the lower specification limit (based on *QL*)

$$\mathbf{Pay\ Factor = 55+0.5TPWL} \quad (3)$$

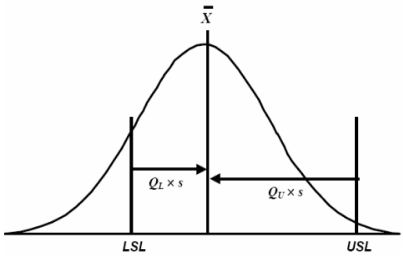


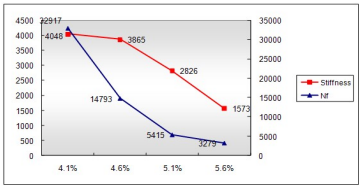
FIG 3. PWL in standard deviation (Q-Value) from the mean (Burati et al., 2003)

CORRELATION BETWEEN FAITIGUE CRACKING AND PAY ADJUSTMENT FACTORS

Relationship between asphalt content and fatigue cracking

The test was proceeded with a controlled air voids and non-controlled air voids to avoid the effect of over compaction. Every specimen reduced its stiffness as the asphalt content increases, and the fatigue life was also reduced as the asphalt content with its stiffness at the same time, like the Figure 4 below.

(a)



(b)

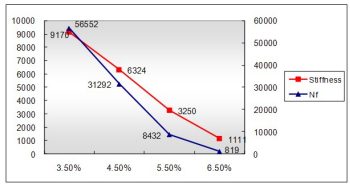


FIG 4. Tendency of fatigue life and stiffness from AP (a) controlled air voids, (b) non-controlled air voids

Relationship between density and fatigue cracking

Density variation was performed manufacturing specimens with the refined compaction frequency, and the result of stiffness and fatigue life was reduced as the density increases like the Figure 5 below. Especially 98% theoretical maximum density showed the highest fatigue life. That seems to be an effect of over compaction.

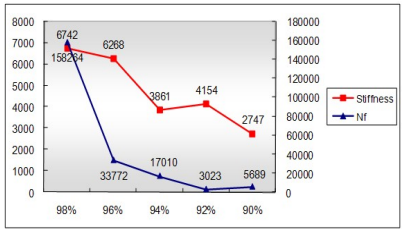


FIG 5. Tendency of fatigue life and stiffness from density

Relationship between fatigue cracking and gradation

In the case of gradation, the test was performed with a standard passing percentage #8. The five specimen was product as follow: 35% as an upper specification, 50% as a lower specification, 32% as an excluded lower limit, 53% as an excluded upper limit, and 40% as a standard passing percentage #8. The following Figure 6 is the result of this test.

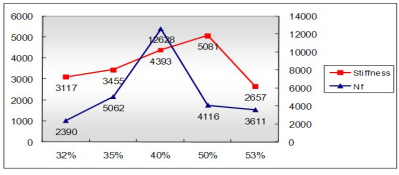


FIG 6. Analysis Tendency of fatigue life and stiffness from gradation

In the case of gradation, stiffness and fatigue life of 35% and 50% caused higher result until the fracture than those of 32% and 53% which were out of specification. Through this result, we found that the asphalt mixture becomes fragile since it didn't correspond the limit of specification which has 40% of standard passing percentage #8.

CONCLUSIONS

- Forty U.S. states apply the pay adjustment method, using their own factors which affect performance of pavement such as density and asphalt content. The density, asphalt content, gradation and smoothness are mostly applied factors. Thus we assumed five pay adjustment standard factors, the four factors just mentioned and the thickness of the pavement.
- Many U.S states use pay adjustment and the PWL is calculated using their quality index tables. Thus we assumed that PWL was a reasonable approach to adjust pavement quality.
- We performed an indirect tensile test to analyze the relationship between fatigue cracking and pay adjustment factors. The tendency of fatigue cracking was very clear, according to the density, asphalt content, gradation.

In the case of asphalt content, every specimen reduced its stiffness as asphalt content increases, and the fatigue life was reduced as the asphalt content with its stiffness at the same time. Especially 98% theoretical maximum density showed the highest fatigue life. That seems to be an effect of over compaction. In the case of gradation, stiffness and fatigue life of 35% and 50% caused higher result until the fracture than those of 32% and 53% which were out of specification.

ACKNOWLEDGMENTS

This research described in this paper was sponsored by Korea Institute of Construction and Transportation Technology Evaluation and Planning, and was part of a study on the standardization of construction criteria based on performance.

REFERENCES

Burati, J. L., Weed, R. M., Hughes C. S., and Hill, H. S. (2003). *Optimal Procedures for Quality Assurance Specifications*, *Report FHWA-RD-02-095*, Civil Engineering Department of Clemson University.

Asphalt Research Program Institute of Transportation Studies University of California, Berkeley. (1994). *Fatigue Response of Asphalt-Aggregate Mixes*. Strategic Highway Research Program.

Temperature Calibration of EICM Model in New Mexico

Bin Zhang[1], S.M. ASCE and Jie Zhang[2], M. ASCE, Ph.D., P.E.

[1] Graduate Student, Department of Civil Engineering, New Mexico State University, P.O. Box 30001, MSC-3CE, Las Cruces, NM 88003-8001; Phone: 575-645-9000; e-mail: bzhang@nmsu.edu
[2] Assistant Professor, Department of Civil Engineering, New Mexico State University, P.O. Box 30001, MSC-3CE, Las Cruces, NM 88003-8001; Phone: 575-646-6012; e-mail: jzhang@nmsu.edu

Abstract: The Enhanced Integrated Climate Model (EICM) is a program that integrates most of the climate conditions to simulate climate effects on pavements. It was originally designed for all regions in the United States. However, it was proposed on the basis of the nation wide average climate data and not accurate for regional conditions. Therefore, it is necessary to calibrate the EICM using local climate data before its application by state DOTs and other agencies. In the State of New Mexico, because of its special climate condition, the calibration of EICM is very important. In this paper, the EICM was used to predict pavement temperature profile with the input data obtained from the LTPP Datapave. Then the EICM-predicted temperatures were compared with the measured temperatures to validate the feasibility of the current EICM in New Mexico. Finally, the correlation between the EICM-predicted and measured temperatures is provided.

INTRODUCTION

Temperature and moisture are the two main climate factors that influence the pavement design and performance (Ahmed et al., 2005). However, the two factors vary with time and seasons. It is not easy to analyze their effects on pavement design and performance. The Enhanced Integrated Climate Model (EICM) integrates most of the climate conditions modeling climate effects on pavements.

The EICM was originally designed for applications in all regions in the United States. However, it was developed on the basis of the nation-wide average climate data and may not accurate for regional conditions. It is necessary to calibrate the EICM model using local climate data before its application by state DOTs and other agencies. Validations of EICM were carried out in New Jersey (Ahmed et al., 2005) and Idaho (Bayomy and Salem, 2005). However, neither of them shows a very good capability in temperature prediction. In New Mexico, the temperature fluctuates more

than many other states. Therefore, the calibration of the EICM model is very important in New Mexico.

In this paper, the latest EICM program – version 3.2 was used to predict pavement surface temperature and temperature profile with depth. To check the consistency, comparisons between the predicted and the field measured temperatures were carried out. Finally, the correlation between the EICM-predicted temperature and field measured temperature is established.

REQUIRED CLIMATE DATA IN THE EICM

To execute the EICM program, certain climatic data are required as inputs, which include air temperature, wind speed, percentage of sunshine, precipitation, humidity, and ground water table depth (Larson and Dempsey, 2003). Air temperature is used to determine the air temperature at each time increment. Wind speed is used to calculate the convection at the pavement surface. Percentage of sunshine is for calculating the amount of solar radiation on pavement surface during day light hours and the amount of cloud cover for radiational cooling at night.

INPUT DATA

In this paper, most input data are from the LTPP Datapave. In the Datapave, only several test sites in New Mexico, i.e., SHRP 1002, SHRP 1003, SHRP 1005, SHRP 1112, SHRP 2118, SHRP 3010 (see Figure 1), have the required humidity and wind speed data. The test site number, e.g. SHRP 1002, is coded with specific site ID by the LTPP for easy understanding (FHWA Website, 2005). Of these sites, SHRP 1002 and SHRP 1003 are close to each other in the same route, the same for test sites SHRP 1112 and SHRP 3010. Sites that are close to each other and in the same route share the same climate and pavement conditions. As a result, four test sites, i.e., SHRP 1002, SHRP 1005, SHRP 1112, SHRP 2118, are selected in the analysis.

The EICM requires either the minimum/maximum or hourly temperature values to be input for each day. In this analysis, the input of air temperature was chosen from the minimum and maximum temperatures of each day, as recorded in LTPP Datapave. However, because of the large amount of data, not all the everyday temperature data is required as input. For each month, only the temperatures of the 1st, 10th, and 20th date were chosen as input. Then temperatures of the rest days in a month will be generated by the EICM program according to the variation trend of the input temperature. The generated temperature has the same seasonal variation trend as the LTPP data. In addition, in the LTPP Datapave, the precipitation data is the total amount of daily precipitation, and humidity is the maximum daily humidity. Both precipitation and humidity are input into the EICM in a similar way as temperature. For the input of wind speed, the daily mean wind speed was used. Other required

climate input data are the ground water table depth and the percentage of sunshine (SS). Because these data are not recorded in the LTPP Datapave for New Mexico State, it is necessary to determine acceptable values that will not cause large errors in the analysis.

For the ground water table depth, data from the U.S. Geology Survey (USGS) were used. For each site, the average recorded water table depth was used in the analysis. The determined water table depths for each site are listed in Table 1. Take the test site SHRP 1002 as an example. The ground water table recorded near the SHRP 1002 fluctuates from 6 to 15 ft in 2007 with the average of 10 ft. Therefore, 10 ft is selected as the ground water table depth for the SHRP 1002. In a same way, water table depths for other sites can be determined.

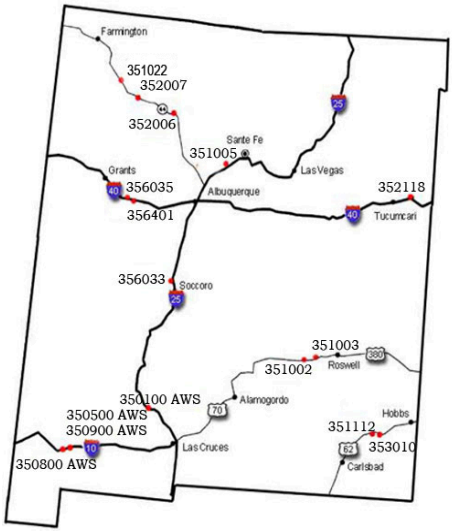


Figure 1. LTPP sites in New Mexico

In this analysis, the SS, which is one of the required climate data in the EICM, is not available for the above mentioned four test sites. Assumptions were made for every site to get the SS value. For example, the test site SHRP 1002 has 106 wet days in 2002, which is about 30% of the whole year. Therefore, a default value of 70% was used for the SS in the SHRP 1002. The same approach was applied to determine the default values of SS for other sites. Table 1 also gives the default values of SS for each test site in the analysis.

Table 1. Selected ground water table depths and default values of SS

Test Site	Water Table Depth (ft)	Percentage of Sunshine (SS, %)
1002	10	70
1005	65	79
1112	45	84
2118	50	80

TEMPERATURE VALIDATION

After inputting all the required data, the EICM program can be run. The output data in the EICM program include predicted pavement temperature profile with depth, water content, pore water pressure, ice content, frost heave and penetration, etc (Larson et al., 2003). In this research, because of the limited data, only comparisons on pavement surface temperature and pavement temperature profile with depth were made to check the feasibility of the EICM.

Comparisons for the test site SHRP 1002 are presented in this paper, as shown in Figure 2 and Figure 3. In Figure 2, comparisons were made among the EICM-predicted pavement surface temperatures and the measured ones. Temperatures used for comparison were selected from the temperatures at 12:00 pm in the first day of each month of year 2002. It can be seen that the measured pavement surface temperature is always higher than the EICM-predicted ones. This may be attributed to the special soil condition in New Mexico. Because the site SHRP 1002 is located in southern New Mexico which is in sand area, for the same density and moisture, sand has higher thermal conductivity than clay and silt (Bu-Hamdeh and Reeder, 2000). Therefore, comparing with clay and silt, sands may cause higher ground temperature at noon. From Figure 2, it can be seen that the measured temperatures in July is much higher than the EICM predicted ones. This can be explained by the specific climate condition during that period. In the area of the test site SHRP 1002, July is the rain season with rains happening in the late afternoon or at night, which leads to limited influence on pavement surface temperature at noon. So the drop of temperature in this period is not large. However, the EICM program takes the total amount of daily precipitation to predict pavement temperature. That daily precipitation will cause a sharp drop on predicted temperature. Therefore, the differences between the predicted and the field measured temperatures in this season are larger than other seasons.

To obtain the influence of percentage of sunshine on pavement temperature, comparisons among the EICM-predicted pavement surface temperatures with different SS values were carried out. As shown in Figure 2, for the site SHRP 1002, the SS values were set as 50%, 70%, and 90%. Figure 2 also shows that, the higher the SS value, the higher the predicted pavement surface temperature.

Figure **3** gives the comparisons between the EICM-predicted and the field measured temperature profiles. For the test site SHRP 1002, there is only one group of temperature profile data recorded in LTPP Datapave. This group of temperature profile data was measured on May 12, 2002. Therefore, comparison was performed based on these data. From

Figure **3**, it can be seen that there are some differences between the EICM-predicted and the measured pavement temperature profiles with depth at the SHRP1002. After comparisons were made for all test sites, it can be concluded that for different test sites, the differences between the EICM-predicted and measured temperature profiles vary. Therefore, the current EICM can not be directly used in New Mexico. It still needs further calibration with local data.

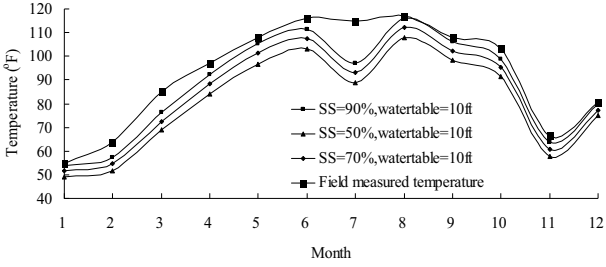


Figure 2. Comparison among the EICM-predicted and measured pavement surface temperatures at SHRP 1002

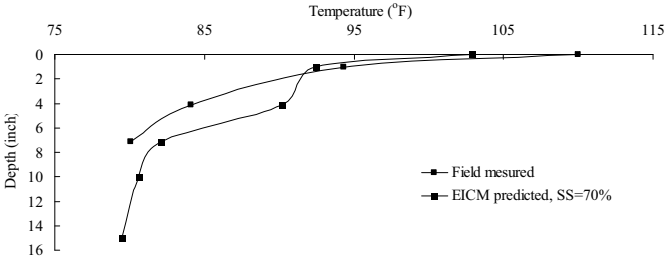


Figure 3. Comparison of EICM predicted and field measured pavement temperature depth profile at SHRP 1002

CORRELATION ANALYSIS

Because of the differences as above mentioned, a correlation should be established between the EICM-predicted and the field measured pavement temperatures. In this

research, it is not possible to find the relationship between the EICM predicted and measured temperature profile with depth based on the data available, so only pavement surface temperature correlation was established for all the test sites, based on the predicted pavement surface temperature under the selected SS value (Table 1). Eq. (1) gives the relationship between the field measured pavement surface temperature and the EICM-predicted ones. Because of the page limitation, the deduction process was not described here.

$$y = 0.9193x + 14.085 \quad (1)$$

where y = field measured temperature ($^{\circ}F$), x = EICM-predicted temperature ($^{\circ}F$). Through statistical analysis, about 97% of the data which were used to develop the model satisfy this relationship, with the $R^2 = 0.968$. The relationship between the EICM predicted and measured pavement surface temperature is acceptable.

Based on the particular climate in New Mexico, the correlation analysis should be carried out seasonally to show the particular climate condition in July. However, with very limited data, it is not easy to show a good result by seasonal analysis. Future work is necessary to be done on the theoretical part of the EICM based on seasonal analysis.

CONCLUSIONS

In this research, a temperature evaluation on EICM was carried out to validate of the application of EICM program in New Mexico. Through the temperature validation, it is concluded that the current version of EICM can not be directly used in New Mexico due to the differences between the EICM-predicted and the field measured temperature. Finally, because it is not possible to find the relationship between the EICM predicted and measured temperature profile with depth based on the data available, a correlation between the EICM-predicted and the measured pavement surface temperature was established.

REFERENCES

Ahmed, Z., Marukic, I., Zaghloul, S., and Vitillo, N. (2005). “Validation of enhanced integrated climatic model predictions with New Jersey seasonal monitoring data.” *Transportation Research Record*, No. 1913.

Bayomy, F., and Salem, H. (2005). “Monitoring and modeling subgrade soil moisture for pavement design and rehabilitation in Idaho, Phase III: data collection and analysis.” *National Institute for Advanced Transportation Technology.*

Larson, G. and Dempsey, B. (2003). “Enhanced integrated climatic model user’s

guide version 3.0" - *7 -Page 7 of 7. Federal Highway Administration*.

FHWA Website. (Visited 2008). "Long Term Pavement Performance program (LTPP)" [WWW Document]. URL: http://www.ltpp-products.com.

Bu-Hamdeh, N.H. and Reeder, R.C. (2000). "Soil thermal conductivity: Effects of density, moisture, salt concentration, and organic matter." *Soil Science Society of America Journal.* Vol.64, 1285-1290.

Improvement of Coastal Silty Sand of Saudi Arabia Using Preloading Technique

Dafalla, M. A. PhD

Researcher, College of Engineering, King Saud University, Saudi Arabia
mdafalla@ksu.edu.sa

ABSTRACT: The subsurface formation at sites along the western Red Sea coast of Saudi Arabia often have loose to medium dense silty sand at several parts. This type of material was encountered at levels immediately below the foundation depth commonly used in practice. These soils undergo excessive settlement when supporting concrete structures, slab on grade systems and pavement structures. This work was aimed at studying the improvement provided by preloading technique to these coastal deposits. Technical College Building Complex site located at Al Qunfoda was selected for this study. The site was preloaded using 4.5 to 6m height of sand over six month period. The settlement was monitored every week throughout the period of preloading. The density and compressibility of the formation was noted to improve in different stages; an initial fast stage occurring within the first four weeks, intermediate stage which continued for 12 weeks and a slow stage which is noted to continue for more than 26 weeks. A final stable stage is considered when no variation in settlement can be reported over a satisfactory period. The process improved the site and established a close to uniform density across the area studied. Plate load tests carried out on improved areas confirmed that the settlement after preloading was reduced to tolerable limits for a particular foundation stress range. This paper provides a guide for monitoring, verification and decision making tool for practicing geotechnical engineers.

INTRODUCTION

This paper is aimed at investigating the performance of preloading technique as used in practice along the Red Sea coast of Saudi Arabia where loose silty sand material is encountered. Damage in the form of excessive settlement was noted in different types of structures and pavements. History of severe damage was reported in the major urban areas along the coast. Jizan city and the nearby towns and settlements were known to be the most affected. A report prepared by the Ministry of Municipality and Rural affairs (Saudi Arabia) in 1985 surveyed the problem and suggested some approaches to improve foundation design. The preloading technique is among these methods. Preloading means placing a temporary load to exert stresses on the ground equal to or higher than stresses to be applied by a proposed structure. This will cause the substrata to densify and form a stiffer support which will help in reducing the compressibility when the actual structure is built. Normally an earth fill of a predetermined height and soil density is placed and the settlement is observed over a period of time until the deformation is stopped or becoming extremely small. Other methods of soil improvement include dynamic compaction, heavy tamping, use of RIC (rapid impact compaction) compacters, stone columns, soil replacement and or soil treatment using a cementing agent. The preloading is found practical, economical and

easy to apply. The concept of preloading was known since long time. The documented approach is tracked as early as 1930s. Busiman (1936) presented a study on a long duration settlement test at the First International Conference on Soil Mechanics and Foundation Engineering. Johnson (1970) used the term precompression for improving soil density. He suggested sand drains to reduce the time of consolidation. Although the method is simple and straightforward it was found that several pitfalls can make the process not successful (Ramli Mohamed 1992). These include: designing for compensation of primary settlement only, removing surcharge too early and inadequate instrumentation and monitoring.

The preloading technique can also help in reducing liquefaction risks in areas with seismic hazards.

SITE BACKGROUND AND CHARACTERISTICS OF THE SUBSTRATA

The site for this study is located at the south west of Saudi Arabia along the Red Sea coast at Al Qunfoda town. The project is a Technical College Complex which consists of several buildings, roads and boundary walls. The soil investigation was conducted by AMNK Consulting Engineers. It was found that the site is underlain by medium dense silty sand followed by very loose to medium dense silty sand to sandy silt. Standard penetration test results reported values as low as 4 blows per 300 mm in some sections. The groundwater is encountered at 2.8 to 3.4m below ground level. The recommendations of the consulting firm suggested alternative solutions to be considered including preloading, stone columns or cast in place pile foundation to support the proposed structures. The geotechnical firm suggested to limit the width of foundation to 2.4m and to adopt narrow strips so that the significantly high stresses would be within the top improved soil layers. The client decided to adopt the preloading option as being economical and easy to apply. Figure 1 shows a generalized subsurface profile.

The subsurface material is predominantly classified as SM. ML and SC. The clayey material is very limited and it is encountered as thin films. The measured plasticity index varied from 3 to 7 except for a few samples indicating some values of 8 to 17. The fine material passing sieve number 200 (75 microns) is in the range of 16.9 to 53.8%. This is mostly silt or clay with low plasticity.

The soil profile given in this study does not represent the worst loose condition along the Red Sea coast. Very loose silty sand with SPT blows of 1 and 2 blows/300 mm down to depths of 20m were noted in Gizan region. The ground water table is variable and influenced by the low and high tide sea levels. The seismic ground acceleration of 10% probability of exceedance in 100 years in western Saudi Arabia indicates the highest relative level of ground motion in the site area (Thenhaus et al 1989). Therefore density improvement of the near surface liquefiable layers is of great concern.

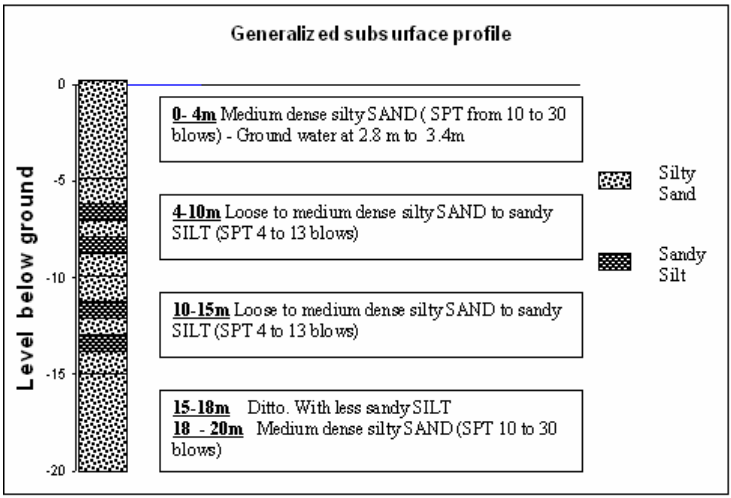


Figure 1. Generalized subsurface profile.

PRELOADING PROCEDURE AND MONITORING

It was agreed to precompress the site with an earth fill to exert a stress of not less than100 kN/m^2 to reduce the total settlement. To achieve this, 6m fill of a material with a density not less than 16.67kN/m^2 was considered. Sand is abundant within close vicinity and can attain the required density with minimum compaction effort. The fill was dumped and leveled up in layers of about 1m until the required height of 6m was reached. The process took about four weeks. Prior to placing the fill settlement plates fitted with extension pipes were installed in 6 locations. Surveying works were carried out to establish the level of each plate before and during execution of the fill. After the required level was reached settlement measurements were taken in a weekly basis. Initially it was expected that settlement stabilization was likely to take place in a few months. No sand or wick drains were suggested because of the granular nature of the formation soils and the cost of constructing sand or wick drains. The lack of sand drains would make the precompression process slower and would require more time to achieve the required settlement stabilization. The site was 73.8m in length and 25.6m in width. Points 1, 2 and 3 were located near three corners while Points 4, 5 and 6 were placed at the centre of the site.

A plate load bearing test using 76cm diameter plate was carried out on natural ground without earth fill to act as a base line information (Figure 2). Observations of the settlement in the 6 points over a period of 32 weeks are shown in graphical form in Figures 3 and 4. The earth fill was removed based on the results showing stable or very small settlements. New soil borings were conducted and a series of plate load tests were carried out to see how much improvement was achieved.

DISCUSSION OF THE RESULTS

As can be seen from the settlement data the site is compressed by 15 to 30 cm. The width of the earth fill is 25.6 m, and the pressure bulb will extend to a depth of more than 30m with the top layers subjected to 100 kN/m^2. The improvement in the soil density depends on the magnitude of the applied stresses. The top layers were compressed more than the bottom layers. The results of the new borings indicated improvement within top zone of 3 to 4m and hardly noticeable improvement below this level. It was noticed that the SPT within the top zone increased to a minimum value of 17 blows/300 mm all over the site. This explains the differences of the overall settlement achieved for the 6 monitoring points. Examining the rate of settlement we can see that three different rates dominate in the six points. At first a rapid rate, within the first four weeks (2.5 to 5 cm/week) followed by an intermediate rate from 4 to 12 weeks (0.25 to 0.5 cm/week) and a slow rate from 12 to 32 weeks (0.1 to 0.25 cm/ week). The last three weeks indicated very slow rate but entire stabilization was not achieved. This was considered sufficient by the client who instructed the removal of the fill. On removal of the fill several plate load tests were carried out and the settlement for 4.5 Kg/ cm^2 (441 kPa) was examined and compared. The table below shows the maximum settlement recorded for 4.5 Kg/ cm^2.

Table 1. Plate load test settlement on natural ground and preloaded area

Plate Load Test Reference	Settlement (mm) at 4.5 Kg/cm^2	Plate Load Test Reference	Settlement (mm) at 4.5 Kg/cm^2
# 1 preloaded area	4.1	# 6 preloaded area	-
# 2 preloaded area	8.0	#7 preloaded area	8.0
#3 preloaded area	12.0	#8 preloaded area	12.0
#4 preloaded area	8.2	#9 preloaded area	8.0
#5 preloaded area	10.5	#10 natural ground	15.0

The plate load tests after removal of the earth fill showed improvement in the total settlement of a plate subjected to 441 kPa from 20 to 50%. The settlement for low stresses is improved in a similar way.

CONCLUSIONS

Preloading can be a better option for structures and pavements in coastal soils of low density. The process can reduce the amount of settlement by the order of 20 to 50% provided that sufficient time is allowed for deformation to stop. The preloading process involves settlement rates which can be classified as fast, intermediate and slow rates. The geotechnical engineer shall make sure that stabilization is reached and the primary consolidation is complete by comparing rates at different stages. Improvement of the density of the near surface soil can reduce the risk of liquefaction.

ACKNOWLEDGEMENTS

The author would like to acknowledge the support and information supplied by AMNK Consulting Engineers, Al-Jazzar Geotechnical, Archiplan Geotechnical, Abuttahir Consulting office, Alsaleem Establishment and the General Directorate of

Technical Education of Saudi Arabia. Proofreading conducted by Dr Jose L.M. Clemente of Bechtel Mining and Metals, USA is highly appreciated.

REFERENCES

Al-Shamrani, Mosleh A. and Dhowian, A.W. (1997). "Preloading for reduction of compressibility characteristics of sabkha soil profiles" *J. Engineering Geology 48 (1997)* pp 19-41

Johnson, S.J. (1970). "Precompression for improving foundation soils." *J. Soil Mech. and Found. Engg., Amer. Soc. of Civ. Engrs. SM1* pp 111-144

Ramli Mohamad (1992)." Engineering the North-South Expressway on soft ground." *Keynote paper, Geotropika '02. Univ. Teknologi Malaysia, Johor Bahru, Malaysia.*

Busiman, A..S. K. (1936). "Results of long duration settlement tests." *Proceedings of the 1st International Conference of Soil Mechnics and Foundation Engineering. Vol 1* pp 103- 106

Thenhaus, P.C., S.T. Algermissen, D.M. Perkins, S.L. Hanson, and W.H. Diment, 1989, Probabilistic Estimates of the Seismic Ground-Motion Hazard in Western Saudi Arabia. *US Geological Survey Bulletin* 1868, 42 pp.

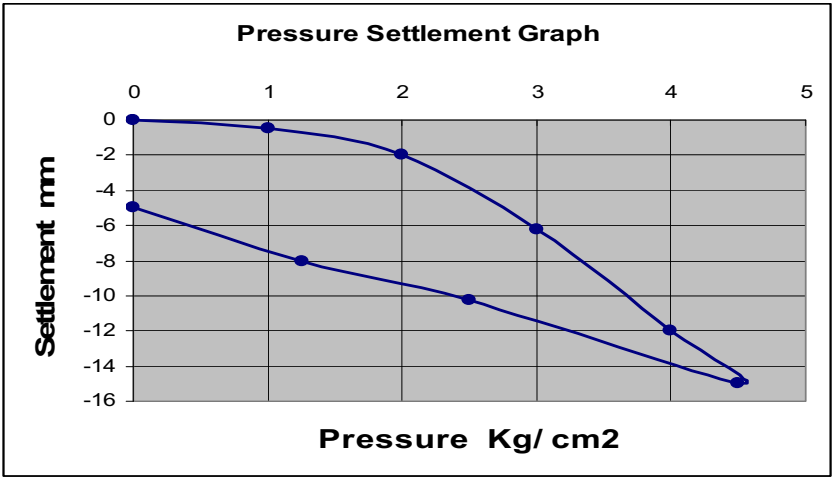


FIG. 2 Typical pressure settlement graph-natural soil.

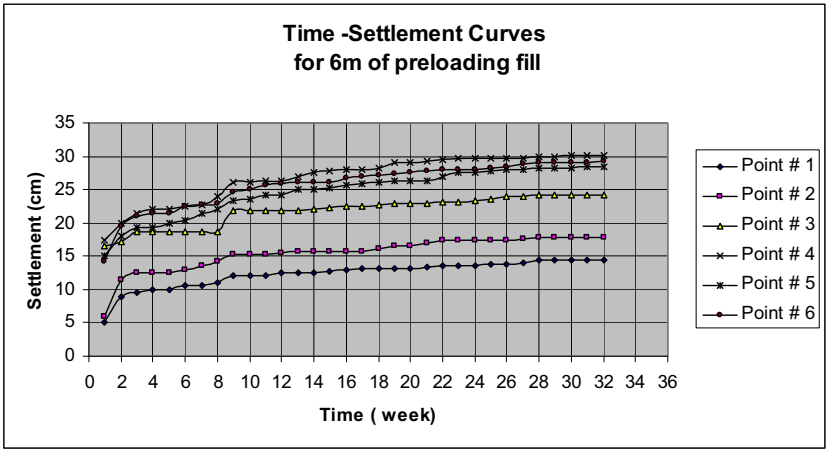


FIG. 3 Settlement at control points over 32 weeks preloading time.

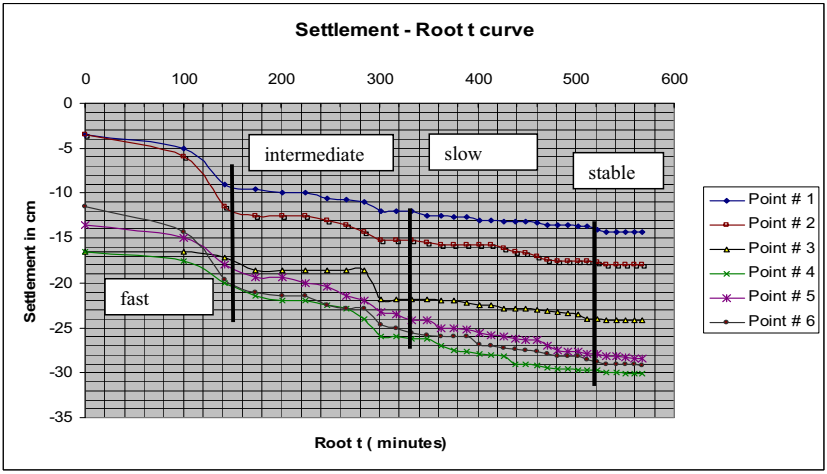


FIG. 4 Zones for rate of settlement.

Comparative Study on GTM Method and Marshall Mixes Design Method for Large Stone Asphalt Mixes

Xinjun Feng[1], Zhuo Gao[2], and Peiwen Hao[3]

[1] Associate professor, School of Communication and Transportation Engineering, Changsha University of Science and Technology, Chiling Road 45#, Changsha,Hunan,China,410076; fxjasphalt@yahoo.com.cn.

[2] Engineer, China Airport Construction Corp. of CAAC, North Sihuan East Road 111#, Beijing,China, 100101; gaozh303@126.com.

[3] Professor, School of Highway, Chang'an University, South Erhuan Road Middle Section, Xi'an, China; 710064; haopw@yahoo.com.cn.

ABSTRACT: Three types of aggregate gradation with different nominal maximum size were designed by Bailey method for large stone asphalt mixes (LSAM). The optimum asphalt content was then determined by Gyratory Testing Machine (GTM) method and Marshall method, respectively. A series of tests were carried out to investigate the performance of the obtained LSAM. The optimum asphalt content(OAC), volume of voids(VV),voids in mineral aggregate(VMA) and voids filled with asphalt(VFA) of specimens prepared by GTM method showed smaller values whereas bulk density is larger. Furthermore, higher temperature stability and poorer crack resistance at low temperature of the former can also be observed.

INTRODUCTION

In recent years, the early damage of asphalt pavement such as rutting, cracking and moisture destruction has become a serious issue in the world (Kandhal, 1990; WU Kuang-huai, 2005; Williams, 1988). LSAM is favorable for its distinguished stability at high temperature, fatigue resistance and water stability(Anderson 1991; Donald, 1990; Kandhal, 1990). LSAM are generally defined as the asphalt mixes with a nominal maximum size of 25~53 mm. Marshall method is commonly used for mix design of LSAM. Marshall mix design method, however, is characterized by two drawbacks: first, compacting process of specimens by Marshall method cannot perfectly simulate the real condition; second, parameters (Marshall stability and flow value) obtained from it cannot sometimes correlate well with the pavement

performance in practice. GTM method was superior especially for its simulation of the real compaction of vehicles on pavement. Usually, asphalt mixtures by GTM method show better rutting resistance. The two methods for LSAM design were investigated and compared in this study.

EXPEREMETAL PROGRAM

Raw materials

A-70 asphalt was used in this study. The properties was tested and tabulated in Table 1. Coarse aggregate, fine aggregate and mineral filler used in this study come from a quarry in Zhao county, Hebei province. Their performance can also meet the requirements specified in the specification. The apparent densities were shown in Table 2.

Table 1. Technical Characteristics of Asphalt

Item		Test value	Technical Requirement
Penetration (0.1mm)		66.0	60～70
Ductility (cm)		>100	≥100
Softening Point(℃)		47.4	≥46
Wax Content%		1.8	<2.2
Density(g/cm^3)		1.015	-
Solubility(%)		99.9	<99.5
Thin-film Oven Test	**Mass Loss(%)**	－0.12	-0.8～+0.8
	Penetration Ratio(%)	69.7	≥61
	Ductility(cm)	>100	≥15

Table 2. Apparent Density of Aggregate

Sieve Sizes(mm)	**37.5**	**31.5**	**26.5**	**19**	**16**	**13.2**	**9.5**	**4.75**
Apparent Density（g/cm^3）	2.722	2.721	2.72	2.72	2.722	2.729	2.73	2.728
Sieve Sizes(mm)	**2.36**	**1.18**	**0.6**	**0.3**	**0.15**	**0.075**	**Filling**	
Apparent Density（g/cm^3）	2.721	2.709	2.703	2.703	2.683	2.69	2.842	

GRADATION DESIGN OF LSAM

Three mixture gradations of 26.5mm, 31.5mm and 37.5mm nominal maximum aggregate sizes were designed by Bailey design method. The grading curves are shown in FIG.1.

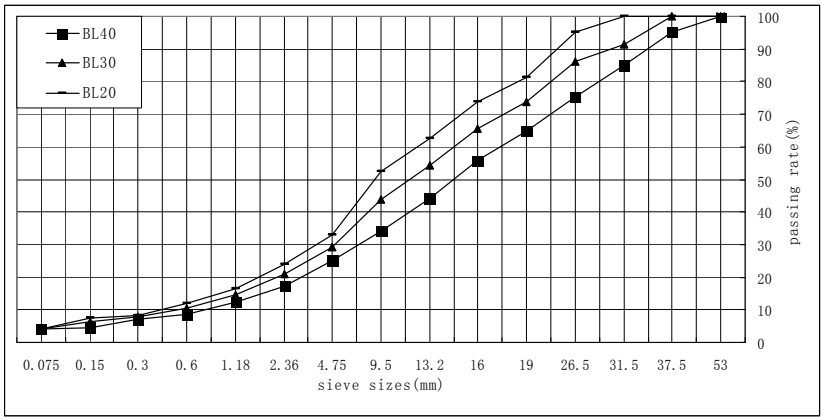


FIG. 1. Three gradations of LSMA by Bailey method

DETERMINATION OF OPTIMUM OIL-STONE RATE OF LSAM

The specimens with 152.4 mm in diameter and 95.3 mm in height were prepared for Marshall method. The number of blows on each side of specimens is 112. The optimum oil-stone rates for BL40, BL30 and BL25 were then determined. After that, the optimum oil-stone rates for BL40, BL30 and BL25 were designed by GTM method. For GTM method, the same size specimens were prepared with a gyratory compaction angle of 1.4 degree.

The comparison results by two methods are shown in Table 3. It shows that the optimum oil-stone rate, VV, VMA and VFA of LSAM designed by GTM method are smaller than those by Marshall method except bulk density. The bulk density and stability of the former are larger than the latter. Compared with the results by Marshall method, there is a reduction of 0.4% to 0.6% of the optimum oil-stone rate, a decrease of 0% to 0.7% of VMA by GTM method. However, bulk density designed by GTM shows an increase of 0.9% to 1.6%. It also shows an stability increase of 41.5% to 64.7% by GTM method. This is mainly due to the relatively compaction effect by GTM than the Marshall compaction machine.

Table 3. Comparison of the Parameters Designed by Marshall Method and GTM Method

Index	BL40		BL30		BL25	
	Marshall method	GTM method	Marshall method	GTM method	Marshall method	GTM method
Optimum Oil-stone Rate（%）	3.8	3.2	3.8	3.4	3.9	3.5
Bulk Density（g/cm^3）	2.441	2.480	2.430	2.453	2.437	2.461
VV（%）	4.8	4.1	5.1	4.7	4.7	4.3
VMA（%）	13.3	11.4	13.5	12.3	13.2	12.0
VFA（%）	63.9	63.9	62.2	61.5	64.3	64.0
Marshall Stability（kN）	20.0	28.3	20.5	32.3	21.8	35.9

PAVEMENT PERFORMANCE OF LSAM

A series of tests were carried out to study the pavement performance of the LSAM designed by Marshall method and GTM method, respectively. High temperature stability, crack resistance at low temperature and water stability of specimens designed according to the above methods were compared.

High temperature stability

Specimens with a size of 300mm×300mm×100mm were prepared for rutting test. The results are shown in table 4.

Table 4. Comparison of High Temperature Stability of LSAM

Test Index	BL40		BL30		BL25	
	Marshall method	GTM method	Marshall method	GTM method	Marshall method	GTM method
Dynamic Stability（times/mm）	3592	3758	1500	2932	2780	4846
Rutting Depth（mm）	2.33	4.66	4.00	4.48	3.37	4.64

It can be seen that the specimens designed by GTM method has higher dynamic

stability than that by traditional Marshall method. It indicates that asphalt mixtures designed according to GTM method can achieve better high temperature stability.

Crack-resistance at low temperature

Bending test at low temperature of various specimens were conducted using 250mm×40mm×40mm prisms. The test results were shown in table 5.

Table 5. Comparison of Crack-resistance Performance of the LSAM

Test Index	BL40		BL30		BL25	
	Marshall method	GTM method	Marshall method	GTM method	Marshall method	GTM method
Bending Tensile Strength（MPa）	7.66	8.45	9.39	9.27	9.92	9.81
The Maximum Bending Tensile Strain (με)	1487	1122	2395	1573	2021	1578
Bending Tensile Stiffness Module（MPa）	5058	7530	4201	5890	5014	6210
Strain Energy（J）	0.207	0.112	0.394	0.154	0.354	0.179

It shows that strain energy of the LSAM designed by GTM method is smaller when compared to that designed by Marshall method. It can also be seen that the former has inferior low temperature crack-resistance than the latter.

Water stability

Immersion Marshall stability test and freezing and thawing splitting test were conducted to check the water stability. The results were given in Table 6.

Table 6. Comparison of Water Stability of the LSAM

Test Index	BL40		BL30		BL25	
	Marshall method	GTM method	Marshall method	GTM method	Marshall method	GTM method
Retained Stability（%）	92.7	98.3	90.9	94.6	96.5	99.2
Retained Tensile Strength Ratio（%）	85.3	90.6	83.1	92.7	91.0	95.9

CONCLUSIONS

(1) The optimum oil-stone rate, VV, VMA and VFA of the LSAM designed by GTM method are smaller than those by Marshall method whereas higher bulk density and stability of the former can be observed.

(2) The LSAM designed by GTM method has better high temperature stability and water stability than the LSAM by Marshall method, but the former has worse low temperature crack-resistance.

REFERENCES

Anderson R.M., Epley L.E.,Walker D. (1991). “Kentucky’S experience with large size aggregate in bituminous hot-mix”. *Asphalt Paving Technologists*，Vol. 60(1): 1-18.

Donald K.C.(1990). “Designing asphaltic concrete mixes which are more readily compacted”. *Asphalt Paving Technologists*，Vol.59(1)；341-359.

Kandhal P.S. (1990). “Large stone asphalt mixes: design and construction”. *Washington, DC: National Center for Asphalt Technology.*

Kandhal, P.S. (1990). “Design of Large Stone Asphalt Mixes to Minimize Rutting.” *Transportation Research Board No. 1259,* National Research Council, Washington, DC: 153-162.

WU Kuang-huai, ZHANG Xiao-ning. (2005). “Summarization on methods of asphalt mixture design”.*Journal of Guangzhou University*：*Natural Science Edition,* 4(5): 456-461.

Williams E.G. (1988). “Design and construction of large stone HMA base in Kentucky”. *Hot Mix Asphalt Technology*，Vol.31(1):37-42.

Use of Fly Ash Alongwith Blast Furnace Slag as Partial Replacement of Fine Aggregate and Mineral Filler in Asphalt Mix, at High Temperature

Liaqat Ali[1] and Akmal Fiaz[2]

[1] National University of Science and Technology (NUST), Islamabad, Pakistan, akmal.fiaz@yahoo.com
[2] National University of Science and Technology (NUST), Islamabad, Pakistan, liaqatnit@yahoo.com

ABSTRACT. The problems associated with the environmentally safe and efficient disposal of waste continue to grow. In many areas, existing landfills are beginning to fill up, and a "not-in-my-backyard" philosophy has made the establishment of new landfills very difficult. The cost of disposal continues to increase while the types of wastes accepted at municipal solid waste landfills are becoming more and more restricted. One answer to all of these problems lies in the ability of society to develop beneficial uses for these waste products. Pakistan is a developing country and in order to open new avenues of prosperity there is a need to develop roads network throughout the country. The use of waste byproducts would also relieve some of the burden on the natural resources / virgin materials. A research was undertaken to study the use of fly ash and granulated blast furnace slag as road construction materials and to see how these can improve the properties of asphalt mix design at high temperatures.

INTRODUCTION

The creation of non decaying waste materials, combined with a growing consumer population, has resulted in a waste disposal crisis. The use of waste materials and by-products in road construction can help in solving the disposal of waste material in an economical way and can play an important part in conserving the natural resources, removing or reducing in heaps waste size and improving the economy of the country. Keeping all these facts in view, a research was undertaken with the following objectives:-

- Ascertain the performance of fly ash as filler alongwith blast furnace slag as partial replacement of fine aggregates in asphalt concrete mix.
- Study the effect of fly ash as filler alongwith blast furnace slag as partial replacement of fine aggregates on Marshall stability and flow at high temperatures.
- Determine the best ranges of fly ash and blast furnace slag to be used as filler (within the limits of specifications) which give best AC mix performance.

MATERIALS USED

Coarse and Fine Natural Aggregates. According to ASTM (C 125–88), aggregates retained on # 4 sieve are coarse and those passing # 4 sieve and retained on # 200 sieve fine aggregates. Coarse and fine aggregates used in the study were obtained from Margalla Hills, which are located 60 kms northeast of Islamabad, Pakistan.

Mineral Filler, Stone dust used as filler was also collected from Margalla Hills; it was sieved for gradation, dried in the oven and then preserved in airtight bags for use.

Fly Ash. The fly ash was obtained from Lakhra Fluidized Bed Combustion power plant, Hyderabad (Pakistan); the power plant was manufactured by Foster Wheeler Energy Corporation, USA. Chemical analysis of Lakhra fly ash is shown in tables 1.

Blast Furnace Slag. Blast furnace slag, a waste by-product of iron making industry, can be used only as fine aggregate in the wearing course because of its particle size (0-4 mm). The slag used in this study was granulated blast furnace slag obtained from Karachi Steel Mills. The chemical composition and sieve analysis of the slag is presented in table 2 and figure 1 respectively.

Bitumen. In Pakistan, generally 60/70 penetration grade bitumen is used for asphaltic wearing course in hot regions. 60/70 penetration grade bitumen used in this study was obtained from National Refinery Karachi, Pakistan.

Physical Properties. Standard tests on natural aggregates, bitumen, filler, fly ash and blast furnace slag were carried out in the lab using standard ASTM and AASHTO procedures. Table 3 shows the physical properties of the materials used in the research.

Table 1. Chemical Analysis of Lakhra Fly Ash and Bottom Ash

Constituents	Fly Ash (%)	Bottom Ash (%)
C_aO	25.6	37.15
C_aCO_3	1.24	1.89
C_aCO_4	24.1	36.3
M_gO	1.72	1.83
S_iO_2	18.75	9.90
AI_2O_3	11.7	6.17
Fe_2O_3	7.4	3.90
K_2O & Na_2O	0.6	0.32
SO_3	1.68	0.88
M_gCO_3	0.04	1.2
Loss on Ignition	6.0	1.2

Table 2. Chemical Composition of Karachi Steel Mill Blast Furnace Slag

Constituents	Chemical Notation	Percentage Range
Silica	SiO2	36-39%
Iron Oxide	FeO	0.5% Max
Alumina	$A1_2O_3$	14-16%
Calcium Oxide	CaO	36-40%
Magnesium Oxide	MgO	9% Max
Sulphur	S	1.5% Max
Manganese	MnO	1.3% Max
Titanium	TiO_2	0.881%
Alkali		0.4% Max

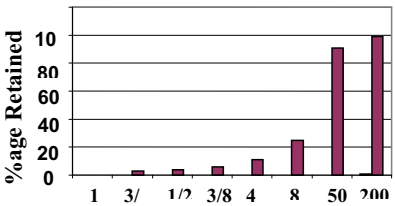


Fig 1. Particle size distribution of the granulated blast furnance

Table 3. Tests, Designation, and Results

Test	AASHTO/ASTM Designation	Result	
Abrasion value (%)	AASHTO-T96, ASTM C131	21.1	
Impact value (%)	BS 812 PART : 3 : 1975	13.55	
Crushing value(%)		22.97	
Flakiness & Elongation	ASTM D3398	11.37-13.1	
		Bulk	APP
Specific gravity of coarse agg.	AASHTO-T 85-88, ASTMC C 127-84	2.666	2.719
Specific gravity of fine agg.	AASHTO-T 84-88, ASTMC C 128-84	2.652	2.752
Specific gravity of filler	AASHTO-T 100-90, ASTM C 854-83	2.708	
Specific gravity of b.f.slag	AASHTO-T 84-88, ASTM C 128-84	2.4923	2.628
Specific gravity of fly ash	AASHTO-T 84-88, ASTM C 128-84	2.7027	
Penetration test	AASHTO-T 49-89, ASTM D 5-73	67.2	
Ductility test	ASTM D 113-79	>100	
Marshall test	AASHTO-T 245-90, ASTM D 1559	Variable	
Bulk sp gravity calculation compacted bituminous mixture	AASHTO-T 166-68	Variable	
Maximum specific gravity (Gmm) of bituminous paving mixtures	AASHTO-T 209-90, ASTM D 2041-78	Variable	
Flash point, coc, deg C.	ASTM D 92	300	
Specific gravity of bitumen	ASTM D 70	1.021	

EXPERIMENTAL MATRIX AND MARSHAL TESTING PROCEDURE

Marshall Method. The Marshall Method of mix design is followed by most of the USA State Highway Departments and African and Asian countries including Pakistan. Stability and flow are the two important parameters obtained from the test.

Table 4. Weight Calculation for Various Marshall Mixes

Passing	Retained on	Actual (%)	For 1200	30% Rep of fine agg. & fines		40% Rep of fine agg. & fines				50% Rep of fine agg. & fines		
				Weight of (gm)		Weight of (gm)				Weight of (gm)		
				St-one agg	Slag	Fly Ash	Sto-ne agg	Slag	Fly Ash	St-one agg	Slag	Fly Ash
1”	¾”	5	60	60			60			60		
¾”	½”	32	384									
½”	3/8”											
3/8”	#4	20.5	246	246			246			246		
#4	#8	13.5	162	113.4	48.6		97.2	64.8		81	81	
#8	#50	20.0	246	172.2	73.8		147.6	98.4		123	123	
#50	#200	3.5	42	29.4	12.6		25.2	16.8		21	21	
#200	Pan	5	60	42		18	36		24	30		30
Bitumen Content (%)				4%			4.5%			5%		
Bitumen Content (gm)				50			56.54			63.16		

Methodology Marshall mix behaviour was studied using partial replacement of fine aggregate by fly ash and blast furnace slag at different temperatures, using National Highway Authority (NHA) Pakistan Class A gradation (NHA, 1991). For the design mix, the mid values of gradation “A” were selected. For each sample preparation 1200 grams of aggregate batch was taken.

The partial replacement of fine aggregate (agg.) and mineral filler at 30%, 40% and 50% replacement (rep.) level by fly ash and blast furnace slag was made by weight. Table 5 shows weight calculations used for preparation of various Marshall mixes. In this study, the specimens were prepared as per ASTM D 1559. One hundred and eight specimens with different combinations, as shown in table 5, were tested for Marshall stability and flow to evaluate the performance of blast furnace slag and fly ash as partial replacement of fine aggregate and mineral filler at different replacement levels. The design matrix shows four different types of mix designs. In these mixes, bitumen used was 4%, 4.5% and 5%. For each cell, three batches were prepared containing three samples each.

Table 5. Experimental Design Matrix

(X = 3 x Sample)

Type of fine agg.	%age of fine agg. & fines	Bitumen Content %age								
		4.0			4.5			5.0		
		Temp °C			Temp °C			Temp °C		
		60	65	70	60	65	70	60	65	70
Stone Dust	100	X	X	X	X	X	X	X	X	X
Blast Furnace Slag & Fly ash	50	X	X	X	X	X	X	X	X	X
	40	X	X	X	X	X	X	X	X	X
	30	X	X	X	X	X	X	X	X	X

Table 6. Summary of Test Results at Various Temperatures for Different Type of Mixes

Temp	**60 °C**			**65 °C**			**70 °C**		
Bitumen (%)	**4**	**4.5**	**5**	**4**	**4.5**	**5**	**4**	**4.5**	**5**
Marshall Stability (KN)									
All Agg.	11.2	12.0	10.0	10.6	11.5	9.54	10.19	10.7	8.86
30%Rep.	10.8	11.8	11.5	9.96	11.1	9.62	9.86	10.0	9.6
40% Rep.	10.4	11.1	10.5	9.94	10.2	10.1	9.68	9.98	9.88
50% Rep.	10.3	11.1	10.6	9.84	10.1	9.94	9.48	9.96	9.82
Marshall Flow (mm)									
All Agg.	2.97	3.27	3.75	3.1	3.3	3.6	3.15	3.32	3.56
30% Rep.	3.02	3.3	3.6	2.82	2.92	3.22	2.76	2.87	3.14
40% Rep.	2.87	3.05	3.5	2.76	2.9	3.11	2.65	2.72	3.01
50% Rep.	2.62	2.72	3.09	2.68	2.72	2.95	2.81	2.92	3.18
Air Voids (%)									
All Agg.	6.61	5.14	4.19	6.42	3.86	2.91	6.2	3.55	2.87
30% Rep.	8.01	6.66	5.65	8.03	6.8	5.74	7.8	6.22	5.72
40% Rep.	8.42	6.77	5.82	8.18	6.85	5.78	8.4	6.61	5.75
50% Rep.	8.67	7.1	6.08	8.55	6.89	5.26	8.4	6.78	6.23
VMA (%)									
All Agg.	14.6	14.4	14.6	14.4	13.4	13.5	14.3	12.9	13.47
30% Rep.	16.2	16.1	16.2	16.3	16.2	16.3	16.1	15.7	16.34
40% Re.p	16.7	15.8	16.5	16.5	16.3	16.5	16.7	16.2	16.5
50% Rep.	17.1	16.8	16.9	17.0	16.0	16.5	16.9	16.5	17.1
VFA (%)									
All Agg.	54.8	64.2	71.3	55.6	70.8	78.4	56.2	72.5	78.68
30% Rep.	50.8	58.7	65.2	50.7	58.2	64.9	51.4	60.7	65.01
40% Rep.	49.8	61.0	64.8	50.6	58.7	65.0	49.9	59.2	65.17
50% Rep.	49.4	57.7	64.1	49.8	60.8	65.9	50.1	58.9	63.56

Testing. Twenty four hours after preparation of samples, they were cleaned, weighed in air, and then submerged in water at 60°C, 65°C and 70°C for 30 minutes. Then they were tested by loading at constant deformation rate of 50 mm/min, until failure occurred. The temperature effects on the Marshall stability and flow parameters along with percent air voids in mix (AV), percent voids in mineral aggregates (VMA) and percent voids filled with bitumen (VFA) were determined

using standard procedures. To serve as control mix, specimens for the whole natural aggregate mix were prepared and tested.

TEST RESULTS AND DISCUSSION

The summary of average Marshall stability test, flow test results, and volumetric analysis results are tabulated in table 6.

Mixes with 100% Natural Aggregates – Control Mix

It can be observed that in general the stability value decreases with increase in water bath temperature as shown in figure 2. All the specimen prepared at 4% and 4.5% bitumen content met the NHA stability (min 9.81 kN) and flow (2-3.5 mm) requirements at all the temperatures while the specimen with 5% bitumen content at 65°C and 70°C did not meet the NHA stability requirements.

The best stability and flow results, i.e., 12.09 kN and 3.27 mm, respectively, were obtained at 60°C with 4.5% bitumen content. None of the samples except with 4.5% asphalt content at 60°C could fulfill the AV, VMA and VFA requirements. Samples with 4% asphalt content at 60°C met AV & VMA requirement of NHA specification but could not meet the VFA requirements. Samples with 5% asphalt content at 60°C met VMA and VFA requirements but could not meet the AV requirements.

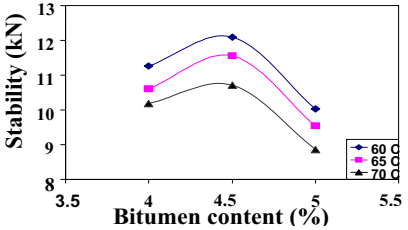


Fig 2. Stability of 100% aggregates.

Mixes with 30% Replacement of Fine Aggregates and Mineral Filler with Blast Furnace Slag and Fly Ash

Like the control mix, generally, a decrease in stability with increase in water bath temperature, at respective bitumen contents was observed (figure 3). All the samples tested at 60°C met the NHA stability and flow requirements; and best result of the stability and flow, i.e., 11.80 kN and 3.30 mm respectively, was observed at 4.5% bitumen content; the corresponding stability and flow at 65°C and 70°C were 11.14 kN, 2.92 mm and 10.06 kN, 2.87 mm respectively. All the samples tested at 65°C and 70°C met the NHA flow requirement. The samples with 5% bitumen contents tested at 65°C to 70°C could not meet the NHA stability requirements. Compared with control mix results, the stability and flow decreased overall but VMA and AV increased which indicates that addition of blast furnace slag and fly ash although effect stability and flow, but their addition may help in increasing VMA and AV in the compacted mix and provide the best result even at high temperature.

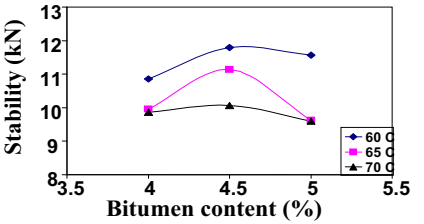


Fig 3: Stability of 30% representative samples, at different temperatures.

Mixes with 40% Replacement of Fine Aggregates and Mineral Filler with Blast Furnace Slag and Fly Ash

The samples also generally showed a decrease in stability with increase in water bath temperature at different bitumen contents as shown in Figure 4. All the samples tested at 60^{O}C met the NHA stability and flow requirements and best result was observed at 4.5% bitumen content at which stability and flow values were 11.14 kN and 3.05 mm, respectively; the corresponding stability and flow at 65^{o}C and 70^{o}C were 10.24 kN and 2.90 mm, and 9.98 kN and 2.72 mm respectively, which is slightly on lowers side for stability. With the comparison of the results (table 6), it can be observed that as the blast furnace slag and fly ash was increased from 30% to 40%, the stability and flow further decreased as compared with control mix. The VMA and AV on the other hand improved.

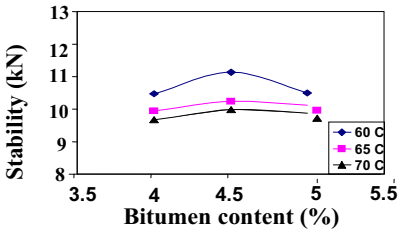


Fig 4: Stability of 40% representative samples, at different temperatures.

Mixes with 50% Replacement of Fine Aggregates and Mineral Filler with Blast Furnace Slag and Fly Ash

Like control mixes, generally a decrease in stability with increase in water bath temperature, at respective bitumen content was observed (figure 5). All the samples tested at 60^{o}C met the NHA stability and flow requirements and the best result was observed at 4.5% bitumen content at which stability and flow were 11.17 kN and 2.72 mm respectively. The corresponding stability and flow at 4.5% bitumen for 65^{o}C and 70^{o}C were 10.12 kN, and 2.72 mm and 9.96 kN and 2.92 mm respectively. From the comparison of results (table 6), it may be seen that flow decreased further as the proportion of blast furnace slag and fly ash were further increased from 40% to 50%. Also the VMA and AV can be observed to be improving.

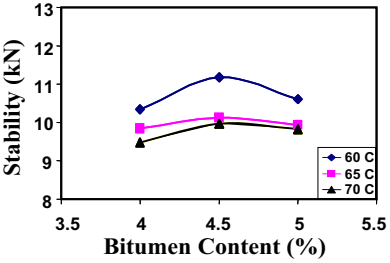


Fig 5. Stability 50% representative samples at different temperatures.

CONCLUSIONS

This lab study has shown the usefulness of blast furnace slag and fly ash in highway pavements; not only that the use of these waste materials will facilitate their disposal but will also help to preserve the natural aggregates. It is planned to construct trial roads/ pavements based on this lab study and further verify the results. Following important conclusions may be drawn from this study:

- The fly ash along with blast furnace slag can be used as partial replacement material in asphalt concrete pavements.
- Increase in temperature causes a decrease in stability of all the samples tested.

- Best results in terms of stability were obtained at 30% replacement level with 4.5% asphalt content for the samples prepared with blast furnace slag and fly ash.
- The best results which satisfying all the specification requirement according to NHA specification A were obtained at 50% replacement level with fly ash and blast furnace slag at 5% bitumen content at 65^{o}C.
- Generally stability and flow decreased gradually with increase in replacement level with these two waste products but on the other hand there is increase in the value of AV and VMA. The increase in AV and VMA can be beneficial in overcoming the bleeding problem during summers.
- VFA generally decreases with increase in replacement level with blast furnace slag and fly ash but increases with increase in bitumen contents.
- Compared with control mix, although all samples with blast furnace slag and fly ash showed lower stability, but this difference was not significant. Considering other properties like flow, AV, VMA and waste management aspects, its use can be beneficial for road construction in Pakistan and other countries experiencing high temperature during summer season. The samples prepared with blast furnace slag alongwith fly ash showed lesser variation in stability at higher temperatures as compared to control mix; as the percentage of these two waste products increased, the samples showed better performance against temperature variations.

REFERENCES

Organization for Economic Co-operation and Development (1977). “Use of Waste Materials and By-products in Road Construction”. Paris, France.

US Corps of Engineers (1991). “Hot Mix Asphalt Paving Handbook UN-13 (CENT-ET)”. USA.

National Highway Authority (1991), “General Specifications”. Government of Pakistan.

National Institute for Transport and Road Research (1978). “Selection and Design of Hot Mix Asphalt Surfacing for Highways, Technical Recommendation for Highway”. Pretoria.

Annual Book of ASTM Standards (1990). Section 4, Volume 4.02.

Foster Wheeler Energy Corporation, (1992). “Foster Fluidized Bed Systems”, New Jersey 08809, U.S.A.

Swamy R.N. (1986). ”Cement Replacement Materials”, Surrey University Press, UK. Scottish.

2D Numerical Settlement Analysis of A Slag Aggregated Test Road on Weak Soils

Aykut SENOL[1] and Bilal EROL[2]

[1] Assist. Prof., PhD, Civil Engineering Faculty of Istanbul Technical University, 34469 Istanbul, TURKEY, senol@itu.edu.tr
[2] MS Civil Engineer, Istanbul Greater Municipality, 34360 Istanbul, TURKEY, bilal.erol@ibb.gov.tr

ABSTRACT: In the past decade, numerous industrial and public initiatives have been launched in order to make knowledge, practices, and mentalities evolve in relation to the acceptability of using waste instead of raw materials as construction materials (Ahmed, 1993). The objectives of the initiatives have been to evaluate current practices and to make new solutions and channels for beneficial use emerge. At the same time, the scientific and standardization communities have developed methodologies and tools to fit the assessment needs (Sherwood, 2001). This part of the research presents the results of research involving metal slag as the base material for road constructions in Istanbul, Turkey. The design parameters for the roads constructed using the discarded metal slag were presented based on laboratory model studies. Numerical analysis and field performances were also conducted for the metal slag. Groundwater and surface water analyses conducted before and after the construction were taken into consideration. The metal slag contains some compounds that have pollution potential. Although the leachability of most compounds is low (below the maximum limit) for conditions in civil engineering applications, corrosion occurs at the exposed parts of the metal slag in poor drainage conditions. The conclusion of this research supports the view that the selected waste material is an environmentally acceptable base material for use as an alternative soil stabilization method in road construction. Consequently, it is concluded that the usage of metal slag waste material as the base of road construction is possible for every aspect of this research.

INTRODUCTION

The problems faced in road construction on soft bases are one of the common problems in Turkey, as in most part of the world (Edinçliler et. al., 2004). In recent years, because of the high cost of most road base stabilization methods, a need to search for alternative methods of road construction on soft bases has arisen (Edil et. al., 2002). One possibility is to use metal slag as a base material in road construction. In the production of liquid steel, 8–10% slag is formed. It is known that a hundred thousand tons of slag was identified in 2005. There is no scientific method for the

disposal of this slag. For these reasons, a prototype road was constructed using metal slag as the base material. The performance of this road has been evaluated. Depending on the environmental evaluation, the first stage of the research has been completed.

METAL SLAG

Metal slag is the name given to the lighter metals accumulated on the surface by density when mixed metals are melted. It is composed of silicate, lime, and aluminum oxide, and also contains iron oxide, magnesium oxide, and sodium oxide. In order to have an easy allocation of light metals, physical features must be taken into account, such as having a density difference and low fusion in order to flow easily when heated. It is formed by oxidation by the air and known as metal rot.

The metal slag sample was tested according to the standard method given in *Standard Methods for the Examination of Water and Wastewater* (APHA, AWWA, WEF, 1995, 19th edition) and was evaluated to conduct the analysis of the parameters according to the "Regulations Controlling Dangerous Waste". 50 g was left in a shaker in 500 ml pure water (in 150 rpm for 24 hours). Then filtrated and analyzed eluate was obtained. The total organic carbon analysis experiments done on eluate were conducted using SIEVERS 2244AP equipment. Heavy metals were measured by an atomic absorption spectrophotometer (Perkins SIMAA 6000). The phenol index, fluoride, and sulfate were measured using a Photometer Merk (SQ 118). Other parameters were examined using titrimetric analytical methods (Table 1).

Table 1. Criteria for methodical storage of waste, and results of analysis

	Waste transacted as dangerous waste (mg/L)	Results of analysis (slag sample) (mg/L)
Arsenic	< 0.2–2.5	0.005
Barium	< 10–30	5.4
Cadmium	< 0.1–0.5	0.002
Copper	< 5–10	0.005
Mercury	< 0.02–0.2	0.01
Molybdenum	< 1–3	0.06
Nickel	< 1–4	0.003
Lead	< 1–5	0.17
Selenium	< 0.05–0.7	0.0002
Zinc	< 5–20	0.16
Chloride	< 1500–2500	2
Fluoride	< 15–50	0.3
Sulfate	< 2000–5000	100

APPLICATION

The application of this part of the research was done in the campus area of Istanbul Technical University (ITU) located in the Sarıyer district of Istanbul. The application area is from the gym road and the satellite building of ITU. Approximately 170.00 m

of the road length was constructed on 3.00 m fill. The general topography of the land is almost flat and there is a slight inclination of 2% from the northwest towards the southeast. The underground water table level is deep and facile flow exists. Two different section types were projected in the construction. The first 50.00 m of the 170.00 m was constructed using the metal slag as the base. The remaining 120.00 m was built according to the Highway Technical Code of Turkey, 2006.

In the first, 50 m road section, the metal slag was used. 0.20 m of compacted ballast was selected for the subbase. On top of this layer, 0.20 m of compacted metal slag was applied (Figure 1). The 0.22 m concrete body was constructed over the 0.10 m ballast resolution layer. The road construction was completed by the application of 0.08 m of asphalt.



FIG. 1. Road base with metal slag



FIG. 2. Standard road section

In the 120 m regular road section, a 0.20 m compacted ballast subbase layer was applied over a 0.20 m compacted ballast base layer (Figure 2). A concrete body of 0.22 m in thickness was constructed over a 0.10 m ballast resolution layer. The road construction was completed by laying an asphalt layer of 0.08 m over the body (Figs. 3–8).



FIG. 3. Initial excavation



FIG. 4. Subbase ballast material

MEASUREMENTS

If measurement observations are made along the x, y, and z coordinates, an electronic total station device is suitable as the most efficient way to determine the probable settlements.

A quick check is done first to prevent physical damage or movement of the coordinates. If the check conditions are appropriate, the observation process can begin. According to the current polygon web, in the completed coordinate route the sections are formed at 5.00 m intervals by the regular software. The detailed points of the formed sections are coordinated by AutoCAD and then transferred to the electronic total station. The current land check points are taken as a reference for the application of the coordinate values. Basic mark systems are done after the application of the 3D (x, y, z) platform. These operations are repeated for all present points and then the measurements are also repeated according to the time periods mentioned in the measurement report. As a result, the difference between the first and the last measurement shows the amount of settlement.

The atmospheric conditions and time of day or night are considered during the examination of the area. It was decided to work using a local coordinate system. A road axis is placed on the area by considering the route of the road and the topography of the land and also by having a polygon route. The coordinates of the road axis are calculated for every 5.00 m of the road.

After using the current polygon route, the device is reset. The installed data is recalled for application to the land. The elevation differences are confirmed by repeating the operation every 2 days for a period of 60 days. Thus, data for the settlement of the road were obtained.



FIG. 5. Metal slag base material



FIG. 6. Resolution layer



FIG. 7. Concrete layer



FIG. 8. Asphalt layer of road

RESULTS

The aim of this research is to identify an improved alternative technique for soil stabilization in road construction by using metal slag such as waste material coming from the industry, taking recovery into consideration. Using the measured and calculated data from the site gathered just after the construction of the road built using the metal slag, the average settlements were determined. In the first 50.00 m section of the road, which was stabilized by the metal slag, the maximum settlement value was obtained as 0.042 mm. However, 0.103 mm of settlement was found in the second, 120.00 m, section that had been stabilized according to the usual standard method. These settlements were also clearly seen on the road. One main observation was the cracks in the connection between the first and second sections of the road (Figure 9). This undesired minor problem is due to the differing rigidities of the sections causing cracks in the transition part (Erol, 2008).



FIG. 9. Cracks formed in the transition part

The following conclusions can be drawn from the evaluation above:

- The usage of metal slag will increase the resistance and service life of the road.

- From the comparison of the two methods, it is determined that soil stabilization using metal slag is a new and effective alternative method of road construction that may be employed instead of regular methods. It is observed that the road section with the ballast base settles 200% more than the one with the metal slag base.

REFERENCES

Ahmed, I. (1993) "Use of Waste Materials in Highway Construction", Noyes Data Corporation, New Jersey, USA.

Erol, B. (2008) "Using Waste Materials As Road Base For Road Construction", ITU, The Institute of Science and Technology, MS Thesis, Istanbul, Turkey [In Turkish with an English summary]

Edil, T.B., Benson, C.H., Bin-Shafique, M. S., Kim, W., Tanyu, B.F. and Senol, A. (2002). "Field Evaluation of Construction Alternatives for Roadway over Soft Subgrade", *Journal of Transportation Research Record* 1786, National Research Council, Paper No: 02-3808, pp. 36-48

Edinçliler, A., Baykal, G., Dengili, K. (2004) "Determination of Static and Dynamic Behavior of Recycled Materials for Highways", *Resources, Conservation and Recycling* vol. 42, pp. 223–237

Sherwood, P. (2001). "Alternative Materials in Road Construction", Thomas Telford Publishing, London.

Experimental Study of Pervious Concrete on Parking Lot

Ming-Gin Lee[1], Chui-Te Chiu[2], Yu-Cheng Kan[3], Tsong Yen[3]

[1]Associate Prof., Department of Construction Engineering, Chaoyang University of Technology, Taichung County, 413, Taiwan, R.O.C.; mglee@mail.cyut.edu.tw
[2]Prof., Department of Civil Engineering, Chung-Hua University, Hsin-Chu 300, Taiwan, R.O.C.; ctc@chu.edu.tw
[3]Prof., Department of Construction Engineering, Chaoyang University of Technology, Taichung County, 413, Taiwan, R.O.C.; ce@mail.cyut.edu.tw

ABSTRACT: In order to resolve the runoff of rainwater resource, to prevent the spoliation of ecology, and to reduce the effect of heat island, the search for a suitable mix design of the pervious concrete for Taiwan is not a trivial issue. The main purpose of this study is to find the suitable pervious concrete mix for pavement engineering. The two experiments included in this study are: (1) test the suitable mix design of pervious concrete; and (2) test certification in the field construction of pervious concrete on parking lot. Pervious pavement composed of 8-in surface layer (pervious concrete) and a 4-in base layer (gravel) were made. The results showed that the compression strength of the two pervious concrete core specimens from test certification in the field construction (parking lot) exceeds the ordinary concrete structure specification (175 kg/cm^2). The field permeability test for the parking lot is about 1000 ml/15sec. The water penetration of the above pervious concrete is very good and no cracks were present on surface. Therefore, it is an environment-friendly material for pavement.

INTRODUCTION

Pervious concrete was referred to as a parking lot pavement material in the central Florida area as early as the 1970s. The concept developed as a means of handling the enormous quantities of water runoff within a parking lot during a heavy rain or storm; pervious concrete allows the water to percolate into the ground under the pavement. The Environmental Protection Agency (EPA) in Unite States has adopted a policy that recommends the use of pervious pavements as a part of their best management practice as a way for communities to mitigate the problem of storm water runoff. Pervious concrete parking lots have also been selected as an integral solution to the problem of hot pavements in the Cool Communities program. The hot pavements bring the phenomenon of heat island effects in the big city. Generally, the air temperature over pervious concrete parking lots is cooler than the temperature over

asphalt parking lots. Pervious concrete parking lots also reduce snow and ice buildup. In addition, pervious concrete is considered a non-pollutant to the environment. The practical range of design thicknesses for pervious concrete pavements is from 5 to 10 inches for plain parking lots (ACI 2006).

Trees planted in parking lots and city sidewalks may offer shade and produce a cooling effect in the area which further reduces the heat island effects. Pervious concrete pavement is ideal for protecting trees in a paved environment. Many plants have difficulty growing in areas covered by impervious pavements, sidewalks, and landscaping, because air and water have difficulty getting to the roots. Pervious concrete allows adjacent trees to receive more air and water while still permitting full use of the pavement. Pervious concrete provides a solution for landscapers and architects who wish to use greenery in parking lots and paved urban areas (Tennis et al 2004). The pervious concrete pavement possesses many advantages that improve city environment as follows (Yang and Jiang 2003):

1. Rainwater can quickly filter into ground, allowing groundwater resources to renew in time.
2. As the pavement is air permeable and water permeable, the soil underneath can be kept wet and further improves the environment of road surface.
3. The pervious concrete pavement can absorb the noise of vehicles, creating a quiet and comfortable environment. On rainy days, the pervious concrete pavement has no plash on the surface and does not glisten at night. This further improves the comfort and safety of drivers.
4. The pervious concrete pavement materials have holes that can cumulate heat. Such pavement can adjust to the temperature and humidity of the Earth's surface and eliminates the phenomenon of heat island in cities.

Pervious concrete is a special type of concrete with a high porosity used for concrete flatwork applications that allows water from precipitation and other sources to pass through it, thereby reducing the runoff from a site and recharging ground water levels. The void content can range from 18 to 35% with compressive strengths of 400 to 4000 psi (2.8 to 28 MPa). The drainage rate of pervious concrete pavement will fall into the range of 2 to 18 gal./min/ft^2 (81 to 730 L/min/m^2). Typically pervious concrete has little to no fine aggregate and has just enough cement paste to coat the coarse aggregate particles while preserving the interconnectivity of the voids (NRMCA 2004). Pervious concrete is traditionally used in parking areas, areas with light traffic, pedestrian walkways, and greenhouses. Pervious Concrete is an important application for sustainable development (Obla 2007).

The main objective of this study is to evaluate the performance of pervious concrete parking lots in Taiwan in order to provide guidance as to how to construct durable pervious concrete pavements based on Taiwan's climate. The secondary objective is to evaluate and develop a test method for determining the in-place permeability of pavement.

EXPERIMENTS

Pervious Concrete Materials and Mixtures

The cement used in this study was Type I Portland cement conforming to ASTM C

150 which was manufactured by a local cement company. The coarse aggregate used was a commonly-used crushed stone with diameter range from 6 to 3 mm. Fine aggregates are nonexistent in pervious concrete mixture because they tend to compromise the connectedness of the pore system. The superplasticizer (SP) is liquor of the phenolic aldehyde; its specific gravity is 1.05 and has 30% solid content. The above materials including cement, crushed gravel, SP and water were used to make the pervious concrete mixture.

Pervious concrete mixture has zero inch slump and water to cement ratio of 0.31. Table 1 shows pervious concrete mixture designs used in this study. The pervious concrete mixture has a wet metallic appearance or sheen. A handful of mixture formed into a ball will not crumble or lose its void structure as the paste flows into the spaces between the aggregates. The above optimum mixture design was depend on typical ranges of materials proportions in pervious concrete and be tested in many trial batches to reach proper proportions and expected behavior.

Table 1. Mixture designs for Pervious Concrete

W/C	Aggregate Diameter	Coarse Aggregate kg/m^3)	Cement (kg/m^3)	Water (kg/m^3)	SP (kg/m^3)
0.31	3 – 6 mm	1498	344	105	2.3

Design and Construction

The elements in the design of pervious concrete pavement systems which includes pavement thickness, joint spacing, and drainage details are very important. When pervious concrete pavements were built on freely draining sandy soils, the water can flow straight through the pavement and into the soil. This type of installation, where the water flows directly downward through the pavement layers, may be referred to as open systems. The installation of above open system was used at the Chaoyang University of Technology parking lot demonstration project. On July 6 and 11, 2007, part of an existing gravel parking lot was removed in order to construct a demonstration pervious concrete pavement site. The parking lot is shown in Figure 1. A 5.5 by 14.4 meters strip of existing parking lot was removed, and 4 inches (100 mm) of subbase was placed and compacted. At last, six strips were paved with 8 inch (200 mm) thick pervious concrete. Joint spacing is about 2.4 meters, demonstration pervious concrete pavement have been divided into six parking spaces.

Field and Laboratory Testing

For this research, the field evaluations included visual observation, in-place permeability test, and core test. The cores were taken in accordance with ASTM Standard C 42 / C 42 M-99. The core barrel was 4 inches in diameter which extracted a core sample with a diameter of 3.75 inches. Twenty-four cores were taken from the parking lot demonstration, where 4 cores were taken for each of the parking spaces. The laboratory tests included void ratio, unit weight, coefficient of permeability, and compressive strength.

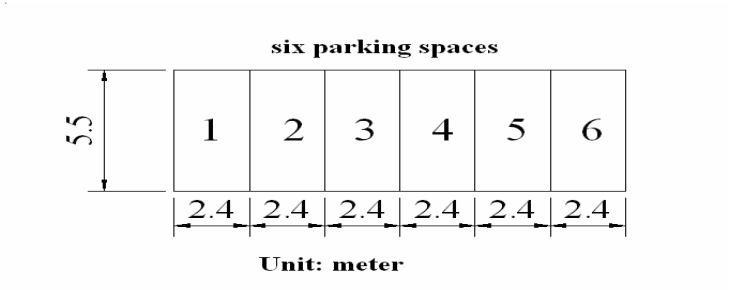


FIG. 1. Parking Lot Demonstration

An in-place permeability test is described as follows: A simple in-place permeability apparatus of pavements was evaluated as part of this research. The equipment consisted of a stop watch, water container (glass cylinder), and an in-place permeability apparatus which was used in the porous asphalt pavement. Rubber dough was attached to seal between the bottom of in-place permeability apparatus and the surface of pavement, and a glass cylinder of permeability apparatus was filled for water to flow out. The water to drain from the x1 initial head of glass cylinder to the x2 final head (free flow) was about 400 ml. The apparatus is shown in Figure 2. The time in seconds T required for the 400 ml water to drain from glass cylinder to the pavement was measured. Precautions should be taken not to allow water to freely flow around the seal of rubber dough. The test may also be used before and after maintenance to quantify the effectiveness of an in-place permeability technique. The content of in-place permeability K (ml/15sec) can be expressed as equation (1).

$$K\ (ml/15sec) = (400ml/T) \times 15 \quad \cdots\cdots (1)$$

Where T = the measured time in seconds



FIG. 2. In-place Permeability Apparatus

RESULTS AND DISCUSSION

Visual Observations

Visual observations provided information on the overall performance of the pervious concrete pavement. This parking lot isn't prone to refrains from clogging by

sand and debris. There is no cracking, but there is partly raveling at the #4 and #5 parking spaces. The raveling is shown in Figure 3. It was due to extreme temperatures at the time of placement, and a dry mixture in the last batch of pervious concrete. After the in-place permeability testing, core samples were taken from six different parking spaces of the pervious concrete for further testing.



FIG. 3. Partly Raveling at the #4 and #5 Parking Spaces

In-place Permeability Testing

The in-place permeability testing method developed for asphalt pavements has been found to work and perform well to pervious concrete pavement (Lee et al 2008). The 28 days and one year test results are recorded in Table 2. The in-place water permeability of pervious concrete pavement ranged from 796.8 to 1176.5 ml/15sec after installation. The six parking spaces are examined again and performing well after a year of use. A critical value of in-place permeability is 400 ml/15sec, anything more than the critical value is a fair penetration rate, and anything less 400 ml/15sec is a poor penetration rate. All six parking spaces have shown to belonged in a very fair penetration rate. This test may be used to assess penetration capability of newly built pavements, or to determine whether maintenance is needed. It would be useful to track results over time, in order to assess the need for and effectiveness of different maintenance treatments.

Table 2. In-place permeability results for parking lot (ml/15sec)

28 days		1	2	3	4	Mean (cv*)	1 year
No. of Parking spacing	#1	796.8	967.7	1071.4	1043.4	969.8 (12.7%)	722.6
	#2	1176.4	1094.9	1121.5	1125.7	1129.6 (3.0%)	1108.2
	#3	1147.2	1096.9	967.7	1081.1	1073.2 (7.0%)	1021.6
	#4	1153.8	1176.5	1153.9	1071.4	1138.9 (4.0%)	1064.1
	#5	1153.9	1071.4	1132.1	1081.1	1109.6 (3.5%)	1048.2
	#6	1098.9	1140.7	1062.0	1162.0	1115.9 (4.0%)	1111.4

cv*: Coefficient of Variability

Testing of Cores

It was possible to extract cores from four of the six parking spaces for laboratory

testing. Failed attempts were made to extract a whole core from both #4 and #5 parking spaces due to dry mixture and material segregation. In total 16 cores were taken from four different parking spaces and were brought back to the laboratory to be tested for void ratio, unit weight, compressive strength, and coefficient of permeability. Some of the cores were cut into top and bottom specimens to compare the properties through the pavement thickness. The test results are recorded in Table 3.

Table 3. Test result of cored samples from different parking spaces

No. of Parking spacing		unit weight (kg/m^3)	void ratio (%)	compressive strength (kg/cm^2)	coefficient of permeability (cm/sec)
#1	1(top/bottom)	2042/2208	7.1/3.5	/	0.003/0.01
	2	2136	4.3	192	0.05
	3	1955	9.8	106	0.05
	4(top/bottom)	1983/1856	12.1/19.7	/	0.01/0.22
#2	1(top/bottom)	2083/2089	11.2/9.8	/	0.13/0.02
	2 (top/bottom)	1982/2055	15.2/11.1	/	0.10/0.05
	3	2079	9.8	180.5	0.05
	4	1984	13.3	146.1	0.13
#3	1 (top/bottom)	2039/2089	13.3/10.3	/	0.04/0.02
	2 (top/bottom)	2277/2052	3.3/12.2	/	0.003/0.05
	3	2081	10.8	105.5	0.12
	4	1994	14.8	82.4	0.10
#6	1	2101	10.0	117.5	0.08
	2	1890	17.8	76.3	0.11
	3(top/bottom)	2168/1661	5/28.6	/	0.01/0.15
	4(top/bottom)	1980/1985	14.1/10.9	/	0.12/0.01
Mean (cv*)		2032 (5.5%)	11.6(52.5%)	125.8 (25.3%)	0.07 (93.8%)

Coefficient of Variability and significant differences were observed among testing of cores due to extreme temperatures at the time of placement, and a dry mixture in the last batch of pervious concrete. For example, it found that the void ratio and unit weight at the top of a pervious concrete core could not match with those at the bottom. Usually, the void ratio at the top of a pervious concrete pavement was much lower than that at the bottom. The tests results reported in this section denied that finding. The results of pervious concrete core specimens showed that the compression strength decreases as the void ratio increases, unit weight decreases as the void ratio increases, and permeability increases as the void ratio increases, with a rapid increase in permeability at void ratios greater than 15%. The results also showed that the compression strength of two pervious concrete core specimens exceeds the ordinary concrete structure specification (175 kg/cm^2).

SUMMARY

1. There is no cracking, but there is partly raveling at the #4 and #5 parking spaces.

Both #4 and #5 parking spaces had very dry mixture and failed to extract with a whole core due to improper installation.

2. The in-place permeability testing method developed for asphalt pavements has been found to work and perform well to pervious concrete pavement. The field permeability for the parking lot is about 1000 ml/15sec, which belongs to a very fair penetration rate. The six parking spaces are examined again and performing well after a year of use.
3. The compression strength of two pervious concrete core specimens exceeds the ordinary concrete structure specification of 175 kg/cm^2.

ACKNOWLEDGMENTS

The authors would like to thank Dr. Yung-fang Chiu, Mr. Tao-kuang Chang and the Ministry of Transportation and Communications for the financial support under the grant MOTC-IOT-96-H1DB004.

REFERENCES

ACI 522R-06. (2006). *Pervious Concrete.* American Concrete Institute, Farmington Hills, MI:1-25.

Lee, M. G., Chiu, C. T., and Yen, T. (2008). *Application of Pervious Concrete on Transportation Engineering (2/2),* Ministry of Transportation and Communications, Taiwan: 1-188.

National Ready Mixed Concrete Association. (2004). *Freeze Thaw Resistance of Pervious Concrete*, Silver Spring, MD: 1-17.

Obla, K. (2007). "Pervious Concrete for Sustainable Development." *Proc., 1st Int. Conf. on Recent Advances in Concrete Technology,* Washington DC.

Tennis, P., Leming. M.L., and Akers, D.J. (2004). "*Pervious Concrete Pavements*." EB 302, Portland Cement Association (PCA), Skokie, Illinois: 1-25.

Yang, J. and Jiang, G. (2003)." Experimental study on properties of pervious concrete pavement materials." *Cement Concrete Research*, Vol. 33(6): 381–386.

An Experimental Study on Pulverized Fuel Ash Concrete

Wen Yi [1], Yonghe Wang[2] , and Yihua Nie[3]

[1]Central South University, 932 Lushan South Road, Changsha 410083; Central South Forestry University of Science and Technology, 498 ShaoShan South Road, Changsha, 410004;yiwengangbiao@163.com,

[2]Central South University .932 Lushan South Road, Changsha 410083; yonghewang@163.com

[3]Central South Forestry University of Science and Technology, 498 ShaoShan South Road, Changsha, 410004; nieyihua@sohu.com

ABSTRACT: It is well known that the quality of cement concrete highway surface has significant influence on the vehicle running speed. This paper discusses the performance of cement concrete mixed with pulverized coal ash based on the experimental study. Results show that when adding with pulverized coal ash, the anti-booklet intensity will be enhanced, the abrasion resistance can be improved and water gain rates and the cement hydration speed can be cut down effectively. It should be noted that the pulverized coal ash cement concrete must consume massive pulverized fuel ash which will occupy land area and pollute the environment.

1. LABORATORY TEST

1.1 Summarization

The pulverized fuel ash includes many active materials, e.g. SiO_2, CaO_2, CO_2.,etc. The pulverized coal ash accumulation not only takes massive lands, but also pollutes the environment. It will improve pavement's mechanical properties and obtains the good economic efficiency if it can be used in the concrete pavement construction [1][2]. Due to the difference of the combustion and recycling technology, the quality of pulverized coal ash has very obvious difference. It is required to use dry and ground powder coal ash in cement concrete pavement project, and the technical class should be above level Ⅱ [3]. The pulverized coal ash used in this experiment is produced by Zhuzhou Power plant. Its main technology test data is as following: water requirement is 100%, water content is 0.11%, KOSS content is 4.51%, SO_3 content is 0.44% and degree of fineness is 19.9% (45um sieves).

Each index of level Ⅲ ash can't satisfy the request of the road surface concrete, which can only be used in the base course.

1.2 The experiment for different contents of pulverized fuel ash

Theoretical study indicates that Ca (OH) $_2$ and gypsum released out from Portland cement can only make maximum 28% powder coal ash get hydration reaction, which improves the strength as a result [4]. It is assumed that 1 m^3 cement concrete needs 360 kg water at least. When 1 m^3 cement concrete uses 360 kg cement, 525# average

calcium silicate cements, water cement ratio is 0.41, the sand aggregate ratio is 37%, powder coal ash in different case is tried to add in 20 kg, 25 kg, 30 kg, 35 kg, 40 kg, 45 kg, 50 kg and 55 kg, respectively. by calculating we know that water amount for 1 m^3 cement concrete is m_w = 180 kg, and k= 0.4, L = 0.86, from the equations (1) and (2):

$$m_c = \frac{lm_w}{w/c - F} \tag{1}$$

$$F = \frac{\frac{Lm_w}{w/c} - m_c}{k} = 44k_g \tag{2}$$

where

m_c is the cement dosages in pulverized fuel ash concrete

L is fine coal ash subtraction water modulus

m_w is water content of concrete

w/c is water cement ratio in concrete

k is fine coal ash's gelatinizes efficiency coefficient

Study shows that the best overall performance of the concrete can be obtained when adding 45kg pulverized coal ash, the pulverized coal ash content was 12.5%, which is among the 8%~20% demanding range in the requirement.

1.3 The mixture designs for pulverized ash cement concrete

The excess coefficient method is used to design the pulverized ash cement concrete[5][6]. Excess coefficient k can be got by $k=m_f/(m_c-m_{c0})$, where m_f is fly ash content, (m_c-m_{c0}) is the substitutes for cement quantity in the concretes. According to the data gives by Zhuzhou power plant, the excess coefficient of 1.5 is used in the study.

In the test, cement grade is 30, slump is 30~50mm, density of 525# ordinary Portland cement is 3700kg/m^3; intensity extra coefficient is 1.06; maximum particle size of crushed stone is 40mm, sand is 2.6mm granulated middle-sized and its density is 2650kg/m^3, the gravel is 5~40mm of crushed stone, the apparent density is 2700kg/m^3 (the parameters above are for dry environment).

1.3.1 *Computing mixture proportion*

In order to calculate the mixture proportion, the following steps are adopted in the study

(1) Configuration strength is $f_{cu,t}$=30+1.645×5=38.2Mpa,

(2) Water cement ratio is $w/c = \frac{Af_{cu}}{f_{cu,t} + ABf_{cu}}$,where A =0.48, B =0.52, so

w/c=0.51.

Based on the standard table, we take the water ash ratio is 0.41 because of w/c≤0.65 in the dry environment.

(3) Determining water dosages (m_w)

Based on the standard, water consumption per $1m^3$ concretes may select m_w=175kg when maximum particle size of crushed stone is 40mm according to 30~50mm slump.

(4) Determining cement dosages (m_c)

According to the following equation:

$$m_c = \frac{m_w}{w/c} = 175/0.51 = 343\left(k_g/m^3\right) \tag{4}$$

In the working conditions, the minimum cement dosages requested is $760kg/m^3$, so the cement dosages may take $343kg/m^3$.

(5) Determining sand ratio

Based on the standard, sand ratio may take $\beta_s = 37\%$ when w/c=0.51, the maximum particle size of crushed stone is 40mm.

(6) Calculating sand and crushed stone amount (m_s, m_g) per $1m^3$

The volumetric method is used to do such as:

$$\frac{m_c}{\rho_c} + \frac{m_w}{\rho_w} + \frac{m_s}{\rho_s} + \frac{m_g}{\rho_g} + 0.01 \times 1 = 1 \tag{5}$$

Based on above analysis and calculating, we can get various materials consumption for $1m^3$ concretes material as follows: cement amount (m_c), water amount (m_w), sand amount (m_s) gravel amount (m_g) are 343kg, 175kg, 768kg, 1306kg separately.

1.3.2 *Adjustment with excess substitution method*

(1) According to applied technology regulations table, pulverized coal ash is selected. Its substitution cement ratio is 15%, and cement amount is 292 kg/m^3;

(2)Figures out the pulverized coal ash amount according to the excess coefficient, m_f=1.5× (343-292)=77(kg/m^3);

(3)Computing absolute volumes of cement, pulverized fuel ash and sand, extracting the volume of pulverized coal ash which surpass the cement part, and deducting the same volume sand amount according to γ_c=3.7,γ_f=2.2,γ_s=2.6. So

$$w_s = w_{so} - \left(\frac{m_c}{\gamma_c} + \frac{m_f}{\gamma_f} + \frac{m_s}{\gamma_s} \right) \times \gamma_s$$

$$= 768 - (29213.7 + 7312.2 - 34313.7) \times 2.6 = 718 \left({}^{k_g}\!/\!_{m^3} \right)$$

(4) Making $g=g_0$ and $w=w_0$, then m_c=292 kg/m^3, m_w=175 kg/m^3, m_s=718 kg/m^3, m_g=1306 kg/m^3,m_f=77 kg/m^3;

(5) Mixture design results

Because we try to match and gain the pulverized coal ash concrete's actual unit weight is 2910kg/m^3 (computation unit weight is 2865kg/m^3) by splining fit approximation. Correction coefficient k is 1.02 (k=2910/2865), so we get the material amount of pulverized coal ash concrete is as following: m_c=298kg/m^3, m_w=179 kg/m^3, m_s=732 kg/m^3, m_g=1332 kg/m^3, m_f=79 kg/m^3.

2. THE INFLUENCE OF PULVERIZED COAL ASH TO CEMENT CONCRETE

2.1 The influence of operating performance

When the cement concrete adds some pulverized coal ash, the total quantity of the gelled materials will increase, and the operating performance of concrete will improve greatly. It is more suitable to slip form construction [7].

(1) The vibration viscosity coefficient of pulverized coal ash reduces, which is benefit to dense in the vibration.

(2) When static slump become smaller, it can prevent slump.

(3) Gelled material's total quantity increases, which is benefit to smooth surface.

(4) The workability improves and spreader's load reduces.

The performances are improved due to the pulverized coal ash which affects the flowing deformation with specific surface area and the spherical micro bead. To spread cement concrete without pulverized coal ash, in order to vibrate densely, we must increase the slump of concrete, and such concrete is easy to collapse. In order to prevent collapse, we must reduce the concrete's slump, so we must enlarge the vibration frequency of tampers. Therefore, the machine advance's resistance and the working load increase. After adding the pulverized coal ash, this contradictory can be solved effectively.

2.2 Increasing bending strength

When pulverized fuel ash is used in the slip form construction for the cement concrete, the bending strength can be increased [8], especially the long-term strength can be significantly increased. In the paper, cement amount is instead of 12.5%level Ⅱ pulverized coal ash. The testing results of bending strength is shown in Fig.1.

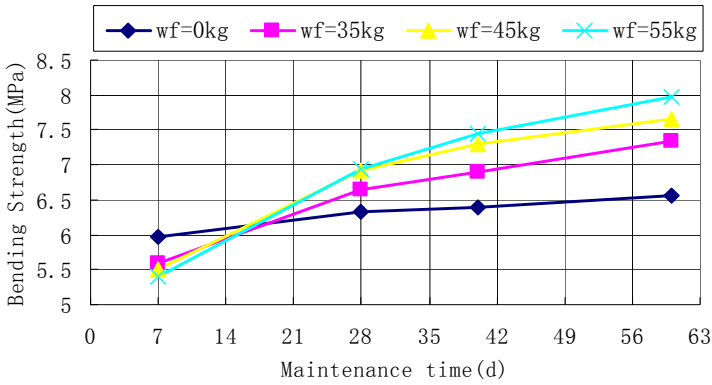


Fig.1. Pulverized fuel ash concrete bending strength and maintenance time relationship curves (MP_a)

According to table 1 and figure 1, the bending strength of concrete with pulverized fuel ash after maintenance 28d, 40d, 60d, the bending strength increase 5%~10%, 8%~16%, 12%~22% than plain concrete separately. The regular is that the bending strength increases with the content of pulverized coal ash and maintenance time.

2.3 Abrasion resistant improvement

The relationship between the abrasion resistance and the intensity in cement concrete pavement is linear. The abrasion resistance increases with pavement bending strength increases [9]. Through the abrasion resistant experiment of test sample in 48d maintenance age, when the mixing quantity of pulverized coal ash is 12.5%, the abrasion resistance of pulverized coal ash concrete increase about 23%. The testing results of bending strength is shown in Table 1.

Table 1. Abrasion resistance contrast experiments tests for pulverized fuel ash concrete

mixing quantity of level Ⅱ pulverized coal ash (kg)	Abrasion amount (kg/m^2)	
	Experimental value	Specification
0	1.20	⩽3.6
45	0.923	

2.4 Reducing water gain ratio

Owing to the limit of machine forming a complete set, the self-discharging trucks

are used to transport mixture during the slip-form construction using domestic slip-form concrete machine [10]. The serious water grain will reduce the blend operating performance during the transportation process, and will induce discharging, and cut the working efficiency down, and increase the labor strength. If the pulverized coal ash is used in the concrete, it can reduce the water grain ratio, which will benefit the transportation of concrete mixture.

2.5Reducing cement hydration speed

To pulverize fuel ash concrete, the cement hydration speed will be reduced, and the time of setting will be prolonged, which is advantageous to high temperature construction and long-distance transportation.

3. SOCIAL AND ECONOMIC BENEFITS

3.1 Social efficiency

The social efficiency mainly reflects in the environment contribution. The total length of 75 km cement pavement in Long –Chang highway have used pulverized coal ash about 22,500 tons. So much pulverized coal ash is used which has saved the depot land 1094 Chinese acres for the thermal power plant, and saved 525# cement about 10,800 tons. At the same time, they reduced the CO_2 emissions resulting in direct pollution to the atmospheric, and improve project qualities for pavement smoothness, strength and outward appearance etc.

3.2 Direct economic efficiency

All 22,500 tons pulverized coal ash used in the cement concrete pavement has saved the fund 3,000,000 Yuan to deposit pulverized coal ash, and saved the project cost 2,280,000 Yuan to buy 10,800 tons cement for the power plant. The cost 30500 Yuan has been saved in each 1km road surface. They have obtained the direct economic efficiency about 70,400 Yuan.

4. CONCLUSIONS

After adding the pulverized coal ash suitably in the cement concrete, the operating performance of the cement concrete can be improved evidently, the water grain rate and the cement hydration speed can be reduced. It is more suitable to construct in slip-form paving. Bending strength and the abrasion resistance of pavement can been enhanced. Highway's project quality can be improved. The environment can be protected. The considerable social and economic efficiency can be obtained. Although the air shrinkage is big, and early strength is low, we can strengthen construction management and use the reasonable technical measure to solve. It does not interrupt the use of pulverized coal ash. The pulverized coal ash cement concrete

is worthy promoting in cement concrete pavement projects in the high grade highway.

ACKNOWLEDGMENTS

The authors appreciate the support of Hunan Education Office. Project No. 06C899

REFERENCES

1. Wenjun KONG. (1995). "Ash resources ways explore."*Explore nature*, (01):13-17.
2. CHEN Hong (2006). "New ways explore to utilization of fly ash." *Western coal chemical industry*, (02):75-77.
3. Quanjin ZU, Wei SUN, Yunsheng ZHANG, Jinyang ZHANG (2005). "Fly ash concrete life of the multi-factor model." *Journal of Southeast University* (Natural Science), (S1):148-151+160.
4. Weizu QIN(2006). "The use of fly ash in concrete."*Commodity Concrete*. (02):13-17
5. "Plain concrete mixture ratio design regulations JGJ55-2000 (2001). " *China Building Industry Publishing House*. Beijing.
6. Linming LIU, CUI Yan(2007)."Discussion about fly ash concrete mix design." *Commodity concrete,* (04):49-51
7. ZhiQin QIAO(2004). "Ash on the properties of concrete." *Science and technology in Monggole*, (02): 59-60
8. Ching CHENG, Hongjuan LIU(2006). "PFA performance of steel fiber reinforced concrete and its components by bending test of the study."*Commodity concrete*, (04):8-12
9. Zongcai DENG, etc (2003). "Basics performance characteristics and flexural toughness of dumb-bell steel fiber reinforced fly ash concretes." *Road,*(9):149-155.
10. QIAO Defu, Qunguo LI, Dajun LI(2006). "Fly ash high-performance concrete production and application." *Jilin traffic science and technology*, (01):31-34

Investigation of High Temperature Properties of Asphalt Mixture Containing Fibers

Liang Zhou[1], Peilong Li[2] and Zhengqi Zhang[3]

[1]PhD Candidate, Key Laboratory of Road and Traffic Engineering of Ministry of Education, Tongji University, Shanghai P.R. China, 201804. Email:tinyzhou2014@sina.com

[2]PhD Candidate, Key Laboratory for Special Area Highway Engineering of Ministry of Education, Chang'An University, Xi'an P.R. China, 710064. Email: li_peilong@sohu.com

[3]Professor, Key Laboratory for Special Area Highway Engineering of Ministry of Education, Chang'An University, Xi'an P.R. China, 710064. Email:z_zhengqi@126.com

ABSTRACT: Fibers are extensively used in civil engineering applications for many years. The fibers provide three-dimensional reinforcement of the mixture. The main objective of paper is to evaluate effect of fibers on performances of asphalt mixture at high temperature. Three different fibers were used as modifiers: polypropylene fiber, polyester fiber and cellulose fibers. An SHRP's Dynamic-Shear-Rheometer (DSR) was employed to investigate the rheology property of asphalt-fiber mortar. The wheel tracking device was employed to evaluate rutting resistance of asphalt mixture. The strengthening mechanism in fiber-reinforced asphalt mixture was studied. DSR test results demonstrated that fiber asphalt mortar showed remarkable improvement of properties in comparison with the control asphalt mortar. The wheel tracking test results showed that fiber performed different performance level but showed more resistance to permanent deformation according to the fiber type and fiber contents.

KEY WORDS: fiber; asphalt mixture; asphalt mortar; high temperature performance

INTRODUCTION

Pavements made from asphalt and aggregate are expected to be mechanically highly durable, however, the increases in traffic volumes in recent years has resulted in heavy damage including rutting and cracks in the pavement. Fibers, as one of various modifiers for asphalt, have gotten much attention for their excellent improvement effects (WU, 2006). Fibers are extensively used in civil engineering applications for many years. Many earlier research projects focused on the influence of fiber additives

on the engineering properties of asphalt or asphalt mixture (Serkan, 2008). In this study, the investigation of high temperature property of fiber reinforced asphalt mortar and asphalt mixture were further developed and tested.

MATERIAL AND EXPERIMENTAL PROGRAM

Materials

The asphalt employed was graded as AH-70# according to Technical Specification for Construction of Highway Asphalt Pavement (JTG F40-2004), with a penetration of 67dmm at 25^0C, and softening point of 61^0C. This asphalt material, supplied by the KOCH Asphalt Co. Ltd (Shaanxi Province, China), is the usual asphalt grade used for asphalt pavement construction in China. Andesite aggregate was used in the experimental program. Three types of fibers including polypropylene fiber, polyester fiber, and cellulose fibers were used as stabilizer to mix with asphalt. Table1 lists the basic properties of fibers.

Table 1 The physical properties of fibers

Items	polypropylene fiber	polyester fiber	cellulose fiber
Diameter / mm	0.013	0.02±0.0025	0.045
Length / mm	4～6	6.35±1.58	1.1
Tensile strength / MPa	>910	517±34.5	
Elongation / %	8～12	33±9	
Melting point / ^{0}C	>240	>249	>200

Dynamic-Shear-Rheometer (DSR)

The rheological properties of asphalt-fiber mortar were measured by a dynamic shear rheometer (DSR) over a wide range of temperatures. For tests at 46^0C to 82^0C, a 1-mm gap and a 25-mm diameter plate were used. After heating to the test temperature of the binder, the top plate was brought into contact with the sample and the sample was trimmed. An actuator then applied a sinusoidal strain. A specific strain level was kept at 12%. Each testing temperature for each sample running a frequency of 10 rad/s.

Wheel Tracking

Wheel Tracking device was adopted to evaluate the high-temperature performance (rutting resistance) of asphalt mixture. The fiber-asphalt specimen was prepared in a

$300mm^{L} \times 300mm^{W} \times 50mm^{H}$ steel mould. The wheel load with a solid-rubber wheel contact pressure was 0.7±0.05MPa. The traveling distance of the wheel was 230±10mm, the number of cycles of the wheel was 42±1 rpm, the whole test time was 60min, and the test temperature was 60 ± 1^{0}C. The wheel tracking results was calculated as follows:

$$DS = \frac{S \times T}{d_{60} - d_{45}}$$

Where: d_{60}, the deflection at the elapsed loading time of 60 minutes, mm; d_{45}, the deflection at the elapsed loading time of 45 minutes, mm; S is the wheel speed, 42 cycle/min; and T is the time difference, 15 minute.

RESULTS AND DISCUSSION

DSR Results

Strategic Highway Research Program (SHRP) adopted rutting parameter ($G^*/\sin\delta$) to estimate the durability of rutting resistance of asphalt mix. The higher $G^*/\sin\delta$ is at high temperature, the durability of rutting resistance of its relevant mix.

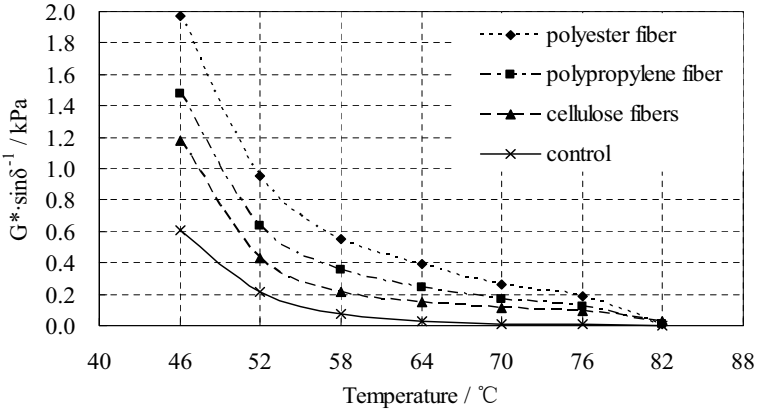


Fig.1. $G^*/\sin\delta$ **versus temperature**

As showed in Fig.1, the rutting parameter of asphalt mortar with or without fibers are decreased with the increase of temperature. These decreases are more significant at lower temperature than at high temperature, which is beneficial to asphalt mortar. The general trend is similar, but it must be noted that the decrease tend of the asphalt-fiber specimens is much better when compared with control specimen which is not added

with any kind of fiber. It means that the addition of different fiber improve the high temperature performance (WU,2008).

Studies before showed that the microstructure of polyester and polypropylene fibers differ from that of cellulose fibers since the cross-section of polyester and polypropylene fibers is quite round, with a smooth surface and a smaller surface area(Jian-shiuh,2005). Therefore, they can be soaked easily by surface active components in the asphalt, which indicates that these fibers can absorb the asphalt. On the other hand, the microstructure of cellulose fibers appears to be so rough. Therefore, the specific surface area is much larger than other two fibers, which leads to the efficiency of binding more asphalt.

Wheel tracking results

Effect of fiber type

The influence of fiber showed different effect between fiber-asphalt mortar and fiber-asphalt mixture. The durability of rutting resistance of fiber-asphalt mixture was investigated in reduced scale using the wheel tracking test. A higher wheel tracking results represents a higher rutting resistance of asphalt mixture.

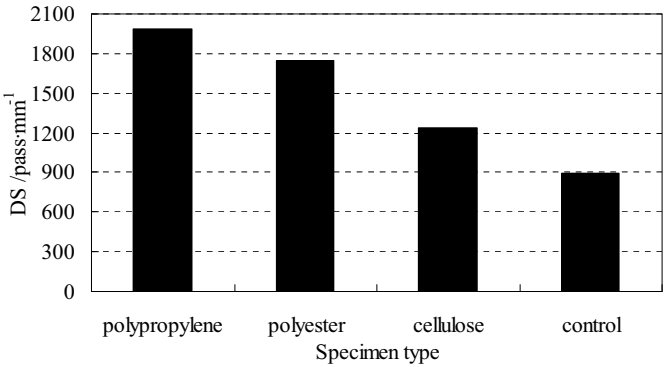


Fig. 2. Dynamic Stability versus Fiber type

It can be seen from Fig.2, the addition of fiber greatly improves the high temperature performance of fiber-asphalt mixture. The fiber added mixtures had a 24–117% higher DS results than the control mixture. In other words, the addition of fibers cause asphalt-fiber mixture demonstrated a permanent deformation response. However, the order of performance improvement of wheel tracking result was not consistent with the DSR data. It can be explained the strengthening mechanism of fiber added in mortar was different from that added in mixture.

The addition of fiber made the fiber-asphalt a more composite material. And the properties of these composite materials are strongly dependent on the arrangement and distribution of the fibers. The composite will generally have anisotropic properties

unless randomly orientated fiber arrays are used, in which case the composite will exhibit quasi-isotropic properties. The direction of the fiber such as unidirectional or bi-directional or angle ply determines the strength and stiffness of the composite. Studies showed that these fibers could form a three directional network in bitumen, which retained bitumen when mixed at high temperatures. This three dimensional structure of fibers could assist in the formation of a thicker coating of mastics to resist the deflection. According to the stress transfer theory of composite material, if there is good adhesion in the fiber-filled composite, the fibers carry some of the tensile loads, and the stress is transmitted from the asphalt mortar to the fiber. Part of the stress can be carried by the fiber.

Effect of fiber content

In order to study the effect of fiber content, tests were conducted to investigate on the effect of content of polypropylene fibers (Chen, 2008). In this study, the asphalt mixture with 0.15%, 0.30% and 0.45% of polypropylene fibers were investigated. Fig. 3 exhibits the effect of fiber content on Dynamic Stability results.

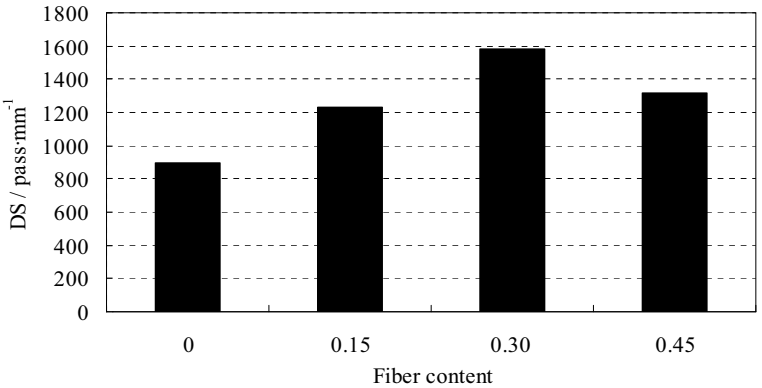


Fig. 3. Dynamic Stability versus Fiber content

There is a limited increase in DS at the content of 0.15% because the fibers act only as a dispersing material. At 0.3% fiber concentration, the DS increases sharply because the fibers begin to form a localized network structure, and the local networks interact to initiate a continuous network throughout asphalt. This formation results in an increase in the DS with the increasing fiber content. This network acts as a support structure, reinforcing the asphalt and resisting deformation. The reduction of DS after the peak value is also observed in the study. Special attention should, however, be paid when excessive fibers are used. The overcrowding fibers may result in voids during the mixing process and lead to poor pavement performance. Moreover, mixing more fibers than the optimum content is not economical, because too much reinforcement could lead to brittle mortar, thus deteriorating the pavement performance.

CONCLUSION

The DSR test results have shown that the addition of different fiber improve the rutting resistance performance. Asphalt-fiber mortar showed decreases with the increase of temperature. These decreases are more significant at lower temperature than at high temperature. The microstructures of different fiber account for different performances. The addition of fibers cause asphalt-fiber mixture demonstrated a permanent deformation response. The strengthening mechanism of fiber added in mortar was different from that added in mixture. In the results of wheel tracking device, there is a peak value of DS with the increase of fibers content. The optimal fiber content could be determined on the test result.

ACKNOWLEDGMENTS

The laboratory tests were performed previously at the Key Laboratory for Special area Highway Engineering of China's Ministry of Education at Chang'an University, and the data analysis was performed in Tongji University in 2008.

REFERENCES

WU Shao-peng, LIU Gang, MO Lian-tong, et al (2006). "Effect of fiber types on relevant properties of porous asphalt". *Trans. Nonferous Met. Soc. China* Vol. 16 791-795

Serkan Tapkin (2008). "The effect of polypropylene fibers on asphalt performance". Building and Environment. Vol. 43 1065–1071

WU Shao-peng, YE Qun-shan, LI Ning (2008). "Investigation of rheological and fatigue properties of asphalt mixtures containing polyester fibers". *Construction and Building Materials* Vol. 22 2111–2115

Jian-shiuh CHEN, Kuei-Yi LIN (2005). "Mechanism and behavior of bitumen strength reinforcement using fibers". *JOURNAL OF MATERIALS SCIENCE* Vol. 40 87– 95

CHEN Hua-xin, XU Qin-wu, CHEN Shuan-fa, et al (2008). "Evaluation and Design of Fiber Reinforced Asphalt Mixtures". Materials and Design

Principles of Designing Asphalt Pavement for Orthotropic Steel Bridge Decks

Xianhua CHEN[1], Wei HUANG[1], Jun YANG[1], Dawei WANG[2]

[1] Transportation College, Southeast University, Nanjing, China, 210096. E-Mail: pavchen@gmail.com
[2] ISAC, RWTH-AACHEN University, AACHEN, German, D-52075

Abstract: The existing studies on distresses in deck pavement indicate further research into the structural behaviours of orthotropic steel bridge decks is necessary to better understand this important issue. In this regard, this paper first presented a brief review of principles for the design of pavement on orthotropic steel plate decks. Second, critical issues including local displacement and negative bending behaviour under truck loading, main distresses in asphalt deck surfacing and their mechanism, and basic requirements for the asphalt surfacing were discussed in detail. Finally, a fatigue based mechanical-experimental design procedure was proposed for the designing of deck pavement. In addition, it is recommended that based on this study, a new theory to accurately describe the composite interaction between asphalt layer and steel deck plates, interaction between asphalt layer's fatigue and bonding membrane damage and their influences, and a more precise performance based design method can be established.

Keyword: asphalt pavement; orthotropic steel bridge deck; local deflection behaviour; composite action; fatigue cracking; designing principle

1 Introduction

Steel Orthotropic decks have been widely used in newly-constructed long-spanned bridges as well as re-decking of existing bridges, due to their light weight, strength, high degree of pre-fabrication or rapid erection, and long-term economy etc [1]. An orthotropic steel bridge deck should be paved to provide skid resistance, smooth riding, and corrosion protection. Asphalt surfacing on steel orthotropic decks act compositely with the steel deck plate and must be regarded as an integral part of the structural deck system [2]. The wearing surfacing is subjected to the impact of loaded truck wheels imposed by the passage of millions of trucks during its service life. It should be watertight, resisting cracks and well bonded to steel deck plate, besides provide a smooth riding surface with high skid resistance for the vehicles passing through the bridges [3-5].

Many asphalt materials, including gussasphalt with TLA, SMA with SBS and epoxy asphalt, and some other type of thermal plastic materials, have been used as wearing surfacing for orthotropic steel deck plate bridges around the world. Their performances vary from excellent to poor depending largely on local climate, deck plate flexibility, volume of heavy truck traffic using the bridge, and, in particular, the type and thickness of the pavement. Many problems, including cracking, rutting and shoving, de-bonding and potholes have been reported nationally and internationally in recent years, and these problems were found very severe in some cases [6-8]. While the fatigue problems of welded steel bridge decks have been largely resolved, reliable and durable pavement structures still remain to be sought for the long-spanned orthotropic steel bridges.

2 Characteristic of paved orthotropic steel bridge decks

2.1 Local Deflection and Negative Bending

The behaviour of paved steel orthotropic decks under heavy truck traffic and environmental conditions is very complex with localization characteristics, and dependent on the geometry of the decks, the wheels position, wheel footprints, and other uncertain factors.

One of the characteristics of orthotropic bridge decks is the relatively large local deflection caused by the passage of truck wheel loads, as shown in figure 1. The displacement response of a typical orthotropic deck with varies load positions are shown in figure 2. Load case I (dual-wheel load crawls on one rib) and load case II (dual-wheel load crawls on one webs of a rib) are detrimental position to pavement, under which larger local displacement and transversal tensile stress will occur. For load case II, the responses are even detrimental as there is negative bending.

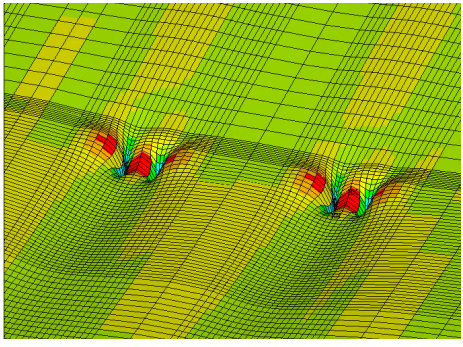


Fig. 1 Local displacement response of deck pavement

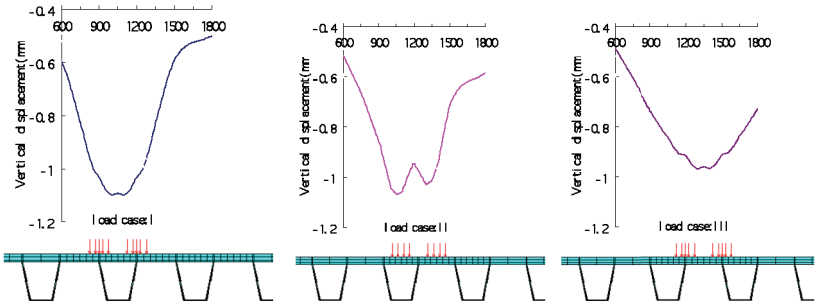


Fig. 2 Vertical displacement of deck pavement under dual-wheel load

2.2 Local tensile stress

Considering the overall behaviour, the complex stress field in the surfacing of an orthotropic deck is the result of three actions [9]: (1) Primary stresses arising from the main girder effect. These membrane stresses are due to the bending of the main girder, when the orthotropic deck is simply considered as the upper flange; (2) Secondary stresses arising from the distribution of the loads corresponding to the rigidities of the ribs and cross beams; (3) Tertiary stresses arising from the local bending of the isotropic deck plate under direct wheel loading.

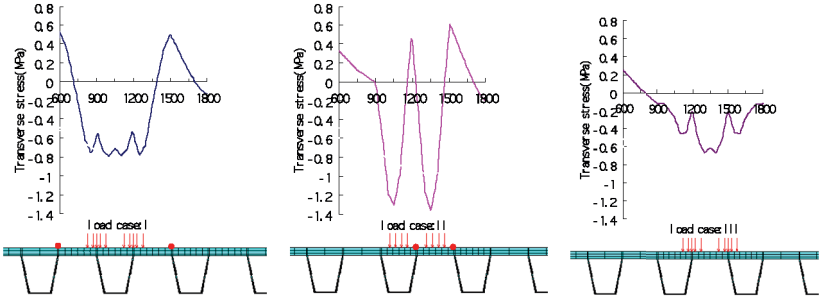


Fig. 3 Transverse Stress of deck pavement under dual-wheel load

To determine the local stresses due to traffic loading, the Finite Element (FE) method is applied. The FE-model should have a fine mesh density to get an accurate result. Critical points under different load case with large tensile stresses are shown as in figure 3 with red circle marks. Transverse tensile stress occurs at the top of pavement over webs of ribs adjacent to wheel load, and for longitudinal tensile stress, the max value occurs at the top of pavement over webs of diaphragms near to wheel load.

Transverse tensile will be dominate stress for the most time. However, numerical results reveal that longitudinal tensile stress will increase rapidly when the HMA is very stiff as in extremely low temperature, as shown in figure 4.

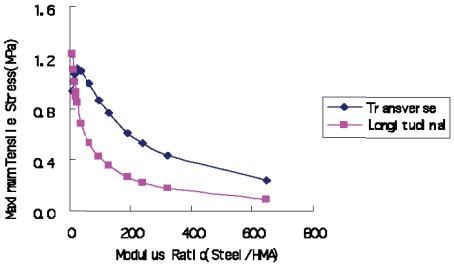


Fig. 4 Response curves of the maximum tensile stress with modulus ratio (Sutong Bridge)

FE-calculations for this study are found time-consuming and the results obtained are strongly dependent on the geometric configuration of the deck, position of the wheels, wheel footprints, and composite contribution of the surfacing and other uncertain factors [6-7].

2.3 Composite action between asphalt pavement and steel deck plates

Asphalt pavement on steel orthotropic decks act compositely with the steel deck plate and must be regarded as an integral part of the structural deck system. Most of HMA and bonding materials are thermal-plastic materials. Their properties are strongly temperature-dependent and behave elastically only at low temperatures. In semi-plastic condition flexural strain distribution through the surfacing thickness becomes non-linear. With a soft bonding layer, shear slip occurs at the interface.

In the so-called composite action theories, the complex geometry of the structure is simplified into a single span or, at most, 2-span beam model, with different support conditions. Engineers often use these theories for estimation of the stresses and strains in the bridge section. Three basic assumptions had been adopted by most of these theories [10-12]: (1) linear material properties; (2) the steel and the wearing course layers have the same radius of curvature and plane cross-sections before and after loading; (3) the gradients of the strain distribution along the depth of the asphalt and steel are equal. However, those assumptions may be valid only under certain conditions according to the test results of Hameau et al.[13] and Chen et al.[14]. New efforts [5-6][15] have been made to describe the interaction between HMA layer and steel deck plate. While new composite theories are still be desirable for bonding membrane design and more reliable stress calculation for the deck pavement.

3 Main Distresses and their mechanisms

Many bridges have frequently been reported with severe embarrassing and costly distresses in the asphalt surfacing on orthotropic steel bridge decks. The main distresses are cracking, slippage and de-bonding, rutting and shoving, pothole, and bleeding etc.

3.1 Regular Cracking

Regular cracking [8] is the most occurring type of distress in asphaltic pavement on orthotropic steel bridges, normally occurring in the surfacing above ribs of the longitudinal and transverse stiffeners shown as figure 5. They will propagate downwards and in length firstly, then will soon develop into parallel cracks and finally alligators or block cracking if they are not properly sealed, as shown in figure 6.

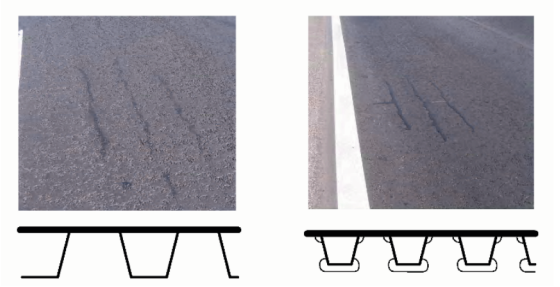


Fig. 5 Crack initiation in deck pavement



Fig. 6 Propagation of cracking in deck pavement

3.2 Slippage and de-bonding

As figure 7 shows, slippage cracks usually are U-shaped with the corrugation and shoving of the pavement. The cracks generally have a width of 2 cm to 10 cm covering at least lane.



Fig. 7 Slippage cracks in asphalt layer

However, the de-bonding is almost impossible to detect recently. According to the repairing practice, asphalt layer adjacent the alligators or potholes will lose bonding as water can penetrate down to steel deck plate surface. Experience in the many countries indicates that once the bond between the steel deck and HMA layer is destroyed, failure of the pavement follows after a short time.

3.3 Pothole

Generally, a pothole is developed from bubbles as shown in figure 8. It can also be observed near cracks during the freezing and thawing cycles in winter or in the stormy and sunny summer.



Fig. 8 Development of bubble crack into pothole

3.4 Other Type of Distresses

Other types of distresses observed in the deck pavement include rutting and shoving, bleeding due to deformation of bituminous materials with too high bitumen content and low voids content, polishing of surfacing aggregates by tyres, repaired block, and ravelling.

3.5 Distress Mechanisms

Fatigue cracking is mainly caused by repeated stresses (shear or tensile) induced by traffic, environment and poor construction. However, repetitive large local deflection and assignable negative bending, exceptionally high stresses induced by heavy traffic or freezing, exceeding the material's tensile or shear strength can also be attributable to the regular cracking [6]. When the bond between the asphalt and steel is weak, tension forces may occur at the bottom of the wearing course, thus leading to cracks starting at the bottom of the wearing course and propagating to the top.

The causes of slippage and de-bonding are mainly due to weak bonding membrane, extremely high temperature and horizontal force with traffic braking or accelerating

could also attribute to these distresses. Permanent deformations are generally caused by high and/or repeated compressive or shear stresses in hot summer. Corrugations may also result from tangential forces caused by braking and accelerating vehicles. For the purpose of fatigue resistance and corrosion protection, asphalt surfacing materials need to be rich in binder. Thus the deck pavement will lead to be susceptible for rutting even very hard polymer modified asphalt. However, with the use of thermo-set materials such as epoxy asphalt as binder, this problem can be totally reduced [7].

It is known that different types of distresses are caused by different mechanisms, but there can be considerable interaction among different distress types. However, it is sometimes difficult to determine the real cause or causes of an occurring damage.

4 Principles for Design deck pavement

4.1 Basic Requirements of orthotropic steel bridge decks

In general, the materials and pavement structure for orthotropic steel bridge decks should be designed to include the following properties [3-7].

- Skid Resistance: Provide a safe skid-resistant surface with polish-resisting aggregates for millions of wheel passages during the service life of the surfacing.
- Ride Quality: Provide a smooth riding surface to bridge users.
- Bond Strength: Be well-bonded to the steel deck to provide composite action between the asphalt layer and the steel deck to reduce fatigue stresses in the laminated structure, and to resist delaminations from shear stresses caused by flexure and by differential thermal expansion or contraction.
- Enough strength and suitable stiffness: to bear the heavy duty trucks loading and disperse the fatigue stress causes by trucks in the welded deck plates.
- Fatigue resistance: Against fatigue cracking under millions of repetitions of loaded truck-wheels.
- High temperature stabilities: Be resistant to shoving, rutting, and ravelling by millions of wheel passages and extremely high temperature.
- Water Proofing and resistance to moisture damage: Be impervious to the passage of water through the surfacing and have good resistance to moisture damage.
- Durability: Be resistant to environmental factors, such as sunlight, oxidation, and temperature changes, and impervious to salt water and to fuel and oil droppings from traffic.
- Corrosion Protection: In addition to being impervious, provides a corrosion-resisting coating to protect the steel plate.
- Workability: Easily to be constructed on steel deck plate and quality control
- Easily to be repaired and removed under traffic.

These requirements should always keep in mind during the processes of material selection, mixture design and structure design of the composite.

4.2 Typical Materials and structures for steel bridges

Figure 9 shows typical structures of deck pavement used in China. Gussasphalt and SMA are thermo-plastic materials with polymer-modified asphalt binders and Epoxy Asphalt Concrete(EAC) is thermo-set by using a reaction-curing material of epoxy asphalt which will not rut under 70°C temperatures, which has been measured on

orthotropic deck pavement in 2nd Nanjing Bridge. EAC is proved to be the super durable surfacing material for heavy duty traffic and extremely high temperature, and now it is widely used in China although its construction cost is 2~3 times that SMA. However special attentions should be paid when applying this material to extremely cold area and to the construction process.

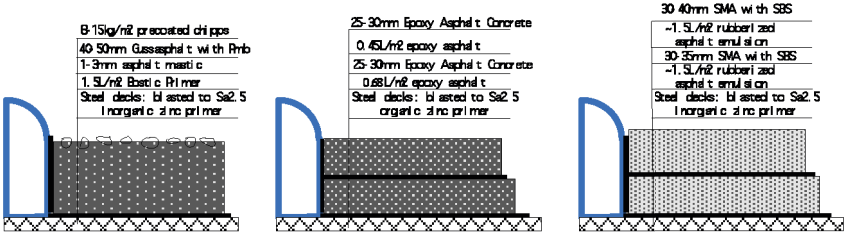


Fig. 9 Typical structures of deck pavement used in China

4.3 Design procedure

The main distresses and failures in asphalt surfacing on steel bridges may generally be attributed to insufficient understanding of the surfacing behaviour on orthotropic steel bridge decks, underestimating the environment and traffic and their influences. They may also be due to the use of incompatible materials, the extremely high/low temperature, and heavy duty traffic as well as severe overloading. A fatigue based mechanical-experimental design principle [16-17] should be adopted for the design on a new bridge deck, or for the design of a replacement wearing surfacing of an existing bridge on which the wearing surfacing has failed. The major steps include the following aspects:

1. Assess the environment factors such as temperature and humidity, traffic and percent trucks.
2. Select a representative axle load and determine allowable ratio of overloading and allowable percent of overloaded trucks.
3. Check the stiffness of unpaved orthotropic steel bridge decks. For an unpaved orthotropic steel bridge deck, the negative bending deflection under designing axle load should be less than 0.8mm. The super structure should be optimized if this requirement is not meted.
4. Select one or several candidate surfacing materials based on previous good performance, the availability of the material, or other rational reasons.
5. Design the HMA mixtures, test their ductility and fatigue resistance with semi-circular bending samples or four point beam bending sample.
6. Test the adhesive strength and shear strength of bonding materials to blasted steel plate with varies thickness to determine the optimum thickness of bonding membranes.
7. Test the deflection responses of the composite structure to back-propagate material character parameters for Finite Element Analysis.
8. Calculate the tension stress and shear stress demand that truck wheels impose on the deck pavement, and determine the equivalent fatigue load for laboratory test on composite beams.

9. Inspect whether the responses of relative deflection of paved orthotropic is less than 0.4mm.

10. Calculate the ESAL will impose on the surfacing for the target service life of the surfacing.

11. Test the integral performance of the composite beams with pull-out test, shear test, and fatigue test. The fatigue loading on the test specimens should reproduce the tension and shear stress levels calculated for the bridge deck in Step 8 above. Pull-out test and horizontal shear test should be done on the samples before and after fatigue test to evaluate the damage of bonding membrane.

12. Compare the performance of the fatigue resistance with the fatigue demand to determine optimum materials and structure for the specific project.

13. Establish the final specification on material, mixture and structure.

14. Investigate the construction conditions, conduct technological test, establish the specification of construction and propose a suitable construction methods.

15. Build test section and modify the construction specification if necessary.

5 Summary and Discussion

This paper investigated issues on the local displacement and negative bending behaviour under truck loading, main distresses in asphalt surfacing and their mechanism, basic requirements for the deck pavement and typical surfacing materials, and proposed a fatigue based mechanical-experimental design procedure for steel deck pavement.

The behaviours of deck pavement on orthotropic steel bridge deck under truck load are complex. It is described by the characteristic of local displacement and tensile stress and negative bending. Deck pavement is an integral part of the structural deck system and acts compositely with the steel deck plate, while more accurate composite theories are still desirable. Fatigue cracking and de-bonding are structure-dependent distresses, while their interaction and effects are still needed to be further investigated. A successful deck pavement design should be based on sufficient understanding the structural behaviours and proper estimation the environment, traffic and construction conditions. It should also incorporate pavement design into superstructure design of the bridges. In addition, improvement of the integral performance of deck pavement, paying much attention to the aspects of construction and ensuring the designed materials to be constructed with designing specification are all important factors to lead to a successful deck pavement project.

Reference:

[1] Sukhen C., The Design of Modern Steel Bridges. *Boston: London Edinburgh*. 1992.

[2] AASHTO, LRFD Bridge Design Specifications, *American Association of State Highway and Transportation Officials, Washington, D.C.*, 1994.

[3] Roman W., Structural behaviour of surfacings on steel orthotropic decks and considerations for practical design, *Structural Engineering International*. 2002, (2): 124-129.

[4] Chen X.H, Huang W., Wang J.W., On design methods of asphalt mixture for the steel orthotropic decks on long-spanned steel box girder bridge, *Highway*, 2004, (8): 34-38. (in Chinese).
[5] Chen X.H., Fatigue Characters of deck pavement on steel orthotropic bridge decks based on composite beam, Ph D Dissertation, *Nanjing: Southeast University*, 2006, April. (in Chinese).
[6] Medani T.O., Design principles of surfacings on orthotropic steel bridge decks, Ph. D Dissertation. *Netherland: Delft University of Technology*, Jan, 2006.
[7] Huang W., Theory and Method of deck paving design for long-span bridges, *Construction Industry Press, Beijing*, China, 2006, 10. (in Chinese).
[8] Chen X.H., Huang W., Yang J., et al, Cracking of wearing courses on steel orthotropic bridge decks, *6th RILEM International Conference on Cracking in Pavements*, Chicago USA, June 16-18, 2008.
[9] Wolchuk R., Steel orthotropic decks-developments in the 1990's, *Transportaion Research Record*, 1999, 1688(04): 30-37.
[10] Cullimore M.S.G., Flett I.D., Smith J.W., Flexure of Steel Bridge Deck Plate with Asphalt Surfacing, *IABSE Periodica*, 1983, (1): 1-15.
[11] Kolstein M.H. and Wardenier J., Stress Reduction Due to Surfacing on Orthotropic Steel Decks, *IABSE Reports, Switzerland*, 1997.pp. 109-118.
[12] Nakanishi N. and Okochi T., The structural evaluation for an asphalt pavement on a steel plate deck[C], *Proceedings of the First International Conference, AAPA*, Sydney, Australia, 2000.
[13] Hamaue G., Puch C., Ajour A.M., Comportement à la Fatigue en Flexion sous Moment Négative, *Revétments de Chaussées sùr platelages métalliques*, 1981.(in French).
[14] Chen X.H., Chen Y., Huang W., Flexure Characters of Epoxy Asphalt Surfacing on Steel Decks, *Journal of Highway and Transportation Research and Development*, 2007, 24(11): 5-8. (in Chinese).
[15] Chen X.H., Huang W., Qian Z.D., Interfacial behaviours of epoxy asphalt surfacing on steel decks, *Journal of Southeast University (English Edition)*, 2007, 23(4): 599-602.
[16] Huang W. and Liu Z.Q., Research on theory and design methods of pavement on orthotropic steel bridge decks, *China Civil Engineering Journal*, 2005, 38(1): 51-59. (in Chinese).
[17] Huang W., Design of deck pavement for long-span steel bridges. *China Civil Engineering Journal*, 2007, 40(9): 65-77. (in Chinese).

Analysis of Semi-Rigid Asphalt Pavement with Flexible Base as a Sandwich Layer

Ruibo Ren[1]， Hiwen Li[2] , Zheren Wang[3]

[1]Professor, School of civil engineering, Shandong Jianzhu University, China.
rrbgq@sdjzu.edu.cn
[2]Assistant Researcher, Shandong Provincial Academy of Building Research, China.
lihiwen@sina.com
[3]Professor, School of Communications Science and Engineering, Harbin Institute of Technology,China. wangzheren@sina.com

ABSTRACT: Reflective cracking is one of main distresses for cement/lime/flyash stabilized base in China. Although flexible base can be and has been utilized as sandwich layer to reduce reflecting cracks from stabilized base, the repetitive truck traffic load may cause higher tensile stress at the bottom of asphalt surface course because of large deformation from flexible base. The high tensile stress may lead to fatigue cracking. To minimize the tensile stress at the bottom of the asphalt layer and to establish optimum structures to reduce reflective cracking, nonlinear finite element technique was utilized to support three experimental pavements in Tonghua Highway in Jilin province. Base on the analyses, pavement structures 1 and 2 are recommended. In addition, for pavement structure 1, the optimal design is to include 7-12cm of AM-30, 10-15cm of flexible base, and 30-45cm of semi-rigid subbase (lime-flyash stabilized soil or cement treated base). Furthermore, for pavement structure 2, the optimal design is to include 15-20cm of flexible base, and 25-40cm of semi-rigid subbase (lime-flyash stabilized base or cement treated base).

INTRODUCTION

Reflective cracking is a major and costly problem in China. It occurs in the top surface layers above existing cracks in the lower stabilized layer. This type of cracking can lead to premature deterioration of the pavement structure through the infiltration of moisture. Flexible base has been utilized with success to reduce reflecting cracks from cement/lime/flyash stabilized base [1]. Flexible base is placed between asphalt surface and cement/lime/flyash stabilized base (sandwich structure). But higher tensile stress could be produced at the bottom of asphalt surface course for structure with flexible base as the sandwich layer. Therefore, under the repetitive actions of heavy vehicle loads, asphalt surface course can not meet the need of fatigue resistance performance, because flexible base material can produce elasto-plastic deformation. This phenomenon has been demonstrated with dynamic triaxial tests [2]. Since the elastic layered system theory is much different

than the actual state of pavement, finite element technique was utilized by characterizing flexible base as nonlinear (elasto-plastic) material. The nonlinear finite element technique was utilized to support three experimental pavements in Tonghua Highway in Jilin province. Lesson learns from the finite element analyses and three experimental pavements in Tonghua Highway are expected to be applicable to a wide range of pavement projects.

MATERIAL ELASTO-PLASTICITY AND YIELDING RULE

The characteristics of the elasto-plastic materials are that deformation will be irreversible and perpetual when unloaded, as shown in Fig. 1. When material is loaded, it is impossible to tell if it is nonlinear elastic or nonlinear elasto-plastic. However, when material is unloaded, the difference is obvious as nonlinear elastic and/or elastic material will return to the original location (refer to Fig. 1). As shown in Fig. 1, elasto-plastic material yielded permanent deformation depending on different loading history [5, 6, 7]. Based on the dynamic triaxial test results, the behavior of flexible base deformation can be characterized as elasto-plastic material. Thus, to simulate the field condition, elasto-plastic finite element technique was utilized to describe the pavement behavior.

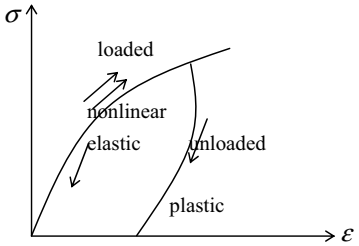


FIG.1. Nonlinear elastic and elasto-plastic.

This paper adopted linear Drucker-Prager yielding rule to describe the elasto-plastic behavior of flexible base. The linear Drucker-Prager yielding rule is very similar to that of Mohr-Coulomb, which modified yielding rule of VonMises [6, 7]. The main difference for VonMises from linear Drucker-Prager and linear Mohr-Coulomb is that the yielding rule takes into account the influence of lateral pressure. According to reference [7], linear Drucker-Prager yielding function is given as:

$$F = \sqrt{3}\alpha I_1 + \sqrt{3J_2} - \sigma_y = 0 \qquad (1)$$

where, I_1 is lateral pressure (in MPa); J_2 is the second stress invariable; σ_y is the yielding stress which relates to material's cohesion and internal frictional angle.

The yielding function of linear Mohr-Coulomb is shown in Eq. 2:

$$F = \frac{1}{2}(\sigma_3 - \sigma_1) + \frac{1}{2}(\sigma_3 + \sigma_1)\sin\phi - \cos\phi = 0 \qquad (2)$$

Where, ϕ is internal frictional angle; $\sigma_1, \sigma_2, \sigma_3$ are principal stresses. When flexible base material was analyzed with Drucker-Prager yielding rule by elasto-plastic finite element method, first of all, according to Equation 1, it should be judged that yielding state is achieved or not, if achieved, it should be calculated with elasto-plastic theory, if not, it should be calculated with elastic theory.

The laboratory test results indicate that the cohesion of flexible base material is near 0 and the internal frictional angle range from 35^0 to 40^0. It has been observed that when there is a better construction quality control, the internal frictional angle can be increased to approximately 45^0 [1]. The internal frictional angle of 40^0 was selected in this study.

SURFACE COURSE AND SEMI-RIGID BASE BOTTOM TENSILE STRESS ANALYSIS OF THREE EXPERIMENTAL PAVEMENTS IN TONGHUA HIGHWAY WITH NONLINEAR FINITE ELEMENT METHOD

Analysis Model

The typical structures with layer thickness and layer modulus of the three experimental pavement sections in Tonghua Highway are presented in Figures 2, 3, and 4. Single circular load with uniform pressure of 0.7MPa was adopted. The circular diameter is 30.4cm. Although the behaviors of asphalt surface course and soil subgrade are all nonlinear, relative to flexible base they are insignificant. Therefore, except for flexible base, all other materials were treated as elastic materials.

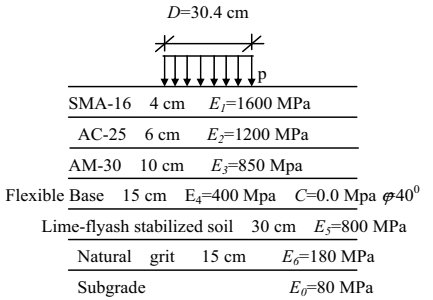


FIG.2. Experimental Pavement Structure 1 of Tonghua Highway.

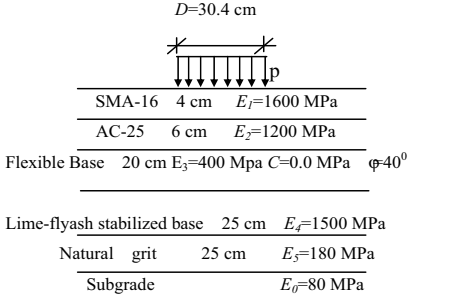


FIG.3. Experimental Pavement Structure 2 of Tonghua Highway.

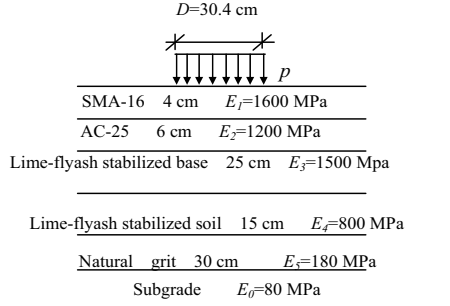


FIG.4. Experimental Pavement Structure 3 of Tonghua Highway.

Since the load and geometric is symmetric, to simply the analyses, two dimensional axisymmetric model was adopted. In addition, Four-node element was

utilized in the analyses. Except subgrade Possion Ratio μ of 0.35, all other pavement layers have Possion Ratio μ of 0.25 [1].

Analysis Results

To evaluate the impacts of the semi-rigid base modulus on the maximum tensile stress at the bottom of asphalt surface course, the moduli of lime-flyash stabilized soil in pavement structure 1 varied from 800, 1000, 1500, 2000, 2500, to 3000MPa. Similarly, the moduli of lime-flyash stabilized soil in pavement structures 2 and 3 varied from 1000, 1500, 2000, 2500, 3000, to 3500MPa. The maximum tensile stresses at the bottom of SMA-16 and AC-25, are presented in Figure 5 and 6, respectively.

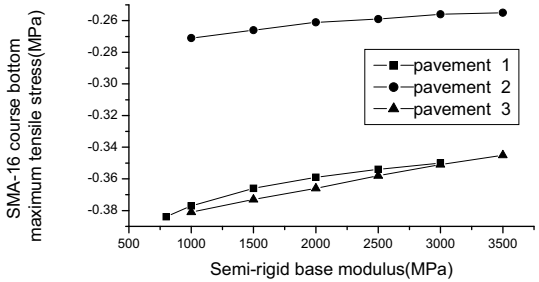


FIG.5. Maximum tensile stress at the bottom of SMA-16 with varying semi-rigid base modulus.

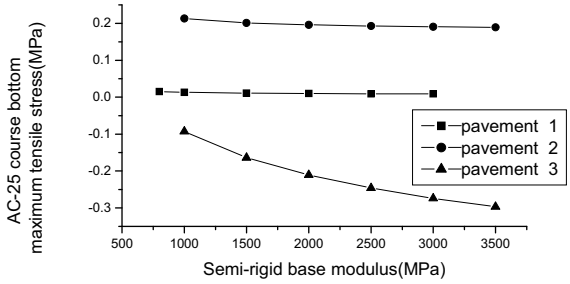


FIG.6. Maximum tensile stress at the bottom of AC-25 with varying semi-rigid base modulus.

In view of Figures 5 and 6, it indicates that the impacts of semi-rigid base moduli on the maximum tensile stresses at the bottom of asphalt surface course vary significantly among pavement structures 1, 2 and 3. It was observed that the greatest and the least impacts of semi-rigid base moduli on the maximum tensile stresses are pavement structures 3 and 1, respectively. One of the main reasons is because the pavement structure 1 has 10cm of AM-30 (just above the flexible base layer) which reduces the impacts of semi-rigid base moduli. Note that AM-30 is a large stone asphalt mixture. As expected, the maximum tensile stresses at the bottom of AC-25 for pavement structure 2 are higher than those for pavement structure 1. The main reason is believed to be the contribution of the 10cm of AM-30 layer.

To study the influences of thickness and modulus of large stone asphalt mixture (AM-30) on maximum tensile stresses of SMA-16 and AC-25 layers for pavement structure 1 (refers to Figure 2), various thicknesses and moduli of AM-30 were employed in the analyses. Due to space limitation, only limited results are presented in the paper. Figure 7 illustrates the brief analysis results. It was observed that the tensile stresses at the bottom of AC-25 decreased with increasing AM-30 thickness. In particular, the influences of thicknesses on maximum tensile stresses are greater than those from moduli's. For example, when thickness of AM-30 decreased from 7 cm to 4cm, the maximum tensile stress at the bottom of AC-25 increased from 0.061MPa to 0.146MPa. Interestingly, when thickness of AM-30 increased to 12cm, the maximum tensile stress at the bottom of AC-25 becomes negative (refers to Figure 7). It indicates that when the thickness of AM-30 thicker than 12cm, the bottom of AC-25 is under compression not tension. By considering the cost, the most economical structure to reduce tensile stress or reflecting cracks is to include 7-12cm of AM-30, 10-15cm of flexible base, and 30-45cm of semi-rigid subbase (lime-flyash stabilized soil or cement treated base).

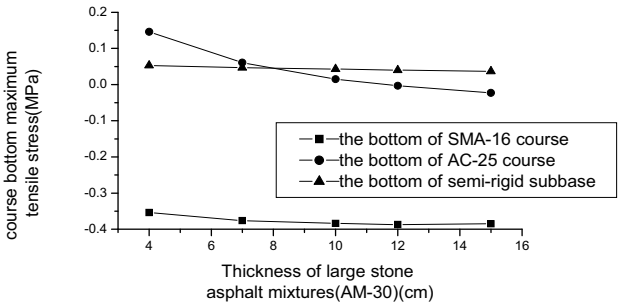


FIG.7. Comparisons of maximum tensile stresses with varying AM-30 thicknesses for pavement structure 1.

Similarly, to optimize the design for pavement structure 2 (refers to Figure 3), various thicknesses and moduli of flexible base and semi-rigid subbase were included in the analyses. Figure 8 presents the comparisons of maximum tensile stresses at the bottom of SMA-16 and AC-25 layers with varying flexible base thicknesses for pavement structure 2. It was found that, although not all results are presented, the maximum tensile stresses at the bottom of AC-25 decreased with increasing moduli of flexible base, and semi-rigid subbase thickness and its modulus. However, the maximum tensile stresses at the bottom of AC-25 increased with increasing thickness of flexible base (refers to Fig. 8). For example, when the flexible base thickness was increased from 10cm to 20cm, the maximum tensile stresses at the bottom of AC-25 increased from 0.082MPa to 0.200MPa. Among the factors considered, the most sensitive factor that impact the maximum tensile stresses at the bottom of AC-25 is the thickness of flexible base thickness. The analysis results suggested that the most economical design for pavement structure 2 is to include 15-20cm of flexible base, and 25-40cm of semi-rigid subbase (lime-flyash stabilized base or cement treated base).

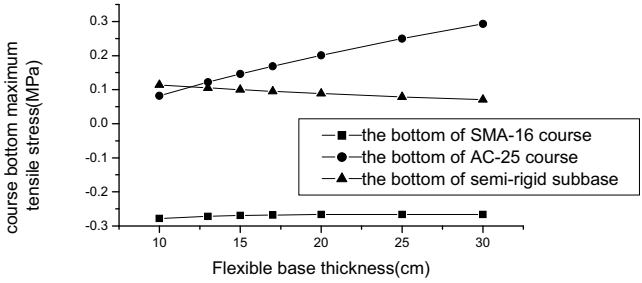


FIG.8. Comparisons of maximum tensile stresses with varying thickness of flexible base for pavement structure 2.

CONCLUSIONS

Reflective cracking is a major concern for cement/lime/flyash stabilized base in China. Although flexible base can be and has been utilized as sandwich layer to reduce reflecting cracks from stabilized base, higher tensile stress could be produced at the bottom of asphalt surface course when it subjected to heavy truck traffic load. The high tensile stress may lead to fatigue cracking. In this study, the nonlinear finite element technique was utilized to support three experimental pavements in Tonghua Highway in Jilin province. The main goal is to establish optimum structures to

reduce reflective cracking. Base on the analyses, the observations and conclusions are given as follows:
(1) Pavement structures 1 and 2 are recommended.
(2) For pavement structure 1, the optimal design is to include 7-12cm of AM-30, 10-15cm of flexible base, and 30-45cm of semi-rigid subbase (lime-flyash stabilized soil or cement treated base).
(3) For pavement structure 2, the optimal design is to include 15-20cm of flexible base, and 25-40cm of semi-rigid subbase (lime-flyash stabilized base or cement treated base).

ACKNOWLEDGEMENTS

Special thanks go out to Hai Luan researcher of Jilin Highway Survey and Design Institute for providing the surveyed parameters of Tonghua highway.

REFERENCES

1.Zhaoyi He.(1997).”Study on preventing semi-rigid asphalt pavement reflecting cracks and road performance.”*Ph.D.dissertation of South-east university*:35-56.
2.Tianqing Ling, Shijie Wang and Zhihong Xu (1999).”Displacement and stress analysis of materials nonlinear performance.”*China Journal Highway and Transport.* Vol.12(1):1-6.
3.Ruibo Ren,Yiqiu Tan and Xiaoning Zhang.(2001).”Solution for solving asphalt pavement multilayered viscoelastic body surface deflection in the FWD dynamic case.” *China Journal Highway and Transport.*Vol.14(2):9-12.
4.Bathe K J and Wilson E L.(1976)”Numerical methods in finite element analysis.”*Prentice-Hall,Inc.*/VA:31-82.
5.Shouyi,Xue.(2005).”Finite element method.”*China Building Material Industry Press*./88-131.
6.Drucker D C.(1952).”A more fundamental approach to plastic stress strain relations“*Proc.1st U.S.Nat.Congr.Appl.Mech.* / VA 86-197.
7.Zhixi Xia.(1991).”Plastic mechanics.”*China Tongji University Press./*77-132.
8.(2006).”Specification for Design of highway asphalt pavement.”*China People Pommunication Press./*10-45.

Properties and Early-Age Cracking Potential of Blended Cement Concrete

Zhi Ge[1], Kejin Wang[2], and Zhili Gao[3]

[1]Assistant Professor, Department of Construction Management and Engineering, North Dakota State University, Fargo, ND 58108; zhi.ge@ndsu.edu
[2]Associate Professor, Department of Civil, Construction, and Environmental Engineering, Iowa State University, Ames, IA 50010; kejinw@iastate.edu
[3]Assistant Professor, Department of Construction Management and Engineering, North Dakota State University, Fargo, ND 58108; zhili.gao@ndsu.edu

ABSTRACT: Stress due to the temperature and moisture gradients in concrete slab often causes pavement curling and warping that may further cause concrete crack if the slab is under restraint conditions. The adding of supplementary cementitious materials (SCMs) can reduce the risk of cracking by reducing the temperature stress. However, under cold weather condition, the slower strength development due to SCMs could increase the risk. This paper reported a study result of using blended cement to reduce such as risk. In this study, the properties of ternary cement concrete, such as setting time, heat of hydration, and datum temperature, were investigated. The risk of early-age cracking for different concrete mixes under different weather conditions was evaluated by the HIPERPAV. The test results indicated that fly ash replacement generally increase the setting time; while the slag replacement reduced the setting time. Both fly ash and slag replacement reduced the generated heat. When the amount of slag increased, the datum temperature and activation energy increased. HIPERPAV analysis indicated that there was little risk of early-age cracking for binary or ternary cement concrete under average summer weather conditions due to proper strength development of the concrete. However, the risk of early-age cracking for the concrete pavement increased under spring or fall weather conditions.

INTRODUCTION

The early-age properties of concrete pavement, such as temperature and moisture, are very important to the service life of the pavement (Andersen et al, 1992; Hankins et al. 1991, McCullough et al. 1998). Stress due to the temperature and moisture gradients in concrete slab often causes pavement curling and warping. Under restraint conditions, the stress may cause concrete to crack. In an effort to solve this problem, recently, supplementary cementitious materials (SCMs) are being increasingly used in concrete pavement due to its economic and environmental benefits, and improvements of concrete properties, such as workability, impermeability, ultimate strength and durability (Strategic Development Council, 2002). Concrete practice has

shown that the performance of concrete containing SCMs, such as workability, setting time, and strength development, varies significantly with the type and amount of the SCMs as well as curing conditions.

The adding of SCMs can reduce the risk of cracking by reducing the temperature stress. However, under cold weather condition, the slower strength development due to SCMs could increase the risk. Therefore, it is important to analyze the risk for different concrete mixes under different curing conditions. Additionally, maturity, expressed by either the time-temperature factor or the equivalent age, is a non-destructive testing and widely used for quality control and determination of the time for concrete framework removal and the time for concrete pavement to open to traffic (Carino, 1994). The datum temperature or activation energy is important for maturity calculation and is a function of concrete materials, mix proportions, and curing conditions. However, there is lack of test data on concrete containing SCMs.

This paper reported a study on concrete properties of blended cement made with different types and amounts of SCMs. The blended cement is made of Type I cement clinker with various amount of ground granulated blast-furnace slag (GGBFS) and fly ash (Class C). The paste setting time, datum temperature, activation energy, and heat of hydration were measured. The HIPERPAV, a computer program developed by Transtec Group, Inc. for the Federal Highway Administration, was used to assess the effect of fly ash and slag on the risk of early-age cracking.

CONCRETE MATERIALS

In this study, types I cement (HI), Grade 100 GGBFS (S), and class C fly ash (FA) were used as cementitious materials. Table 1 summarizes their chemical and physical properties. The slag was blended with type I cement by cement manufacture. The slag contents in the blended cement were 20, 25, and 35%. The mean particle sizes of the cement, fly ash, and slag were 24.5, 13.6, and 8.86 μm, respectively. The type I cement contained 1.74% gypsum, 2.34% bassanite, and 1.46% anhydrite. Rive sand (F.M.=2.92) and limestone (NMSA=25 mm or 1 inch) were used to mix mortar or concrete samples. Mortar with a sand-to-cement ratio of 2.19 and a water-to-binder ratio of 0.4 was prepared for the datum temperature and activation energy test. The mix proportion for one cubic yard of concrete is 1,706 lbs limestone; 1,366 lbs sand; 562 lbs binder; and 225 lbs water. Water reducing agent (104 ml per 100 lbs binder) and air entraining agent (34 ml per 100 lbs binder) were also used in the concrete.

EXPERIMENTAL TEST

The setting time of cement paste was tested according to ASTM 191. The datum temperature and activation energy were determined following the ASTM C 1074. The samples were cured under 10, 21, and 32 ℃. The heat of hydration of concrete was tested using IQdrum from Digital Site Systems, Inc. The Concrete was mixed according to ASTM 192, and placed into a 6"x12" plastic cylinder. A sensor was inserted into the middle of the specimen. Then, the specimen was put into a semi-adiabatic drum. The sensor recorded concrete temperature every 15 minutes for a total testing time of approximate 10 days. The initial temperature for all concrete samples was controlled under 25±1°C.

Table 1. Chemical and Physical Properties of Cementitious Materials

Compound	Type I Cement	Slag	Fly Ash
CaO	64.24	37.09	24.88
SiO_2	20.80	36.79	34.86
Al_2O_3	5.55	9.20	19.80
Fe_2O_3	2.25	0.76	5.38
MgO	1.91	9.50	5.33
K_2O	0.50	0.41	0.52
Na_2O	0.19	0.34	3.19
SO_3	2.96	-	2.09
S	-	1.07	-
LOI	0.82		0.29
Specific Gravity	3.14	2.93	2.66
Fineness (m^2/Kg)	399	534	

RESULTS AND DISCUSSION

Table 2 shows that, compared with the pure cement paste, 15% fly ash replacement increased the setting time. The incensement was 105 minutes for the initial setting time and 113 minutes for the final setting time. Adding GGBFS to the binary cement (HI-15% FA) decreased the setting time but still higher than the cement paste. The pastes with different amount of slag had similar initial setting time. The difference was within 10 minutes. The same trend was also observed for concrete setting time (Wang and Ge, 2003). Table 2 also indicates that, for a given consistency, fly ash reduced the water requirement. However, the slag increased the water required. The water-to-binder ratio for the ternary mix was similar to the cement paste.

Table 2. Setting Time of Cement Paste

	HI	HI-15%FA	HI-15%FA-20%S	HI-15%FA-25%S	HI-15%FA-35%S
Initial Set Time (min)	98	203	178	174	169
Initial Set Time (min)	195	308	270	255	240
W/B	0.252	0.245	0.251	0.250	0.250

The heat evolution of concretes made with different levels of fly ash and slag replacement are shown in Fig. 1 and 2. Fly ash and slag can significantly reduce the heat generation at early age. The reduction increases as the SCMs replacement increase.

It should be mentioned that the reduction is not proportional to the slag replacement level. As the time increases, the difference is reduced due to the Pozzolanic reaction.

As a result, the concrete with fly ash and slag might have reduced risk of thermal shrinkage cracking in concrete when compared with Portland cement concrete.

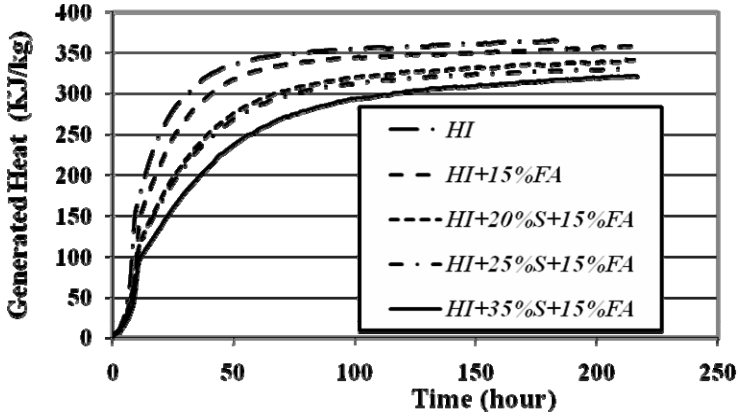


FIG. 1. Heat evolution for concrete containing different blended cement.

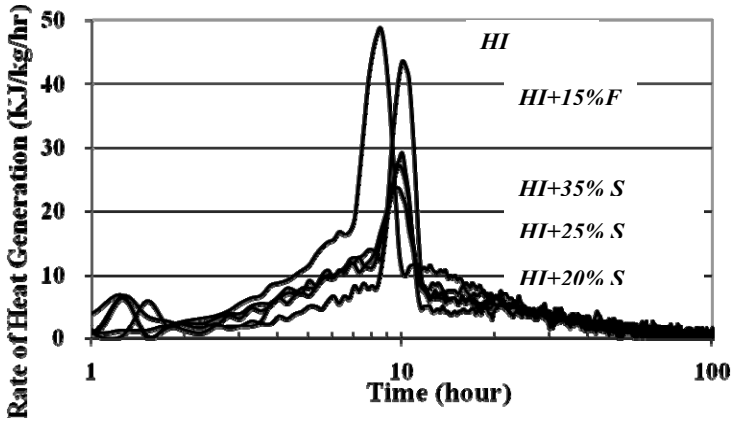


FIG. 2. Rate of heat evolution for concrete containing different blended cement.

Fig. 2 indicates that fly ash replacement postponed cement hydration and also reduced the rate of hydration. The peak of the rate of heat generation was delayed for about 1.5 hours by replacing 15% type I cement with fly ash. The delay could be caused by the reduced water demand of fly ash concrete (Sánchez de Rojas et al, 1993). Slag replacement also reduced the rate of cement hydration. However, the time

for slag concrete to reach the peak of the rate of heat generation kept unchanged or slightly decreased compared with the concrete without slag.

Table 3 shows that concrete made with binder containing fly ash and/or slag had higher datum temperature than -10°C, which is a traditionally recommended value for concrete (Metha and Monteiro, 2006). This means blended cement concrete can stop strength development at a higher temperature than Portland cement concrete. Therefore, the blended cement should be placed and cured at a relative higher temperature to gain certain strength at certain age. Concrete made with slag-blended cement had higher activation energy than concrete without slag. These results are consistent with previous research (Ma et al, 1994).

Table 3 also indicates that, as slag content increased the datum temperature and activation energy of concrete increases linearly. Concrete that has higher activation energy is more sensitive to curing temperature.

Table 3. Datum Temperature and Activation Energy

	HI-15%FA	**HI-15%FA-20%S**	**HI-15%FA-25%S**	**HI-15%FA-35%S**
Datum Temperature (℃)	-7.2	-2.7	-2.9	-0.8
Activation Energy (J/mol)	26,576	32,895	32,571	40,006

HIPERPAV ANALYSIS

HIPERPAV program considers the structural design, concrete materials properties, mix proportion, and environmental and construction conditions in its input. In this study, typical 3-day temperature curves of spring, summer, and fall in Iowa were used. The winter condition was not studied because there are few concrete construction activities in the season. The replacement levels of 15% for fly ash and 0%, 20%, 25%, and 35% for slag were considered. A 12-inch thick, 12-foot wide concrete slab with transverse joint spacing of 15 feet on a 6-inch thick unbound aggregate subbase with a K-value of 200 psi/inch was selected. It was assumed that the single layer liquid curing compound was applied at a half hour after the paving. The joint were cut at the optimum time.

Fig. 3 through 5 and Table 4 summarize the HIPERPAV analysis results. It was observed that, in summer (Fig. 3), the rate of concrete strength development is desirable. On the other hand, the critical stresses developed in the concrete slab due to thermal and moisture change are relatively low, partially because of the small temperature difference between the surface and internal concrete. The critical stresses are similar for all different concrete mixes. As a result, concrete strength is always higher than the stress within 3 days after paving, and the minimum difference between concrete strength and critical stress is relatively large (23-37.7 psi, depending on the amount of slag replacement; see Table 4). Therefore, base on the HIPERPAV analysis, cracking would not likely occur in these concrete pavements within 3 days after paving.

In spring and fall (Fig. 4 and 5), the rate of concrete strength development slows down due to a lower curing temperature than that in summer, and the stresses developed in concrete is higher due to a larger thermal and moisture gradient along the depth of the concrete slab. The minimum difference between concrete strength and stress becomes smaller (as low as 6.2 psi for spring, see Table 4). However, the concrete stresses still do not exceed strength, and the HIPERPAV program predicts no cracking in the concrete pavements.

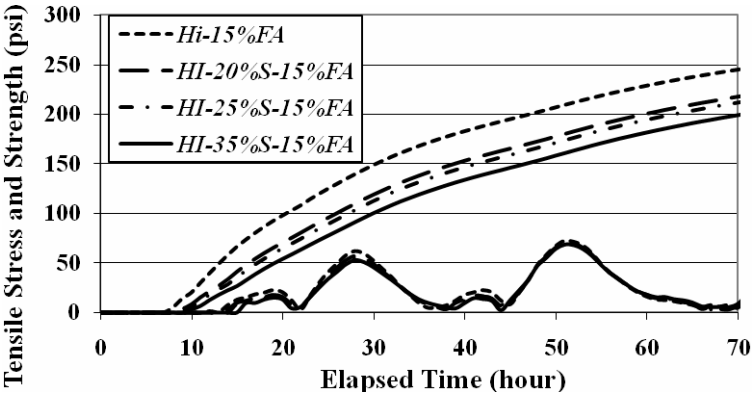


FIG. 3. Concrete strength vs. critical stress for summer conditions.

Table 4. Minimum Difference between Concrete Strength and Stress

	Minimum Difference between Strength and Stress (Psi)			
	HI-15%FA	**HI-15%FA-20%S**	**HI-15%FA-25%S**	**HI-15%FA-35%S**
Spring	21.3	14.6	11.3	6.2
Summer	37.7	30.0	26.9	23
Fall	30.9	18.1	17.1	31

It should be mentioned that the weather conditions selected for this study are the typical/average temperatures of the seasons. In early spring or later fall, actual weather temperature may be lower than the average weather temperature, and potential cracking may occur in actual field practice. Also, if there is a sudden temperature drop, there will be higher risk of thermal cracking in spring and fall conditions than summer conditions due to the smaller difference between the strength and stress. In addition, the current program does not provide information on the effects of characteristics of SMCs on concrete performances. Further research on SCM concrete cracking resistance is needed.

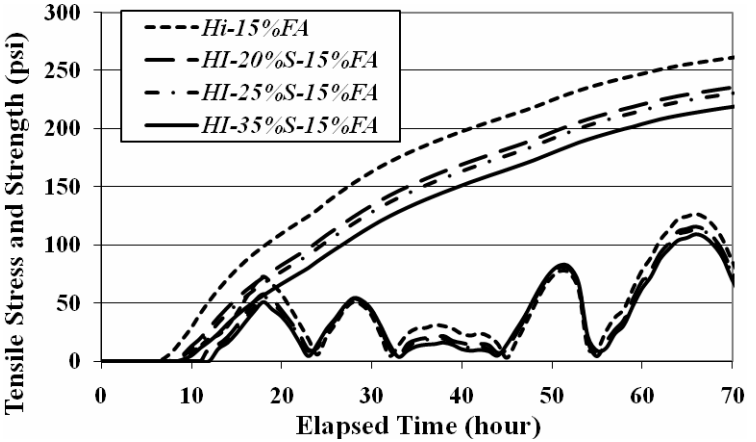


FIG. 4. Concrete strength vs. critical stress for spring conditions.

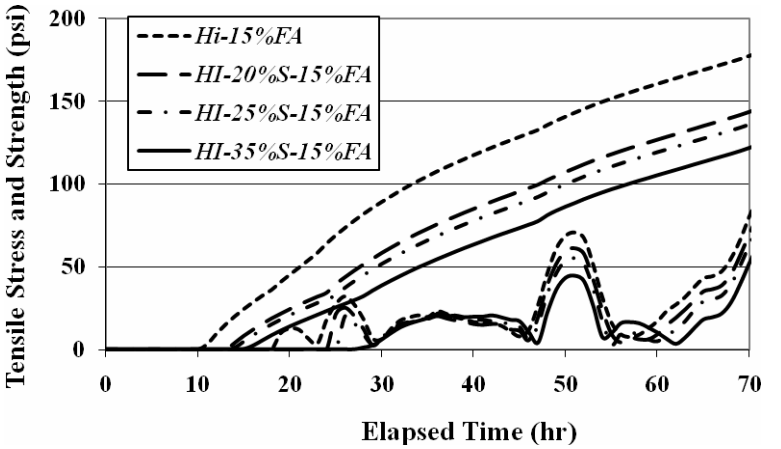


FIG. 5. Concrete strength vs. critical stress for fall conditions.

CONCLUSIONS

The following conclusions can be drawn from this study:

1. Fly ash replacement increased setting time of the paste, while slag replacement in ternary cements does not further delay the setting time. In fact, the slag replacement reduced the extended setting times caused by fly ash.
2. Fly ash and slag replacement both reduced the generated heat. However, the

heat reduction was not proportional to slag replacement level due to the pozzolanic reaction. Fly ash replacement postponed the peak time of the rate of heat generation. Concrete with different slag replacement level had similar peak time.

3. The datum temperature and activation energy of concrete increased with the amount of fly ash and slag replacements. That means the concrete with blended cement could stop hydration at a higher temperature than concrete without fly ash and slag.
4. Based on the HIPERPAV analysis, under typical spring, summer, or fall weather conditions in Iowa, concrete made with 15% fly ash and 20%–35% slag replacement would have no early-age cracking potential. However, in spring or fall, the stresses developed in the concrete become much closer to the strength developed in the concrete, indicating a higher risk of cracking than the concrete cast in summer.

ACKNOWLEDGEMENTS

The study was sponsored by the Center for Portland Cement Concrete Pavement Technology, Iowa State University, and the Iowa Department of Transportation (Iowa DOT). Some concrete strength and maturity tests were performed at Iowa DOT.

REFERENCES

Andersen, P.J., Andersen, M.E., and Whiting, D. (1992). "A guide to evaluating thermal effects in concrete pavements." SHRP-C-321, Strategic Highway Research Program, National Research Council.

Carino, N.J. (1994). "The maturity methods: theory and application." *Cement Concrete and Aggregate*, Vol. 6(2): 61-73.

Hankins, K., Suh, Y.C., and McCullough, B.F. (1991). "Field evaluation of coarse Aggregate types: criteria for test sections." Research Report 422/1244-1, Center for Transportation Research, The University of Texas at Austin.

Ma, W., Sample, D., Martin, R., and Brown, P.W. (1994). "Calorimetric study of cement blends containing fly ash, silica fume, and slag at elevated temperature." *Cement Concrete and Aggregate*, Vol. 16 (2): 93-99.

McCullough, B.F., Zollinger, D., and Dossey, T. (1998). "Evaluation of the performance of Texas pavements made with different coarse aggregates." Research Report 3925-1F, Center for Transportation Research, The University of Texas at Austin.

Mehta, P.K. and Monteiro, J.M. (2006). Concrete: Microstructure, Properties, and Materials. McGraw-Hill:392-394.

Sánchez de Rojas, M. I. Luxán, M. P. Frías, M., and García, N. (1993). "The influence of different additions on Portland cement hydration." *Cement and Concrete Research*, Vol. 23: 46-54.

Strategic Development Council (2002). "Roadmap 2030: The U.S. concrete industry technology roadmap. " Strategic Development Council.

Wang, K.J. and Ge, Z. (2003). "Evaluating properties of blended cements for concrete pavement (project report)." The Center for Portland Cement Concrete Pavement.

Evotherm Warm Mix Asphalt Technology Applied on Ultra-thin Pavement in China

Zhuohui Tao[1], Fujian Ni[2], Jinhai Yan [3], Wenyuan Huang [4]

[1]Technical Engineer, Shanghai application center, MeadWestvaco Corporation, China 200231;
Email: zt7 @meadwestvaco.com
[2]Professor, School of Transportation, Southeast University, Jiangsu Province, China 210096;
Email:nifujian@gmail.com
[3]Ph.D, School of Transportation, Southeast University , Jiangsu Province, China 210096;
Email: jason.yan1@gmail.com
[4]Technical manager, Shanghai application center, MeadWestvaco Corporation, China 200231;
Email: wh13@meadwestvaco.com

ABSTRACT: With the characteristics of Evotherm warm mix asphalt technology introduced, the existing problem about hot mix asphalt technology applied on ultra-thin pavement was put forward. The research on the workability of Evotherm warm asphalt mixture was conducted by measuring the Brookfield dynamic viscosity of Evotherm warm mix asphalt and hot mix asphalt (HMA) at different temperatures, which can guide the mixing and compaction temperature range. Based on test results of laboratory performance, the warm mix asphalt ultra-thin pavement was paved in China at low air temperature. The temperature vs. time curve of Evotherm warm asphalt mixture was derived theoretically by Pavecool® software in advance. The field temperature vs. time curve was also obtained by field test result of Evotherm trial road, which can guide the compaction occasion of the Evotherm warm mixture. The pavement performance of trial road was positive, which demonstrated that the application of Evotherm warm mix asphalt on ultra-thin pavement was successful at low air temperature in China.

INTRODUCTION

A study tour was sponsored by the National Asphalt Pavement Association in 2002 and since then, interest in warm mix asphalt technologies has grown in the United States. The first generation Evotherm technology, which was based on the emulsion asphalt technology, was developed in 2003. The third generation Evotherm- dispersive asphalt (DAT) technology, which was based on a chemistry solution technology, was developed successfully in 2007 [1].

Evotherm WMA is produced at temperatures about 30°C to 60°C lower than typical Hot Mix asphalt (HMA). Compared to HMA, Evotherm warm asphalt mixtures have some advantages, such as saving energy and reducing fumes release during production and placement, in addition, WMA can be compacted more easily because the compaction temperature range of Evotherm warm asphalt mixture is wider, which can also prolong the warm asphalt mixture compaction time at low air temperatures. An Evotherm DAT application of an ultra-thin pavement was proven to be successful at a low air temperature in December of 2007 in China [2].

BROOKFIELD DYNAMIC VISCOSITY VS. TEMPERATURE CURVE

The Evotherm chemistry solution diluted by water was added into SBS modified asphalt directly in order to simulate the field mixing process of Evotherm DAT warm mix asphalt .The process of adding the solution to the asphalt must be well controlled because water is converted into vapor when mixed with hot asphalt. The weight of the asphalt sample was 500 g and the weight ratio of asphalt vs. the solution is 95:5. The asphalt temperature was 165°C, the solution temperature was 20°C. Mixing can not be stopped until the vapor disappears. The duration of mixing time was 30 minutes, and then the Evotherm asphalt was put into oven for 2 hours at a temperature of 140°C after mixing. The Brookfield dynamic viscosity vs. temperature of Evotherm asphalt and original asphalt were tested respectively. These results are shown in Figure 1 [3].

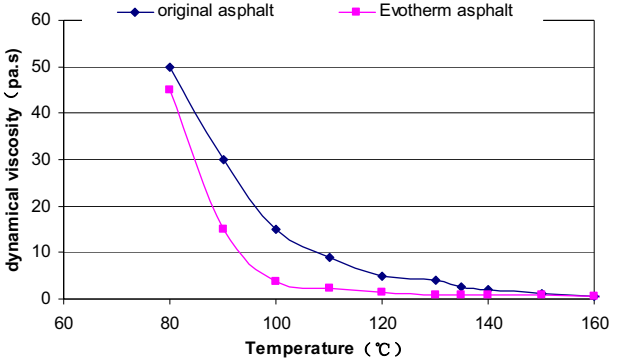


FIG.1. Brookfield Dynamical viscosity vs. Temperature

The results indicate that the Evotherm solution reduced the Brookfield dynamic viscosity of original asphalt by two thirds when the temperature range is 100°C~140°C which also prove that Evotherm WMA could be mixed and compacted easily when the mixture temperature was between 100°C and 140°C .

EVOTHERM WARM ASPHALT MIXTURE DESIGN

The ultra-thin asphalt concrete (subsequently called the “UTAC”) was designed based on a combination of the Marshall Design method and the Gyratory compaction method [4].

Design Aggregate Gradation and Asphalt Content

The UTAC-10 design aggregate gradation is shown in Table 1

Table1. UTAC-10 design aggregate gradation

Sieve size(mm)	UTAC-10
16	100
13.2	100
9.5	83.2
6.7	47.8
4.75	32.8
2.36	24.4
1.18	18.3
0.6	11.2
0.3	8.6
0.15	7.5
0.075	6.2
Optimal asphalt content (%)	5.0

Laboratory Performance Testing

During construction of the test sections, samples of each asphalt mixture were obtained and used to produce test samples used for laboratory performance testing. Contractors compacted samples at the asphalt plant without reheating; although, many agencies transport the mixture to a central laboratory where it was reheated prior to compaction. The laboratory performances of warm asphalt mixture were evaluated. These test results are shown in Table 2.

Table2. Laboratory performance test results

Item	UTAC-10	Specification
Density(g/cm^3)	2.429	--
Void (%)	4.2	3~5%
Marshall Stability(KN)	11.0	>8.0
Flow value(0.1mm)	39	15~40
VFA（%）	69	65~75

As shown in table 2, the air void and Marshall Stability of Evotherm warm asphalt mixture met the requirement of specification.

CONSTRUCTION

The UTAC-10 Evotherm trial road was paved successfully in December of 2007 in China. The trial road was 1km long, the thickness was about 2.5cm, the width was 11m. Production started in the morning by firstly manufacturing 500 tons of mix using the Evotherm DAT process. The trial road was paved at a wind speed of 10mph and an air temperature of 10°C. Flow rate of the plant was 240 tons/hour. Asphalt vs. concentrated solution ratio was 95/5 (pump speed was 1.1kg/second) [5].

Temperature Control Process

Temperature of the aggregates started at 150°C to warm up the plant and decreased gradually to around 130°C (between 125 and 135 °C). It took about three trucks (75 tons) to stabilize the temperature. Temperature of SBS modified asphalt was 165°. The outlet temperature of the warm asphalt mixture was 135~140°C. The temperature of the mix inside the trucks when arriving on the jobsite declined from 135°C to 130°C.

Compaction

The roller compaction pattern consisted of the following: 2 passes of steel wheel roller (in vibratory mode on the first pass) plus 6 passes of pneumatic tire roller plus 2 passes of steel wheel finish roller. The weight of the steel roller was 16 tons, and the weight of the pneumatic tire roller was 30 tons. The vegetable oil was used to brush the tires to stop the mixture from sticking with tires. The velocity of the paving machine was about 3~4m/min.

Temperature Testing and Analysis

Both pavement interior temperature and surface temperature were tested at different times by thermometer at specific position during construction in order to obtain the temperature vs. time curve which can guide the compaction time based on the Evotherm warm asphalt mixture available compaction temperature range. The temperature testing time was 20 minutes in all and the temperature was recorded every 2 minutes. Compaction temperature was 125~130°C under the first steel wheel roller pass (in vibratory mode on pass), was decreased to100~110°C under the pneumatic tire roller pass, and was decreased to 60~70°under the final steel wheel roller pass. Meanwhile, the theoretical temperature at different times was also calculated by using Pavecool® software developed by simulating the field conditions. the parameters of Pavecool® software include asphalt grade, wind speed, time, air temperature, mixture type, mixture thickness and mixture temperature etc. the warm mixture temperature vs. time curve was shown in Figure 4 [6].

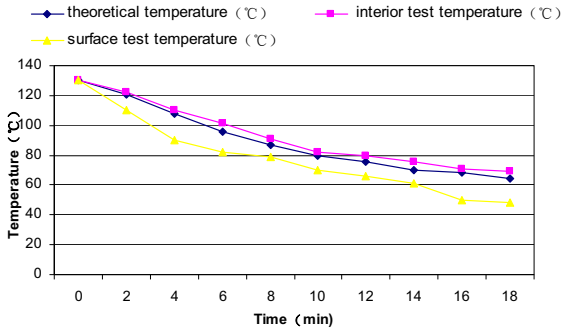


FIG.4. warm mixture temperature vs. time curve

As shown in Figure 4, the theoretical temperature vs. time curve matched with interior test temperature vs. time curve well. It took about 6 minutes for the mixture interior test temperature to fall from 130°C to 100°C at a wind speed of 10 mph and an air temperature of 10°C. It can be also concluded that the pneumatic tire roller compaction must be finished within 6 minutes based on the Brookfield dynamic viscosity vs. temperature at above mentioned circumstances.

FIELD PAVEMENT PERFORMANCE TESTING

Performance properties were tested from cores taken from trial road one day after construction. Test results are shown in Table 3.

Table3. Field performance test results

Mixture type	Height (cm)	Bulk volume density (g/mm)	theoretical maximum density (g/mm)	Void (%)	Marshall compaction (%)	theoretical maximum compaction(%)
UTAC-10	2.7	2.366	2.536	6.6	97.4	93.3
	2.8	2.393	2.536	5.6	98.5	94.3
	2.6	2.395	2.536	5.5	98.6	94.4
	2.5	2.361	2.536	6.9	97.2	93.1
	2.6	2.393	2.536	5.6	98.5	94.4
Specification	---	---	---	3~7	97~100	93~97

As shown in table 3, the compaction of Evotherm warm asphalt mixture trial road met the requirement of specification which proved the Evotherm technology applied on ultra-thin asphalt pavement was successful.

CONCLUSIONS

In this paper, the research on Evotherm warm asphalt mixture applied on ultra-thin asphalt pavement at low air temperature was conducted. Evotherm chemical packages contain surfactants that create micro-dispersions of residual water (<0.05%) within the binder. When sheared under compression, as during compaction, the micro-dispersions form slip planes, effectively reducing the viscosity of the binder phase. This shear-induced viscosity reduction allows for improved compaction at low temperatures. Evotherm WMA could be mixed and compacted easily when its temperature was between 100°C and 140°C.

The laboratory performance of UTAC-10 Evotherm warm asphalt mixture can meet the requirement of the specifications. It can also be concluded that pneumatic tire roller compaction must be finished within 6 minutes when the mixture paving

temperature is about 130°C at a wind speed of 10 mph and an air temperature of 10°C. Theoretical temperature vs. time curve match with field interior test temperature vs. time curve well. Pavecool® software is an effective tool to simulate the field temperature vs. time curve and calculate compaction period of time.

ACKNOWLEDGEMENTS

The work was sponsored by MeadWestvaco Corporation cooperative agreement with Southeast University. The two authors of this paper were employees of MeadWestvaco Corporation. The authors would like to thank Professor Gu Xingyu from Southeast University and doctor Du from Hebei Province Highway Administration Bureau for allowing this research to be conducted at their subsidiaries.

REFERENCES

[1] US. Department of Transportation, Federal Highway Administration .Avaliable online at:
http://www.fhwa.dot.gov/pavement/asphalt/wma.cfm(accessed August 2008).
[2] Zhuohui Tao, “Evotherm warm mix asphalt applied at low air temperature”[R] ISSA, Xian, China. 2008.
[3]JTJ --2004, ' Specifications of asphalt concrete pavement design for highway ', Ministry of Communications of the People’s Republic of China, Beijing, 2004.
[4]Dapeng Li, “The research on the performance of Ultra-thin overlay asphalt concrete.”[D]Dissertation Submitted to Southeast University For the Academic Degree of Master of Science, Nanjing, China, 2007
[5]EVOTHERM DAT JOBSITE Road RD-Charmant [R] MeadWestvaco Corporation
[6] Washington State Department of Transportation.Avaliable online at:
http://www.wsdot.wa.gov/biz/mats/Apps/pavecool.htm (accessed August 2008)

Future Design of Perpetual Pavements: Issues and Options

Rafiqul A. Tarefder[1], A. M. ASCE and Damien Bateman[2]

[1]Assitant Professor of Civil Engineering, University of New Mexico, MSC01 1070, Albuquerque New Mexico, 87113; tarefder@unm.edu

[2]Graduate Research Assistant, Department of Civil Engineering, University of New Mexico, MSC01 1070, Albuquerque New Mexico, 87113; evankias@unm.edu

ABSTRACT: Perpetual pavements are considered by many pavement experts to be the long-term solution to increasing traffic volumes and related pavement rehabilitation costs and user delay costs. The paper reviews the problems that perpetual pavements are experiencing, such as moisture infiltration/damage, and layer debonding. There is no indication that the pavement design methods presented in this paper account for moisture infiltration/damage or debonding in their designs. This is primarily due to the lack of an appropriate design method, which can include infiltration/damage and debonding it its design. Analysis of current field performances of selected perpetual pavements and mechanistic-empirical predicted performances is also shown. From this analysis, three out of six perpetual pavements are performing better than expected; two pavement sections are performing as predicted, and one pavement section performing worse than expected.

INTRODUCTION

Perpetual pavement is defined as an asphalt pavement designed and built to last on the order of 50 years or more without requiring major structural rehabilitation or reconstruction, and needing only periodic surface renewal in response to distresses confined to the top of the pavement. With perpetual pavements, the potential for traditional fatigue cracking is reduced, and pavement distress is typically confined to the upper layer of the structure. Thus, when surface distress reaches a critical level, an economical solution is to remove and replace the top layer. The perpetual pavement concept can be used for any pavement structure where it is desirable to minimize rehabilitation and reconstruction costs as well as minimize closures to traffic.

While there are some successes with perpetual pavements, there is a big gap in our understanding the design of this pavement. One of the critical issues with the current perpetual pavement design method is that it does not ensure optimum structure and/or layers. Another critical issue with perpetual pavement design is that some of the most important factors related to pavement longevity are not adequately addressed by

existing design approaches. In particular, the effects of moisture within the pavement section and interlayer de-bonding can be principal factors in reduction of pavement performance over time, yet both effects are only accounted for in a relatively crude manner. To this end, this study discusses the critical issues and options related to existing perpetual design, materials, moisture infiltration, bonding-debonding, and field performances.

OBJECTIVES AND SCOPE

The objectives of this study are to evaluate current design methods of perpetual pavements, examine the effects of moisture infiltration on the current perpetual pavement, assess the degree of bonding/bonding within a perpetual pavement section.

DATA COLLECTION

All fifty state DOTs have been contacted in regards to design and implementation of perpetual pavements in their respective states. Thirty seven state DOTs responded and out of those that responded, only fourteen have designed or are in the process of designing perpetual pavements. Many of the perpetual pavements found during this review do not have complete data. Only six have complete data. This includes two perpetual pavements from New Mexico, US 70 and US 550, and one from Ohio, Oregon, Texas and Washington. In this study, wherever possible, data is taken from the 13 perpetual pavement sections to examine certain critical issue.

Table 1 presents total pavement thickness, traffic volume, design life and service life of the pavement, and the length of each pavement section. The traffic volume is presented as the average annual daily truck traffic (AADTT) measured for each pavement. The thickness of each pavement varies from 13 to 30 inches. The design life of the pavements varies from 20 to 50 years. Two pavements have a design life of 50 years, Ohio and Washington. Pavements from California, Iowa, Kentucky and Michigan have design lives of 40 years. Illinois, Maryland, Minnesota, New Mexico (US 70), Oregon (I-5) and Texas (SH 114) have design lives of 30 years, and New Jersey, New Mexico's US 550 and Wisconsin pavements designed to last 20 years.

ISSUE OF LAYER MATERIALS & THICKNESS

A perpetual pavement cross-section is presented in Figure 1 based on the the average value of the collected data. Three layers of perpetual pavements can be described as follows: The surface layer (*wearing surface*) is in direct contact with traffic. A wearing surface is used to protect the lower dense-graded layers, to allow rainfall to drain through the open graded layer and off the pavement, to reduce traffic noise and improve visibility in wet weather conditions (Cano 1997). The second layer is known as an *Intermediate layer*. This layer usually consists of a Superpave mix which is a gap-graded bituminous mixture where the aggregate and binder grade are major contributors to its rut-resistant properties. The third layer is a *base layer*. This layer is placed at the bottom of the HMA section. The base layer can a rich binder layer (RBL), which is extra flexible due to higher binder content and this is a major

contributor to its fatigue-resistant performance. The use of polymer modified binders in base layers is rare because polymer modified binder makes the asphalt concrete stiff. However, Illinois DOT decided to use a polymer-modified binder in the base layer instead of a RBL as the potentially higher permeability of Superpave mixtures might allow moisture to infiltrate and become entrapped and this would lead to premature stripping of the hot mix asphalt (HMA). The above layers are placed on a solid foundation, which can be a granular subbase or a treated subgrade or soils.

Table 1. Perpetual Pavement Design Data

Number of State DOT	Pavement Section	AADTT (trucks/day)	Total Pavement Thickness (in)	Design Life (yrs)	Service Life (yrs)	Section Length (mi)
1	California I-710	10000	19	40	19	1
2	Illinois I-70	24000	25.5	30	19	12
3	Iowa US-60	8250	23.5	40	15	-
4	Kansas US-75	712 ESAL/day	16	10	-	4
5	Kentucky I-64	10000	19	40	20	3.3
6	Michigan I-96	8900	30	40	20	-
7	Minnesota I-35	864	15	30	16	-
8	New Jersey I-287	24000	19	20	12	-
9	New Mexico US-70	1338	16	30	8	38
9	New Mexico US-550	1100	13	20	7	118
10	Ohio US-30	3747	22.25	50	20	8
11	Oklahoma SH-152	1820 ESAL/day	15	-	-	10
12	Oregon I-5	12240	24	30	15	-
13	Texas SH-114	18000	23.5	30	20	1.7
14	Washington I-90	5400	28	50	18.5	5.3
14	Wisconsin STH 50	770	21	20	-	6.9

ISSUE OF DESIGN

As mentioned previously, the philosophy of perpetual pavement design is to keep the tensile strains at the bottom of the asphalt layer so small that the fatigue life of the base layer becomes virtually infinite. The limiting strain that leads to this infinite

fatigue life is called endurance limit. To keep the traffic induced strain low at the bottom of the base, the following two main approaches are employed:

- The first approach is the construction of a bottom lift for the base layer with softer binder grade and/or higher binder content.
- The second approach is the increase of the total thickness of asphalt layers (surface and intermediate) and the increase of stiffness for all layers.

Table 2 shows the perpetual pavement concepts used for 14 pavements analyzed. Eleven out of fourteen state DOTs analyzed for this summary use a limiting strain. The remaining 3 state DOTs do not follow this perpetual concept.

Fatigue Endurance Limit

Table 2 presents the fatigue endurance limits of perpetual pavements. It can be seen that the fatigue endurance limit ranges from 60 to 90 micro-strain (με).
For California's I-710, the fatigue endurance limit (FEL) of 70 με is based on the relationship between tensile strain and laboratory fatigue life (Pavement Research Center 1999). The University of Illinois conducted a thorough study of the literature

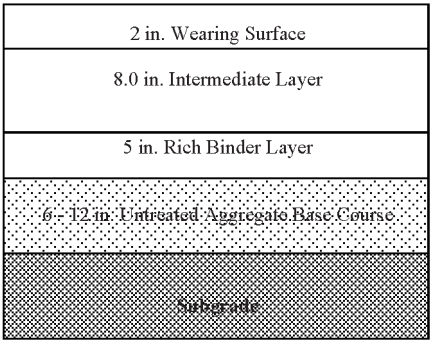


FIG. 1. Cross-section of a Perpetual Pavement

and utilization of the Asphalt Institute equations to examine Illinois binder mixtures and established a fatigue model which was used to generate fatigue endurance limits for its perpetual pavement design mixes. Exhaustive testing indicates no strain value below 70 με needs to be used to have all mixtures exhibit the extraordinarily extended fatigue life associated with an FEL. The strain level associated with the FEL ranges up to around 100 με, but never below 70 με (Carpenter 2006, Romanoschi 2008).

An endurance limit value of 65 με was used for the strain at the bottom of the HMA in Michigan's latest project, I-96 in Detroit (Eacker 2008). The endurance limit used in New Mexico's US 70 is not known but it is known that the base course of this pavement is an asphalt Rich Binder Layer (RBL). A limiting strain of 70 με was used in Ohio's US 30, as tests revealed that no tensile strains at the bottom of the RBL exceeded this value (Ohio DOT 2006). In constructing the perpetual pavement on I-5, analysis was done by Oregon DOT to determine combinations of axle loads and

HMA layer moduli that would result in tensile strains at the bottom of the HMA layer exceeding a threshold value of 70 με (Scholz 2006). Texas perpetual pavements are designed and checked to ensure that the limiting tensile strain at the bottom of the last asphalt layer is below 70 με (Walubita 2007).

In summary, many of the pavements listed in Table 2 show that a limiting strain of 70 με is most commonly used. However, some states such as Illinois and Michigan use limiting endurance strains of 60 and 65 με for their pavements.

Design Method

Table 2 lists the software and structural design methods of the 14 perpetual pavements reviewed in this section. Five out of 14 state DOTs use AASHTO *1993 Pavement Guide* for the design of new or reconstructed perpetual pavements, such as Kansas, Washington, Oregon and New Jersey. Several states have come up with their own mechanistic or mechanistic–empirical design methods such as California, Illinois and Texas, while others are in the process of developing a mechanistic-empirical method for newly constructed pavements. DOTs that use their own method of design usually include software programs which allow them to estimate an appropriate thickness for the pavement. For instance Washington and Texas use EVERSERIES and PerRoad software, respectively.

Perpetual pavements presented in Table 2 are designed using mechanistic, empirical, or mechanistic-empirical analysis. CIRCLY is software for the mechanistic analysis and design of road pavements. It was used to determine the principal strain at the bottom of the rich binder layer in California's I-710 (Pavement Research Center 2006). Since 1989, Illinois DOT has been using a mechanistically based pavement-thickness design procedure, called ILLIPAVE. It includes limiting the maximum tensile strain at the bottom of the lower lift, as well as limiting the subgrade stress(Fee 2001).

Michigan's perpetual pavements were designed using a mechanistic approach employing the ELSYM5 computer program. The program outputs are stresses and strains in the pavement structure. This approach applied the concept of cumulative damage to determine the appropriate section for a design period of up to 40 years. In their latest project, Michigan used EVERSTRESS, PerRoad, and MEPDG which are mechanistic-empirical software, to design the perpetual pavement on I-96 in Detroit (Eacker 2008). The mechanistic-empirical (ME) Asphalt Institute model was used to design the perpetual pavement section on US 70 near New Mexico's Hondo Valley (AMEC 2007).

Ohio's US-30 was designed based on elastic layer analysis. Kenlayer was used with adjusted modulus values for the upper layers based on estimated temperature gradients. The thickness of the asphalt base was adjusted until tensile stains at the bottom of the asphalt base were 70 με or less (Green 2008). Prior to construction the Asphalt Pavement Association of Oregon (APAO) conducted a mechanistic-empirical analysis of the I-5 pavement structure to determine if the structure was likely to meet generally-accepted criteria for perpetual pavements with respect to fatigue cracking. Oregon DOT used the AASHTO 1993 Pavement Design Guide and WESLEA to conduct this analysis (Scholz 2006). The current structural (thickness) design and

analysis of Texas perpetual pavements is mechanistic-empirically based using the Flexible Pavement System (FPS) 19W software. However, the thickness design is also often checked with the PerRoad software (Walubita et al. 2007).

Table 2. Perpetual Pavement Design Concepts

No.	State Pavement	Pavement Section	Limiting Strain in Base Layer	Design Method/ Software	Design Method/ Software
1	California	California I-710	70 με	CIRCLY, Highway Design Manual	Mechanistic
2	Iowa	Illinois I-70	90 με	ILLIPAVE, IDOT ME Design	Mechanistic
3	Illinois	Iowa US-60	60 με	1993 AASHTO	Empirical
4	Kansas	Kansas US-75	70 με	1993 AASHTO, EVERSTRESS	Empirical
5	Kentucky	Kentucky I-64	70 με	ME Design Method	Mechanistic-Empirical
6	Michigan	Michigan I-96	65 με	ELSYM 5, Von Quintus Catalog 2001, EVERSTRESS, PerRoad, MEPDG	Mechanistic, Mechanistic-Empirical
7	Minnesota	Minnesota I-35	None	MnPave, ROADENT	Mechanistic-Empirical
8	New Jersey	New Jersey I-287	None	1993 AASHTO	Empirical
9	New Mexico	New Mexico US-70	no	Asphalt Institute	Mechanistic-Empirical
10	Ohio	Ohio US-30	70 με	Kenlayer	Mechanistic
11	Oklahoma	Oklahoma SH-152	70 με	PerRoad	Mechanistic-Empirical
12	Oregon	Oregon I-5	70 με	AASHTO 1993, WESLEA	Empirical
13	Texas	Texas SH-114	70 με	FPS 19W, PerRoad	Mechanistic-Empirical
14	Washington	Washington I-90	None	AASHTO 1993, EVERSERIES	Empirical

In total, fourteen states are represented and out of those fourteen, five perpetual pavements are designed using mechanistic-empirical analysis, and another five pavement sections are designed using empirical analysis, and the remaining four pavement sections use mechanistic analysis. The majority of state DOTs however are investigating the implementation of MEPDG.

ISSUE OF BONDING/DEBONDING

Six perpetual pavements have been analyzed to determine whether debonding is a critical issue with perpetual pavements. The perpetual pavements discussed are shown in Table 3. California's I-710 does not show any signs of debonding and there is no evidence indicates that indicates that debonding is potential problem. The use of tack coat (AR 8000 binder) between each lift prevents is used as a preventative measure to avoid debonding between layers (Monismith 2008). According to literature pertaining to the design of I-70, the Illinois DOT task group agreed that priming with a polymer material between each lift is required to enhance the durability of the mixtures, to promote bonding and so increase the life of the pavement structure (Asphalt Institute 2001). There is evidence of debonding in New Mexico's US 70. Reason for this is the permeability gradient in the layers above the RBL layer.

Table 3. Debonding of Perpetual Pavements

Pavement Section	Debonding Problems	Preventative Measures	Age Since Rehab (Yrs)
California I-710	No	Prime coats and tack coats used between layers	7
Illinois I-70	No	Polymer Priming between all layers in pavement	5
New Mexico US-70	Yes	-	3
Ohio US-30	No	Tack coats applied between all layers	2.5
Texas SH-114	Yes	Tack coats applied between all layers	2
Washington I-90	Yes	Tack coats applied between all layers	8

According to Ohio DOT officials, there is no long-term debonding problem in Ohio perpetual pavements. Specifications for Ohio pavement design call for the use of tack coats between all layers in a perpetual pavement (Powers 2008). There is a major problem with debonding in Texas perpetual pavements. From a recent study, core samples were taken from six different Texas perpetual pavement sections. Of the six sections investigated recently, five showed evidence of debonding at one or two locations (Scullion 2006).

Through core sampling of pavements prior to rehab, the Washington State DOT have often found debonding between the last overlay and the previous pavement surface. According to WSDOT staff, debonding is a potential cause of top-down cracking of perpetual pavements and in some cases, debonding and delamination occurs even with proper tack application between lifts (Uhlmeyer 2008). In summary, three out of the six (50%) state perpetual pavements analyzed do not show any indication of potential debonding problems.

ISSUE OF MOISTURE INFILTRATION AND/OR DAMAGE

Nine perpetual pavements data were available and they were analyzed to determine whether permeability is a critical issue with perpetual pavements (Table 4).

California's I-710 does not show any signs of moisture infiltration and damage. According to a state DOT official, Caltrans used strict compaction controls for the 1st phase of the I-710 freeway rehabilitation. The upper part of the pavement structure were compacted so that the air void contents of the layers were in the range not more than 6% and not less than 3%. The thick rich bottom mix was compacted so that the air void contents did not exceed 3%. These mixes were 3/4 in. dense-graded mixes so it is likely that permeability would be low (Monismith 2008). Illinois DOT uses liquid additives when a mixture is susceptible to moisture damage (stripping). The IDOT elected to require the use of hydrated lime for all mixtures used in the perpetual pavement. Along with the mandatory use of lime, current IDOT design standards require longitudinal underdrains to be placed under the shoulder/pavement joint on both sides of the pavement (Asphalt Institute 2006). According to a Michigan state DOT official, permeability is not a direct consideration in terms of perpetual pavement performance. There is no evidence of moisture-related problems on any of their perpetual pavements, so there are no preventative measures in place (Eacker 2008). Moisture infiltration/damage is a major concern with New Mexico's US 70 (Hondo Valley). In November 2004, NMDOT and FHWA personnel noted that there were areas of the top mat where water was weeping out of the pavement structure onto the surface due to high permeability of the surfacing course (AMEC 2007).

Table 4. Moisture Infiltration/Damage of Perpetual Pavements

Pavement Section	Moisture Problem	Preventative Measures
California I-710	No	Drainage layers placed in pavement
Illinois I-70	No	AASHTO T-283 test with liquid additives (lime) for all mixes
Michigan I-96	No	Not considered, so no design for permeability
New Mexico US-70	Yes	-
Ohio US-30	No	AASHTO T-283 test for all mixes
Oklahoma SH-152	No	Low Permeability specifications for all mixes (12.5x10^-5 cm/s)
Oregon I-5	Yes	Lime and latex anti-strip
Texas SH-114	Yes	Edged drains and chip seal application
Washington I-90	No	Drainage Layers placed in Pavement, anti-strip modifier (liquid additives), crack seal products

Ohio state DOT officials state that permeability is controlled by gradation and density of surface and intermediate layers. Specifications control this adequately. In terms of stripping, specifications for design mixes require testing, using the AASHTO T-283 test (Powers 2008). Personal communication with Oregon DOT has revealed that they have encountered moisture-related problems, such as stripping, on Oregon's I-5 (south of Cottage Grove). The state DOT uses lime or anti-strip additives when required in design mixes, but the state has been re-examining this policy and the use of lime or latex has been increased in areas where stripping is evident on I-5 (Renteria 2008).

Recent testing using ground penetration radar (GPR) revealed the presence of excessive moisture at layer interfaces in many of Texas's pavement sections, especially above the impermeable RBL. Reasons for this include poor compaction in the 1 in. stone filled (SF) layer which is sitting on the RBL, honeycombing between layers where large voided areas trap moisture (Scullion 2006). There are no indications of permeability problems in Washington's I-90. Construction practices call for drainage layers to be placed in pavement sections, and the use of anti-strip modifiers (liquid additives) and crack seal products to reduce moisture damage and infiltration (Uhlmeyer 2008).In summary, three out of nine (33%) state perpetual pavements show moisture infiltration/damage problem.

CONCLUSIONS

- The most common fatigue endurance limit used among fourteen pavement sections analyzed is 70 με. Endurance limits for some pavement sections were based on fatigue testing of design mixes, and others were based on assumptions from published literature and studies. Five out of fourteen pavements (36%) analyzed used an empirical method of design. Four out of the fourteen (28%) pavements use a mechanistic method of design and the remaining five pavements (36%) used a mechanistic-empirical method of design.
- Three out of six (50%) perpetual pavements analyzed show debonding with five out of six pavements in Texas alone showing major debonding problems. There is no indication that debonding is accounted for in the initial design of these pavement sections, but if so, this suggests that the design method used is unreliable.
- Three out of nine (33%) pavements analyzed have experienced permeability problems in their respective perpetual pavements with Texas indicating widespread moisture and permeability problems in their perpetual pavements. Studies on the performances of Texas pavements suggest that poor compaction methods and the use of a coarse design mix (stone filled HMA) are the source of the moisture-related problems. There is no indication that permeability was considered a factor in the design, and this may be due to lack of an appropriate design method to account for this.

ACKNOWLEDGEMENTS

The authors appreciate the funding of the New Mexico Department of Transportation.

REFERENCES

AMEC Earth and Environmental Inc. (2007). "Forensic Analysis Scoping Report – US 70 Hondo Valley Perpetual Pavement Structure." *Project No. AC-MIP-070-4(35)264,* NMDOT State Materials Bureau, New Mexico Department of Transportation, P.O. Box 1149, Santa Fe, New Mexico 87504-1149.

Asphalt Institute (2006). "Illinois I-70 Technology Showcase." <http://www.asphaltinstitute.org/Upload/ > (May 5, 2008).

Carpenter, S.H. (2006). "Fatigue Performances of IDOT Mixtures." *Research Report FHWA-ICT-07-007,* Illinois Center for Transportation, IL 61801

Eacker, M. (2008): Personal Communication, Pavement Design Engineer, Construction and Technology, Michigan Department of Transportation.

Fee, F. (2001). "Extended Life Asphalt Pavement: New Approaches to Increase Durability." *Transportation Research News.* 215, TRB, Washington, D.C.

Green, R. (2008): Personal Communication, Pavement Research Engineer, Ohio Department of Transportation.

Monismith, C. L. (2008): Personal Communication, Director of the Pavement Research Center, California Department of Transportation.

Pavement Research Center (1999). "Mix Design and Analysis and Structural Section Design for Full Depth Pavement for Interstate Route 710." *Technical Memorandum prepared for the Long Life Pavement Task Force*. Pavement Research Center, University of California, Berkeley, CA

Powers, D. (2008): Personal Communication, Bituminous Engineer, Ohio Department of Transportation.

Powers, D. (2007). "Material Requirements to Meet Perpetual Pavement Performance Expectations." Oregon Office of Materials Management, Oregon Department of Transportation, <http://www.flexiblepavements.org/>, (March 13, 2008).

Renteria, R.A. (2008): Personal Communication, Pavement Design Engineer, Materials Laboratory, Oregon Department of Transportation, Salem, Oregon.

Romanoschi, S.A., Gisi, A.J., Portillo, M., Dumitru, C. (2008). "The First Findings From The Kansas Perpetual Pavements Experiment." *Transportation Research Board Annual Meeting 2007,* Paper #08-1384, Transportation Research Board, 500 Fifth Street, NW, Washington D.C.

Scholz, T.V., Huddleston, J., Hunt, E.A., Lundy, J.R., Shippen, N.C., (2006). "Instrumentation and Analysis of a Perpetual Pavement on an Interstate Freeway in Oregon." *2006 International Conference on Perpetual Pavement,* Ohio Research Institute for Transportation and the Environment, Stocker Center, Athens, Ohio 45701.

Scullion, T. (2006). "Perpetual Pavements in Texas: The State of the Practice." *Report FHWA/TX-05/0-4822-1*, Texas Transportation Institute, Texas.

Uhlmeyer, J. (2008): Personal Communication, State Pavement Design Engineer, Washington State Department of Transportation.

Walubita, L. F., and Scullion, T. (2007). "Perpetual Pavements In Texas: The Fort Worth SH 114 Project In Wise County." *Technical Report 0-4822-2*, Texas Transportation Institute. College Station, TX.

Field Evaluation of Damages from Super Heavy Load Moves

Dar Hao Chen[1], John Bilyeu[2], and Zheng Li[3]

[1] School of Communication and Transportation Engineering, Changsha University of Science and Technology, Chiling Road 45#, Changsha, Hunan, China, 410076. dchen@dot.state.tx.us
[2] Texas Department of Transportation. Email: jbilyeu@dot.state.tx.us
[3] Texas Department of Transportation. Email: zli@dot.state.tx.us

ABSTRACT

The number of superheavy load permits in the last five years has increased by a factor of 13.3. With continued economic development in Texas, superheavy load permits are expected to continue to increase. Significant efforts have been made to monitor, evaluate, and analyze pavement damage caused by the superheavy load moves. This paper documented six cases of pavement surface damage as the result of superheavy load moves. It was found that superheavy loads can cause serious damages to fresh seal coats if not properly routed. Based on these six case histories, it was concluded that seal coats are most vulnerable to damage under one or more of the following factors: (1) time after placement (the first 5 weeks are critical), (2) high temperatures, and (3) steep grades in combination with too few drive axles. The results indicate that even after repairs, the pavement condition is not as good as the original undamaged condition, as the damages are still visible approximately six years after repairs. The findings and lessons learned from these six cases can be used by other transportation authorities to improve their regulations and permitting procedures so that damage caused by superheavy load moves is minimized.

INTRODUCTION

Regulating and permitting superheavy loads is part of the Department of Transportation's routine operation [Chen et al. 2005]. The regulations and policies concerning truck weights and dimensions have important economic consequences [TRB 2002]. Truck weights and dimensions are two of the most complex areas of transportation regulation [Schulman 2003] and there is insufficient information to accurately quantify the damages, especially due to weight. When a gross vehicle weight (GVW) exceeds 115,394 kg (254,400 lb), the Texas Department of Transportation (TxDOT) defines it as a superheavy load. Texas is considered a "commerce friendly state" and the number of the superheavy load permits has increased over the years, as shown in Fig. 1. These permits have increased by a factor of 13.3 over the last 5 years, from 49 in 2002 to 701 in 2007. With the economic development in Texas, TxDOT expects superheavy load permits to increase further. The GVW of superheavy loads range from 115,500 kg (254,400 lb) to over 1,043,000kg (2,300,000 lbs).

While it is known that a superheavy loads may cause substantial damage, most evaluation and analyses is done primarily to prevent a structural failure such as rutting or cracking. Under current policy, carriers are responsible for any damage caused by the superheavy load move, while it is Department's responsibility to prove the damages are due to the superheavy load move. Extensive field monitoring in the last 7 years (2002-2008) has not uncovered any structural failures (rutting or cracking) as a result of superheavy load moves. However, there are six instances of fresh

surface treatments peeling off and/or asphalt bleeding to the surface. These damages were typically occurred on the slopes/hills in hot summer afternoons. Field observations indicated that even with the repairs, the pavement condition is not as good as the original undamaged condition. Permitting superheavy loads during the seal coat season in Texas is a challenge, because TxDOT seal coats approximately 32,187 lane km (20,000 lane miles) every year. The superheavy load route selection and evaluation process sometimes requires multiple iterations due to the seal coat construction schedules. Long detours and permit issuance delays can occur during this construction season because an open corridor is not maintained in each district to allow passage of superheavy loads. However, delays in delivering superheavy loads can interrupt power service to communities, reduce or even halt refinery production, result in penalties and/or added costs that can exceed hundreds of thousands of dollars due to delays in industrial construction schedules.

This paper documents the pavement damage caused by superheavy load moves in Texas in the last 7 years.

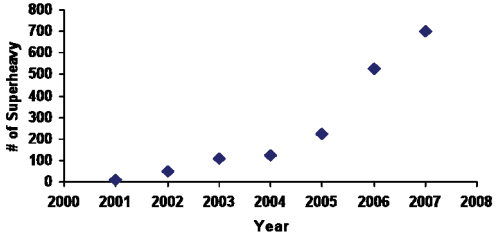


Fig. 1 - Number of Superheavy Load Moves in Texas

Tyler District - SH43

In summer (June 24th) of 2002, there was damage caused by a superheavy load on a 3-week old seal coat pavement on SH43, as shown in Fig. 2. The carrier used one pull truck and a nineteen line Goldhofer trailer to transport a 333,793kg (736,000 lb) generator. The maximum average load per tire on the trailer was 2,086kg (4,600 lb), and the drive axles had 2,268kg/tire (5,000 lbs per tire) for all six tires. SH43 has many rolling hills which are now known to cause problems for fresh seal coat surfaced roads, in the form of peel-ups. This occurs when the temperature is high, the load is heavy, and the carrier does not have the proper equipment to transport loads on steep grades. When the slope is as little as 2.4%, it is best for a superheavy load to have at least one pull truck and one push truck to reduce the shear force between the drive axle tires and seal coat surface. Too much shear force from the driven tires is ultimately responsible for peeling of the seal coat. The benefits of a push truck will be presented in the next section. District personnel performed spot repairs in 2002 and billed the carrier for the damages.

Efforts were made to measure the degree of the slope on the hilly section of SH43. The slope measurements in this area vary from 0.7 to 3 degrees (1.2% to 5.2% grade). One thing worthy of mention is that even after 6 years of repairs and trafficking, the

tire tread marks are still visible on the road, as shown in Fig. 2. The repairs never brought the pavement back to original condition.



Fig. 2 -- Pavement Damage on SH43

Odessa District - US285

On May 30th of 2003, a 300,753kg (663,048 lb) GVW transformer caused damage to a seal coat pavement less than 2 weeks old. The carrier did not have the appropriate permit to move this load legally. The carrier had applied for the permit, but the move occurred before the permit was issued. Based on the load diagram submitted by the carrier, the tire load on the trailer was 2,800kg/tire (6,175 lbs. per tire). However, according to the weighing results provided by the Arizona DOT, the highest tire load on the trailer was 6,758kg (14,900 lbs) on one of the tandem tire sets. This was 20% more than that indicated on the permit request. Note that the heavy load originated from Arizona, and the Arizona DOT did weigh the load. District personnel observed numerous locations where brand new seal coat on US285 had been damaged. Numerous locations had 0.6-1.5m (2-5 feet) long streaks of seal coat peeling off, and the longest one found was 24m (80 feet). The damages were contained entirely in the lanes traveled by the superheavy load. No other damage was observed on adjacent lanes. Interestingly, the same carrier moved a second load about 4 weeks later, with tire loads of only 2,268kg/tire (5,000 lbs per tire) with no observed damage to the then 5~6 week old seal coat. There were no hilly highways in the route, and both push and pull trucks were utilized. Since the damage occurred on flat pavement, there was no slope measurement. Air temperature was in the mid 90's when they went through the same road the second time. It is believed that the combination of heavy tire load and fresh seal coat (not fully cured) were the main factors contributing to the damage.

Based on this instance, TxDOT began to reject superheavy load moves on any seal coat less than 5 weeks old. Research is underway to verify the 5-week criterion for different types of seal coat binders under various conditions (temperature, slope, etc).

Fort Worth District - FM2210

The damage on FM2210 occurred in spring (April 1st) 2004, and is shown in Fig. 3. The age of the seal coat at the time of damage was approximately 1 year. The hilly section is approximately 457.2meters (1,500ft) with slopes varying from 0.6 to 2.4 degrees (1.05% to 4.19% grade). There were two moves (two generators) with slightly more than 0.45 million kg (1 million lbs) each. The maximum average tire load for the 20-line Golhofer trailer was 2,551kg/tire (5,625 lbs. per tire). Only a pull truck was utilized in both moves; there was no push truck. Since the route was fairly

short, the carrier was able to move both generators on the same day. The first move was completed in the morning and it did not cause any damage. The second move was done in the afternoon (around 2:30pm) and the asphalt temperature had increased. With increasing asphalt temperature, the seal coat binder becomes soft, allowing it to bleed to the surface under the superheavy load. Although the load did not cause structural damage, the aesthetics and skid resistance of the road were destroyed. In addition, there were localized areas where the seal coat stuck to the tires and peeled off. Therefore, it is believed that the main contributing factor for the damage on FM2210 was the high temperature. It was the only variable that changed in those two moves. A superheavy move through a hilly section with only a pull truck might exacerbate the damage, but these factors are less important than temperature. The District maintenance forces spot-repaired the worst places in 2004 and billed the carrier for the damage to FM2210. For comparison purposes, pictures were taken in April 2008 at those two locations. Even after the repairs, the damage is still visible after 4 years of trafficking.

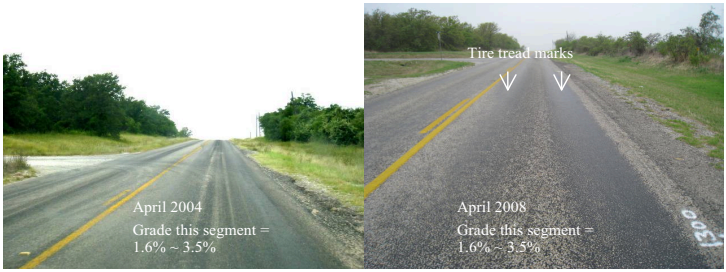


Fig. 3 -- Pavement Damage on FM2210

Yoakum District - FM109

There was a request to move a 225,889kg (498,000 lb) load on FM109. However, in reality, the GVW was about 303,907kg (670,000 lbs), a load 77,110kg (170,000lb) higher than permitted. The damage occurred on a hot summer day (August 10th) of 2004. The permitted tire load was 2,540kg/tire (5,600 lbs per tire). However, the weighed tire load was approximately 3,629kg/tire (8,000 lbs per tire), an increase of 43% over what was permitted. A superheavy load with such high tire loads traveling over hills on a seal coat pavement in August has a very high possibility of causing damage. As reported by district personnel, when the superheavy rig was climbing a hill, its drive axles started spinning on the 3-month old seal coat. It was strongly believed that the damage occurred because the load was towed only by a pull truck without any push truck(s). The damage was exacerbated when the temperature and tire load were high. The rear tires of the pull truck were spinning for approximately 213-244m (700-800ft) as the rig tried to get to the top of the hill. Fig. 4 shows the peeling of the seal coat surface and it sticking to the tires. The carrier backed down the hill and parked the truck on the shoulder waiting for two push trucks. Note that in the permitted loading diagram, there were both pull and push trucks. No additional damage was observed when the load was moved in the evening by a pull truck and two push trucks. This showed that if the load was moved by a pull truck and push

trucks at lower pavement temperature, this would not cause damage. The district maintenance forces did a spot repair, but did not seek reimbursement because the cost was minimal.



Fig. 4 -- Pavement Damage on FM109

Bryan District - FM1371

The damage on FM1371 occurred in summer (June) 2005 with a permitted GVW load of 321,143kg (708,000lb). The construction record indicates that the seal coat was placed several years ago. The permitted maximum trailer tire load was 2,381kg/tire (5,250 lbs per tire). However, the weighed GVW was approximately 359,245kg (792,000lbs) and its tire load was 2,948kg (6,500 lbs) on several tires. Thus, it was over 20% of what had been permitted. TxDOT informed the carrier that it was their decision to move this load, and repairs would be their responsibility if the move caused any damage to the pavement. A precaution was taken by the carrier to move the load over the hilly portion of the route in the early morning to avoid potential damage to the pavement surface. The slopes of the hilly area vary from 0.3 to 3.0 degrees (0.52% to 5.2% grade).

When the truck started climbing the hill, a transmission gear went out, leaving the load stranded on the side of a hill. Due to this malfunction, the carrier had to wait for a second prime mover to be brought in. By 2:00 PM the second prime mover arrived and the load was ready to be moved. However, at 2:00 PM in June, the seal coat surface had heated up making the road much more susceptible to heavy tire loads. This demonstrates that it is not only the age of the seal coat and temperature, but also the slope of the pavement that plays a critical role in this type of damage.

Paris District - SH56

The damage occurred over several miles on August 22nd 2005 at about 3:30 PM on a new seal coat pavement (6 days old). Although the GVW exceeded 114,305kg (252,000lbs) or the threshold value of a superheavy load, no permit request was made to TxDOT. Thus, this move on SH56 was illegal. Police issued a citation and weighed the vehicle. The actual weighed GVW was 166,433kg (367,000 lbs) with an average tire load of approximately 2,631kg/tire (5,800 lbs per trailer tire). Fig. 5 shows the pictures of pavement damage and some temporary spot repairs to stop the bleeding and cover up the places where the seal coat had completely peeled off.



Fig. 5 -- Pavement Damage on SH56

Again, the damage occurred on a hot summer afternoon on a hilly, fresh seal coat pavement. The road was finally repaired by two seal coat treatments over the entire damaged section (several miles). TxDOT billed the carrier for $265,717 for the cost of the repair.

CONCLUSION

Superheavy load permits have increased by a factor of 13.3 over the last 5 years, from 49 in 2002 to 701 in 2007. With the economic development in Texas, TxDOT expects superheavy load permits to continue to increase. The GVW of superheavy loads range from 115,393 kg (254,400 lb) to over 1,043,262kg (2,300,000 lbs). This paper documented 6 cases of pavement surface damage as the result of superheavy load moves. Superheavy loads can cause serious damage to fresh seal coats if not properly routed. Based on these 6 case histories, it was concluded that seal coats are most vulnerable to damage when they are fresh (within 5 weeks of placement), at high temperature, and in hilly areas when there are inadequate push and pull trucks to transport the loads. It was evident that in some instances, the damage was done by illegal moves, or the load levels (GVW and tire loads) were much higher than permitted. Thus, in 2007, Texas legislation empowered TxDOT to penalize carriers when such instances occur. Some of information presented in this paper is only qualitative, because of the limitations of the available personnel and data. Research is still underway to develop criteria that can minimize the future damage.

ACKNOWLEDGEMENTS

This work could not have been completed without the assistance of Paul Rollins and Juan Gonzalez who did the most of the condition surveys.

REFERENCES

- Chen, Dar-Hao, Bilyeu, J. and, Chang, J.R. (2005) “A Review of the Superheavy Load Permitting Program in Texas” International Journal of Pavement Engineering. Vol. 6 (1) June 2005, pp. 45-53.
- Schulman, J.F. “Heavy Truck Weight and Dimension Limits in Canada” http://www.railcan.ca/documents/publications/2003_09_23_heavyTruckWxD_en.pdf
- TRB (2002) Regulation of Weights, Lengths, and Widths of Commercial Motor Vehicle. Special Report 267.

Author Index

Page number refers to the first page of paper

Ali, Liaqat, 112
Alvarez-Lugo, Allex, 1

Bateman, Damien, 177
Bilyeu, John, 187
Boudlal, Omar, 75
Button, Joe W., 1

Cao, Rongji, 1
Ceylan, Halil, 9
Chang, Jia-Ruey, 17
Chao, Sao-Jeng, 17
Chen, Dar Hao, 187
Chen, Xianhua, 145
Chiu, Chui-Te, 125

Dafalla, M. A., 100

Erol, Bilal, 119
Estakhri, Cindy K., 1

Feng, Xinjun, 106
Fiaz, Akmal, 112

Gao, Zhili, 163
Gao, Zhuo, 106
Ge, Zhi, 163
Gopalakrishnan, Kasthurirangan, 9
Guan, Hongxin, 68
Guo, Yanfang, 43

Hao, Peiwen, 106
Huang, Baoshan, 25
Huang, Wei, 145
Huang, Wenyuan, 171
Hwang, Sang-Min, 87

Jia, Jonathan, 37

Kan, Yu-Cheng, 125
Kessler, K., 62
Kim, Seong-Min, 87

Lee, Jeffrey L., 31
Lee, Ming-Gin, 125
Leidy, Joe, 49
Li, Hiwen, 155
Li, Peilong, 139
Li, Zheng, 187

Melbouci, Bachir, 75
Mubaraki, Muhammad, 56

Nam, Boo-Hyun, 31
Ni, Fujian, 81, 171
Nie, Yihua, 132

Ren, Ruibo, 155
Rhee, Suk-Keun, 87

Scullion, Tom, 49
Senol, Aykut, 119
Shu, Xiang, 25
Stokoe, Kenneth H. II, 31

Tao, Zhuohui, 171
Tarefder, Rafiqul, 177

Walubita, Lubinda F., 49
Wang, Dawei, 145
Wang, Kejin, 163
Wang, Yan, 81
Wang, Yonghe, 132
Wang, Zheren, 155
Wu, Yingbiao, 43

Xie, Yongqing, 37

Xu, Liting, 37
Xu, Shifa, 37
Xuan, Weihong, 81

Yan, Jinhai, 171
Yang, Jun, 145
Yen, Tsong, 125
Yi, Wen, 132

Zhang, Bin, 93
Zhang, Jie, 93
Zhang, Xiuli, 43
Zhang, Zhengqi, 139
Zhou, Liang, 139

Subject Index

Page number refers to the first page of paper

Aggregates, 43, 49, 75, 112, 119
Airport runways, 9
Asphalt pavements, 37, 106, 145, 155, 171
Asphalts, 1, 37, 68, 112, 139, 171

Base course, 43, 62, 68, 81, 155
Blasting, 112
Bonding, 68
Bricks, 43
Bridge decks, 145
Bridges, steel, 145

Calibration, 93
Cements, 81, 163
China, 155, 171
Comparative studies, 106
Concrete pavements, 125, 132, 163
Correlation, 25
Cracking, 68, 87, 106, 145, 155, 163

Damage, 187
Deflection, 31, 145
Deformation, 25
Demolition, 75
Design/build, 62
Deterioration, 56
Dewatering, 81

Evaluation, 187
Experimentation, 125, 132

Fatigue, 87
Fibers, 139
Flexible pavements, 9
Florida, 125
Fly ash, 112
Fuzzy sets, 9

Highway and road construction, 119

Korea, South, 87

Load factors, 187

Material properties, 1, 49, 81, 163
Mixtures, 1, 37, 49, 106, 139, 171
Moisture, 93, 163
Mortars, 139

New Mexico, 93
Nondestructive tests, 9

Parking facilities, 125
Pavements, 17, 25, 31, 56, 62, 87, 93, 100, 177, 187
Performance characteristics, 17, 177
Predictions, 56
Preloading, 100
Probe instruments, 31
Pullout, 132

Quality control, 62

Recycling, 43, 75
Rehabilitation, 17
Replacement, 112
Rigid pavements, 155

Sand, 100
Saudi Arabia, 56, 100
Shrinkage, 81
Silts, 100
Soil properties, 119
Specifications, 87
Stiffness, 62
Stones, 43, 49

Structural analysis, 9
Subgrades, 62

Temperature effects, 93, 112, 139, 163
Texas, 187
Tunnels, 37
Two-dimensional analysis, 119